

**Analysis of Potential Conservatism in
Foundation Design for Offshore
Platform Assessment**

by

**Jiun-Yih Chen, Britain A. Matarek, Justin F. Carpenter, and Robert B. Gilbert
Offshore Technology Research Center
The University of Texas at Austin**

and

**Sean Verret and Frank J. Puskar
Energo Engineering, Inc.**

**Final Project Report
Prepared for the Minerals Management Service
Under MMS Award/Contract M08PC20002
MMS Project Number 612**

October 2009

OTRC Library Number: 8/09B198

This report has been reviewed by the Minerals Management Service and approved for publication. Approval does not signify that the contents necessarily reflect the views and policies of the Service, nor does mention of trade names or commercial products constitute endorsement or recommendation for use.



For more information contact:

Offshore Technology Research Center
Texas A&M University
1200 Mariner Drive
College Station, Texas 77845-3400
(979) 845-6000

or

Offshore Technology Research Center
The University of Texas at Austin
1 University Station C3700
Austin, Texas 78712-0318
(512) 471-6989

A National Science Foundation Graduated Engineering Research Center

Analysis of Potential Conservatism in Foundation Design for Offshore Platform Assessment

Table of Contents

Table of Contents	i
List of Tables and Figures	iii
Executive Summary	xiii
1. Introduction.....	1
1.1. Objectives	1
1.2. Methodology	5
1.3. Structure of the Report.....	5
2. Background Information on Pile Foundations	7
2.1. Pile Foundation Design Practice	7
2.2. Potential Sources of Conservatism in Foundation Design.....	10
2.3. Historical Performance of Platform Foundations in Hurricanes.....	14
3. Case Study Platforms	16
3.1. Screening Assessment.....	16
3.2. Platforms Selected for Quantitative Analyses	17
4. Methodology for Quantitative Analyses	20
4.1. 3-Dimensional Finite Element Method Model of Platform Structure	20
4.2. Simplified Plastic Collapse Model of the Foundation	24
4.3. Comparison of Results from Simplified Plasticity Model with 3-Dimensional Finite Element Method Model	29
5. Findings.....	35
5.1. Field Performance Consistent with Design	35
5.2. Importance of Failure Mechanism for Foundation System Capacity	53
5.3. Importance of Structural Factors in Foundation System Capacity	58
5.4. Importance of Sand	59
6. Practical Guidance for Platform Assessments	66
6.1. Guidelines for Modeling Foundations in Platform Assessments.....	66
6.2. General Guidance for Platform Assessments.....	67
6.3. Recommendations for API Recommended Practice	70
6.4. Illustrative Examples for Platform Assessments.....	71
7. Conclusions and Recommendations	76

7.1. Conclusions.....	76
7.2. Recommendations for Practice	78
7.3. Recommendations for Future Work.....	80
8. References.....	81
Appendix A – Excerpt of API RP 2A-WSD	84
Appendix B – Platform Database	101
Appendix C – Description of 3-D FEM Model	107
Appendix D – Description of Simplified Plasticity Model.....	117
Appendix E – Quantitative Analyses of Case Study Platforms	125
Appendix F – Expert Panel Meeting.....	261

List of Tables and Figures

Tables

Table 2.1	Design Parameters for Cohesive (Clay) and Cohesionless (Sand) Soils	10
Table 3.1	Case Study Platforms Selected for Detailed Quantitative Analyses	19
Table 4.1	Output from the Pushover Analysis of Platform 1 in the End-On Loading Direction	23
Table 4.2	Environmental Load Parameters for the Hindcast Analysis of Platform 1	24
Table 5.1	Summary of Results for Quantitative Analysis (Part 1 of 2)	37
Table 5.1	Summary of Results for Quantitative Analysis (Part 2 of 2)	38
Table C.1	Environmental Load Parameters for the Hindcast Analysis of Platform 1 in the End-on Loading Direction	113
Table C.2	Environmental Load Parameters and Results of the Pushover Analysis of Platform 1 in the End-on Direction.....	114
Table C.3	Partial Output from the Pushover Analysis of Platform 1 in the End-on Direction	115
Table E.1	Input Parameters for the Piles of Platform 1 Battered in 2 Directions	129
Table E.2	Input Parameters for the Piles of Platform 1 Battered in 1 Direction.....	129
Table E.3	Input Parameters for the Conductors of Platform 1	130
Table E.4	Design Soil Profile and Parameters for All Piles and Conductors of Platform 1	131
Table E.5	Structural Capacity of the Piles of Platform 1	134
Table E.6	Structural Capacity of the Conductors of Platform 1.....	135
Table E.7	Input Parameters for the Piles of Platform 2 Battered in 2 Directions	143
Table E.8	Input Parameters for the Piles of Platform 2 Battered in 1 Direction.....	143
Table E.9	Input Parameters for the Conductors of Platform 2	144
Table E.10	Design Soil Profile and Parameters for All Piles and Conductors of Platform 2	145
Table E.11	Structural Capacity of the Piles of Platform 2	148
Table E.12	Structural Capacity of the Conductors of Platform 2.....	149
Table E.13	Input Parameters for the Piles of Platform 8.....	154
Table E.14	Input Parameters for the Conductors of Platform 8.....	154
Table E.15	Design Soil Profile and Parameters for All Piles and Conductors of Platform 8	155
Table E.16	Structural Capacity of the Piles of Platform 8	158

Table E.17	Structural Capacity of the Conductors of Platform 8.....	159
Table E.18	Input Parameters for the Piles of Platform 9.....	163
Table E.19	Input Parameters for the Conductor of Platform 9.....	163
Table E.20	Design Soil Profile and Parameters for All Piles and Conductor of Platform 9...	164
Table E.21	Structural Capacity of the Piles of Platform 9	167
Table E.22	Structural Capacity of the Conductor of Platform 9	168
Table E.23	Input Parameters for Pile A of Platform 10.....	173
Table E.24	Input Parameters for Piles B and C of Platform 10	174
Table E.25	Input Parameters for the Conductor of Platform 10.....	174
Table E.26	Design Soil Profile and Parameters for All Piles and Conductor of Platform 10.	175
Table E.27	Structural Capacity of Pile A of Platform 10	180
Table E.28	Structural Capacity of Piles B and C of Platform 10	181
Table E.29	Structural Capacity of the Conductor of Platform 10	181
Table E.30	Input Parameters for the Double Batter Piles of Platform 11	187
Table E.31	Input Parameters for the Single Batter Piles of Platform 11	188
Table E.32	Input Parameters for the 72-inch Diameter Conductor of Platform 11.....	188
Table E.33	Design Soil Profile and Parameters for All Piles and Conductor of Platform 11	189
Table E.34	Structural Capacity of the Double Batter Piles of Platform 11	194
Table E.35	Structural Capacity of the Single Batter Piles of Platform 11	195
Table E.36	Structural Capacity of the Conductor of Platform 11	195
Table E.37	Input Parameters for the Piles of Platform 12.....	199
Table E.38	Input Parameters for the 36-inch Diameter Conductor of Platform 12	200
Table E.39	Input Parameters for the 26-inch Diameter Conductors of Platform 12.....	200
Table E.40	Design Soil Profile and Parameters for All Piles and Conductors of Platform 12	201
Table E.41	Structural Capacity of the Piles of Platform 12	206
Table E.42	Structural Capacity of the 36-inch Diameter Conductor of Platform 12	206
Table E.43	Structural Capacity of the 26-inch Diameter Conductors of Platform 12.....	206
Table E.44	Input Parameters for the Piles of Platform 22.....	211
Table E.45	Design Soil Profile and Parameters for the Piles of Platform 22.....	212
Table E.46	Structural Capacity of the Piles of Platform 22	214
Table E.47	Input Parameters for the Vertical Piles of Platform 25	218
Table E.48	Input Parameters for the Double Batter Piles of Platform 25	218

Table E.49	Input Parameters for the Conductors of Platform 25	219
Table E.50	Design Soil Profile and Parameters for All Piles and Conductors of Platform 25	220
Table E.51	Structural Capacity of the Double Batter Piles of Platform 25	223
Table E.52	Structural Capacity of the Vertical Piles of Platform 25	224
Table E.53	Structural Capacity of the Conductors of Platform 25	224
Table E.54	Input Parameters for the Double Batter Piles of Platform 27	229
Table E.55	Input Parameters for the Single Batter Piles of Platform 27	230
Table E.56	Input Parameters for the Conductors of Platform 27	230
Table E.57	Design Soil Profile and Parameters for All Piles and Conductors of Platform 27	231
Table E.58	Structural Capacity of the Double Batter Piles of Platform 27	236
Table E.59	Structural Capacity of the Single Batter Piles of Platform 27	237
Table E.60	Structural Capacity of the Conductors of Platform 27	237
Table E.61	Input Parameters for the Piles of Platform 29 Battered in 2 Directions	242
Table E.62	Input Parameters for the Piles of Platform 29 Battered in 1 Direction	242
Table E.63	Input Parameters for the Conductors of Platform 29	243
Table E.64	Design Soil Profile and Parameters for All Piles and Conductors of Platform 29	244
Table E.65	Structural Capacity of the Piles of Platform 29	247
Table E.67	Input Parameters for the Piles of Platform 30 Battered in 2 Directions	252
Table E.68	Input Parameters for the Piles of Platform 30 Battered in 1 Direction	253
Table E.69	Input Parameters for the Conductors of Platform 30	253
Table E.70	Design Soil Profile and Parameters for All Piles and Conductors of Platform 30	254
Table E.71	Structural Capacity of the Piles of Platform 30	257
Table E.72	Structural Capacity of the Conductors of Platform 30	258
Table F.1	List of Attendees in the Expert Panel Meeting	261

Figures

Figure 1.1	Results from a Pushover Analysis Showing the Capacity of a Platform Governed by Its Foundation.....	2
Figure 1.2	Platform with “Suspected” Foundation Failure	2
Figure 1.3	Platform with Wave-in-deck Damage	3
Figure 1.4	Damaged X-joint of a Platform.....	3
Figure 1.5	Pancaked Leg of a Platform	4
Figure 1.6	Buckled Underwater Brace of a Platform.....	4
Figure 4.1	An Illustration of the SACSTM model for Platform 1 (Energo 2006)	21
Figure 4.2	Recommended Geotechnical Design Parameters for Platform 1 (McClelland 1979)	22
Figure 4.3	Base Shear versus Deck Displacement for Platform 1 in the End-On Loading Direction	24
Figure 4.4	Schematic of Pile System Collapse Due to the Formation of Plastic Hinges (Lee 2007)	26
Figure 4.5	Schematic of the Updated Plastic Collapse Model for Piles and Wells.....	26
Figure 4.6	System Load Parameters for the Simplified Plastic Collapse Model (Tang and Gilbert 1992).....	27
Figure 4.7	Foundation System Capacity Interaction Curve from Plasticity Model of Platform 1 in the End-on Loading Direction	29
Figure 4.8	Foundation System Capacity Interaction Curve from Plasticity Model of Platform 22 in the End-on Loading Direction	31
Figure 4.9	Foundation System Capacity Interaction Curve from Plasticity Model of Platform 10 in the Hurricane Ike Loading Direction	32
Figure 4.10	Foundation System Capacity Interaction Curve from Plasticity Model of Platform 12 in the End-On Loading Direction.....	33
Figure 4.11	Foundation System Capacity Interaction Curve from Plasticity Model of Platform 1 in the End-On Loading Direction.....	34
Figure 4.12	Foundation System Capacity Interaction Curve from Plasticity Model of Platform 9 in the End-On Loading Direction.....	34
Figure 5.1	Foundation System Capacity Interaction Diagram from Plasticity Model of Platform 8.....	39
Figure 5.2	Foundation System Capacity Interaction Diagram from Plasticity Model of Platform 22.....	40
Figure 5.3	Foundation System Capacity Interaction Diagram from Plasticity Model of Platform 25.....	40

Figure 5.4	Foundation System Capacity Interaction Diagram from Plasticity Model of Platform 27.....	41
Figure 5.5	Foundation System Capacity Interaction Diagram from Plasticity Model of Platform 29.....	41
Figure 5.6	Foundation System Capacity Interaction Diagram from Plasticity Model of Platform 9.....	43
Figure 5.7	Foundation System Capacity Interaction Diagram from Plasticity Model of Platform 11.....	43
Figure 5.8	Foundation System Capacity Interaction Diagram from Plasticity Model of Platform 12.....	44
Figure 5.9	Foundation System Capacity Interaction Diagram from Plasticity Model of Platform 30.....	44
Figure 5.10	Plan View of Foundation System for Platform 10.....	47
Figure 5.11	Foundation System Capacity Interaction Diagram from Plasticity Model of Platform 10.....	47
Figure 5.12	Results of the t-z Analysis of Pile C in Tension	48
Figure 5.13	Sensitivity of the Foundation Overturning Capacity to Loading Direction for Platform 10.....	48
Figure 5.14	Foundation System Capacity Interaction Diagram from Plasticity Model of Platform 1	49
Figure 5.15	Foundation System Capacity Interaction Diagram from Plasticity Model of Platform 2.....	50
Figure 5.16	Schematic of Geologic Setting for Platforms 1 and 2.....	51
Figure 5.17	Sensitivity of the Foundation System Capacity for Platform 1 to Density of Sand Layer at Pile Tips.....	52
Figure 5.18	Sensitivity of the Foundation System Capacity for Platform 2 to Density of Sand Layer at Pile Tips.....	52
Figure 5.19	Schematic Showing Failure Mechanisms for Foundation Systems	54
Figure 5.20	Sensitivity Analyses of Foundation System Capacity to Lateral and Axial Resistance Provided by Soil for Platform 1 in End-On Loading Direction	55
Figure 5.21	Sensitivity Analyses of Foundation System Capacity to Yield Strength of Piles and Conductors for Platform 1 in End-On Loading Direction.....	56
Figure 5.22	Foundation System Capacity Interaction Diagram from Plasticity Model of Platform 11	57
Figure 5.23	Sensitivity Analyses of Foundation System Capacity to Loading Direction for Platform 30.....	58

Figure 5.24	Comparison of Stratigraphy at Two Locations in Similar Geologic Setting....	60
Figure 5.25	Boring Log Used in the Assessments of Platforms 1 and 2 (McClelland 1979)..	61
Figure 5.26	Cone Resistance from a CPT Performed in the Neighboring Block of Platforms 1 and 2 (Fugro-McClelland 2005).....	62
Figure 5.27	Foundation System Capacity Interaction Diagram from Plasticity Model of Platform 1 Comparing the Correct Design Input for the Sand Layers with the Incorrect Input Used in the Pushover Analysis	65
Figure C.1	An Illustration of the SACS™ model for Platform 1 (Energo 2006)	110
Figure C.2	Recommended Geotechnical Design Parameters for Platform 1 (McClelland 1979)	111
Figure C.3	Base Shear versus Deck Displacement for Platform 1 in the End-on Direction ..	116
Figure D.1	Schematic of Pile System Collapse Due to the Formation of Plastic Hinges (Lee 2007)	118
Figure D.2	Schematic of the Updated Plastic Collapse Model for Piles and Wells.....	119
Figure D.3	System Load Parameters for the Simplified Plastic Collapse Model (Tang and Gilbert 1992).....	120
Figure D.4	Orientation of the Skew Angle in the Simplified Plastic Collapse Model (Tang and Gilbert 1992)	121
Figure D.5	Foundation System Capacity Interaction Curve from Plasticity Model of Platform 1 in the End-on Loading Direction	124
Figure E.1	Ultimate Axial Capacities of the Corner Piles of Platform 1	132
Figure E.2	Ultimate Lateral Capacity of the Corner Piles of Platform 1.....	133
Figure E.3	Ultimate Lateral Capacity of the Conductors of Platform 1	134
Figure E.4	Base Case Foundation System Capacity Interaction Diagram of Platform 1 in the End-on Direction.....	135
Figure E.5	Base Case Foundation System Capacity Interaction Diagram of Platform 1 in the Broadside Direction	136
Figure E.6	Base Case Foundation System Capacity Interaction Diagram of Platform 1 in the Diagonal Direction.....	136
Figure E.7	Parametric Analyses for Platform 1 in the End-on Direction Using Capacity Multipliers.....	137
Figure E.8	Parametric Analysis for Platform 1 in the End-on Direction Assuming Static (versus Cyclic) Loading Condition.....	138
Figure E.9	Parametric Analysis for Platform 1 in the End-on Direction Increasing the	

	Density of the Pile Tipping Layer.....	139
Figure E.10	Parametric Analysis for Platform 1 in the End-on Direction Increasing the Yield Strength of the Steel Piles and Conductors.....	140
Figure E.11	Ultimate Axial Capacities of the Corner Piles of Platform 2	146
Figure E.12	Ultimate Lateral Capacity of the Corner Piles of Platform 2	147
Figure E.13	Ultimate Lateral Capacity of the Conductors of Platform 2	148
Figure E.14	Base Case Foundation System Capacity Interaction Diagram of Platform 2 in the End-on Direction	149
Figure E.15	Base Case Foundation System Capacity Interaction Diagram of Platform 2 in the Broadside Direction.....	150
Figure E.16	Base Case Foundation System Capacity Interaction Diagram of Platform 2 in the Diagonal Direction	150
Figure E.17	Parametric Analysis for Platform 2 in the End-on Direction Increasing the Density of the Pile Tipping Layer	151
Figure E.18	Ultimate Axial Capacities of the Piles of Platform 8	156
Figure E.19	Ultimate Lateral Capacity of the Piles of Platform 8	157
Figure E.20	Ultimate Lateral Capacity of the Conductors of Platform 8	158
Figure E.21	Base Case Foundation System Capacity Interaction Diagram of Platform 8 in the End-on Direction	160
Figure E.22	Base Case Foundation System Capacity Interaction Diagram of Platform 8 in the Diagonal Direction	160
Figure E.23	Ultimate Axial Capacities of the Piles of Platform 9	165
Figure E.24	Ultimate Lateral Resistance of the Piles of Platform 9	166
Figure E.25	Ultimate Lateral Resistance of the Conductor of Platform 9	167
Figure E.26	Base Case Foundation System Capacity Interaction Diagram of Platform 9 in the End-on Direction	168
Figure E.27	Base Case Foundation System Capacity Interaction Diagram of Platform 9 in the Diagonal Direction	169
Figure E.28	Parametric Analyses for Platform 9 in the End-on Direction Increasing the Ultimate Lateral Resistance and Yield Strength of the 72-inch Diameter Conductor	170
Figure E.29	Plan View of Foundation System for Platform 10.....	172
Figure E.30	Ultimate Axial Capacities of Pile A of Platform 10	176
Figure E.31	Ultimate Lateral Resistance of Pile A of Platform 10	177
Figure E.32	Ultimate Axial Capacities of Piles B and C of Platform 10	178
Figure E.33	Ultimate Lateral Resistance of Piles B and C of Platform 10	179

Figure E.34	Ultimate Lateral Resistance of the Conductor of Platform 10	180
Figure E.35	Base Case Foundation System Capacity Interaction Diagram of Platform 10 in the Direction of the Waves in Hurricane Ike	182
Figure E.36	Base Case Foundation System Capacity Interaction Diagram of Platform 10 Corresponding to Loading from South to North	182
Figure E.37	Base Case Foundation System Capacity Interaction Diagram of Platform 10 Corresponding to Loading from North to South	183
Figure E.38	Base Case Foundation System Capacity Interaction Diagram of Platform 10 Corresponding to Loading from East to West	183
Figure E.39	Comparison of Foundation Capacities in Different Loading Directions for Platform 10	184
Figure E.40	Parametric Analysis for Platform 10 in the Hindcast Wave Direction Using the Peak Side Shear Capacity	184
Figure E.41	Ultimate Axial Capacities of the Double Batter Piles of Platform 11	190
Figure E.42	Ultimate Lateral Resistance of the Double Batter Piles of Platform 11	191
Figure E.43	Ultimate Axial Capacities of the Single Batter Piles of Platform 11	192
Figure E.44	Ultimate Lateral Resistance of the Single Batter Piles of Platform 11	193
Figure E.45	Ultimate Lateral Resistance of the Conductor of Platform 11	194
Figure E.46	Base Case Foundation System Capacity Interaction Diagram of Platform 11 in the End-on Direction	196
Figure E.47	Parametric Analysis for Platform 11 in the End-on Direction Increasing the Yield Strength of the Steel.....	196
Figure E.48	Ultimate Axial Capacities of the Piles of Platform 12	202
Figure E.49	Ultimate Lateral Resistance of the Piles of Platform 12	203
Figure E.50	Ultimate Lateral Resistance of the 36-inch Diameter Conductor of Platform 12	204
Figure E.51	Ultimate Lateral Resistance of the 26-inch Diameter Conductors of Platform 12	205
Figure E.52	Base Case Foundation System Capacity Interaction Diagram of Platform 12 in the End-on Direction	207
Figure E.53	Base Case Foundation System Capacity Interaction Diagram of Platform 12 in the Diagonal Direction	207
Figure E.54	Parametric Analyses for Platform 12 in the End-on Direction Increasing the Ultimate Lateral Resistance and Yield Strength of the Conductors	208
Figure E.55	Ultimate Axial Capacities of the Piles of Platform 22	213
Figure E.56	Ultimate Lateral Resistance of the Piles of Platform 22	214

Figure E.57	Base Case Foundation System Capacity Interaction Diagram of Platform 22 in the End-on Direction	215
Figure E.58	Ultimate Axial Capacities of the Double Batter Piles of Platform 25	221
Figure E.59	Ultimate Lateral Resistance of the Double Batter Piles of Platform 25	222
Figure E.60	Ultimate Lateral Resistance of the Conductors of Platform 25	223
Figure E.61	Base Case Foundation System Capacity Interaction Diagram of Platform 25 in the End-on Direction	224
Figure E.62	Base Case Foundation System Capacity Interaction Diagram of Platform 25 in the Broadside Direction	225
Figure E.63	Base Case Foundation System Capacity Interaction Diagram of Platform 25 in the Diagonal Direction	225
Figure E.64	Parametric Analyses for Platform 25 in the End-on Direction Increasing the Ultimate Lateral Resistance and Yield Strength of the Conductors	226
Figure E.65	Ultimate Axial Capacities of the Double Batter Piles of Platform 27	232
Figure E.66	Ultimate Lateral Resistance of the Double Batter Piles of Platform 27	233
Figure E.67	Ultimate Axial Capacities of the Single Batter Piles of Platform 27	234
Figure E.68	Ultimate Lateral Resistance of the Single Batter Piles of Platform 27	235
Figure E.69	Ultimate Lateral Resistance of the Conductors of Platform 27	236
Figure E.70	Base Case Foundation System Capacity Interaction Diagram of Platform 27 in the End-on Direction	238
Figure E.71	Comparison of Foundation Capacities in Different Loading Directions for Platform 27	238
Figure E.72	Ultimate Axial Capacities of the Corner Piles of Platform 29	245
Figure E.73	Ultimate Lateral Capacity of the Corner Piles of Platform 29	246
Figure E.74	Ultimate Lateral Capacity of the Conductors of Platform 29	247
Figure E.75	Base Case Foundation System Capacity Interaction Diagram of Platform 29 in the End-on Direction	248
Figure E.76	Base Case Foundation System Capacity Interaction Diagram of Platform 29 in the Broadside Direction	249
Figure E.77	Base Case Foundation System Capacity Interaction Diagram of Platform 29 in the Diagonal Direction	249
Figure E.78	Ultimate Axial Capacities of the Corner Piles of Platform 30	255
Figure E.79	Ultimate Lateral Capacity of the Corner Piles of Platform 30	256
Figure E.80	Ultimate Lateral Capacity of the Conductors of Platform 30	257
Figure E.81	Base Case Foundation System Capacity Interaction Diagram of Platform 30 in the End-on Direction	258

Figure E.82	Base Case Foundation System Capacity Interaction Diagram of Platform 30 in the Broadside Direction.....	259
Figure E.83	Base Case Foundation System Capacity Interaction Diagram of Platform 30 in the Diagonal Direction	259
Figure E.84	Comparison of Foundation Capacities in Different Loading Directions for Platform 30.....	260
Figure F.1	Comments in Dr. Lymon Reese’s Letter (Part 1 of 3).....	263
Figure F.1	Comments in Dr. Lymon Reese’s Letter (Part 2 of 3).....	264
Figure F.1	Comments in Dr. Lymon Reese’s Letter (Part 3 of 3).....	265

Executive Summary

A significant finding from the performance of jacket platforms in major hurricanes, including Andrew (1992), Roxanne (1995), Lili (2002), Ivan (2004), Katrina (2005) and Rita (2005), is that pile foundations performed better than expected (e.g. Aggarwal et al. 1996, Bea et al. 1999 and Energo 2006 and 2007). Jacket platforms are fixed-base offshore structures that are used to produce oil and gas in relatively shallow water, generally less than about 500 feet. The foundation systems consist of driven, open-ended, steel pipe piles. While observed damage or failure in the foundation is rare, assessment of jacket platforms subjected to environmental loads greater than their original design loading frequently indicates that the capacity of the structural system is governed by the foundation. In addition, there were several hundred platforms damaged in these hurricanes and yet there were only a few cases of reported pile foundation failures. Therefore, there is a need to better understand and quantify the potential conservatism in foundation design for the purposes of assessing platforms.

The objectives of this project were to identify and analyze the factors that may contribute to the apparent conservatism in foundation design and to provide guidance on how to incorporate this information in assessing existing platforms. The methodology was to compile and analyze data for existing platforms that have been subjected to hurricane loads near or greater than the design capacity for the foundations. An expert panel of practitioners and researchers was convened to guide the work.

The major conclusion from this work is that the performance of platform foundations in recent hurricanes, based on the available but limited information that we have, is consistent with expectations based on their design and there is no direct evidence of excessive conservatism. In the cases we analyzed in detail, the actual performance of the foundation was either expected or could be explained without conservatism in the design capacity of the foundation.

These results do not preclude the possibility of foundation capacities being greater than expected based on design. One of the limitations of this study was lack of cases from recent hurricanes where the ultimate strength of the foundation system was reached or exceeded in hurricanes. Foundations are designed with a factor of safety, such as a factor of 1.5 for axial loading under 100-year hurricane conditions. The magnitude of hurricane conditions required to reach this value is significant, requiring extreme waves and currents, and was not reached in most of the cases studied (i.e., a foundation failure was not expected and indeed was not observed). Of all the cases obtained from MMS files and industry sources, there were unfortunately only a few that met the high loading condition required to truly test the foundation. In addition, there is redundancy in foundation systems so that overload of a pile, either axially or laterally, does not necessarily lead to collapse or even observable damage. Finally, the study was limited to platforms that were not destroyed since little if any information is available about the performance of platforms that were destroyed.

The major factor contributing to potential conservatism is the effect of long-term set-up (or aging) or pre-loading; there is evidence from laboratory and field studies to suggest that both axial and lateral pile capacities may increase with time beyond the values that are assumed for design. However, in the one case we do have of a foundation failure in a hurricane (an axial pile failure in clay), there is no evidence of the capacity being greater than the design value.

Platform foundations can fail both in shear where the piles are failing laterally (plastic hinges form due to bending) and overturning where the piles are failing axially (plunging or pulling out). Therefore, both axial and lateral capacities are significant for pile foundations in platforms. The axial capacity of piles is derived mostly from the soils in the bottom one-third of the piles. The axial capacity of the piles and, therefore, the overturning capacity of the foundation are approximately proportional to the shear strength of the soils. The lateral capacities of the piles and conductors are derived mostly from the soils in the upper 40 to 50 feet below the mudline depending on their diameters. The lateral capacities of the piles and conductors and the shear capacity of the foundation are much less sensitive to the shear strength of the soils than the axial capacity for typical soil conditions in the Gulf of Mexico.

Structural elements are important to the performance of a foundation system. Well conductors can contribute significantly to the shear capacity of a foundation system, and in some cases to the overturning capacity. The yield strength of steel in the piles also affects the shear capacity of the foundation. Increasing the nominal yield strength to reflect the average value can have a significant effect on the shear capacity for a foundation system, and a much greater effect than increasing the shear strength of the soil by the same amount.

The presence of sand layers contributing significantly to pile capacity was a notable factor in the platforms analyzed herein. Sand is significant because it generally corresponds to a geologic setting where there is significant spatial variability over rather short distances. A soil boring not drilled at the location of a platform when sand is significant to pile capacity, even if the boring is within several thousand feet of the structure, may not provide representative information for the soil conditions at the platform location. In addition, most historical soil borings in the Gulf of Mexico used a Driven Penetration Test to characterize the shear strength of sand layers. This method is generally considered to be outdated, it may not have fully penetrated the sand layers due to sampler refusal, and it has been replaced over the past several decades with Cone Penetration Testing. Finally, pile capacity models when sand layers are present are more complex than for clay layers alone, and we identified numerous cases where sand layers were inappropriately modeled in pushover analyses due to this complexity.

A final conclusion is that general trends in foundation performance cannot be drawn easily based on qualitative assessments. Each platform case, considering the water depth, vintage, structure, geologic setting, hurricane loading and platform performance, is unique and a detailed analysis is required to understand how it performs.

The following guidelines are intended to provide a defensible and consistent approach for modeling pile foundations in platform assessments:

1. When the foundation controls the assessment, include a geotechnical engineer

- familiar with platform assessment.
2. Include well conductors realistically and explicitly in the structural analyses.
 3. Consider using mean rather than nominal yield strength for steel piles and well conductors.
 4. Use static versus cyclic p-y curves for lateral soil capacity.
 5. Be careful in specifying the input for sand layers.

In addition to the specific guidelines for how foundations are modeled in platform assessments, the following general guidance is provided to improve the overall practice of platform assessment:

1. Be careful when relying on a soil boring that was not drilled at the location of the platform or was not drilled using modern methods of sampling and testing (pushed, thin-walled tube sampling for clay layers and Cone Penetration Test for sand layers).
2. Try to obtain pile driving records as well as soil boring logs to help estimate the axial pile capacities and as-built conditions.
3. When the pile foundation system is governing the capacity of the platform in a pushover analysis, check the sensitivity of the foundation system capacity to the lateral and axial capacity of the piles independently.
4. Do not arbitrarily increase the shear strength of the soil to account for perceived conservatism in foundation design.

The following recommendations are intended to improve the API Recommended Practice for Platform Assessment:

1. Provide specific guidance for characterizing pile foundations in platform assessments by incorporating the guidelines developed in this study into RP 2SIM.
2. Update p-y curves for clay in API RP 2A.
3. Better clarify and update design guidance for sand in API RP 2A.
4. Appropriately account for pile flexibility when determining the required pile length.

A major limitation of this study was not analyzing platforms that were destroyed by hurricanes. If detailed analysis could be conducted on these platforms, they may provide

valuable information about how pile systems and the jackets they support performed under extreme loading conditions and may allow us to refine our conclusions. In addition, there may be additional platforms that survived even though the pile systems experienced loads greater than their capacity. Such platforms should be considered for future study. Finally, performing a Cone Penetration Test at the location of the two case study platforms where we are uncertain about the geotechnical properties could provide important information to better understand why these structures survived.

1. Introduction

A significant finding from the performance of jacket platforms in major hurricanes, including Andrew (1992), Roxanne (1995), Lili (2002), Ivan (2004), Katrina (2005) and Rita (2005), is that pile foundations performed better than expected (e.g. Aggarwal et al. 1996, Bea et al. 1999 and Energo 2006 and 2007). Jacket platforms are fixed-base offshore structures that are used to produce oil and gas in relatively shallow water. Most platforms are located in less than 500 feet of water in the Gulf of Mexico. Driven, open-ended, steel pipe piles are typically used to support this type of structures.

Assessment of jacket platforms subjected to environmental loads greater than their original design loading has indicated that the capacity of the structural system is often governed by the pile foundation (Figure 1.1). While there are few cases with “suspected” foundation damages or failures (Figure 1.2), there are no direct observations of such damages and failures during these hurricanes. The majority of platform damages and identifiable failures have been observed to occur in the structures above the mudline (Figures 1.3 to 1.6).

While the lack of definitive foundation failures may be considered acceptable because they are fit for purpose and conservative, this potential conservatism is a cause of concern. The conservatism in foundation design and assessment can lead to costly construction of new platforms or unnecessary limitations on the manning and production levels of existing platforms. In addition, the engineers designing the platform can be misled by overlooking more realistic failure modes of the jacket structure above the mudline, if the foundation is unrealistically governing the calculated capacity of the structural system.

1.1. Objectives

The objectives of this project are to identify and analyze the factors that may contribute to the apparent conservatism in foundation design and assessment and to provide guidance on how to incorporate this information in assessing existing platforms.

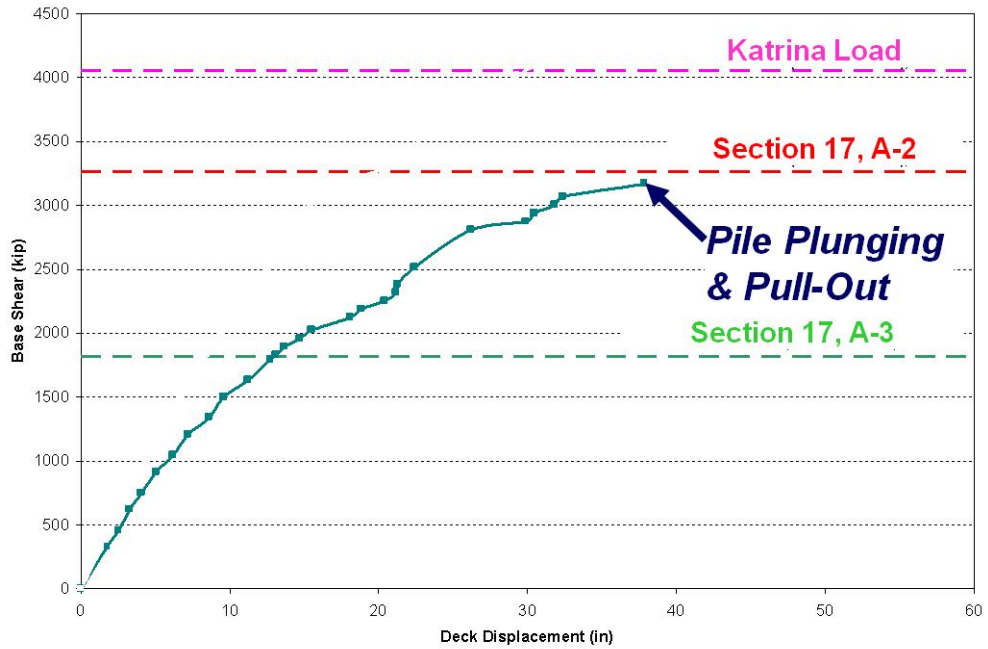


Figure 1.1 Results from a Pushover Analysis Showing the Capacity of a Platform Governed by Its Foundation



Figure 1.2 Platform with “Suspected” Foundation Failure



Figure 1.3 Platform with Wave-in-deck Damage



Figure 1.4 Damaged X-joint of a Platform

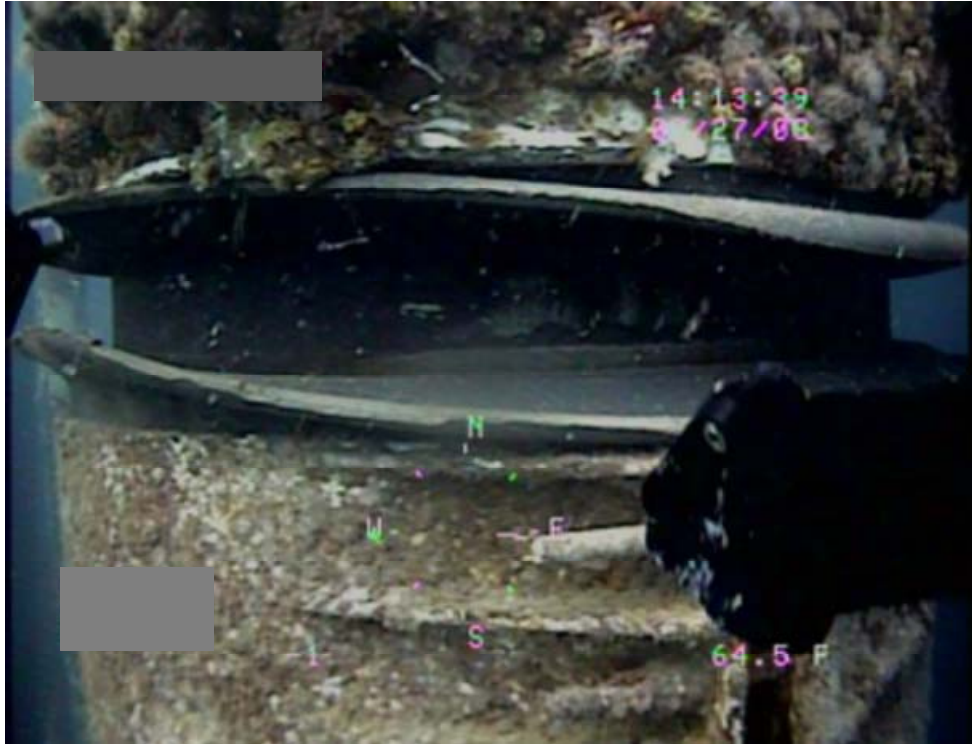


Figure 1.5 Pancaked Leg of a Platform

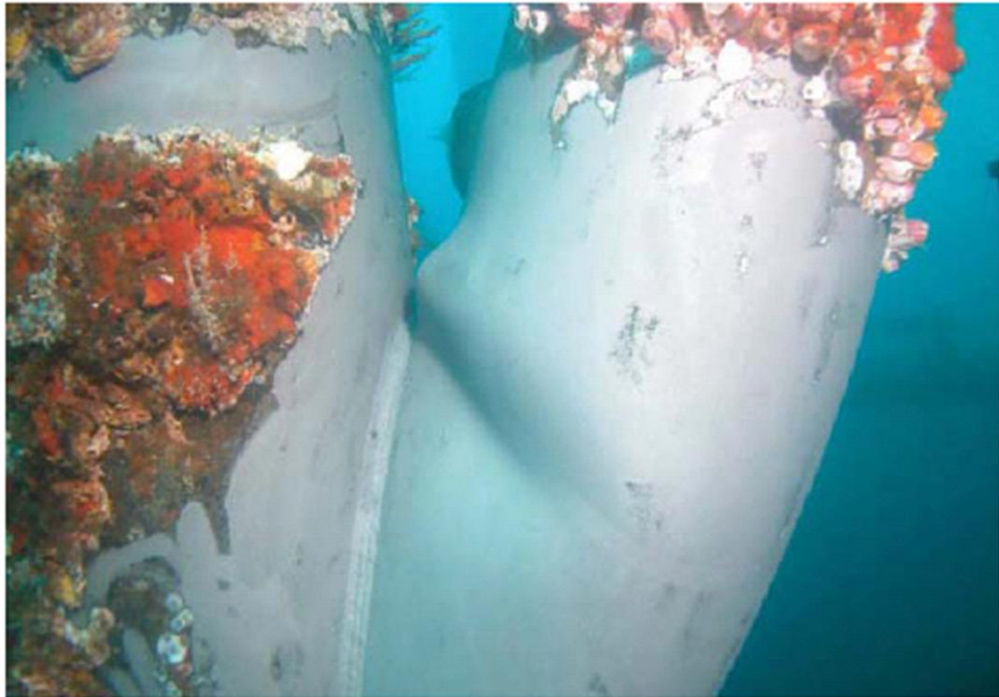


Figure 1.6 Buckled Underwater Brace of a Platform

1.2. Methodology

The project was contracted to the Offshore Technology Research Center (OTRC) at the University of Texas at Austin (UT), under Contract Number M08PC20002 by the Minerals Management Service (MMS) and Contract Number 2007-103130 by the American Petroleum Institute (API). Energo Engineering, Inc. (Energo) was sub-contractor assisting OTRC in the effort of collecting and interpreting platform data. The project started in the spring of 2008.

This project was carried out through data collection, qualitative analysis, quantitative analysis, design and assessment implications and expert panel discussions. Platform data compiled in this project were obtained primarily from the industry. MMS also provided platform data in a confidential format from the post-hurricane assessments submitted by various operators. All available platform data were compiled for the qualitative analysis, which was intended to identify relevant trends for the performance of platforms and their foundations in major hurricanes. The qualitative analysis also served as a screening tool to identify those platforms that potentially experienced hurricane loads close to or beyond their original design capacities for detailed quantitative analyses. The quantitative analyses involved estimating the capacities of the foundation systems using simplified plastic collapse models. Three-dimensional (3-D) finite-element models (FEMs) of the structures and their foundations were also developed to perform hindcast and pushover analyses of selected platforms. The results from the quantitative analyses were synthesized into guidelines for assessments. An expert panel meeting was convened on March 23, 2009 to discuss the findings from this project and solicit input from the expert panel including experienced or knowledgeable members of industry and academia. The guidance from the expert panel was incorporated in this report.

1.3. Structure of the Report

The structure of this report is summarized below.

- Chapter 1 Introduction: The motivation, objectives and methodology for this project are presented.
- Chapter 2 Background Information on Pile Foundations: The practice for designing offshore pile foundation, a discussion of potential sources of conservatism in design,

and the historical performance of piles in hurricanes are provided. The API design method is provided in Appendix A.

- Chapter 3 Case Study Platforms: The database compiled for available platforms where the foundation was tested in a hurricane is presented, and the use of this database to select case study platforms for detailed quantitative analysis is described. The database is provided in Appendix B.
- Chapter 4 Quantitative Analyses: The methodology used to analyze the performance of case study platforms is explained with details included in Appendix C (3-Dimensional Finite Element Method model) and Appendix D (simplified plasticity model).
- Chapter 5 Findings: The major findings from this project are presented with the detailed quantitative analyses that support these findings included in Appendix E.
- Chapter 6 Practical Guidelines for Platform Assessments: Guidelines for how foundations are treated in platform assessments are provided and illustrated. The notes from an expert panel meeting that contributed to formulating these guidelines are included in Appendix F.
- Chapter 7 Conclusions and Recommendations: Conclusions and recommendations are summarized.
- Chapter 8 References: The list of references is provided.

2. Background Information on Pile Foundations

The foundations used for jacket platforms in the Gulf of Mexico are driven piles made of steel pipes (referred to as steel pipe piles or simply piles throughout this report). The practice for designing these piles, a discussion of potential sources of conservatism in design, and the historical performance of piles in hurricanes are provided in this chapter.

2.1. Pile Foundation Design Practice

The design of offshore piles has been guided by API RP 2A for the past 40 years. The most recent version of the foundation design methodology provided in this guidance document, API RP 2A-WSD (2000), is included in Appendix A for reference. The basics are summarized in this section to provide context for the analyses and discussions presented throughout this report.

The design method is for individual piles and considers axial and lateral loading. For axial loading, the resistance of the pile is divided into side shear (or friction) acting along the external wall of the pile over its length and end bearing acting at the tip of the pile. While the piles are open-ended pipes, they generally behave as plugged after set-up so that the end bearing acts over the gross area of the pile tip. The side shear and end bearing resistances require displacement of the pile in the soil to be mobilized. The relationship between side shear and displacement is characterized by a t - z curve (t is unit side shear and z is axial displacement between the pile wall and the soil), while the relationship between end bearing and displacement is characterized by a Q - z curve (Q is end bearing and z is tip displacement). Side shear can act in both directions, i.e., a pile pushing down in compression or pulling up in tension, while end bearing is generally assumed to only act in compression. For a typical pile, the majority of the axial capacity comes from the soils in the lower third of the pile length. For lateral loading the resistance of the pile versus lateral displacement is characterized by a p - y curve (p is the unit lateral resistance and y is the lateral displacement). Cyclic loading during a storm can degrade the lateral resistance due to disturbance of the soil and even a gap possibly opening up between the pile and the soil. Therefore, two sets of p - y curves are provided for design, one for static loading and one for cyclic loading. The more conservative cyclic p - y curves are generally used for design with hurricane loading. For a typical pile, the majority of the lateral

capacity comes from soils in the upper 50 feet of the pile length.

The types of soils are divided into two broad categories: cohesive soils and cohesionless soils. In the Gulf of Mexico, cohesive soils are made up primarily of marine clays that were deposited as sediment dropping through the water column. Since these soils drain relatively slowly under loading during a hurricane, they are characterized by their undrained shear strength (c) for pile design. The undrained shear strength is typically measured in the laboratory using samples of soil that are obtained from a soil boring. These samples have been typically obtained by driving or pushing a sampling tube (2.5-inch outside diameter liner sampler) depending on whether the weight of the percussion sampler is sufficient to push the sampler into the formation. As such, these samples can be relatively disturbed and exhibit undrained shear strengths that are generally lower than those in situ. The liner sampler was, and today still is, used to obtain normally consolidated soft clay (or until the undrained shear strength increases to 250 to 300 psf). Occasionally, the samples have been obtained with a large diameter (e.g., 4-inch diameter) piston sampler. These samples are less disturbed and exhibit higher undrained shear strength. Also, the undrained shear strengths have been obtained by performing in situ testing, such as field vane and piezocone penetration tests, in the soft clay. The undrained shear strengths from in situ testing are generally higher than those from laboratory tests on relatively disturbed samples. This difference in sampling and testing has been implicitly accounted for by the geotechnical engineers who develop a design profile of undrained shear strength versus depth for pile design. The in situ undrained shear strength generally increases linearly with depth below the mudline, at a nominal rate of about 7~10 psf/ft, in the Gulf of Mexico. When a pile is driven, the soil is disturbed and the undrained shear strength is reduced. Over a period of several weeks to months after driving, the undrained shear strength increases back to approximately the undisturbed value. The axial side shear, end bearing and the lateral soil resistance are roughly proportional to the undrained shear strength for a clay layer. The t - z curves for clays generally exhibit strain-softening; the peak unit side shear is mobilized at about 0.4 inch of displacement for typical offshore driven pipe piles and then drops off to a value that is about 0.8 times the peak at larger displacements. For the relatively long and slender piles that are used for jacket platforms, the maximum total side shear that can be mobilized is less than the peak value and generally closer to the residual on average because the axial flexibility of the pile results in mobilizing the peak strengths along the pile at different times. The cyclic p - y curves in clay limit the lateral resistance to about 70 percent of the peak value that is available for static loading.

Cohesionless soils on the shelf in the Gulf of Mexico are generally made up of alluvial (or fluvial) sands that were deposited by rivers during times when the shelf was exposed due to lower sea levels. Since these cohesionless soils drain relatively quickly under loading during a hurricane, these soils are characterized by their drained shear strength, expressed as an internal friction angle (ϕ'), for pile design. The internal friction angle increases with density and with particle size. The internal friction angle has generally been estimated from the number of blows required to drive a sampling tube (essentially a small diameter, open-ended pipe) into the sand. One challenge that arises frequently is that the sampler meets refusal, meaning that it cannot be driven through the sand and greater judgment is needed to estimate ϕ' . The axial side shear is related to the interface friction angle between the sand and pile wall (δ), which is nominally assumed 5 degrees less than the internal friction angle of the sand, ϕ' . The axial side shear is also related to the lateral stress acting on the pile wall, which is expressed as K times the effective vertical overburden stress, where K is assumed to be 0.8 for driven steel pipe piles in the Gulf of Mexico. At depth, approximately 50 to 100 feet below the mudline, the design method constrains the unit side shear to a maximum or limiting value that is also related to ϕ' (the larger ϕ' , the larger the limiting side shear). The t-z curves for sands do not exhibit strain softening. The axial end bearing for sands is also related to ϕ' and is constrained by a maximum or limiting value that is relevant for typical platform piles that are greater than 100 feet in length. Again, the limiting end bearing increases with increasing ϕ' . The ultimate lateral resistance in sands is also related to ϕ' . The lateral resistance corresponding to cyclic loading is also less than that corresponding to static loading. However, the difference is less pronounced for sands than for clays.

A summary of the design parameters for cohesive and cohesionless soils is provided in Table 2.1.

Generally, the axial pile capacity in sand is much higher than the capacity in clay. In a complex soil stratigraphy, such as one with interbedded layers of sand and clay, the pile capacity is assumed to have a smooth transition near the artificially defined layer boundaries. Common practice is to assume that the axial pile capacity in sand cannot be fully mobilized until the pile penetrates a distance of 3 pile diameters into the sand layer. Also, the axial pile capacity is assumed to decrease at a distance of 3 pile diameters above the underlying clay layer. In these transition zones, the axial pile capacity is assumed to vary linearly between the value corresponding to the clay layer above or

below the sand layer and the value corresponding to the sand layer where the capacity is fully mobilized. If the thickness of the sand layer becomes thin enough such that entire layer is within the transition zones, the design parameters are usually downgraded. Also, if there are a few thinly interbedded sand and clay layers, they are usually lumped into a single layer. Offshore geotechnical engineers commonly recommend a design undrained shear strength profile for end bearing capacity calculation and design parameters of sand (K , δ and f_{lim}) for side shear capacity calculation in this layer, which can potentially be conservative as discussed in Section 2.2.

Table 2.1 Design Parameters for Cohesive (Clay) and Cohesionless (Sand) Soils

Design Parameters for Clays	
Parameters	Typical Units
Submerged Unit Weight, γ'	kips-per-cubic-foot (kcf)
Undrained Shear Strength, c	kips-per-square-foot (ksf)
Reference Strain, ϵ_c	dimensionless
Design Parameters for Sands	
Parameters	Typical Units
Submerged Unit Weight, γ'	kips-per-cubic-foot (kcf)
Coefficient of Lateral Earth Pressure, K	Dimensionless
Soil-pile Interface Friction Angle, δ	Degrees
Limiting Skin Friction, f_{lim}	kips-per-square-foot (ksf)
Bearing Capacity Factor, N_q	Dimensionless
Limiting Unit End Bearing, q_{lim}	kips-per-square-foot (ksf)
Initial Modulus of Subgrade Reaction, k	kips-per-cubic-inch (kci)
Internal Friction Angle, ϕ'	Degrees

2.2. Potential Sources of Conservatism in Foundation Design

The foundation design methodology is intended to produce pile foundations that are fit for purpose and is not necessarily intended to predict the actual capacity of piles in a hurricane. The challenge is that there is a great deal of uncertainty in estimating pile capacity under both axial and lateral loading. In order to account for this uncertainty in design, there are numerous assumptions made in design practice that tend to be conservative so that uncertainty does not lead to an unexpected failure. These

assumptions are implicit in the design practice and act in addition to the design factor of safety that is applied to the design capacity.

The following summary of these potential sources of conservatism draws heavily upon the following references: Tang and Gilbert (1992), Murff et al. (1993), Pelletier et al. (1993), Aggarwal et al. (1996) and Bea et al. (1999). Hurricanes Andrew (1992) and Roxanne (1995) provided the primary motivation for documenting this information.

1. Availability of Site-specific Geotechnical Data: When assessing older platforms, site-specific geotechnical data are often unavailable due to various reasons including the time elapsed between the original constructions and current assessments, change of ownership, confidentiality issues, record keeping practice and historical design practice. Even when a site-specific boring is available, it is rarely exactly at the location of the platform and may not reflect variations in subsurface conditions over the length and width of the structure. On the shelf where most jackets are located, the soil stratigraphy tends to be more variable than in deeper water due to interbedded sands and clays and clay layers that may have been desiccated due to exposure when sea levels were lower. In areas with alluvial (fluvial) sand deposits, this variability is particularly pronounced due to the complex geometry from channels that meandered and cut across one another. In order to account for this uncertainty due to spatial variability, design profiles for shear strengths tend to reflect conservatism and are not necessarily the best guess or median value for strength based on the boring data alone.
2. Sampling and Testing Methods for Site Investigations: Sampling and testing methods can have a significant effect on the determination of the engineering properties of soils. Sampling methods have improved over time, meaning that it is not possible to compare directly data from older soil borings with those from newer soil borings. Specifically, driven samples were used to characterize the undrained shear strength of clay layers before about 1980, while pushed samples and in situ methods have been used since. Likewise, driven penetration methods were used to characterize the density and shear strength of sand layers until very recently when more modern Cone Penetration Tests were performed. Uncertainty in the in situ properties of the soil was therefore greater historically, leading to more conservative design assumptions for the vast majority of platforms on the shelf.

3. As-built Conditions of Foundation: The as-built conditions of the foundations may be different from those planned for or assumed in design. For example, pile driving records sometimes show that the as-built pile lengths are different among the piles at the same platform and different from the design pile length, most likely due to denser soils that cause refusals of some piles. These as-built conditions may be significant because the axial capacity of the piles can be higher than expected. Also, the pile wall thickness schedules may be different from those in the design drawings due to pile refusals, which may change the lateral capacity of the piles. Sometimes, jetting or drilling out the pile plugs is performed to advance the piles to the design penetration. These processes can reduce the axial capacity of the piles. The annulus between the pile and jacket leg may be grouted. The grouting connects the pile and jacket leg structurally and increases the effective moment capacity of the pile near the mudline. These details can only be found in the as-built (record) drawings, which are therefore important in assessing the capacity of the foundation. Construction records are often difficult to locate for older platforms, especially after the ownership of the platforms has changed. The foundation conditions may also change with time. For example, scour and subsidence of soils around the foundation may decrease its capacity.

4. Time Effects: Long-term set-up or aging for piles installed in clays and sands may increase the foundation capacity with time. The design method is intended to estimate the capacity after short-term set-up (dissipation of driving-induced pore water pressures), which generally occurs within several months after driving. However, both laboratory and field data suggest that the axial side shear capacity of a driven pile can continue to increase for years after driving (e.g., Seed and Reese 1957; Vijayvergiya et al. 1977; Randolph et al. 1979; Chow et al. 1996; Bogard and Matlock 1998; and O'Neill 2001). This evidence suggests that the increase in side shear capacity several years after driving in clay and sand layers could be as much as a factor of two greater than the value used in design. In addition, the ultimate lateral resistance of the soil can increase with time due to periods of cyclic loading and unloading that can occur over the lifetime of the platform when it is subjected to storm events. Jeanjean (2009) provided data indicating that the ultimate lateral resistance in a clay could be as much as 50 percent greater after repeated cycles of loading and unloading due to reconsolidation of the clay. These potential long-term increases in capacity are not included in design.

5. Rate-of-loading Effects: The design values for axial and lateral capacity are representative of a static load applied over a time duration of several minutes to hours. However, the maximum load in a hurricane will be applied over seconds. The strength of the soil and therefore capacity of the pile will tend to increase with increased loading rate, and could lead to actual capacities that are as much as 100 percent greater than design values (Bea et al. 1999).
6. Strain-softening and Cyclic Degradation: Strain-softening and cyclic loading can cause degradation of the undrained shear strength of clay. These effects, which tend to reduce axial and lateral capacity, are generally included in design. If these degradation effects are not as severe as assumed in design, then the actual capacities will be greater than the design values.
7. Limitations of Design Databases: The design methods were developed from pile load tests on driven piles that were generally much smaller than those used in practice. The published data used to develop the API design methods consist of axial load tests on piles with capacities that average hundreds of kips (e.g., Najjar 2005), while most pile foundations for jacket platforms have design capacities that are thousands of kips. Therefore, significant extrapolation is required to predict the behavior of large offshore piles from these test data. Conservatism is potentially introduced in estimating axial capacity in clay layers where strain-softening is assumed for the long offshore piles (strain softening would have less of an effect for shorter piles). It is potentially introduced in estimating axial capacity in sand layers where limiting values for side shear and end bearing govern the capacity for long offshore piles (these limiting values would have less of an effect for shorter piles). Several sets of data produced since the p-y curves were developed for API RP 2A, including Stevens and Audibert (1979), Murff and Hamilton (1993), Randolph and Houlsby (1984) and Jeanjean (2009), suggest that static and cyclic p-y curves for soft clays may be stiffer and exhibit ultimate resistances that are at least 30 percent greater compared to the curves used in design. The conservatism in design is at least partially motivated by the relatively large uncertainties in environmental loads and pile capacities and the fact that a factor of safety of only 1.5 is used for extreme loading.
8. Engineering Practice for Thinly Interbedded Sand and Clay Layer: Offshore geotechnical engineers historically recommended a design undrained shear strength

profile for end bearing capacity calculation and design parameters of sand (K , δ and f_{lim}) for side shear capacity calculation for a layer with thinly interbedded sand and clay. In reality, the end bearing capacity of piles tipping in this layer is probably between the values calculated assuming that the piles are tipping in either sand or clay. The practice of assigning a design undrained shear strength profile for end bearing capacity calculation is conservative because the end bearing capacity of piles in sand is much higher than the end bearing capacity in clay. As a result, the axial capacity of piles in a geological setting with complex soil stratigraphy can potentially be underestimated.

9. Design Practice for Foundation versus Structure: Typically, jacket foundations are designed for first pile failure. In other words, the piles are sized based on the most critically loaded pile. One pile design is often applied for all the piles supporting a jacket structure; in some cases, there may be up to two different pile designs for a structure. On the contrary, structural members are usually designed and sized separately based on the expected forces in each member considering the entire structural system. Therefore, structural members are usually more optimized than piles and the potential conservatism due to the design practice for piles is higher than that for the structure.

In summary, there are numerous sources of uncertainty involved in estimating the capacity of offshore piles, and this uncertainty has understandably led to a conservative design method. Factors that could reduce the capacity are generally included in design, while factors that could increase the capacity are generally neglected in design. Therefore, a failure is not necessarily expected if a pile foundation is loaded to its design capacity, particularly for piles loaded axially in sand layers and laterally in clay layers. However, it would also be surprising if the axial or lateral capacity of a pile foundation were much more than twice the design value.

2.3. Historical Performance of Platform Foundations in Hurricanes

Previous studies have investigated the performance of pile foundations for offshore platforms subjected to hurricane loads. Aggarwal et al. (1996) describe a detailed analysis of offshore platforms that were subjected to large loads in Hurricane Andrew (1992). They analyzed three jackets that survived without any indication of damage to the pile

foundations. They inferred from these analyses that there was a conservative bias in the lateral capacity of the foundation system, with the actual capacity being between 1 and 1.3 times the design capacity. They also inferred a conservative bias in axial capacity of the system, with the actual capacity being between 1.5 and 1.7 times the design value. A notable qualification of these conclusions however is that the foundation systems in all three cases were not actually loaded to their design capacity. The inference of conservatism was based on the premise that given variability in the actual capacity, there is a possibility of system failure when the system is loaded to less than its expected (or design) capacity but none of these three systems failed.

Bea et al. (1999) performed a similar analysis for offshore platforms subjected to large loads in Hurricane Roxanne (1995). They also concluded that there was a conservative bias in foundation design, with actual pile capacities being about two times the design values. Again, to our knowledge, this inference is not based on any structures where the load was equal to or greater than the design capacity of the foundation

3. Case Study Platforms

The performance of case study platforms where the capacity of the foundation was tested in a hurricane is the focus of this project. In order to select case study platforms for detailed analysis, a database was first compiled and screened for candidate platforms. A description of this screening assessment and the selected platforms is provided in this chapter.

3.1. Screening Assessment

A qualitative evaluation was performed to identify relevant trends for the performance of platforms and their foundations in major hurricanes. It also served as a screening tool to identify those platforms that potentially experienced hurricane loads close to or beyond their original design capacities. The qualitative evaluation was performed through the collection of platform data, review of platform data, compilation of a platform database and evaluation of the database to identify relevant trends for the performance of platforms and their foundations.

A database of platforms evaluated for this project is provided in Appendix B. This information was obtained primarily from the industry (Energo 2006 and 2007, GEMS 2008 and PMB 1993 and 1995). MMS also provided platform data in a confidential format from the post-hurricane assessments submitted by various operators. The database includes 30 platforms that experienced hurricanes Andrew, Ivan, Katrina, Rita and Ike. The following information was compiled for each platform:

- Hurricane Exposure Event(s)
- Number of piles
- Length of piles
- Age of piles
- Soil stratigraphy including the tip bearing stratum
- Sampling and testing methods used to develop geotechnical design parameters
- Water depth
- Number of well conductors
- Approximate ratio of the maximum wave height during the hurricane(s) to the

design wave height

- Expected mode of failure for the piles

The maximum wave heights (H_{\max}) that occurred at the platform locations during hurricanes were estimated from proprietary hindcast studies that were provided to us by MMS. The design wave heights for most of the older platforms are not known because the design practice was not standardized until the 1970's. Even for the platforms installed after the 1970's, the design wave heights are sometimes unknown because detailed design records were lost after the transfers of ownership. In order to provide an indicator of the design wave height (H_{dgn}), the design wave height for each of the platforms was determined using the present-day sudden hurricane wave height criteria that are used in the ultimate strength assessment for a low consequence/ manned-evacuated platform (API Section 17 A-2). Because the base shear of a platform is approximately proportional to the square of the maximum wave height, a ratio of $(H_{\max}/H_{\text{dgn}})^2$ was calculated for each platform to provide a rough indication of how much a platform was overloaded (relative to API Section 17 A-2 criteria) during a particular hurricane. Platform foundations that experienced hurricane loads greater than their original design capacities and unexpectedly survived the hurricane loads are of particular interest in this project.

The platforms are mostly 4 or 8-pile platforms. The length of the piles ranges from 135 to 400 feet. The age of the piles between their installation and the hurricane events ranges from 5 to almost 50 years. The majority of the piles are embedded in interbedded layers of sand and clay. The bearing stratum at the tip of the piles ranges from fine sand, silty fine sand, sandy silt to clay. The most common sampling method utilized in the subsurface explorations is the wireline percussion technique, with a thin-walled sampler driven by a 175-pound hammer falling approximately 5 feet. Water depth at the platform locations ranges from 60 to more than 1,000 feet; however, most of the platforms are located in a water depth of 200 feet or less. The number of well conductors ranges from none to as many as 40. The ratio $(H_{\max}/H_{\text{dgn}})^2$ ranges from 0.7 to 1.6, with the majority having values greater than one.

3.2. Platforms Selected for Quantitative Analyses

The list of platforms selected for detailed quantitative analyses is presented in Table 3.1. The factors involved in the selection of these platforms included:

- High probability of platform foundations being loaded beyond their original design capacities in a hurricane
- Availability of information about how the platform performed in the hurricane
- Availability of detailed geotechnical data
- Availability of detailed structural drawings to develop foundation models
- Availability of detailed structural analyses (3-D FEM pushover analyses) to compare with foundation analyses
- Availability of the hindcast loading information, such as the wind, wave and current conditions at the platform locations to estimate the hindcast base shear and overturning moment acting on the foundation systems

The greatest challenge in selecting platforms was the availability of information about how it performed in a hurricane. Unfortunately, this information is not available for platforms that were destroyed because detailed post-hurricane assessments are not conducted for these structures. Consequently, we have little if any information about how a platform failed, such as in the foundation versus in the jacket, for platforms that were destroyed. Therefore, the focus in this study is on platforms that were loaded heavily and survived the hurricane.

The availability of geotechnical, structural and hindcast information often determined whether a platform was selected for the detailed quantitative analysis. The information of these platforms was obtained almost entirely from the industry (Energo 2006 and 2007 and GEMS 2008). These platforms experienced either Katrina or Rita in 2005 or Ike in 2008. They are mostly 4-pile platforms with some 3-, 6- and 8-pile platforms. Most of them are older platforms installed in the 1960's and 1970's; few of them were installed in the last two decades. The pile foundations of these platforms are mostly tipping in the sand layers (sandy silt, silty fine sand, fine sand and sand), with a few of them tipping in the clay layers (clay, silty clay and interbedded clay and silty fine sand). These platforms are located in relatively shallow water with a maximum water depth of approximately 360 feet. Most of them are equipped with well conductors ranging from one 72-inch diameter conductor to 18 smaller conductors with a diameter between 20 and 30 inches. One of the 4-pile platforms has no conductors.

Table 3.1 Case Study Platforms Selected for Detailed Quantitative Analyses

Platform Database No.	Hurricane Exposure Event(s)	Number of Piles	Length of Piles (ft)	Year of Installation	Age of Piles	Soil Stratigraphy	Tip Bearing Stratum	Water Depth (ft)	Number of Well Conductors
1	Katrina	8	135	1965	40	Stratum 1: very soft to firm clay (90') Stratum 2: fine sand (12') Stratum 3: firm clay (12') Stratum 4: interbedded sandy silt and firm silty clay (19') Stratum 5: sandy silt (10') Stratum 6: silty fine sand (10')	Stratum 5: sandy silt	140	18
2	Katrina	6	140	1966	39	Stratum 1: very soft to firm clay (90') Stratum 2: fine sand (12') Stratum 3: firm clay (12') Stratum 4: interbedded sandy silt and firm silty clay (19') Stratum 5: sandy silt (10') Stratum 6: silty fine sand (10')	Stratum 5: sandy silt	140	12
8	Katrina	4	274	1984	21	Stratum 1: very soft to soft clay (30') Stratum 2: silty fine to fine sand (56') Stratum 3: interbedded firm to stiff clay and fine to silty fine sand (37') Stratum 4: firm to very stiff clay (56') Stratum 5: silty fine sand (101') Stratum 6: very stiff clay (52')	Stratum 5: silty fine sand	220	12
9	Katrina	4	118	1989	16	Stratum 1: silty fine sand (5') Stratum 2: firm clay (20') Stratum 3: silty fine sand (11') Stratum 4: fine sand (71') Stratum 5: interbedded very stiff clay and silty fine sand (44') Stratum 6: fine sand (50')	Stratum 5: interbedded very stiff clay and silty fine sand	60	1
10	Ike	3	220/ 265	2001	7	Stratum 1: very soft clay (11') Stratum 2: soft to hard clay (337')	Stratum 2: very stiff clay	360	1
11	Katrina	4	239/ 309	2000	5	Stratum 1: fine sand (9') Stratum 2: soft to firm clay (27') Stratum 3: fine sand (64') Stratum 4: stiff clay (8') Stratum 5: fine sand (9') Stratum 6: stiff to very stiff clay (6.5') Stratum 7: silty fine to fine sand (13.5') Stratum 8: stiff to very stiff clay (71') Stratum 9: silty fine to fine sand (73') Stratum 10: very stiff silty clay (7') Stratum 11: fine sand (27')	Stratum 9: silty fine to fine sand/ Stratum 11: fine sand	120	4
12	Rita	4	255	1972	33	Stratum 1: stiff to firm clay (37.5') Stratum 2: medium dense silty fine sand grading to clay silt below 56' (34.5') Stratum 3: stiff to very stiff clay (144') Stratum 4: very dense (silty) fine sand (100') Stratum 5: very stiff clay (25') Stratum 6: very dense sandy silt (15') Stratum 7: very stiff clay (N/A)	Stratum 4: very dense (silty) fine sand	190	12
22	Rita	4	290	1976	29	Stratum 1: very soft to firm clay (106') Stratum 2: silty fine sand (21') Stratum 3: stiff clay (13.5') Stratum 4: silty fine sand (27.5') Stratum 5: stiff clay (49.5') Stratum 6: laminated stiff clay and silty fine sand (27.5') Stratum 7: silty fine sand (26') Stratum 8: firm to stiff silty clay (69')	Stratum 8: firm to stiff silty clay	110	0
25	Katrina	4	169	1967	38	Stratum 1: firm clay (5') Stratum 2: medium dense silty fine sand (12') Stratum 3: firm to very stiff clay (146') Stratum 4: dense fine sand (>43')	Stratum 4: dense fine sand	90	4
27	Rita	4	264/ 281	2000	5	Stratum 1: very soft clay (14') Stratum 2: firm to stiff clay (86') Stratum 3: medium dense sand (15') Stratum 4: very stiff clay (>185')	Stratum 4: very stiff clay	300	2
29	Katrina	8	140	1967	38	Stratum 1: very soft to firm clay (75') Stratum 2: dense to very dense sand (80') Stratum 3: silty clay (5.5') Stratum 4: dense to very dense sand (N/A)	Stratum 2: dense to very dense sand	150	12
30	Katrina	6	210	1973	32	Stratum 1: very soft to firm clay (75') Stratum 2: dense to very dense sand (80') Stratum 3: silty clay (5.5') Stratum 4: dense to very dense sand (N/A)	Stratum 4: dense to very dense sand	150	12

4. Methodology for Quantitative Analyses

The objective of the quantitative analyses is to estimate the capacity of the foundation system and compare this estimate with the hurricane loading for each case study platform. Two models were used to estimate the capacity of the foundation system:

- a 3-dimensional finite element model that represents the state of practice for ultimate strength (pushover) analyses in platform assessment; and
- a simplified plasticity model of the foundation system that provides insight into the behavior of the foundation and facilitates sensitivity analyses due to its simplicity.

An overview for these models is provided in this chapter; detailed descriptions for the two models are included as Appendices C and D. Platform 1 (Table 3.1) is used throughout this section to illustrate and explain the models. Results from the two models are compared and discussed at the end of the chapter.

4.1. 3-Dimensional Finite Element Method Model of Platform Structure

Structural Analysis Computer Software (SACS™) was used to conduct 3-Dimensional Finite Element Method analyses of the case study platforms. SACS™ is a package of software developed by Engineering Dynamics, Inc. for use in both offshore structures and general civil engineering applications (Engineering Dynamics 2005). Use of this software was donated in-kind for this project by Engineering Dynamics, Inc. The inputs to this model are the structural properties of all members and connections including the piles, the behavior of the soil surrounding the piles (i.e., t-z and p-y curves as a function of depth along each pile and a Q-z curve at the tip), and the environmental loading including the magnitude and direction of waves, wind and current. The primary output from this model includes the total load on the structure, typically expressed as a base shear, the displacement of the deck, and the loads, moments and deformations in individual members. Details for this model are provided in Appendix C, as well as Engineering Dynamics (2005).

To illustrate, the structural model for Platform 1 developed in SACS™ is shown in Figure 4.1 and the geotechnical design information used to estimate pile capacity and establish

t-z, Q-z and p-y curves is shown in Figure 4.2.

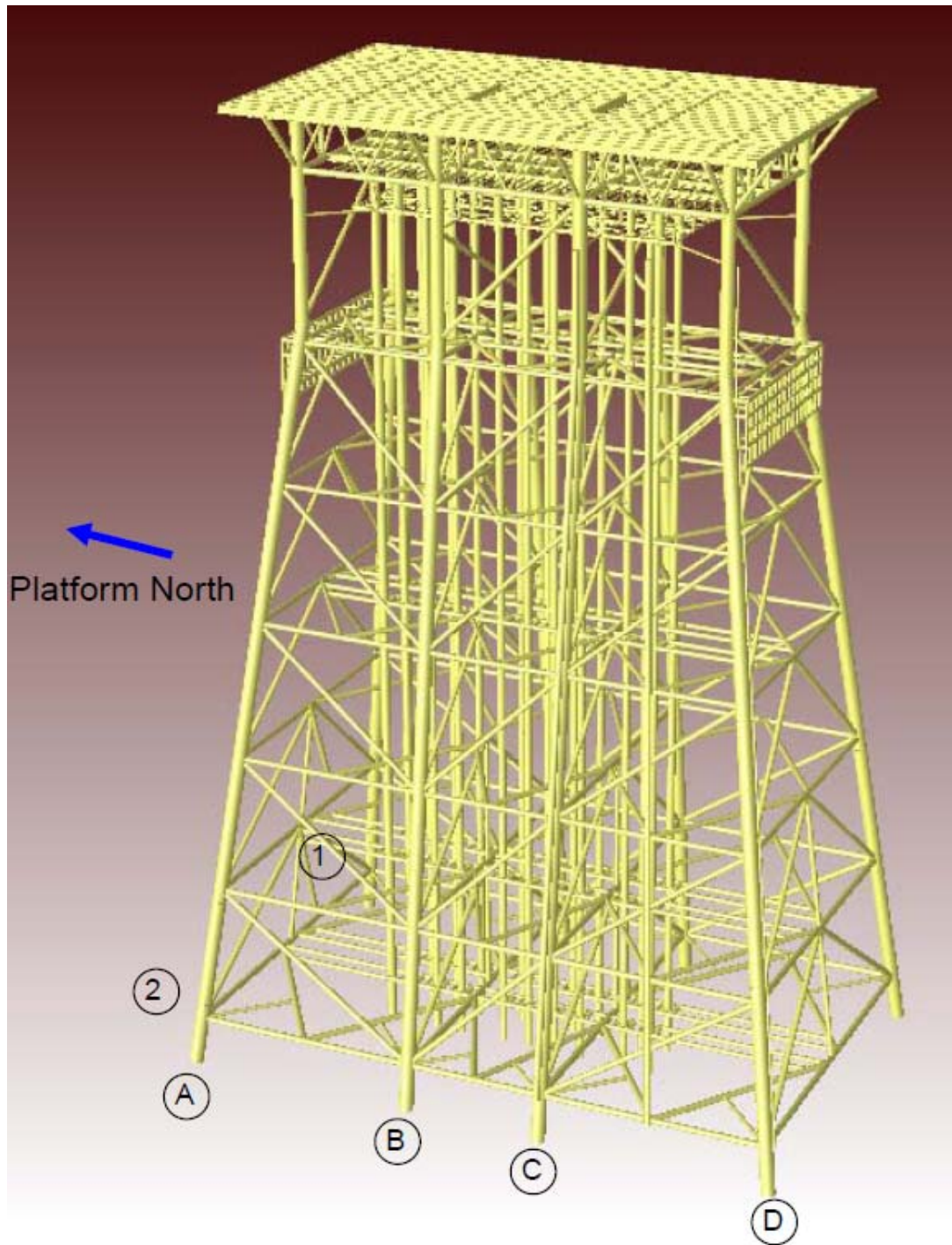


Figure 4.1 An Illustration of the SACS™ model for Platform 1 (Energo 2006)

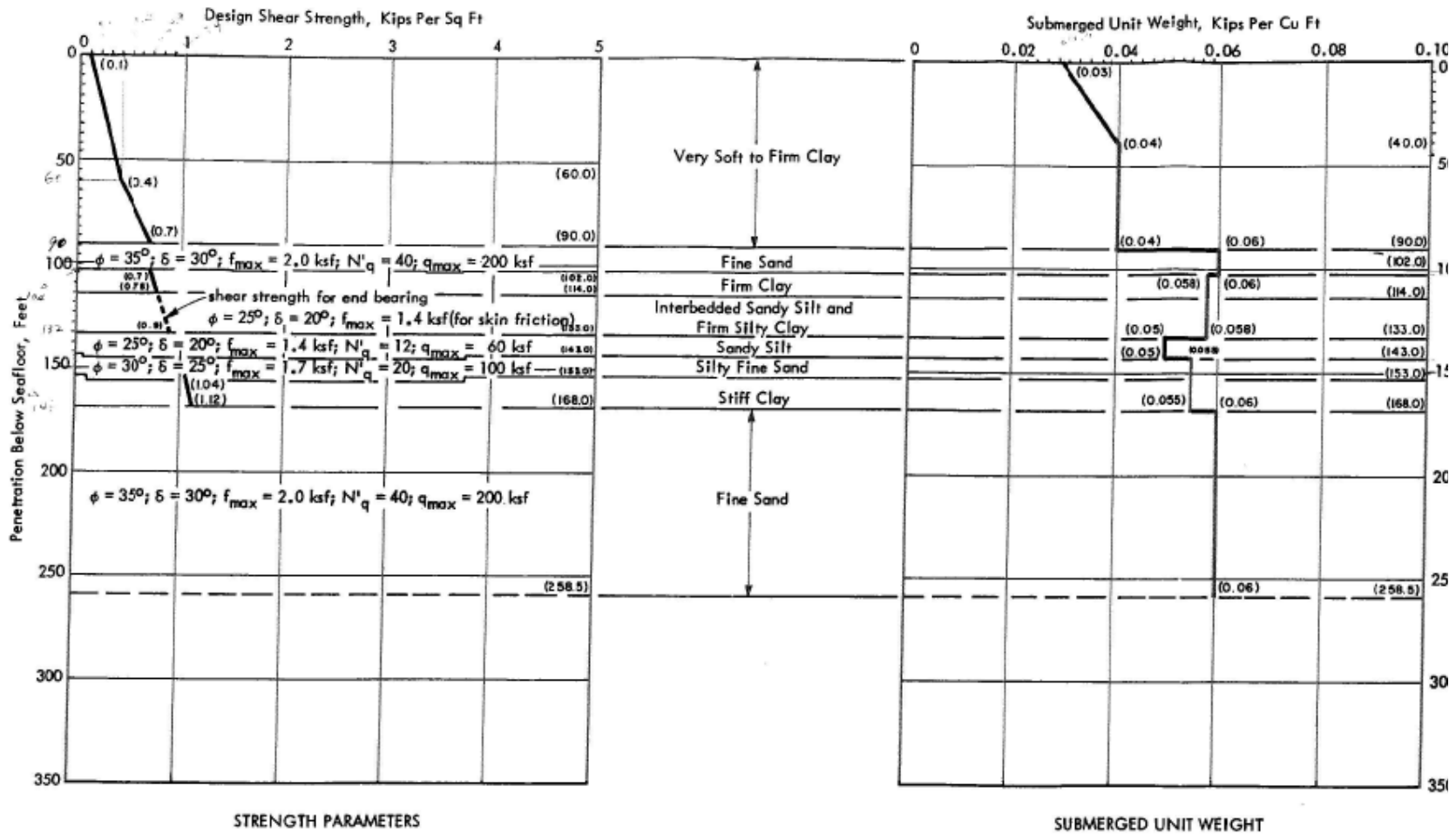


Figure 4.2 Recommended Geotechnical Design Parameters for Platform 1 (McClelland 1979)

The results of the pushover analysis to estimate the structural capacity for Platform 1 are summarized in Table 4.1 and Figure 4.3. This analysis corresponds to waves loading the platform in the end-on direction (toward Platform North in Figure 4.1), which was approximately the direction of waves in Hurricane Katrina. In the analysis, the total load on the structure from the combination of waves, wind and current is increased incrementally using a load factor to develop the relationship between deck displacement and base shear (the total horizontal force acting at the mudline). One challenge in a pushover analysis is to select a base load (the load at a load factor equal to one) such that the platform is on the verge of failure. The results of the analysis for Platform 1 (Table 4.1 and Figure 4.3) indicate that its capacity is reached at a load factor of 0.84 with a deck displacement of 32 inches, a base shear of 2,300 kips and an overturning moment of 215,000 ft-kips. The failure in the pushover analysis is attributed to an axial failure of piles in the foundation, which consequently causes the entire platform to collapse. Specifically, Piles A1 and A2 (Figure 4.1) first plunge and then Piles D1 and D2 pull out as the load is increased further.

Table 4.1 Output from the Pushover Analysis of Platform 1 in the End-On Loading Direction

Load Step	Load Factor	Base Shear (kips)	Overturning Moment (ft-kips)	Deck Displacement (in.)
5	0.19	521	48544	23
10	0.41	1125	104752	6
15	0.58	1591	148186	10
20	0.69	1893	176290	14
25	0.79	2167	201840	27
27	0.84	2305	214614	32
28	0.86	Platform collapsed – numerical analysis did not converge		

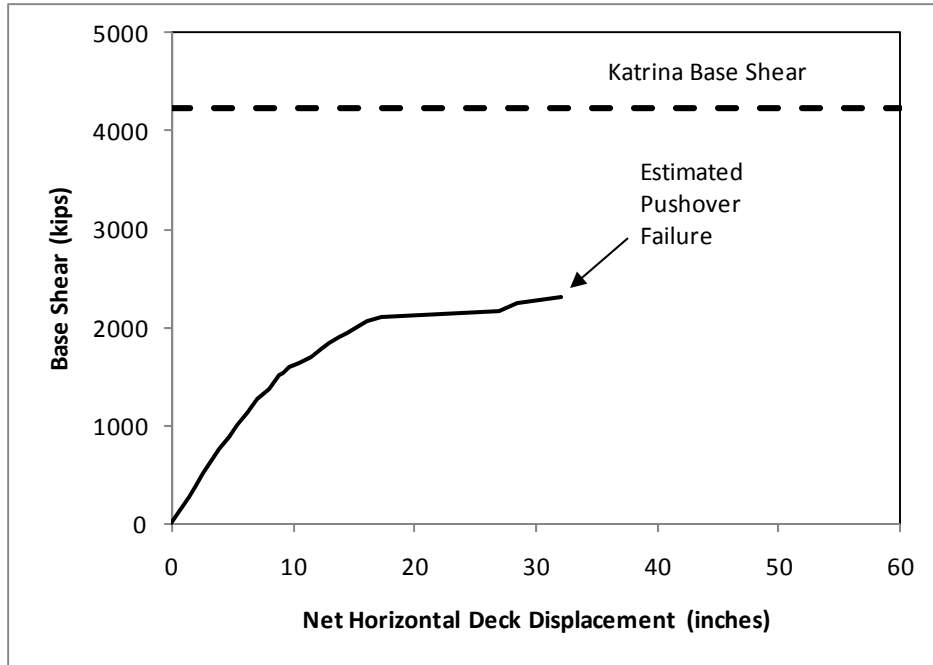


Figure 4.3 Base Shear versus Deck Displacement for Platform 1 in the End-On Loading Direction

For comparison, SACSTM is also used to estimate the hurricane loads to which Platform 1 was subjected in the end-on direction based on hindcast data from Hurricane Katrina (Table 4.2). This analysis indicates that the platform experienced a base shear of approximately 4,000 kips (Table 4.2). As shown on Figure 4.3, the hindcast load is significantly greater than the estimated platform capacity, which was governed in the pushover analysis by the foundation capacity. This platform survived Hurricane Katrina, making it a useful case study platform to explore potential conservatism in foundation design.

Table 4.2 Environmental Load Parameters for the Hindcast Analysis of Platform 1

Platform	Wave Height (ft)	Wave Period (sec)	Wind Speed (knots)	Current Velocity (knots)	Vertical Load (kips)	Base Shear (kips)	Overturning Moment (ft-kips)
Platform 1	58.7	16.1	68.9	1.9	2500	4053	362323

4.2. Simplified Plastic Collapse Model of the Foundation

The simplified plastic collapse model uses an upper-bound kinematically admissible

solution to define the combinations of base shear and overturning moment that cause the complete collapse of the foundation system (Murff and Wesselink 1986). The upper-bound method assumes a plastic collapse mechanism, where all elements of resistance are characterized as rigid and perfectly plastic (Murff 1987). The piles in the system collapse when one hinge forms at the pile head and a second hinge forms at some depth below the pile head. The collapse of the entire system occurs when two hinges form in each of the piles in the system, as shown schematically in Figure 4.4. The solution is an upper-bound approximation to the system capacity because it does not explicitly satisfy force and moment equilibrium. Also, the structure supported by the piles is assumed to be perfectly rigid. Comparisons between this upper-bound solution and more rigorous pushover analyses indicate that the upper-bound model overestimates the total horizontal force causing failure by about 10 percent (Murff and Wesselink 1986).

The original model developed by Murff and Wesselink (1986) and extended by Tang and Gilbert (1992) was updated for this study to incorporate multiple soil layers and pile wall thicknesses below the mudline. In addition, the contribution of well conductors to the foundation system capacity was included. The conductors are modeled as piles that are connected to the structure with rollers (Figure 4.5) such that the structure can move the conductors horizontally but not vertically (that is, the conductors contribute lateral resistance but not axial resistance to the foundation system). Details for this model are provided in Appendix D.

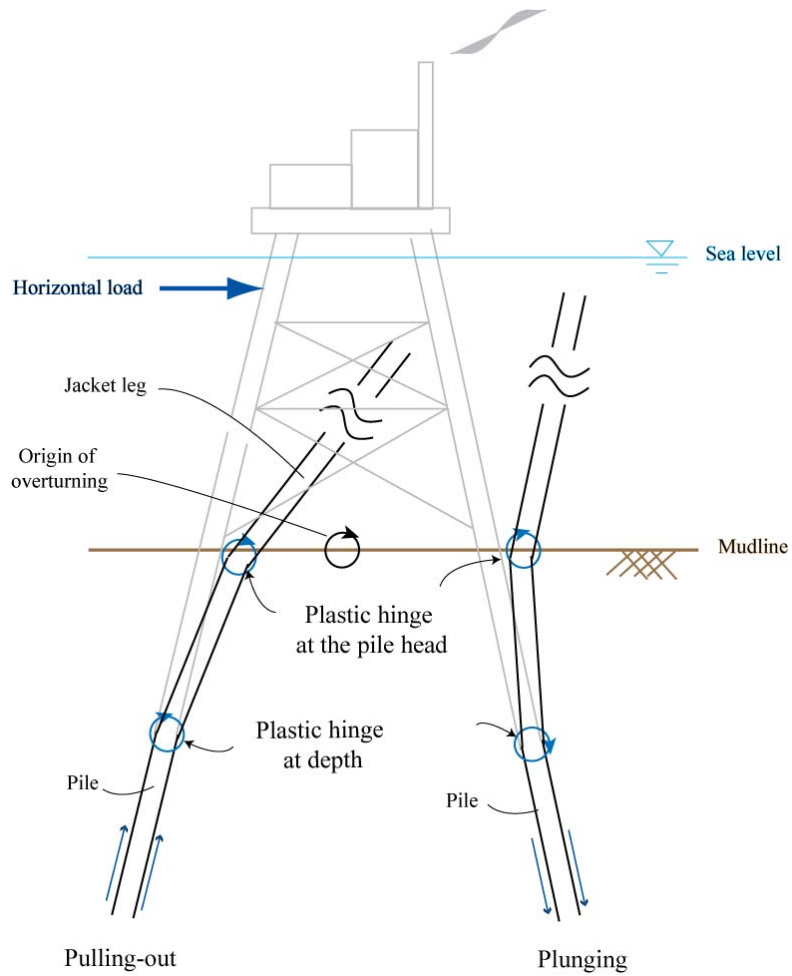


Figure 4.4 Schematic of Pile System Collapse Due to the Formation of Plastic Hinges (Lee 2007)

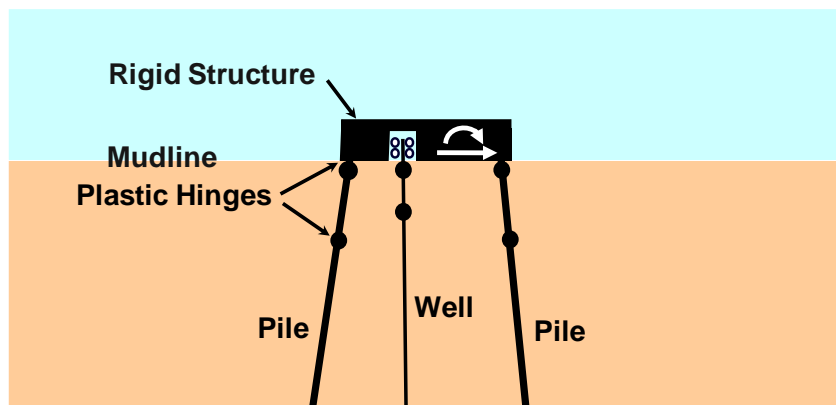


Figure 4.5 Schematic of the Updated Plastic Collapse Model for Piles and Wells

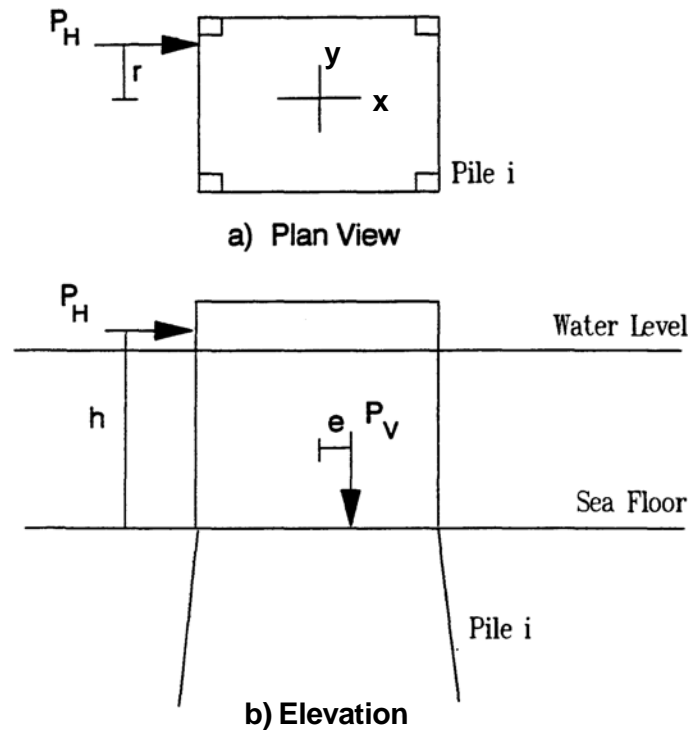


Figure 4.6 System Load Parameters for the Simplified Plastic Collapse Model (Tang and Gilbert 1992)

The inputs to the model are the loads on the foundation system (Figure 4.6), the geometry of the piles and conductors including locations and batters, the axial and lateral resistance versus depth for each pile and conductor, and the structural capacity of each pile and conductor. The critical horizontal collapse load (that is, base shear, P_H) of the foundation system at a specified moment arm above the mudline (h) is determined by varying the horizontal load such that the external work applied by the system load is equal to the internal work associated with the system capacity. A relationship between base shear and overturning moment (M) is developed from the combinations of the critical collapse load and its moment arm.

To illustrate, the foundation system capacity interaction curve for Platform 1 (Figures 4.1 and 4.2) in the end-on loading direction is shown in Figure 4.7. This interaction curve includes the contribution from the 8 piles as well as the 18 well conductors. The interaction curve is an envelope; for hurricane loads located within the envelope, the foundation system is expected to be stable. The first zone corresponds to the shear failure mechanism, which is the initial part of the interaction curve at a small overturning

moment. This part of the interaction curve slopes upward gently (increases in base shear with increasing overturning moment) because of pile batters. In this portion of the interaction curve, the capacity of the foundation system is governed by the lateral capacities of the piles and conductors. The other extreme at a large overturning moment corresponds to an overturning failure mechanism. This part of the interaction curve shows a steep downward slope (critical base shear decreasing rapidly with increasing overturning moment). In this portion of the interaction curve, the capacity of the foundation system is governed by the axial capacities of the piles. The zone between these two extremes on the interaction curve corresponds to a combination of shear and overturning (i.e., both lateral and axial capacities are contributing to total system capacity).

The foundation system capacity interaction curve essentially presents the foundation capacity for all possible scenarios of environmental load profiles (from a small moment arm to a large moment arm). On the contrary, a pushover analysis is typically performed using a given environmental load profile and scaling this load profile with a series of load factors until the platform collapses. In essence, the moment arm does not change throughout the pushover analysis. As such, the result of a pushover analysis is comparable to a point on the foundation system capacity interaction curve. The load path of a pushover analysis, if drawn on the interaction diagram, starts at the origin and follows a straight line leading to the interaction curve. The slope of this linear load path is the inverse of the moment arm.

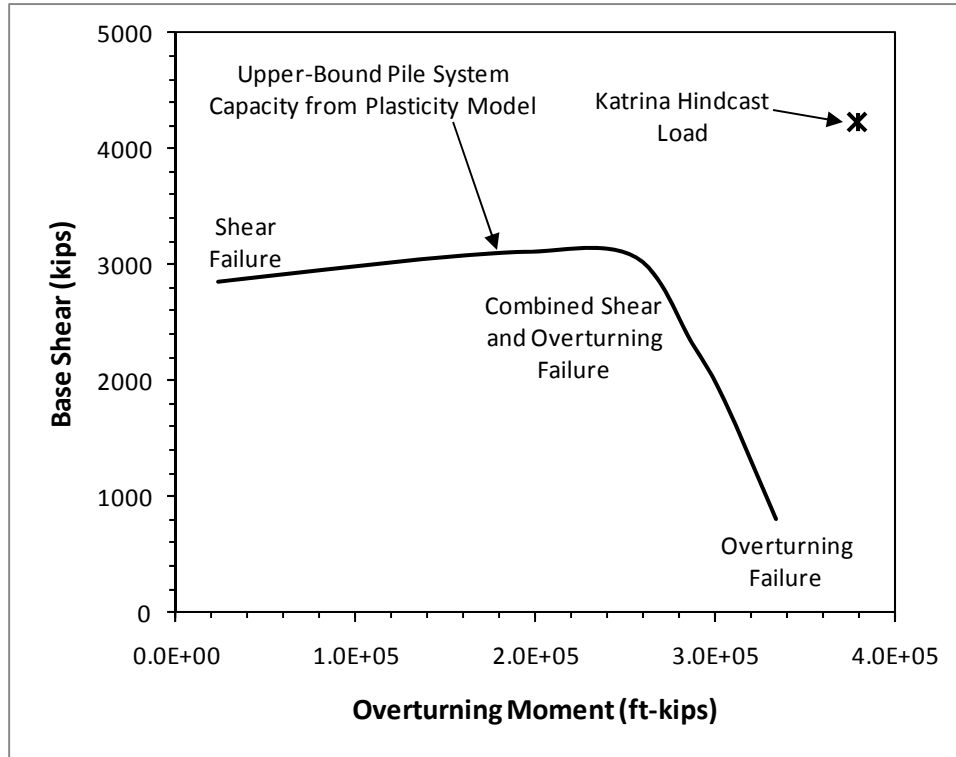


Figure 4.7 Foundation System Capacity Interaction Curve from Plasticity Model of Platform 1 in the End-on Loading Direction

As with the pushover analysis, the capacity can be compared to the hindcast loading. The maximum base shear and overturning moment applied by Hurricane Katrina in the end-on direction (Table 4.2) are plotted in Figure 4.7. As for the pushover analysis, the applied loading is significantly greater than the estimated capacity from the upper-bound plasticity model for this platform. Possible reasons for this discrepancy will be discussed in Sections 5.1.4 and 5.4.

4.3. Comparison of Results from Simplified Plasticity Model with 3-Dimensional Finite Element Method Model

While convenient for analyses, the simplified plasticity model is only useful if it provides a reasonable estimate of the foundation system capacity. The objective of this section is to compare the results from the simplified plasticity model with those from the more rigorous 3-Dimensional Finite Element Method model (SACSTM). Details of these comparisons are provided in Matarek (2009) and Carpenter (2009).

Platform 22 (Table 4.1) provides a convenient basis for comparison because it is a simple structure with 4 piles and no conductors. The results from the two models are compared on the capacity interaction curve in Figure 4.8. As expected and discussed previously, the simplified plasticity model provides an upper-bound solution and overestimates the load causing failure by about 10 percent (Figure 4.8). In order to account for this known bias, the horizontal load causing failure from the plasticity model is reduced by a factor of 0.9; the curve labeled “Estimated Pile System Capacity from Plasticity Model” in Figure 4.8 shows this adjustment. The adjusted capacity interaction curve from the plasticity model and the failure load from the pushover analysis compare well (Figure 4.8). In the pushover analysis, several joints above the foundation started to fail before the system capacity of the foundation was reached, possibly causing a “premature” foundation failure since the damaged structure was not able to redistribute load as effectively. In order to study this possibility, the pushover analysis was repeated by increasing the yield strength for the members in the jacket so that they did not fail before the foundation; this result is labeled “Failure Load from 3-D FEM Pushover Analysis with Strengthened Structure” in Figure 4.8. In this case, the results from the two models are nearly identical (within a few percent of one another). In all subsequent results for the simplified plasticity model presented in this report, the capacity interaction curve will be reduced by a factor of 0.9 to provide a reasonably unbiased estimate.

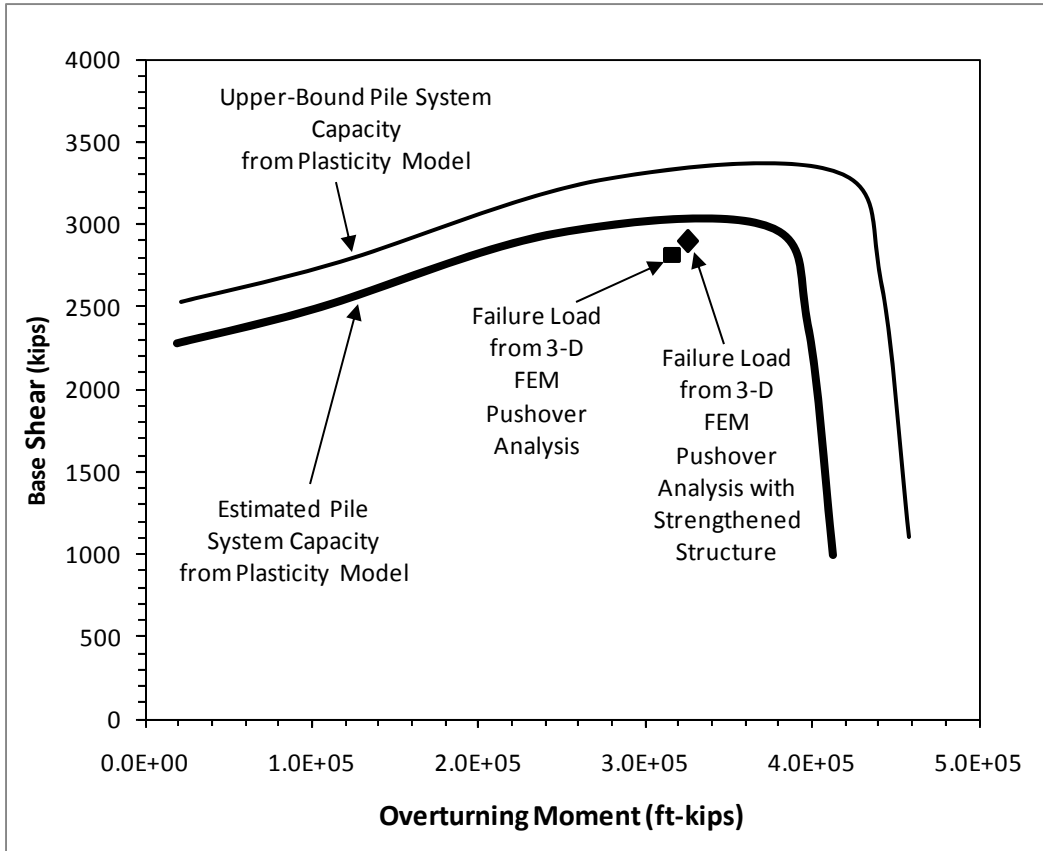


Figure 4.8 Foundation System Capacity Interaction Curve from Plasticity Model of Platform 22 in the End-on Loading Direction

Platform 10 (Table 3.1) also provides a helpful basis for comparison of the two models since it only has one small conductor and the failure mechanism is overturning. The capacity interaction curve for this tripod foundation system is shown in Figure 4.9. One interesting feature of this analysis is that the axial side shear capacity of the piles depends on displacement, which is accounted for explicitly with the t-z curves in the pushover analysis. However, in the simplified plasticity analysis, a governing value of side shear at failure (or collapse) is assumed. Two capacity interaction curves are shown in Figure 4.9; one using the peak unit side shear and the other using the residual unit side shear over the length of the piles. The pushover analysis indicates that the governing capacity at failure is close to the residual side shear, which is consistent with the results from the plasticity model (Figure 4.9).

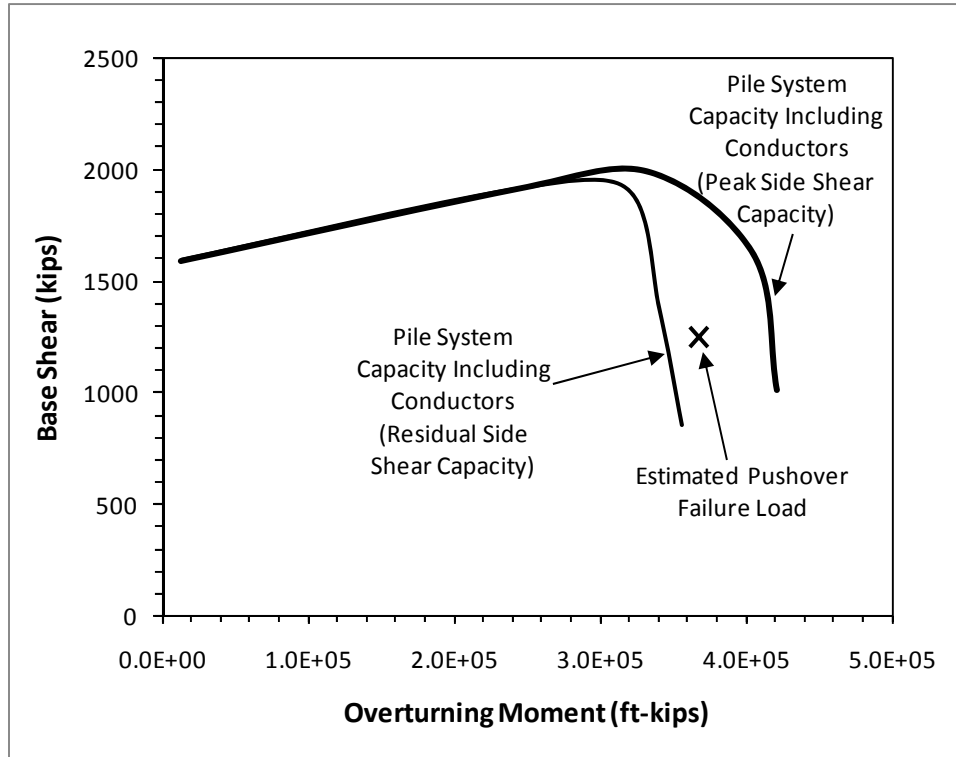


Figure 4.9 Foundation System Capacity Interaction Curve from Plasticity Model of Platform 10 in the Hurricane Ike Loading Direction

The presence of well conductors can have a significant effect on the foundation system capacity, and this effect is difficult to capture in the simplified plasticity model because their relative contribution to the system capacity will depend on displacement (which is not considered in the simplified plasticity model). Comparisons of results from the simplified plasticity model and the pushover analysis are shown in Figures 4.10, 4.11 and 4.12 for Platforms 12, 1 and 9, respectively.

For Platform 12, a pair of results is shown where the conductors were excluded and included in both the simplified plasticity model and the pushover analysis. The failure mechanism for the foundation system is shear, meaning that the lateral capacities of the conductors contribute quite a bit to the total capacity of the foundation (Figure 4.10). The simplified plasticity model provides a very good estimate of the system capacity in this case and is able to account well for the contribution of the conductors (Figure 4.10).

For Platforms 1 and 9, the capacity from the pushover analysis is greater than the capacity from the plasticity model if the conductors have no contribution but less than the capacity from the plasticity model if the conductors provide their full contribution

(Figures 4.11 and 4.12). In these cases, the full plastic capacity of the conductors is not being realized at the deck displacement defined as failure in the pushover analysis. Platform 9 is of particular interest because it has one relatively large conductor that contributes significantly to both the shear and the overturning capacity of the foundation system. In this case, the plastic moment capacity of the large conductor contributes to the overturning capacity of the foundation.

In summary, a set of capacity interaction curves from the simplified plasticity model, one where conductors are not included and one where conductors are included, provide bounds on the capacity of the foundation system (Figures 4.10 to 4.12). The actual system capacity is probably between these curves and closer to the curve including the maximum effect of conductors than the one neglecting the conductors. Both curves will be included in all subsequent results for the simplified plasticity model presented in this report.

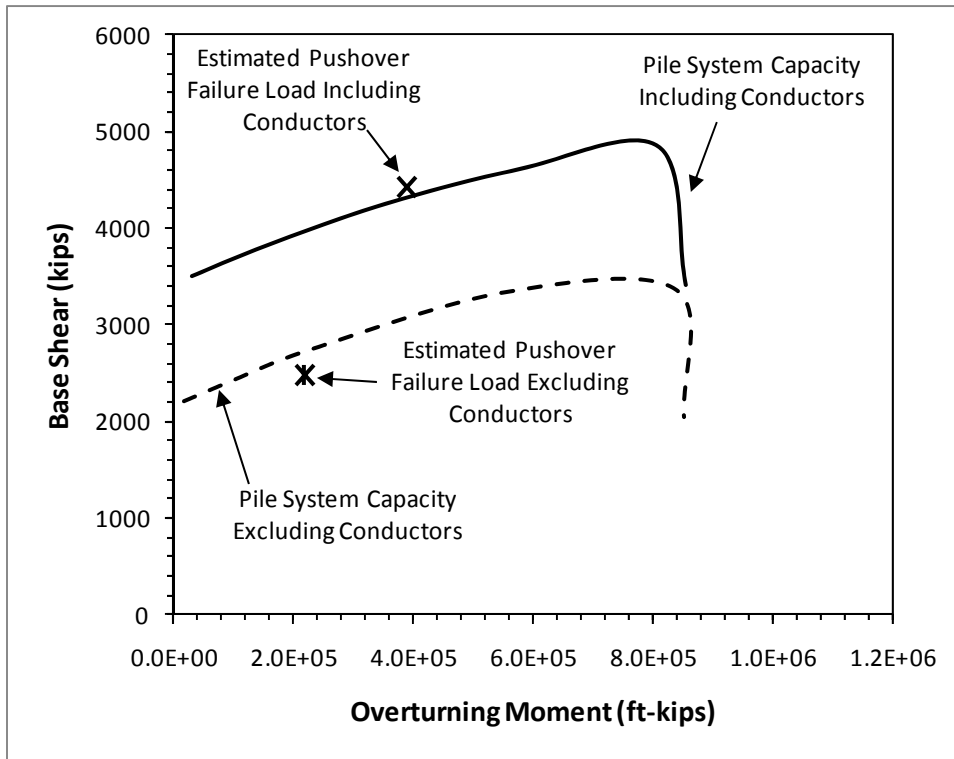


Figure 4.10 Foundation System Capacity Interaction Curve from Plasticity Model of Platform 12 in the End-On Loading Direction

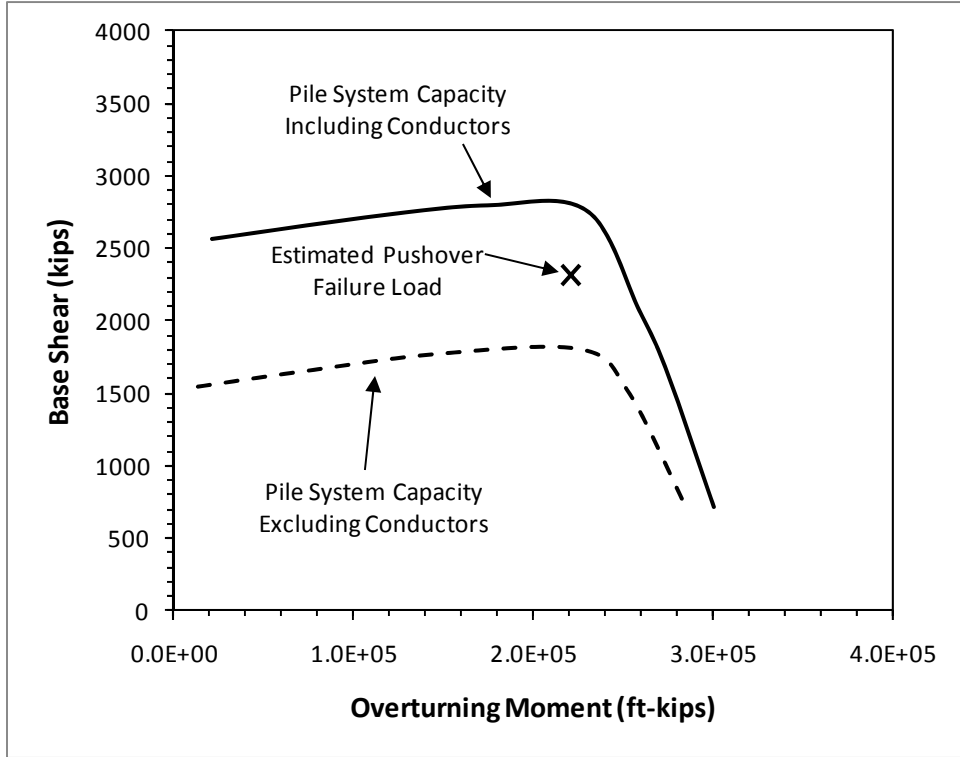


Figure 4.11 Foundation System Capacity Interaction Curve from Plasticity Model of Platform 1 in the End-On Loading Direction

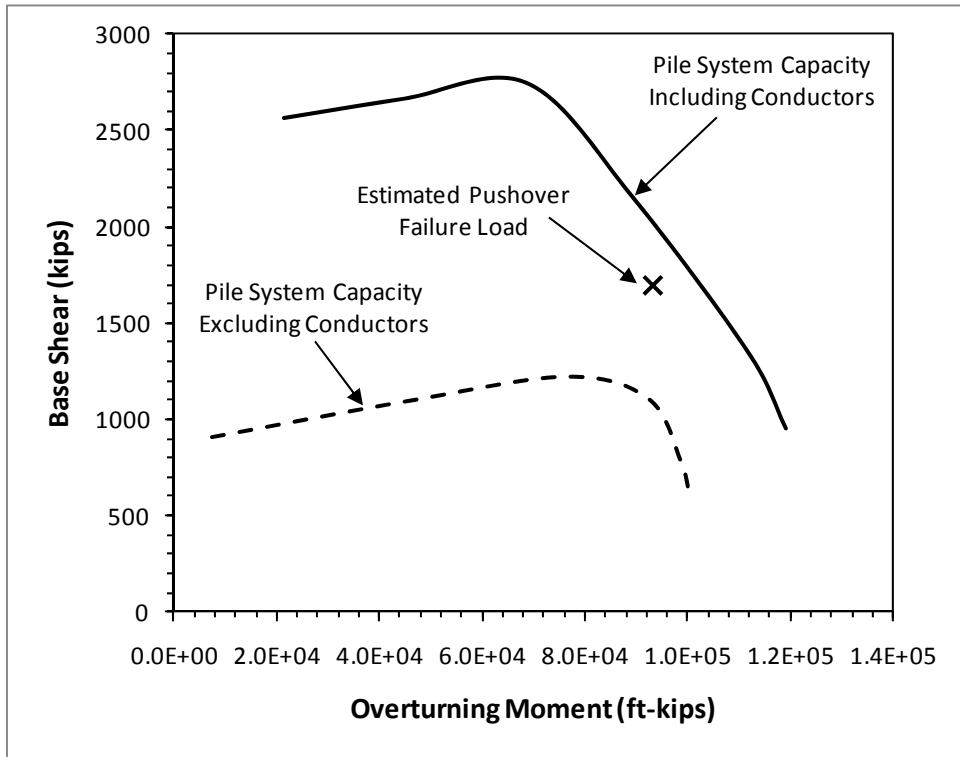


Figure 4.12 Foundation System Capacity Interaction Curve from Plasticity Model of Platform 9 in the End-On Loading Direction

5. Findings

Based on detailed analyses of the 12 case study platforms, the following four major findings were developed:

1. Field performance of foundation systems is consistent with design.
2. The failure mechanism is important in assessing foundation system capacity.
3. Structural factors are important in assessing foundation system capacity.
4. The presence of sand is important in assessing foundation system capacity.

These major findings are discussed and illustrated in this chapter. Details of the analyses that support these findings are provided in Appendix E.

5.1. Field Performance Consistent with Design

Based on the quantitative analyses in this study, the performance of platform foundation systems is consistent with how they were designed and there is no direct evidence of excessive conservatism. Table 5.1 summarizes the results for the 12 platforms that we have analyzed in detail. The performance in the hurricanes generally matches up with what is predicted based on the foundation design.

- In five cases where the platforms were loaded to less than the design capacities of the foundation systems (Platforms 8, 22, 25, 27 and 29), there were no indications of foundation system failures. (Shown in green cells in Table 5.1)
- In four cases where the platforms were loaded to near or beyond the shear capacity of the foundation system (Platforms 9, 11, 12 and 30), there were no indications of foundation system failures. This result is expected because of the reserved structural capacity beyond what is modeled, which can contribute to the shear capacity of the foundation system for a jacket (Sections 5.2 and 5.3). (Shown in yellow cells in Table 5.1)
- In the one case we have of a reasonably definitive foundation failure (Platform 10), the platform was loaded to the design axial capacity of the foundation and an overturning failure of the foundation system apparently occurred. This result is not surprising because the foundation was loaded to its capacity and the platform is a tripod structure with little redundancy to overturning. (Shown in pink cells in Table 5.1)

5.1)

- There is one pair of bridge-connected platforms (Platforms 1 and 2) that did not experience foundation failures even though they were possibly loaded well beyond the overturning capacities of the foundation systems. However, a site-specific soil boring is not available for these platforms and the subsurface conditions in this geologic setting are highly variable with significant layers of sand (Section 5.4), making the inference of design capacities questionable in this case. (Shown in blue cells in Table 5.1)

Table 5.1 Summary of Results for Quantitative Analysis (Part 1 of 2)

Platform No.	Year of Installation	Water Depth (feet)	Indicator of Design Wave Height ¹ (feet)	Maximum Hindcast Wave Height (feet)	Observed Performance	Predicted Performance
8	1984	220	59	77 (Katrina, 2005)	No Evidence of Foundation Failure	Foundation Capacity Not Exceeded
22	1976	110	53	57 (Rita, 2005)	No Evidence of Foundation Failure	Foundation Capacity Not Exceeded
25	1967	90	51	44 (Katrina, 2005)	No Evidence of Foundation Failure	Foundation Capacity Not Exceeded
27	2000	300	61	75 (Rita, 2005)	No Evidence of Foundation Failure	Foundation Capacity Not Exceeded
29	1967	150	56	63 (Katrina, 2005)	No Evidence of Foundation Failure	Foundation Capacity Not Exceeded

¹ Present-day sudden hurricane wave height criteria used in ultimate strength assessment for A-2 (Section 17 of API RP 2A-WSD 2000).

Table 5.1 Summary of Results for Quantitative Analysis (Part 2 of 2)

Platform No.	Year of Installation	Water Depth (feet)	Indicator of Design Wave Height ¹ (feet)	Maximum Hindcast Wave Height (feet)	Observed Performance	Predicted Performance
9	1989	60	45	56 (Katrina, 2005)	No Evidence of Foundation Failure	Shear/Overturning Capacity Reached
11	2000	120	54	67 (Katrina, 2005)	No Evidence of Foundation Failure	Shear Capacity Reached
12	1972	190	58	67 (Rita, 2005)	No Evidence of Foundation Failure	Shear Capacity Reached
30	1973	150	56	63 (Katrina, 2005)	No Evidence of Foundation Failure	Shear Capacity Reached
10	2001	360	61	71 (Ike, 2008)	Evidence of Axial Pile Failure	Overturning Failure
1	1965	140	55	59 (Katrina, 2005)	No Evidence of Foundation Failure	Overturning Failure
2	1966	140	55	59 (Katrina, 2005)	No Evidence of Foundation Failure	Overturning Failure

¹ Present-day sudden hurricane wave height criteria used in ultimate strength assessment for A-2 (Section 17 of API RP 2A-WSD 2000).

5.1.1. Cases of No Foundation System Failures when Hurricane Loads Were Less than Design Capacities

The foundation system capacity interaction curves for Platforms 8, 22, 25, 27 and 29 are shown in Figures 5.1 to 5.5, respectively. Even considering the foundation capacity without the contribution of conductors, the estimated hurricane loads are all less than the foundation capacities for these platforms. Post-hurricane field observations of these platforms also show no evidence of foundation failures, which is consistent with our analyses.

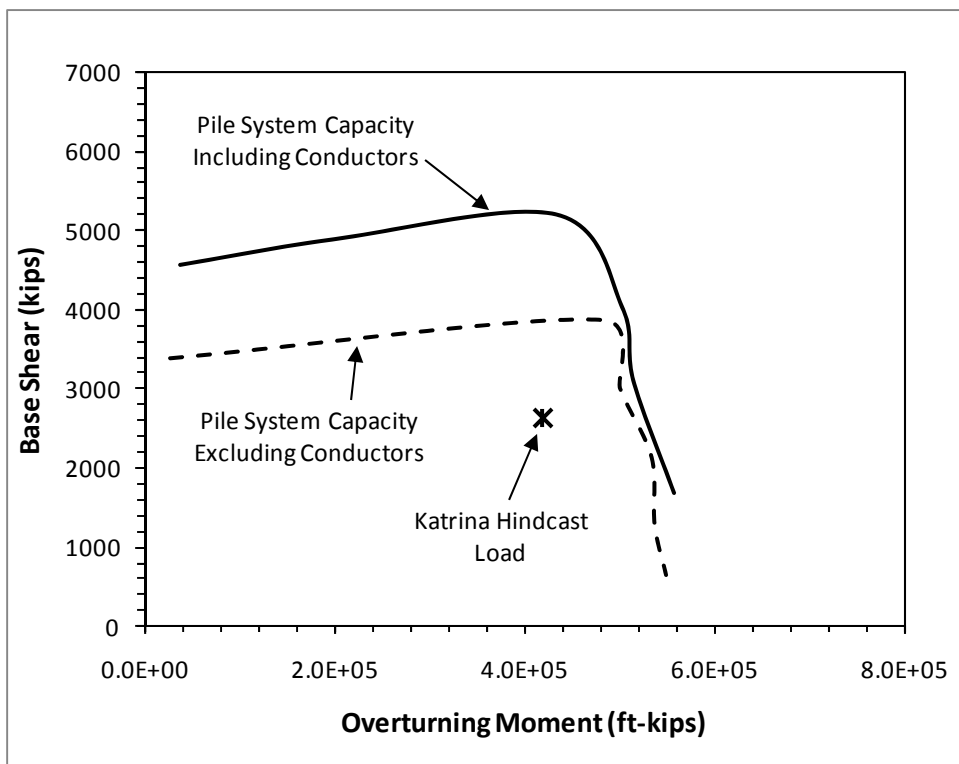


Figure 5.1 Foundation System Capacity Interaction Diagram from Plasticity Model of Platform 8

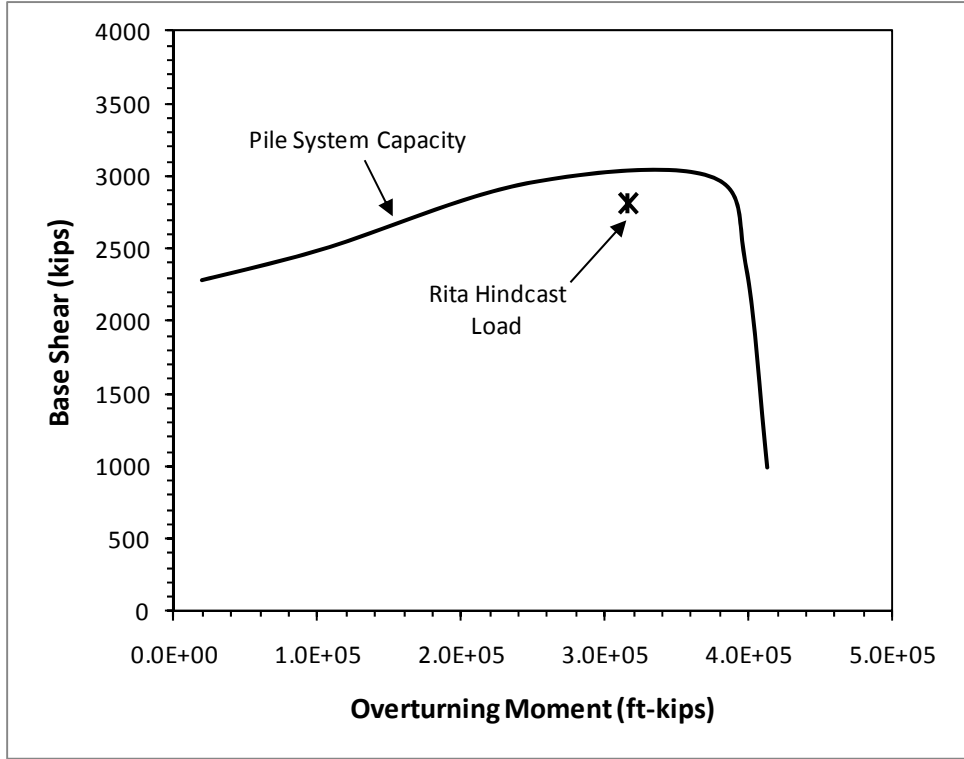


Figure 5.2 Foundation System Capacity Interaction Diagram from Plasticity Model of Platform 22

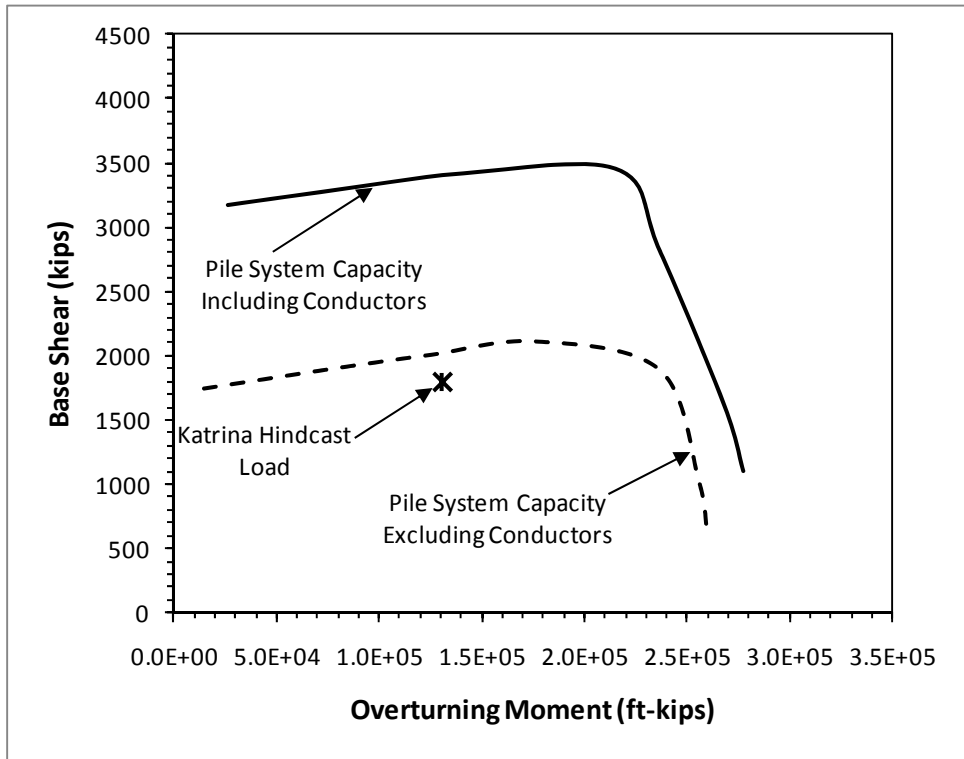


Figure 5.3 Foundation System Capacity Interaction Diagram from Plasticity Model of Platform 25

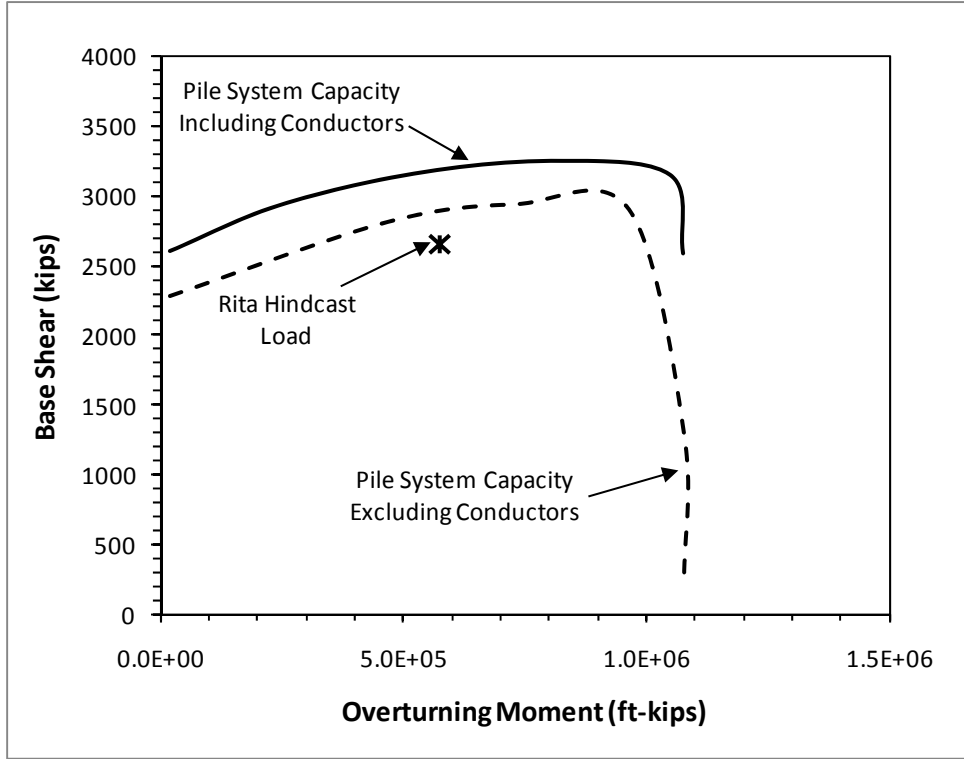


Figure 5.4 Foundation System Capacity Interaction Diagram from Plasticity Model of Platform 27

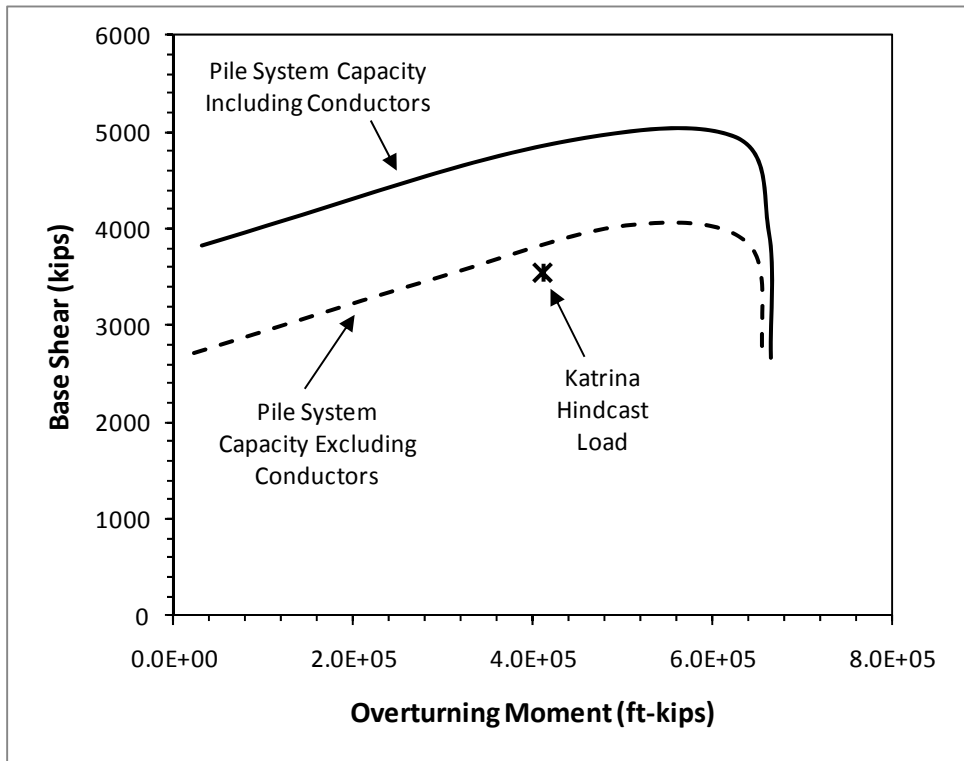


Figure 5.5 Foundation System Capacity Interaction Diagram from Plasticity Model of Platform 29

5.1.2. Cases of No Shear Failures of Foundation Systems when Hurricane Loads Were Near Design Capacities

For Platforms 9, 11, 12 and 30, the estimated hurricane loads are very close to or beyond the shear capacities of the foundation systems without the contribution of conductors (Figures 5.6 to 5.9). However, there was no evidence of foundation system failures in these structures based on post-hurricane inspections and assessments.

Even though they were loaded close to or beyond the design lateral capacities of the piles, it is not surprising that there were no failures of the foundation systems. Structural factors, such as the presence of conductors and yield strengths for steel members that are greater than the nominal values used in assessment, can provide an additional margin of safety for a shear type failure in the foundation. None of these structures were loaded beyond the predicted capacity of the foundation system if the conductors provide their full contribution (Figures 5.6 to 5.9). Additionally, penetration of jacket legs below the mudline and grouting in the annuluses between the legs and piles can increase the effective moment capacities of the piles near the mudline, which also increases the shear capacity of the foundation. Therefore, while there may have been individual piles that were close to or even yielded (which would be very difficult to detect in a post-hurricane inspection), the foundations are not expected to fail as a system when the loads are near the predicted capacities of the foundation systems.

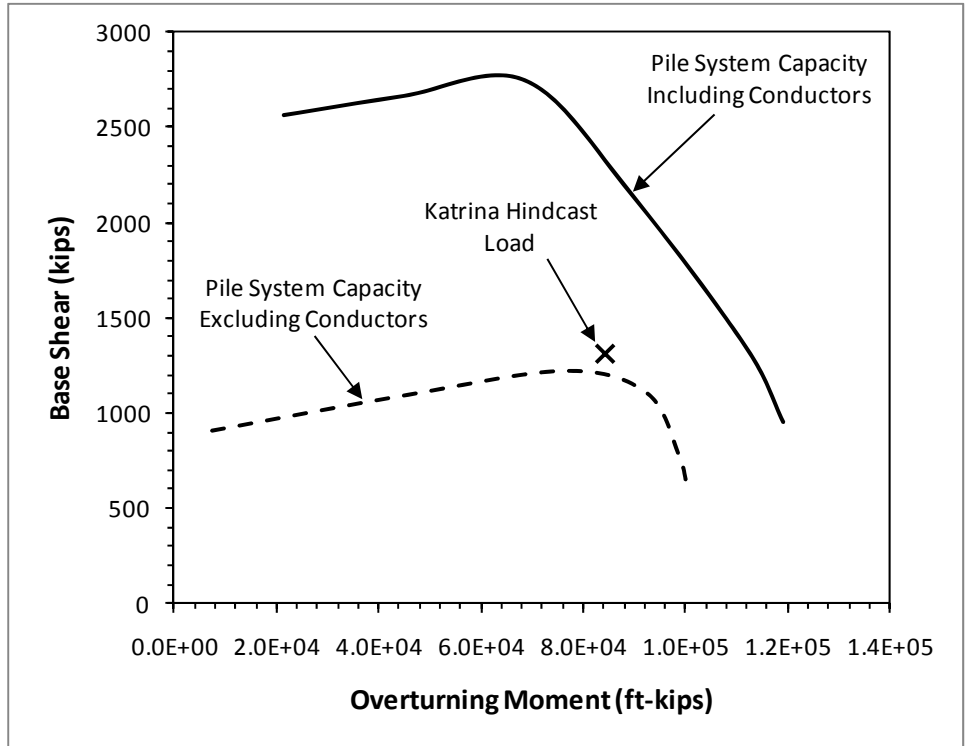


Figure 5.6 Foundation System Capacity Interaction Diagram from Plasticity Model of Platform 9

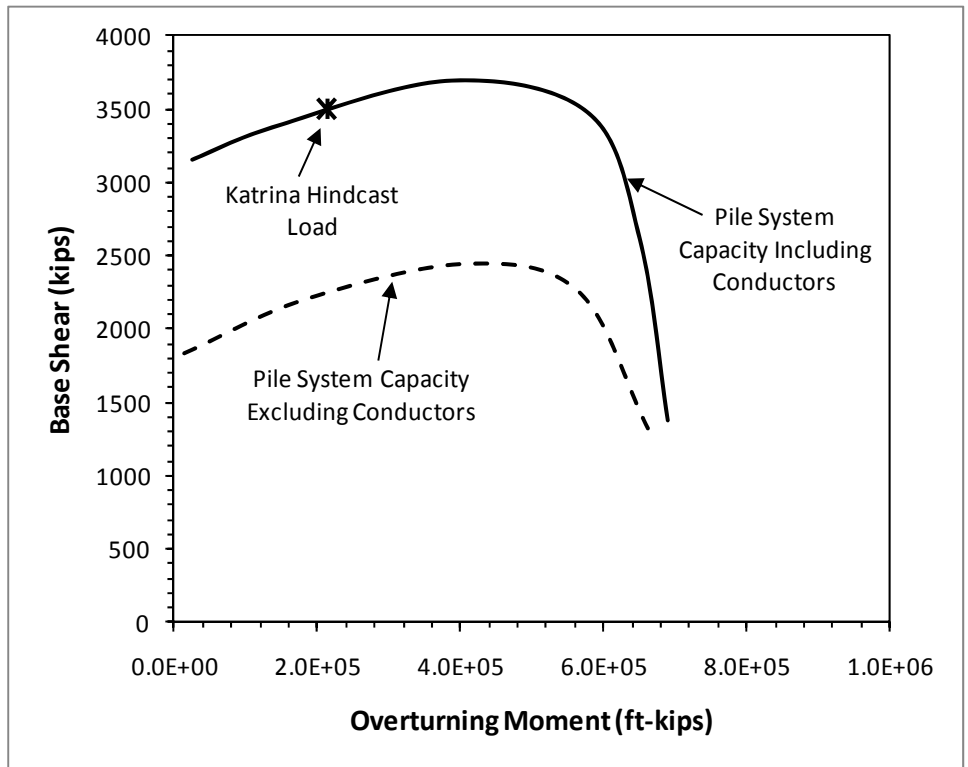


Figure 5.7 Foundation System Capacity Interaction Diagram from Plasticity Model of Platform 11

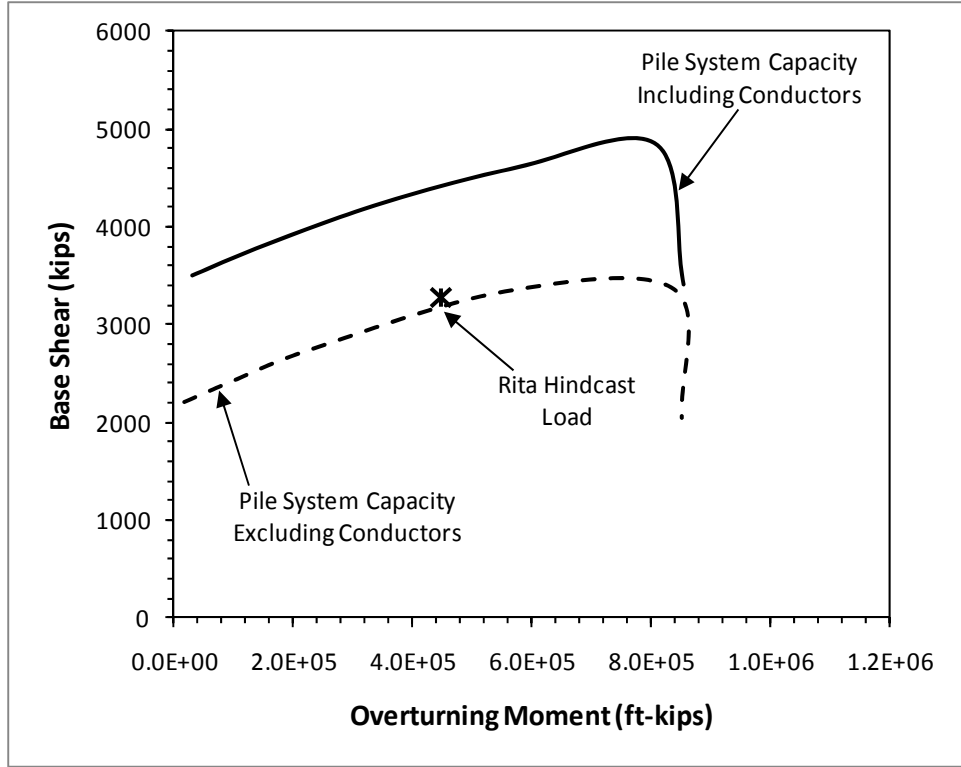


Figure 5.8 Foundation System Capacity Interaction Diagram from Plasticity Model of Platform 12

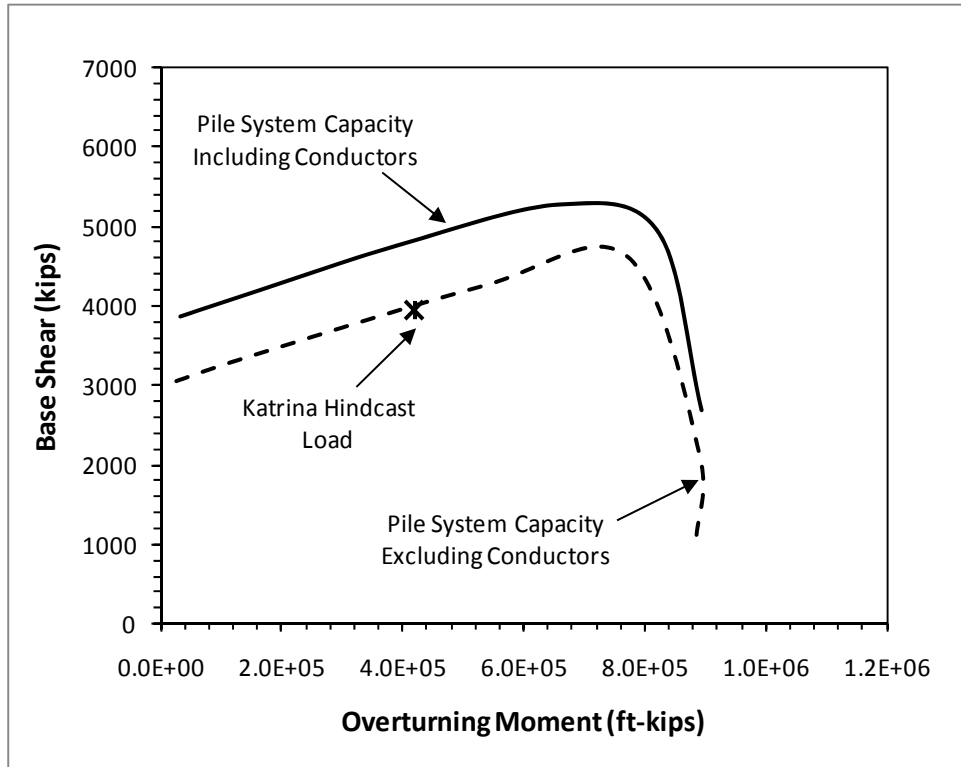


Figure 5.9 Foundation System Capacity Interaction Diagram from Plasticity Model of Platform 30

5.1.3. Case of Overturning Failure of Foundation System when Predicted

Platform 10 is a tripod structure where one of the piles also serves as a well conductor (Pile A in Figure 5.10). The platform was installed in 2003. It was loaded from the east by Hurricane Ike in 2008, and was left leaning to the west after the hurricane. Visual (underwater) inspections have not detected any indication of structural failure to cause the lean, and all indications suggest that the foundation system failed in overturning. The displacement of the piles at the mudline was estimated to be a few feet because the base of jacket including mudmats is below mudline. This platform is the first offshore structure, excluding caissons, available to us to date where a reasonably definitive foundation failure has been observed and documented.

The foundation system capacity interaction curve for Platform 10 (Figure 5.11) shows that the foundation system was probably loaded beyond its overturning capacity. The predicted foundation system failure is initiated by an axial pull-out failure of the back pile in the hurricane loading (Pile C in Figure 5.10). Piles B and C are 205-foot long, 48-inch diameter steel pipes driven into a normally consolidated marine clay. Geotechnical information comes from a site-specific boring that was drilled in 2000 using modern techniques for sampling and testing. The axial side shear on the piles is expected to exhibit strain-softening behavior according to the design method. The residual side shear on the t-z curve used in the pushover analysis for this platform is assumed to be 0.8 times the peak value. When we use the residual side shear and no reverse end bearing for the piles, we predict a foundation capacity that is less than the hurricane load (Figure 5.11). This result indicates that strain softening may have occurred in the field, which is consistent with design practice and what is used for t-z curves in a pushover analyses.

A simplified t-z analysis was performed for Pile C (the back pile in tension). The wall thickness was assumed to be 1 inch, which is the thickness of the majority of the pile length. The load-displacement curve of this pile considering strain softening is presented in Figure 5.12. As shown in this figure, the maximum axial capacity is mobilized at a pile-head displacement of 1.6 inches and then the capacity drops to a residual value at a displacement of 2 inches. The maximum axial capacity is less than ultimate capacity assuming peak side shear is mobilized simultaneously along the pile length, and the available capacity after more than several inches of displacement is smaller than the maximum and equal to the residual capacity (Figure 5.12). This finding is significant because the pile length may be determined by structural engineers using the ultimate

capacity versus pile penetration curves developed by geotechnical engineers. The strain softening behavior is usually not included in these curves because the geotechnical engineers do not know the pile wall thickness schedule at the time when they prepare these curves. Instead, t-z curves are usually provided by the geotechnical engineers. These t-z curves are used by structural engineers in the structural analysis to determine the performance of the structure and its members. However, they are not necessarily used to size the piles. As a result, the axial capacity of the piles can be 10 to 30 percent less than its intended value for long, flexible piles embedded in normally consolidated marine clays that exhibit strain softening.

The geometry of this tripod platform makes it less redundant than a 4, 6 or 8-leg structure. The wave loading direction in Ike put single pile into tension (Pile C Figure 5.10). The pull-out failure of that single pile would lead to the collapse of the foundation system (or excessive rotation of the jacket). Pile A on the north side of the tripod also serves as a well conductor, meaning that its axial capacity is probably greater than the pile alone due to grouted connections within the casing strings. However, this potential reserve is not effective in increasing the overturning capacity in the Hurricane Ike loading direction because the system capacity is governed by pull-out of Pile C. The foundation capacity in overturning is very sensitive to loading direction, as shown in Figure 5.13. This sensitivity also indicates a lack of redundancy to overturning. Ironically, the greatest capacity corresponds to a load from the north, which is not likely in a hurricane.

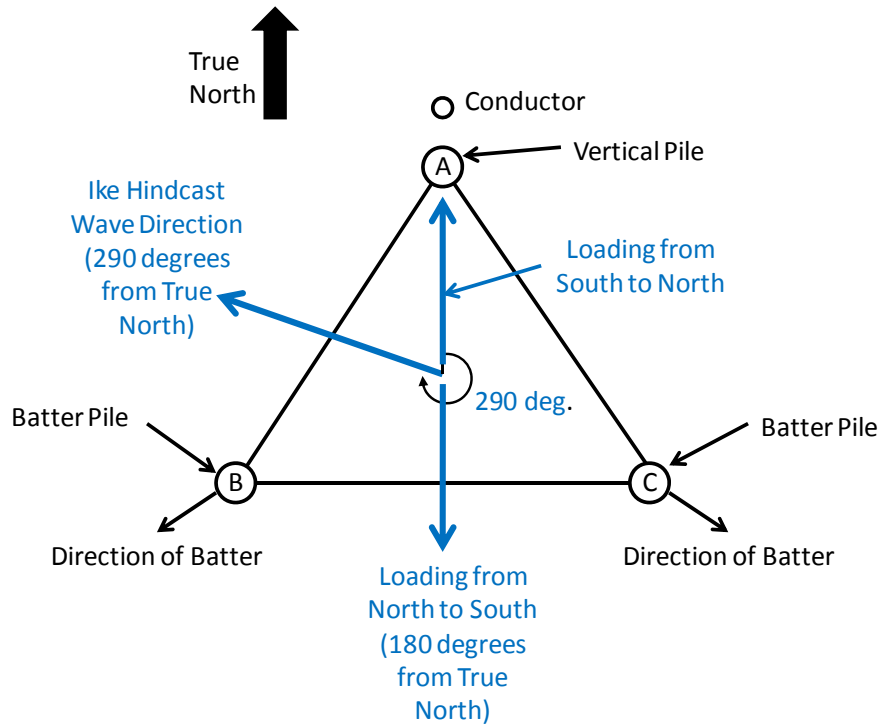


Figure 5.10 Plan View of Foundation System for Platform 10

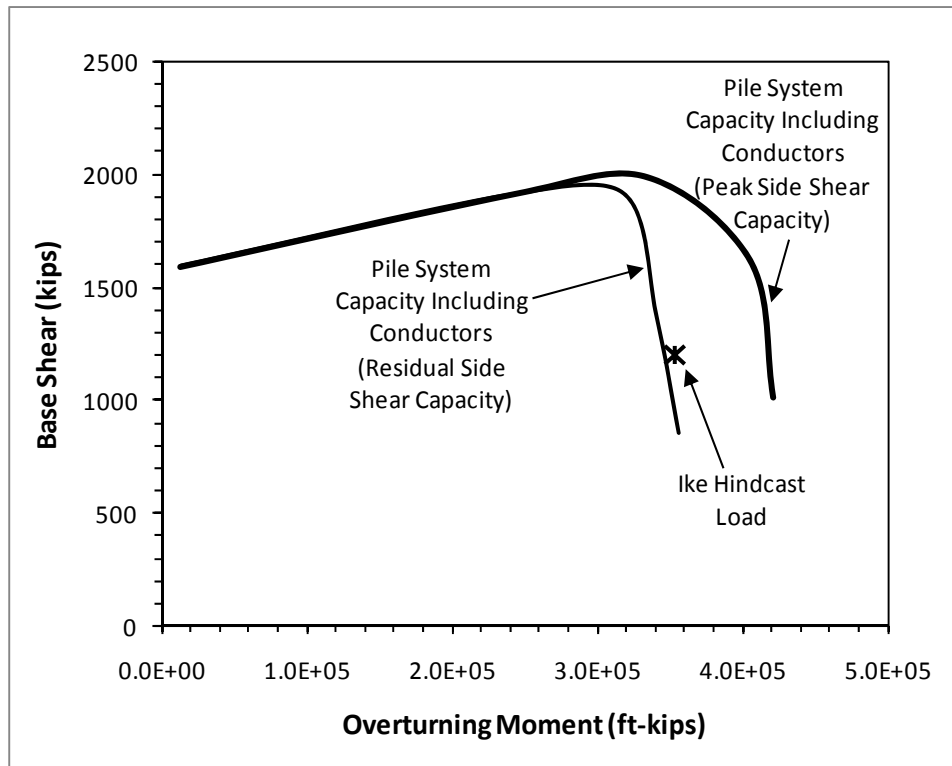


Figure 5.11 Foundation System Capacity Interaction Diagram from Plasticity Model of Platform 10

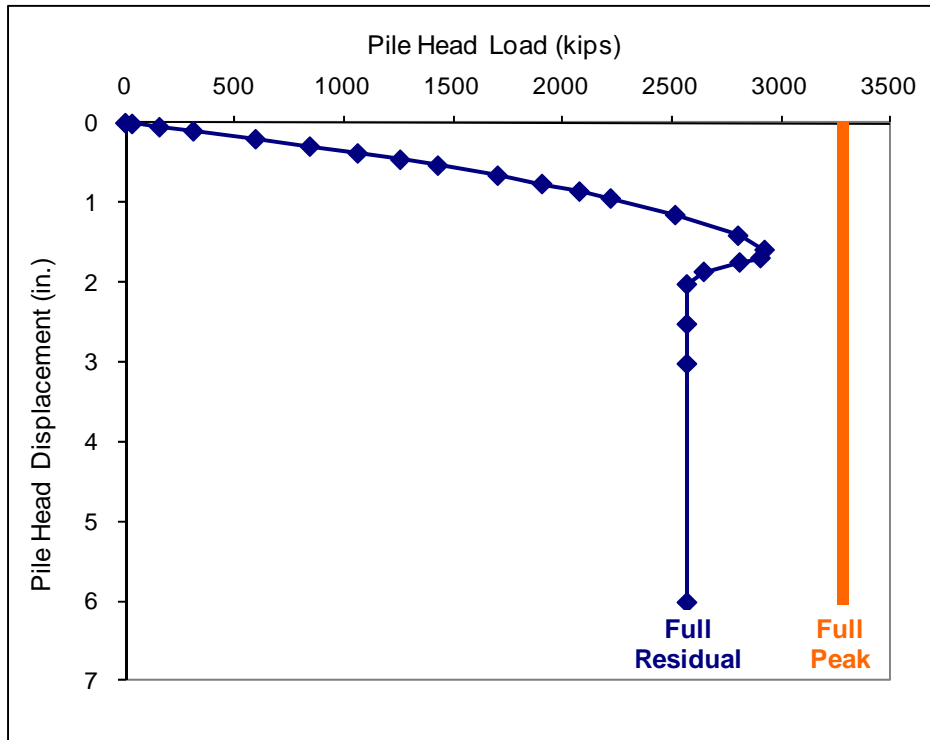


Figure 5.12 Results of the t-z Analysis of Pile C in Tension

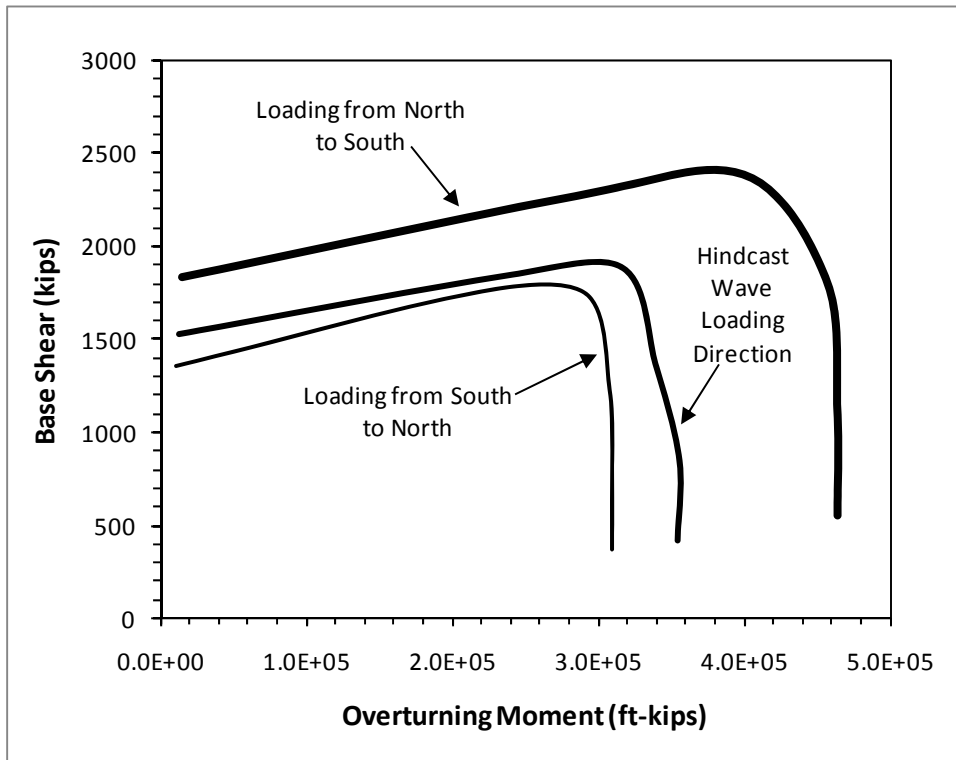


Figure 5.13 Sensitivity of the Foundation Overturning Capacity to Loading Direction for Platform 10

5.1.4. Cases of No Overturning Failures of Foundation Systems when Predicted

Platforms 1 and 2 are 8 and 6-pile structures that are in the same location (connected by a bridge). The foundation system capacity interaction curves for these platforms predict overturning failures of the foundation systems because the predicted capacities are well below the estimated hindcast loading from Hurricane Katrina (Figures 5.14 and 5.15). However, both structures survived the hurricane intact and there is no evidence of distress in the foundation system.

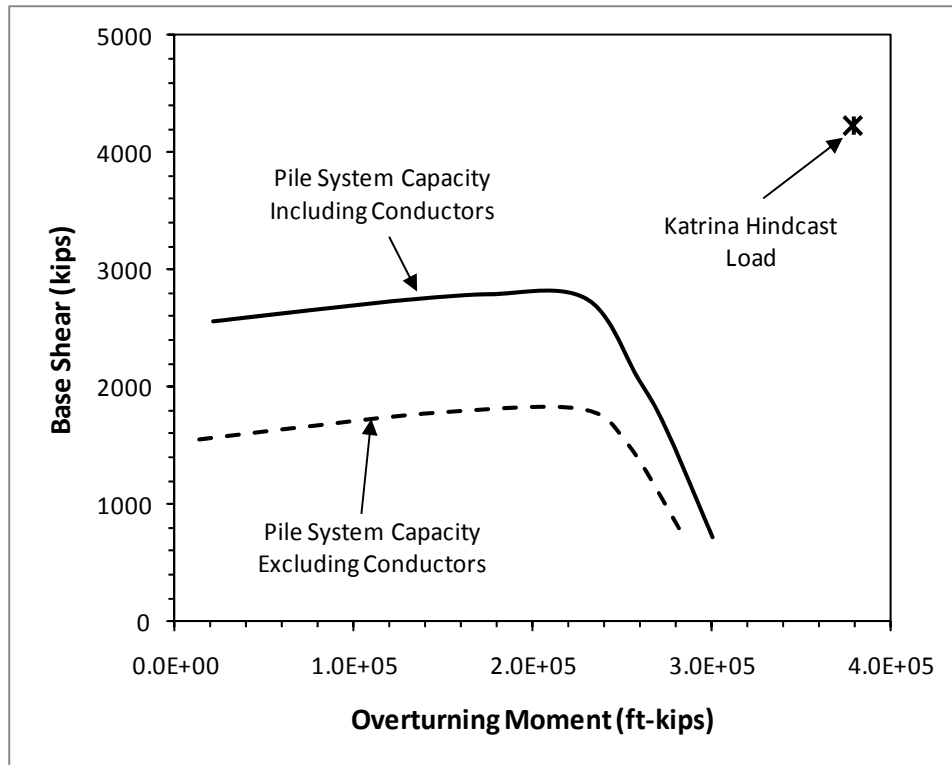


Figure 5.14 Foundation System Capacity Interaction Diagram from Plasticity Model of Platform 1

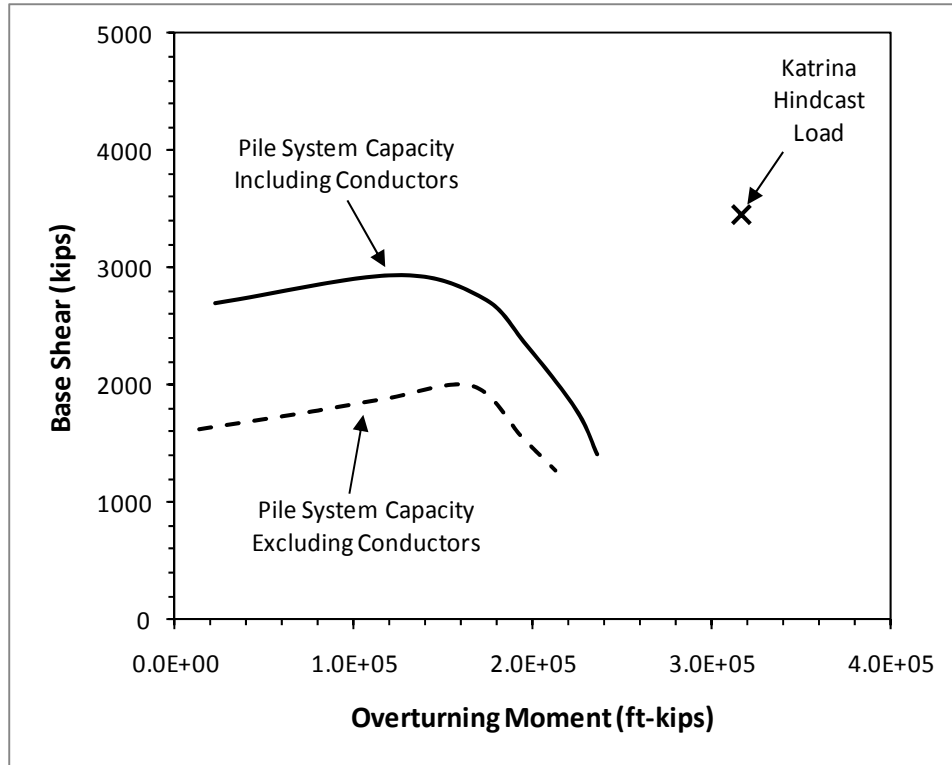


Figure 5.15 Foundation System Capacity Interaction Diagram from Plasticity Model of Platform 2

While it is possible that these two cases provide evidence of conservatism in foundation design, the most probable explanation for the apparent discrepancy between observed and predicted performance is that the predicted capacities are based on an inappropriate soil boring. We have not yet been able to locate a site-specific boring for these structures, which were installed in the mid 1960's. The closest boring that is available, and the boring that was used in the assessment, was drilled in 1979 about 1,000 feet away. The geologic setting is a complex and variable alluvial (fluvatile) deposit with interbedded layers of clay and sand, making it difficult to extrapolate conditions over more than hundreds or even tens of feet. In addition, the method used in the 1979 soil boring to estimate the density and therefore shear strength of the sand layers was an outdated Driven Penetration Test that generally met refusal and did not fully characterize these layers.

There are two strong pieces of evidence suggesting that this boring does not properly reflect the geotechnical conditions at the site. First, the piles were designed to tip in a layer that did not optimize their axial capacity. As shown in Figure 5.16, if the piles had been driven less than 10 feet deeper, the tip capacity would have been 70 percent greater

and the total axial capacity almost 50 percent greater. Figures 5.17 and 5.18 show how sensitive the foundation system capacity is to the density of the sand layer at the pile tips. For Platform 2, this difference alone is enough to make the predicted capacity nearly the same as the hurricane loading. For Platform 1, this difference is enough to change the failure mechanism for the foundation system from overturning to shear, where there are other sources of reserve in the structural system that can increase the foundation capacity (see Section 5.1.2). The selection of pile length for these structures is not consistent with typical practice if this soil boring accurately reflects the geotechnical conditions at the site.

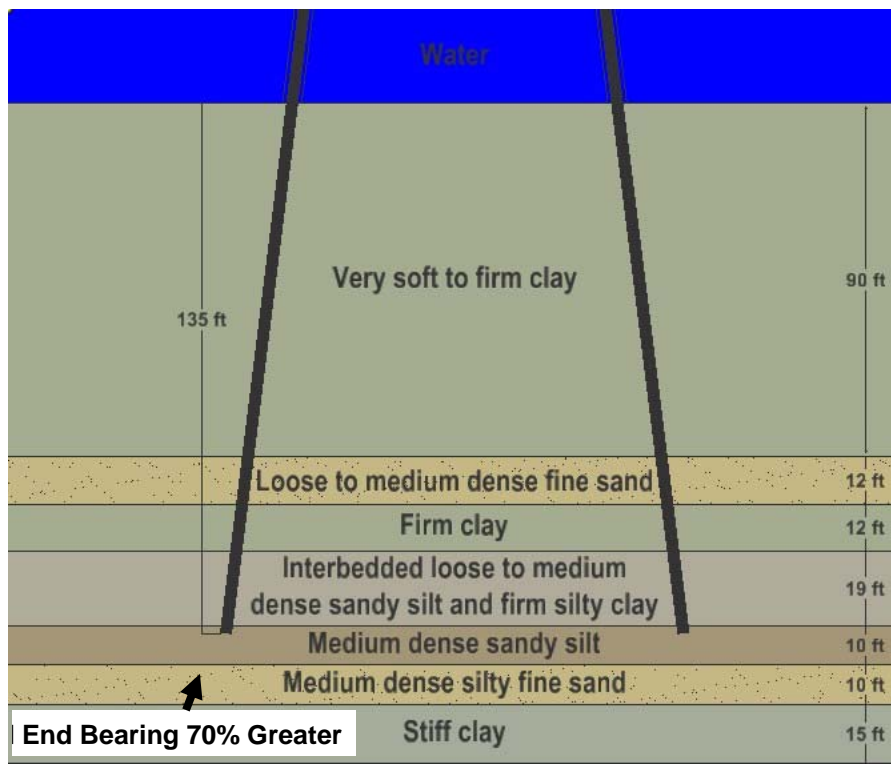


Figure 5.16 Schematic of Geologic Setting for Platforms 1 and 2

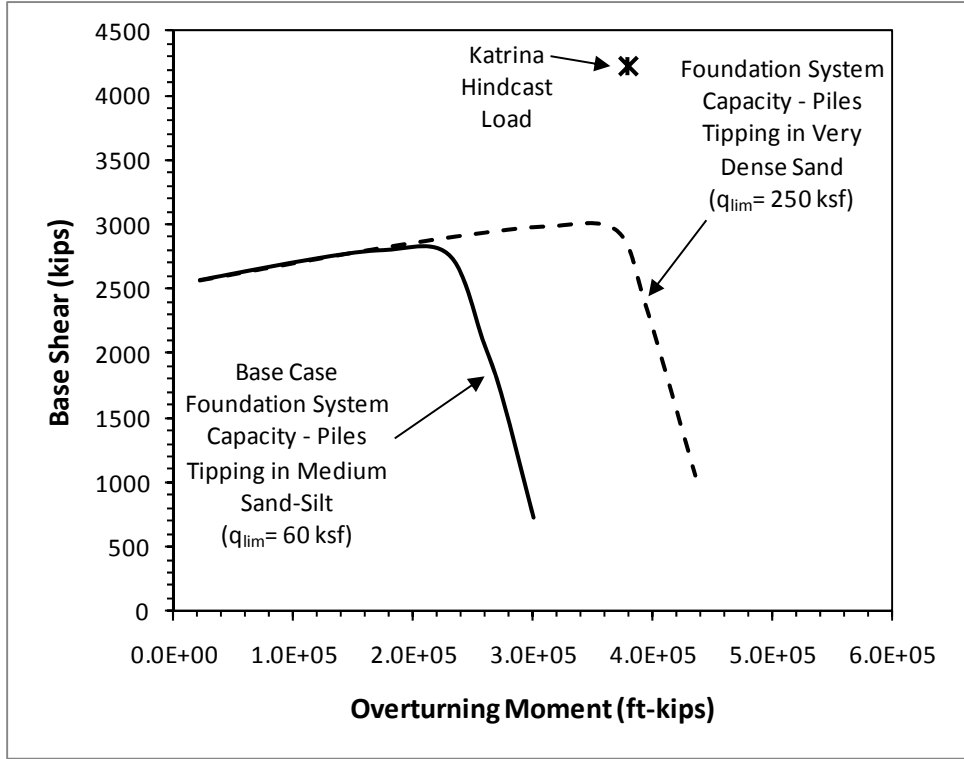


Figure 5.17 Sensitivity of the Foundation System Capacity for Platform 1 to Density of Sand Layer at Pile Tips

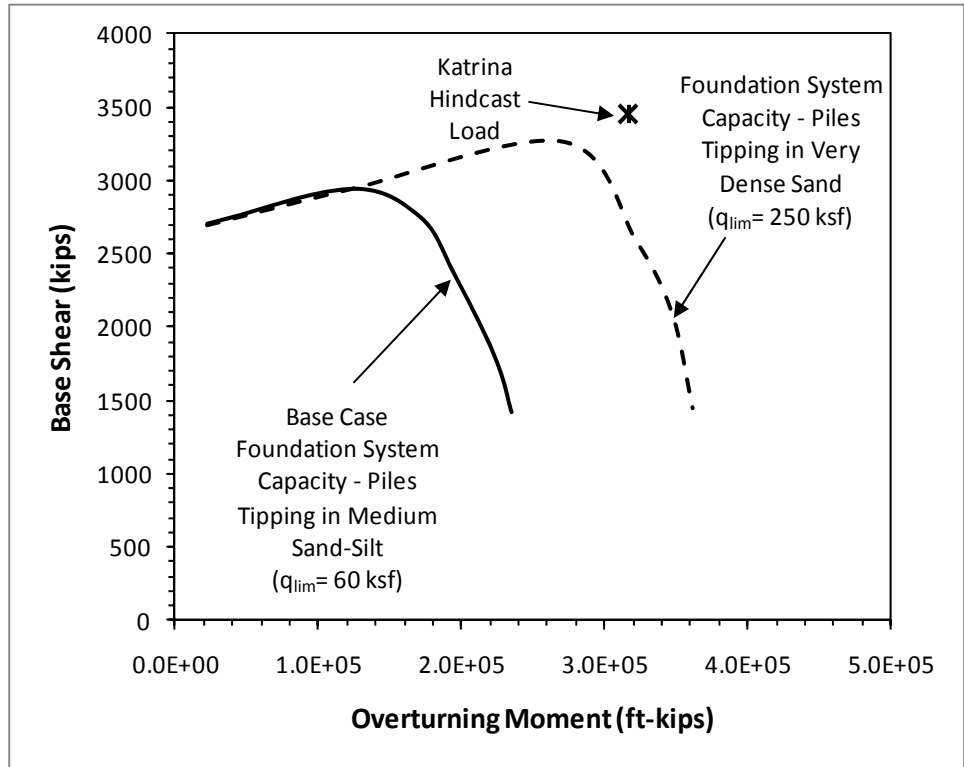


Figure 5.18 Sensitivity of the Foundation System Capacity for Platform 2 to Density of Sand Layer at Pile Tips

Second, the large discrepancy between the hurricane loading and the predicted foundation capacity in overturning is not consistent with any of the other structures that we have analyzed (compare Figures 5.14 and 5.15 with Figures 5.1 to 5.9 and 5.11). The maximum wave height at this location in Hurricane Katrina was 59 feet. For comparison, the design maximum wave height for a present-day A-2 ultimate strength assessment is 55 feet. If we use the predicted capacity in Figures 5.14 and 5.15 as a guide, these platforms were designed using a maximum wave height of less than 45 feet. While the design standards in the mid 1960's were not the same as today, they were not that much lower, particularly considering that a major operator designed and installed these two structures.

Therefore, we suspect that the explanation for the large discrepancy between observed and predicted performance (Figures 5.14 and 5.15) reflects an underestimate of the actual design capacity (the design capacity that would be obtained with a site-specific, modern soil boring) and not conservatism in the design method.

5.2. Importance of Failure Mechanism for Foundation System Capacity

The type of failure mechanism is important in assessing the capacity of the foundation system. There are two broad categories of failure mechanisms for the foundation system: shear failure where the piles and conductors exceed their lateral capacities and overturning failure where the piles exceed their axial capacities (Figure 5.19). For a shear failure mechanism,

- the system capacity is relatively insensitive to the shear strength of soil;
- the system capacity is relatively sensitive to the yield strength of steel;
- the system capacity is relatively sensitive to conductors; and
- the system capacity is relatively insensitive to loading direction.

Conversely, for an overturning failure mechanism,

- the system capacity is relatively sensitive to the shear strength of soil;
- the system capacity is relatively insensitive to the yield strength of steel;
- the system capacity is relatively insensitive to conductors; and
- the system capacity is relatively sensitive to loading direction.

The importance of the failure mechanism is demonstrated in the following sections using sensitivity analyses with the Case Study Platforms.

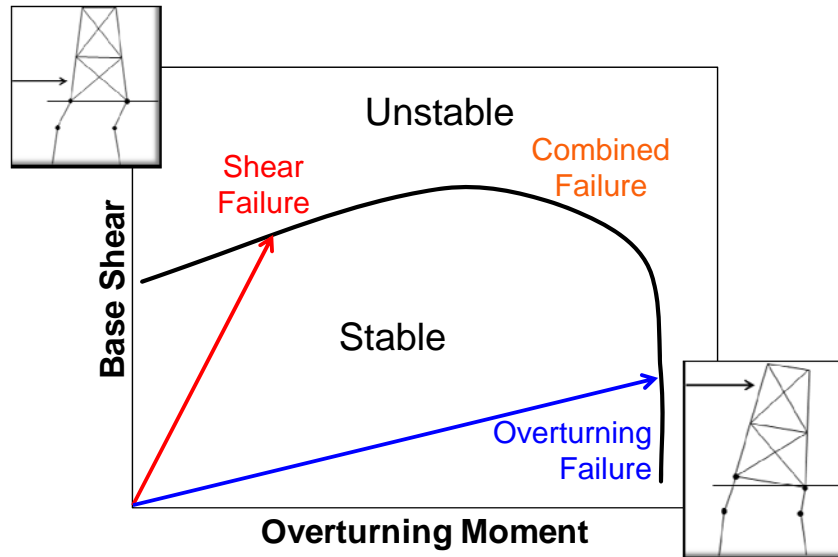


Figure 5.19 Schematic Showing Failure Mechanisms for Foundation Systems

5.2.1. Sensitivity of Shear versus Overturning Capacity to Shear Strength of Soil

The capacity of a foundation system in shear is much less sensitive to the shear strength of the soil than the capacity of the system in overturning. A sensitivity analysis for the foundation system capacity of Platform 1 is shown in Figure 5.20. First, the lateral resistance provided by the soil, which is roughly proportional to the shear strength of the soil over the upper 50 feet of the pile or conductor, was increased by 50 percent (the curve labeled “ $NQ_{lat} = 1.5$ ” in Figure 5.20). The results in Figure 5.20 show that increasing the shear strength of the soil by 50 percent increases the load causing a shear failure by about 10 percent. For comparison, the axial resistance provided by the soil to an overturning failure mechanism was also increased by 50 percent (the curve labeled “ $NQ_{ax} = 1.5$ ” in Figure 5.20). Again, this axial soil resistance is roughly proportional to the shear strength of the soil, particularly over the lower third of the pile length. In this case, increasing the shear strength of the soil by 50 percent increases the moment causing an overturning failure by about 50 percent.

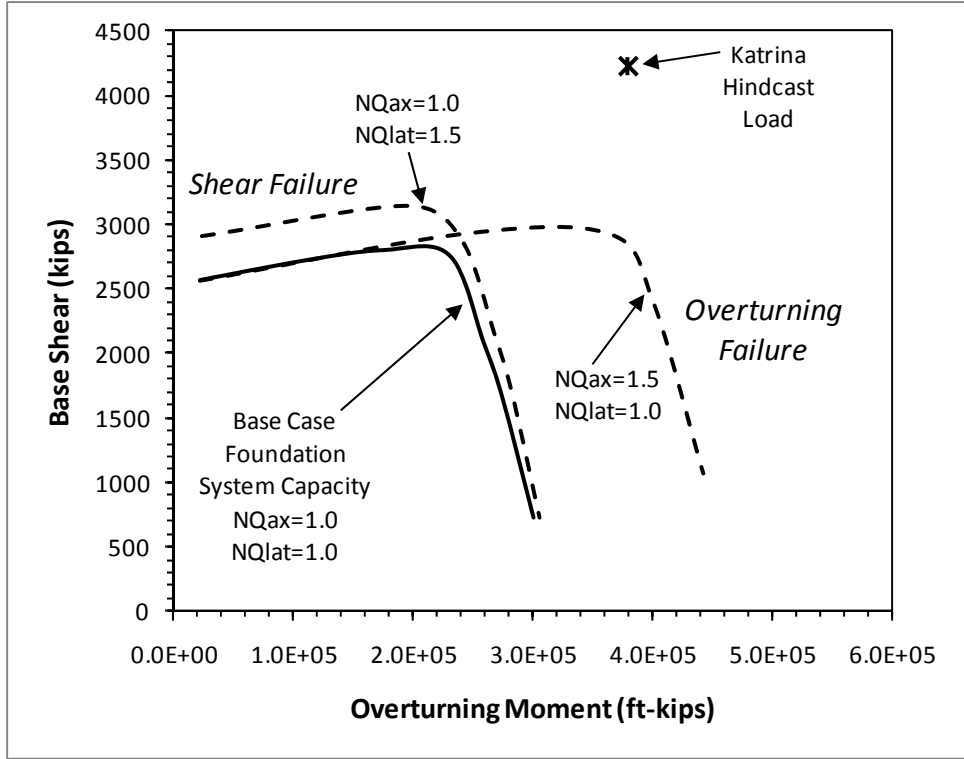


Figure 5.20 Sensitivity Analyses of Foundation System Capacity to Lateral and Axial Resistance Provided by Soil for Platform 1 in End-On Loading Direction

This relatively insensitivity of the shear capacity of the foundation system to the shear strength of the soil may explain why structural engineers sometimes increase the shear strength of the soil by factors of two or more to explain survival of platforms in hurricanes. This practice is not appropriate for several reasons. First, we do not have any evidence to suggest that the lateral resistance provided by the soil would be more than two times greater than what the design method predicts. Second, arbitrarily changing the shear strength of the soil along the entire pile length will have a much larger effect on the axial resistance, which might change the governing failure mechanism from overturning to shear (as illustrated in Figure 5.17).

5.2.2. Sensitivity of Shear versus Overturning Capacity to Yield Strength of Steel

The shear capacity of the foundation system is much more sensitive than the overturning capacity to the yield strength of the steel piles and conductors. A sensitivity analysis for the yield strength of the piles and conductors is shown on Figure 5.21. Pushover analyses are typically conducted assuming that the yield strength of the steel in the members is equal to the nominal yield strength, which is 36 ksi for the platform shown in Figure 5.21.

However, the actual yield strength is expected to be greater than the nominal value and generally the increase is on the order of 5 to 20 percent (Energo 2009). The yield strength for the piles and conductors was increased by 15 percent in Figure 5.21. A 15 percent increase in the yield strength increases the shear capacity of the foundation by roughly 10 percent, while it has a very small effect on the overturning capacity (Figure 5.21). A comparison of Figures 5.20 and 5.21 shows that the shear capacity of this foundation system is about three times more sensitive to the yield strength of the steel than the shear strength of the soil.

The moment capacities of the piles and conductors can also be increased due to other factors, such as the jacket leg penetration below the mudline, grouting between the jacket legs and piles, and grouting between casing strings in conductors. All of these factors can have a significant impact on the shear capacity of the foundation system.

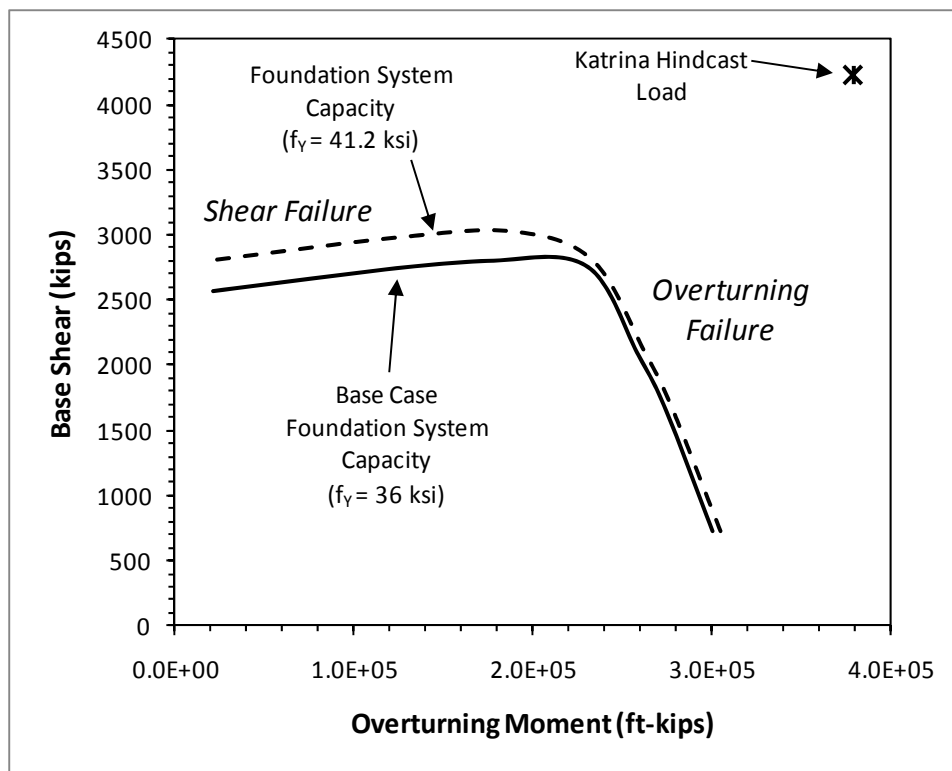


Figure 5.21 Sensitivity Analyses of Foundation System Capacity to Yield Strength of Piles and Conductors for Platform 1 in End-On Loading Direction

5.2.3. Sensitivity of Shear versus Overturning Capacity to Well Conductors

The shear capacity of the foundation system is much more sensitive than the overturning capacity to the lateral resistance provided by well conductors. Figure 5.22 illustrates this effect with Platform 11. This platform is equipped with four conductors, including one large, 72-inch diameter conductor. The conductors serve to increase the shear capacity of the foundation system by about 70 percent. If the conductors did not contribute to the foundation capacity, it is possible that this foundation would have failed in Hurricane Katrina (Figure 5.22).

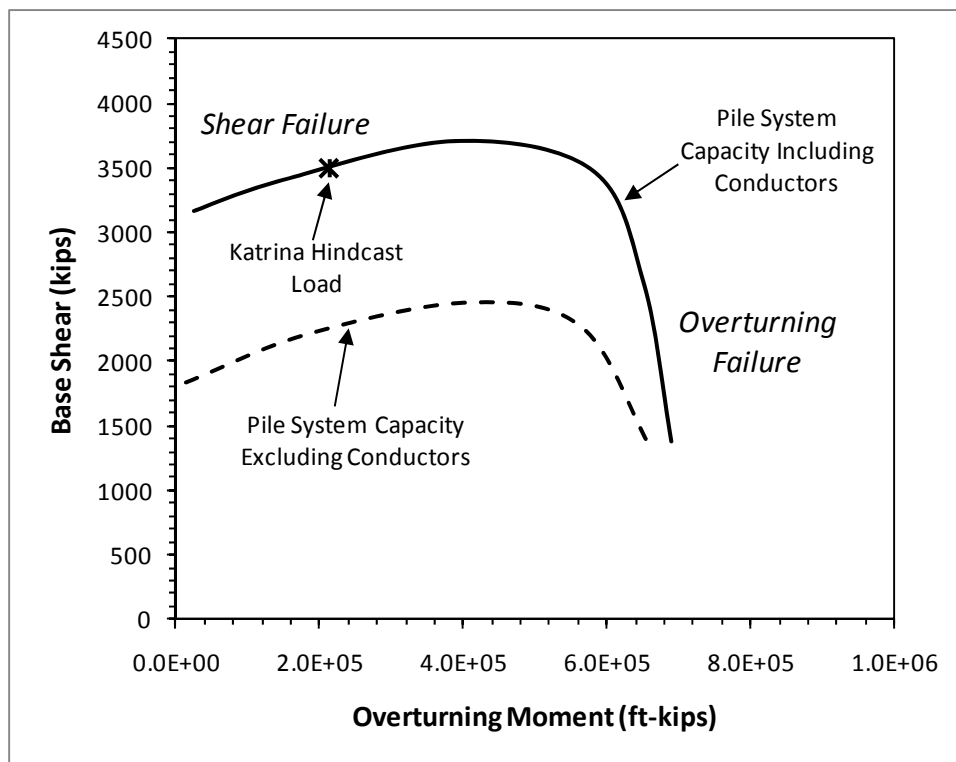


Figure 5.22 Foundation System Capacity Interaction Diagram from Plasticity Model of Platform 11

5.2.4. Sensitivity of Shear versus Overturning Capacity to Loading Direction

The shear capacity of a foundation system is relatively insensitive to the loading direction compared to the overturning capacity. The foundation capacity for Platform 30, a 6-pile rectangular platform, is shown as a function of loading direction in Figure 5.23. In the portion of the capacity interaction curve corresponding to a shear failure mechanism, the capacity is insensitive to the loading direction. Essentially, each pile contributes roughly

equally to the lateral capacity. Conversely in the portion of the capacity interaction curve corresponding to an overturning failure mechanism, the capacity is sensitive to loading direction since each individual pile contributes differently depending on the moment arm between the pile and the center of the rotation for the platform in the direction of loading. The tripod platform (Platform 10) illustrates an extreme example of the sensitivity of overturning capacity to loading direction due to its geometry (Figure 5.13).

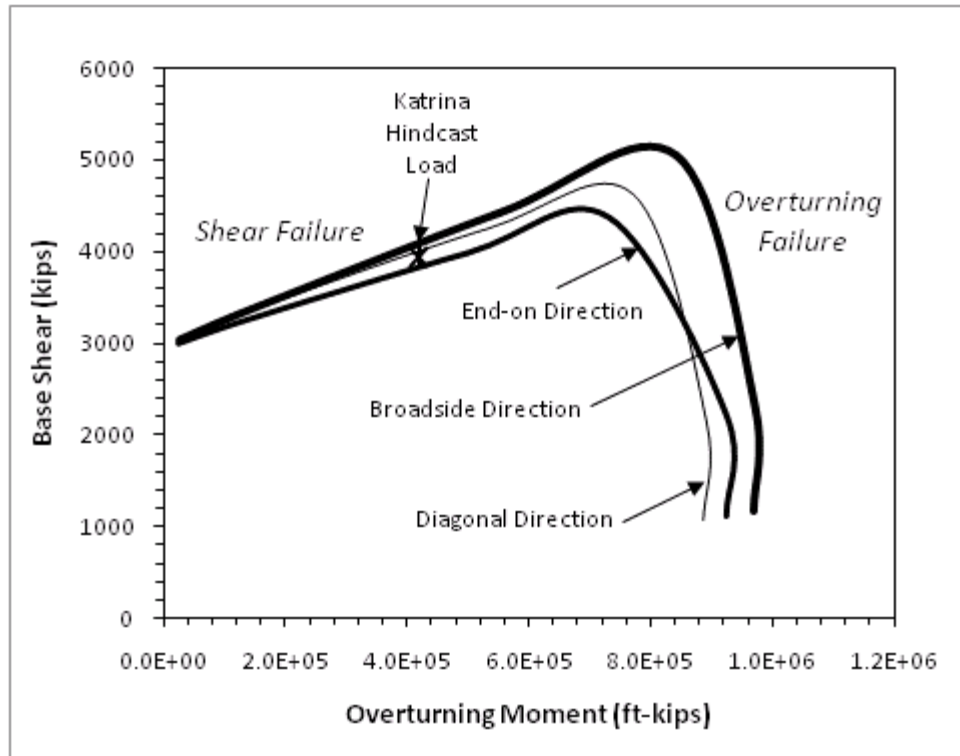


Figure 5.23 Sensitivity Analyses of Foundation System Capacity to Loading Direction for Platform 30

5.3. Importance of Structural Factors in Foundation System Capacity

While foundation capacity is generally associated with geotechnical factors such as the strength of the soil, structural factors also affect the capacity of the foundation system:

- The moment capacity of piles and conductors affects the shear capacity of the foundation system (e.g., Figure 5.21).
- Well conductors can provide a significant contribution to the shear capacity of the foundation system if the structural framing allows the development of this

- contribution (e.g., Figure 5.22).
- The relative flexibility of an individual pile can affect its axial capacity in clay layers that are susceptible to strain softening (e.g., Figures 4.9, 5.11 and 5.12).
 - The rigidity or strength of the jacket structure can affect the capacity of the foundation system because it affects the ability of the structure to redistribute loads as individual piles are loaded to their capacity (e.g., Figure 4.8).
 - Mudmats and other structural framing at the mudline can potentially contribute to resisting overturning if they bear on or in the soil. However, the contribution of these elements to the overturning capacity of the foundation is typically small since they are bearing on the relatively weak soils near the mudline and would require deformation much greater than that required to mobilize pile capacity. For the few cases where these elements bear on relatively strong soils, the presence of these elements can potentially help in understanding the discrepancy between the observed and calculated capacities.

These points underscore the importance of considering the piles and conductors as one of many members that make up the structural system.

5.4. Importance of Sand

Sand layers contribute to the axial and lateral pile capacity in 11 out of the 12 Case Study Platforms (Platform 10 is the single exception). Furthermore, the contribution of sand layers to pile capacity is substantial in the majority of these platforms. This finding was unexpected as marine clays are the dominant soil type for pile foundations in the areas of production in the Gulf of Mexico. However, many of the platforms that were loaded heavily in these recent hurricanes are located on the shelf in areas where there are significant deposits of sand.

Sand layers are generally associated with a complex and variable geologic setting, such as alluvial (or fluvial) deposits laid down by meandering streams and rivers. There can be large variations in soil stratigraphy and properties over relatively short distances of less than one hundred feet in these settings. As an illustration, the soil profile for Platform 1 is compared with that for Platform 30 in Figure 5.24. While these two locations are from the same geologic setting several miles apart, the stratigraphy is significantly different.

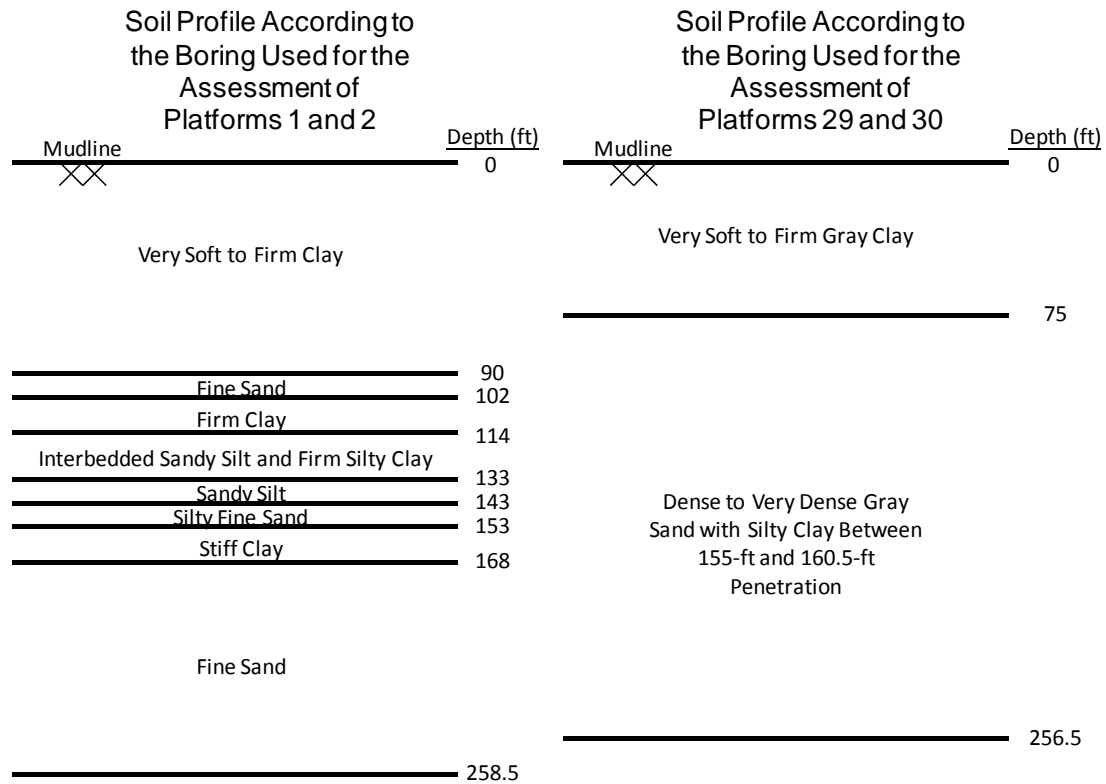


Figure 5.24 Comparison of Stratigraphy at Two Locations in Similar Geologic Setting

Sand layers can be difficult to characterize with soil borings if the layers are too dense to penetrate. The boring log from the 1979 boring drilled in the vicinity of Platforms 1 and 2 is shown in Figure 5.25. The density and strength of the sand layers is determined from the penetration resistance for the driven sampler in the column labeled “Blow Count” in Figure 5.25. For the sand layers at and below the tip of the pile, the sampler met refusal as indicated by the entry of 30 for the blow count; once 30 blows were reached, they would stop driving the sampler if it had not penetrated at least 2 feet. Therefore, the inferred classification of this sand layer as Medium Dense in the API Design Method versus higher categories of Dense or Very Dense is debatable. The log for a more modern Cone Penetration Test conducted about 3 miles away in the same geologic setting is shown in Figure 5.26. This log shows that even the cone was not able to penetrate the sand layers about 140 feet below the mudline (which may or may not be the same sand layers as those at the location of the boring in Figure 5.25), and that these layers were classified as Very Dense at this location. The sensitivity of the foundation capacity to this classification of density is illustrated in Figures 5.17 and 5.18.

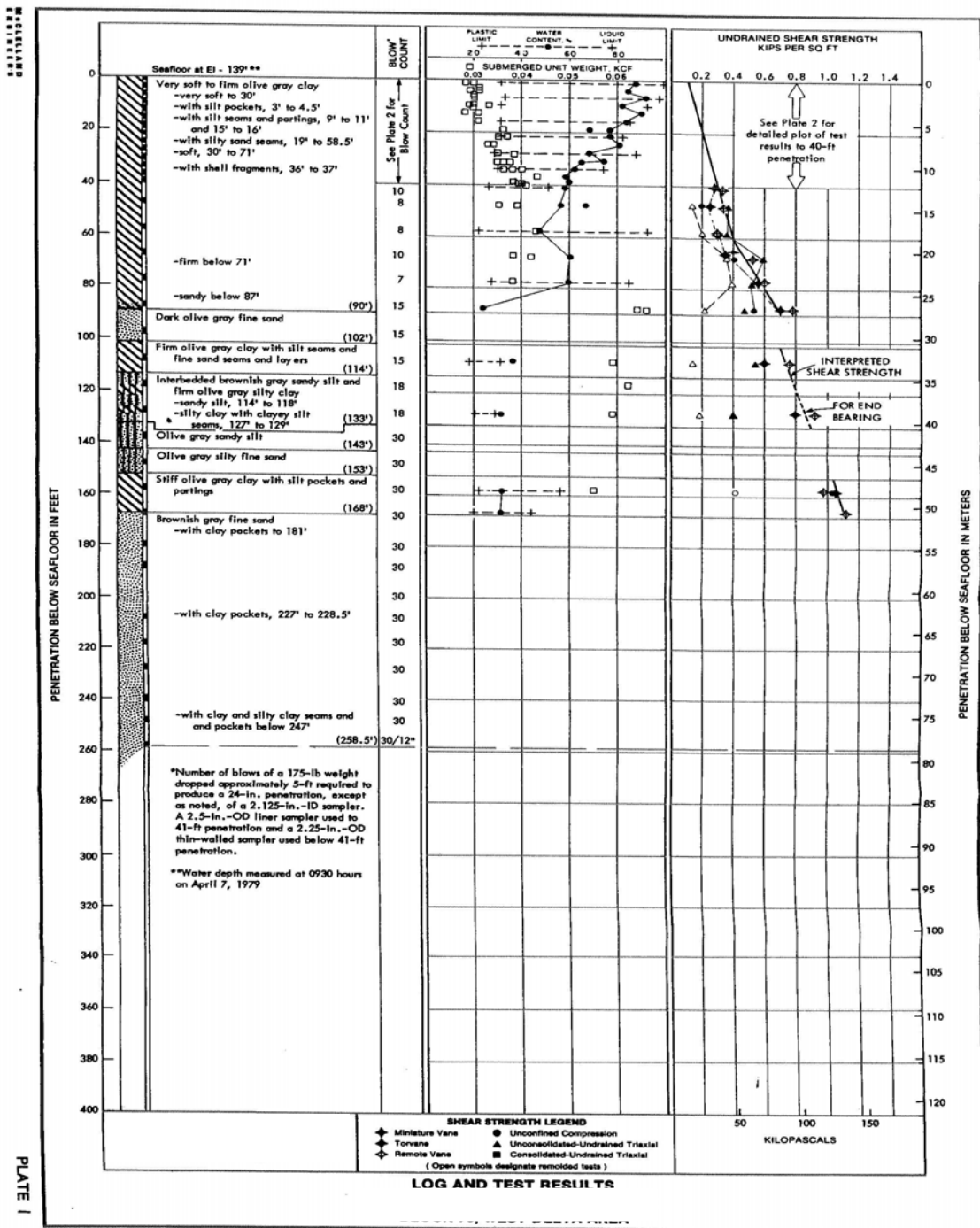


Figure 5.25 Boring Log Used in the Assessments of Platforms 1 and 2 (McClelland 1979)

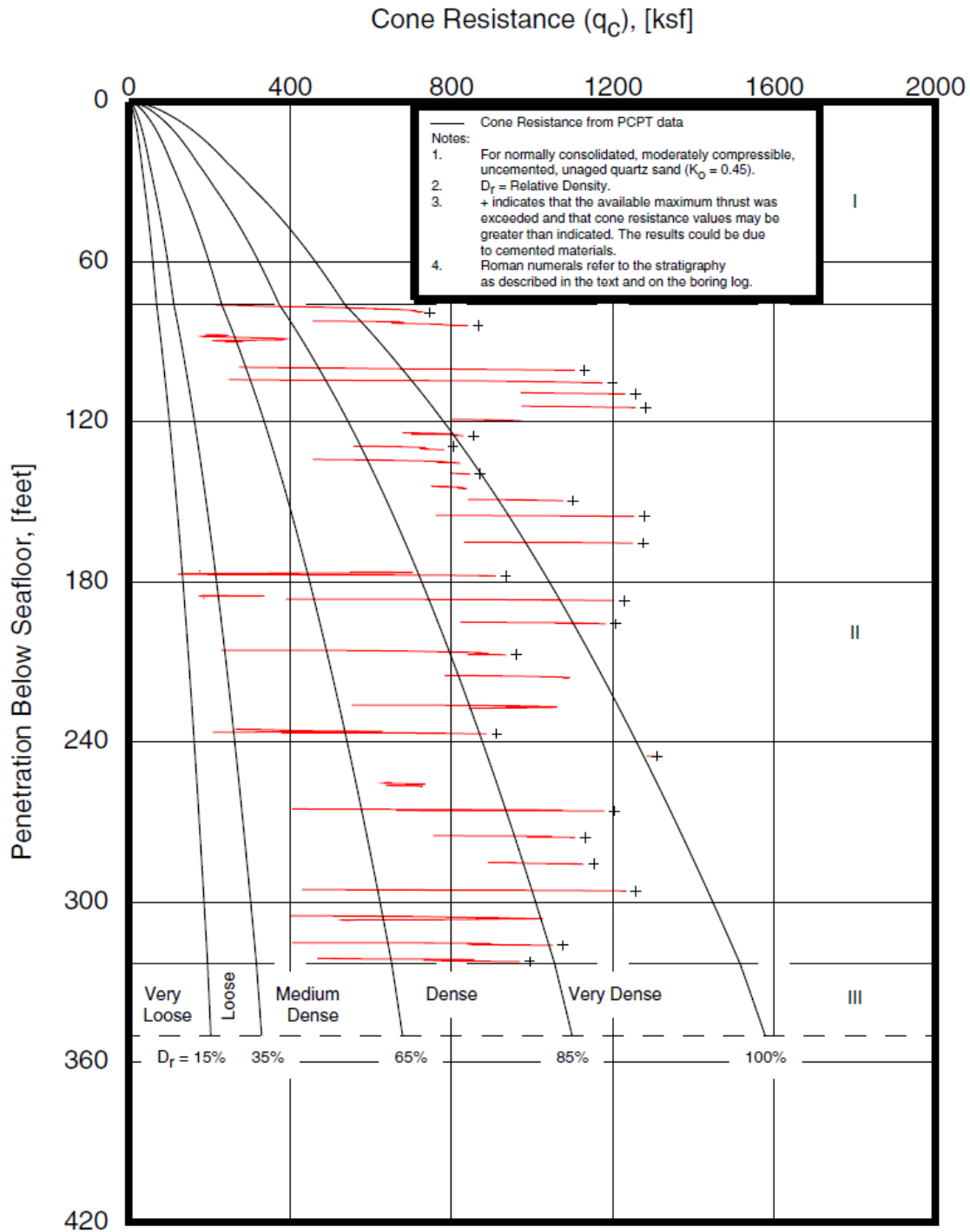


Figure 5.26 Cone Resistance from a CPT Performed in the Neighboring Block of Platforms 1 and 2 (Fugro-McClelland 2005)

The refusal of the cone penetrometer and the practice of performing cone penetration tests in a borehole in most offshore applications result in a discontinuous cone tip

resistance profile (Figure 5.26). Furthermore, the cone tip resistance value increases significantly from the beginning of the push to cone refusal. Engineering judgment is required to develop a “design” cone tip resistance profile in order to use CPT-based methods to estimate axial pile capacity. This process naturally introduces uncertainty in the estimated axial pile capacity (that is, the capacity estimated by different geotechnical engineers will likely be different). As such, qualified geotechnical engineers who are experienced in interpreting CPT data and understand the limitations and reliability of these CPT-based methods are required to provide a sound estimate of pile capacity.

Sand layers are also more complicated to model in a pushover analysis. In order to calculate pile capacity for axial and lateral loading, clay layers require three input parameters while sand layers require eight input parameters (Table 2.1). In reviewing pushover analyses, we commonly found errors in the input values used for sand layers. Examples of errors included using $K = 1.0$ (the program default) instead of $K = 0.8$ (the API design method¹), inter-changing the soil-pile interface friction angle δ and the internal friction angle ϕ' (δ is used to calculate axial capacity and is generally assumed 5 degrees smaller than ϕ' , which is used to calculate lateral capacity), and using values of limiting unit side shear or unit end bearing that were not consistent with the other input parameters for that layer. These seemingly small errors in modeling can have a large impact on the assessment, as shown in Figure 5.27.

The most recent errata and supplement of API RP 2A published in October 2007 (Errata and Supplement #3) presents a new table (Table 6.4.3-1) for the design parameters of sand. In this table, K and δ are combined into a dimensionless shaft friction factor, β , which relates the effective overburden pressure to the unit side shear (shaft friction). With the introduction of this new table and future updates of the software packages used for pushover analyses, it is less likely for structural engineers to make the mistakes discussed

¹ API RP 2A-WSD (2000) recommends a K value of 0.8 for both tension and compression loadings of open-ended pipe piles driven unplugged and a K value of 1.0 for full-displacement piles (plugged or closed end). The default value of K in the software for pushover analyses is often set to be 1.0. It is common practice for offshore geotechnical engineers to use a K value of 0.8 for open-ended pipe piles in both tension and compression loadings because the “coring mode” usually dominates when the open-ended pipe piles are driven and, therefore, they are driven unplugged. Unfortunately, K values are not typically recommended or specified in the geotechnical reports. Consequently, most pushover analyses we reviewed were performed with a default K value of 1.0 and the foundation capacities were overestimated.

previously. However, care is still warranted to make sure that the design parameters (β , f_{lim} , N_q and q_{lim}) are consistent for a given sand layer.

In addition to the new table for the design parameters of sand, the errata and supplement also present four different CPT-based methods to estimate the axial capacity of piles in sand. These methods are all based on direct correlations of pile unit friction and end bearing data with cone tip resistance (q_c) value from cone penetration tests. These CPT-based methods are considered more reliable than the method presented in the main text. However, more experience is required before any single method can be recommended for the purposes of design or assessment.

Estimating pile capacity in sand layers is generally considered to be more difficult than for clay layers, and there is more uncertainty in these estimates (e.g., Pelletier et al. 1993 and Tang and Gilbert 1993). Greater uncertainty naturally leads to greater conservatism in estimating the capacity for the purposes of design. Therefore, all other factors aside, it is not surprising that the two platforms with the largest discrepancy between the observed and predicted performance, Platforms 1 and 2, have sand layers that contribute significantly to the pile capacity (e.g., more than 70 percent of the axial capacity for the piles in Platform 1 is contributed by sand layers).

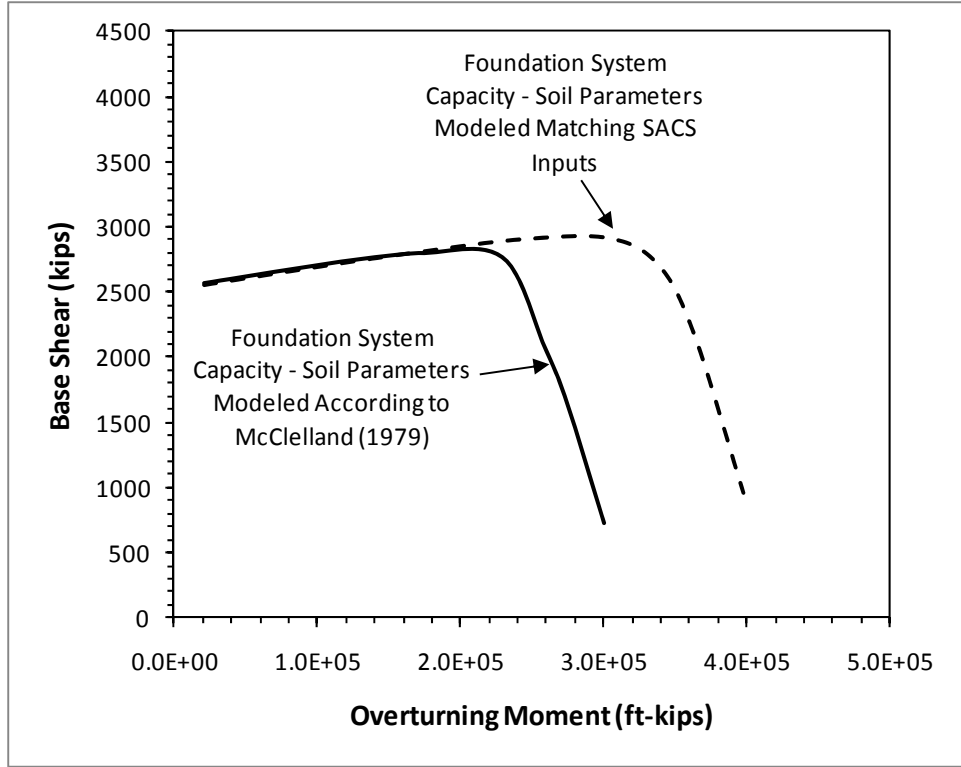


Figure 5.27 Foundation System Capacity Interaction Diagram from Plasticity Model of Platform 1 Comparing the Correct Design Input for the Sand Layers with the Incorrect Input Used in the Pushover Analysis

6. Practical Guidance for Platform Assessments

Guidance developed from the findings of this project are summarized in this chapter. The guidance is organized into four categories: (1) Specific guidelines for how foundations are modeled in platform assessments; (2) General guidance to improve the practice of platform assessment; and (3) Recommendations for updating the API Recommended Practice documents for platform design and assessment. Three illustrative examples are presented at the end to demonstrate how to implement this guidance in practice. The notes from an expert panel meeting that was held to help formulate this guidance are provided in Appendix F.

6.1. Guidelines for Modeling Foundations in Platform Assessments

The following guidelines are intended to provide a defensible and consistent approach for modeling pile foundations in platform assessments:

1. When the foundation controls the assessment, include a geotechnical engineer familiar with platform assessment. As in structural engineering, there are aspects of geotechnical engineering that cannot be fully captured in a design standard or recommended practice, including the basis and context for design recommendations. Practical experience and expertise as a geotechnical engineer is essential to understand how pile foundations should be modeled in platform assessment. In addition, assessment is different than design so, as with structural engineering, there is a need for the geotechnical engineers involved in a platform assessment to be familiar with assessment as well as design.
2. Include well conductors realistically and explicitly in the structural analyses. Well conductors should be modeled the same as pile foundations below the mudline, considering compatibility between forces and displacements in the conductors and the soil. Care should be exercised in how the jacket framing that constrains and engages the conductors is modeled so that the lateral displacements of the conductors at the mudline are consistent with the behavior of the overall jacket under a given loading condition, and that the conductor framing will fail at the appropriate loading levels. In structural analyses, conductors should not be pinned at the mudline and should not be connected rigidly to the jacket.

3. Consider using mean rather than nominal yield strength for steel piles and well conductors. The nominal yield strength is not the most likely or expected value, rather a conservative estimate (Energo 2009). In a platform assessment, the objective is to model the structure and the soil as accurately as possible and to assess its ultimate capacity without any additional factor or margin of safety. Therefore, unbiased, not conservative, estimates for input values should be used.
4. Use static versus cyclic p-y curves for lateral soil capacity. As pointed out by Aggarwal et al. (1996) in conducting pushover analyses on platforms loaded by Hurricane Andrew, the ultimate capacity of the platform system in shear is reached as the piles push laterally at large displacements into undisturbed soil. Therefore, the degradation effects of cyclic loading at relatively small displacements prior to the point at which the ultimate capacity is reached will not affect the ultimate lateral capacity at large displacements. This approach is supported by both experimental data and numerical analyses (e.g., Murff and Hamilton 1993; Hamilton and Murff 1995 and Jeanjean 2009).
5. Be careful in specifying the input for sand layers. Make sure that the earth pressure coefficient, K , is set to 0.8 unless otherwise specified by geotechnical engineers. Make sure that the soil-pile interface friction angle, δ , is not inter-changed with the soil internal friction angle, ϕ' (δ should be less than ϕ' by about 5 degrees). Make sure that the values for limiting side shear and limiting end bearing are consistent with the values input for δ and the end bearing factor, N_q (all four values should correspond to the same API category). The newest supplement for foundation design in API RP 2A (Errata and Supplement #3) is an attempt to minimize errors in modeling sand layers by reducing the number of parameters that are specified, and can be used for quality control to back check the input by ensuring that the input values for K and δ produce the equivalent value for β in Errata and Supplement #3. However, the commercial software packages available for pushover analyses need to be updated to incorporate this simpler approach for modeling sand layers.

6.2. General Guidance for Platform Assessments

In addition to the specific guidelines for how foundations are modeled in platform assessments, the following general guidance is provided to improve the overall practice of platform assessment:

1. Be careful when relying on a soil boring that was not drilled at the location of the platform or was not drilled using modern methods of sampling and testing (pushed, thin-walled tube sampling for clay layers and Cone Penetration Test for sand layers). Particular care is needed in geologic settings that are spatially variable, as in areas with fluvatile deposits where clay and sand layers are interbedded. In such deposits, even having a boring within the 500 foot distance required by MMS (30CFR 250.907) is not necessarily an accurate reflection of the depth, thickness and density of sand layers at the platform site. When a modern, site-specific boring is not available, sensitivity analyses are warranted. Information from several borings in the platform vicinity together with consultations with geotechnical engineers will help to guide these sensitivity analyses.
2. Try to obtain pile driving records as well as soil boring logs to help estimate the axial pile capacities. Pile driving records could be particularly useful in cases where there are questions about the stratigraphy or densities of sand layers or the actual final penetrations of the piles. In addition, pile driving records will indicate the actual depths where the pile wall thickness changes, which can be important for lateral pile capacity. Finally, these records may indicate that stronger steel was used for piles or conductors than was specified in design.
3. When the pile foundation system is governing the capacity of the platform in a pushover analysis, check the sensitivity of the foundation system capacity to the lateral and axial capacity of the piles independently. This sensitivity analysis can be implemented in practice by first changing the shear strength of the soils (the shear strength is being used here as a surrogate for the lateral soil resistance) in the upper 50 feet of the piles to assess the sensitivity to lateral resistance in piles and conductors and then changing the shear strength of the soils below 50 feet to check the sensitivity to axial resistance (the shear strength is being used here as a surrogate for the axial side shear and end bearing resistance). If the foundation system capacity is more sensitive to the lateral soil resistance, then the failure mechanism is probably shear and there are a variety of structural factors to consider in the assessment, especially the bending moment capacities of the piles and conductors. If the foundation system capacity is more sensitive to the axial soil resistance, then the failure mechanism is probably overturning and geotechnical factors such as the stratigraphy and the soil properties are an important consideration in the assessment. Also, carefully check to see if other

structural members are prematurely failing and reducing the effectiveness of the structure to redistribute loads among the piles and well conductors.

4. Do not arbitrarily increase the shear strength of the soil to account for perceived conservatism in foundation design. The information we have to date suggests that the performance of platform foundations in hurricanes is consistent with their design. While there are well-documented sources of potential conservatism in foundation design, with the primary factor probably being increases in capacity with time due to long-term set-up (or aging) and preloading, increasing the shear strength used to calculate lateral or axial capacity by more than a factor of two is not supported by any available information. In addition, we do have evidence from Hurricane Ike of an axial pile failure in a normally consolidated clay occurring approximately five years after installation at a load essentially equal to the design capacity. When large increases in soil shear strength (factors of two or more) are needed to explain a platform survival in a hurricane, look for the following explanations to these large increases:

- If the axial capacity of the pile is mostly due to sand layers acting in side shear or end bearing, then increasing the undrained shear strength of clay layers alone (which is common practice due to simplicity) may have very little impact on the axial capacity. A large increase in clay shear strength may be necessary to achieve a relatively modest increase in axial pile capacity.
- If the pile system is failing in shear, then the capacity of the system is much more sensitive to the bending capacity of the piles and conductors than to the shear strength of the soil. A relatively small increase in bending moment capacity (such as steel yield strength change from nominal to mean) may have a larger effect on the capacity of the pile system than a relatively large increase in the shear strength of the soil.
- Recognize that the shear strength of the soil is being used as a convenient surrogate for lateral and axial soil resistance since the soil shear strength can be changed easily as input to a pushover analysis. However, the relationship between lateral or axial soil resistance and shear strength is not direct or proportional. Increasing the undrained shear strength of clay layers causes the clay to be treated as more heavily overconsolidated in the design recipe for axial side shear; in this case, the greater the undrained shear strength the less sensitive the axial capacity will be to an increase in the undrained shear strength. For example with a normally consolidated clay,

increasing the undrained shear strength by two times only increases axial side shear by 40 percent; increasing undrained shear strength by four times only increases axial side shear by two times; and increasing undrained shear strength by ten times only increases axial side shear by four times. Also, increasing the shear strength for sand layers may have no impact if limiting values control axial side shear or end bearing.

6.3. Recommendations for API Recommended Practice

The following recommendations are intended to improve the API Recommended Practice for Platform Assessment:

1. Provide specific guidance for characterizing pile foundations in platform assessments, incorporating the information in Sections 6.1 and 6.2 of this report into a code format suitable for RP 2SIM.
2. Update p-y curves for clay in API RP 2A. There is ample evidence now available (e.g., Jeanjean 2009) that the ultimate lateral capacity and the lateral soil stiffness for piles in normally consolidated clay layers are both greater than what is recommended at present by API. While this change will not impact many new designs since newer platforms are generally in deeper water and the foundation capacity is governed by overturning, this change is important in assessing older platforms and should be included in RP 2SIM per the previous recommendation.
3. Better clarify and update design guidance for sand in API RP 2A. Include the simpler approach for specifying design parameters for sand that has been published as a supplement (Errata and Supplement #3) into the main document. Provide specific guidance on how to incorporate split spoon sampler or cone refusal in estimating density or unit side shear and unit end bearing. Also provide specific guidance on how to treat layered profiles with interbedded clay and sand layers, particularly in estimating unit end bearing.
4. Appropriately account for pile flexibility when determining the required pile length. While the API RP 2A recommends that pile flexibility be included, our understanding of current practice is that pile lengths are selected on the basis of design curves provided in geotechnical reports that may assume a perfectly rigid pile. The discussion about this issue in RP 2A should be made more forceful and specific guidance should be provided so that pile flexibility can be included practically in design calculations.

6.4. Illustrative Examples for Platform Assessments

Three illustrative examples are provided in this section to demonstrate how to incorporate the practical guidelines discussed in Sections 6.1 to 6.3 in the post-hurricane assessments of platforms.

6.4.1. Pushover Capacity Governed by Foundation Overturning when Piles Embedded in Inter-bedded Layers of Sands and Clays

Inter-bedded layers of sands and clays are commonly found in water depths less than about 300 feet, especially in the areas where old river or stream valleys formed during periods of low sea level. Because these areas are generally closer to the coastline, platforms located in these areas tend to be older ones, designed with older soil borings and older versions of the API RP 2A. The presence of even a relatively small amount of sand can have a large impact on pile capacity because sand layers generally provide greater side shear, end bearing and lateral resistance than clay layers.

Geotechnical engineers tend to be more conservative in making foundation recommendations when inter-bedded layers of sands and clays are present. Driving piles through inter-bedded layers of sands and clays can result in the dragdown of fine-grained materials (silts or clays) through the soil-pile interface into the coarse-grained materials (sands or gravels) below. Dragdown of fine-grained materials causes a reduction in the side shear capacity of piles. As a result, the geotechnical engineers tend to recommend a lower design category for the sands, either by assigning a material type with fines or a lower density than measured in the boring. Also, the densities of sands can be underestimated due to the standard of practice for drilling and sampling in the past, Driven Penetration Testing. When a refusal blowcount of 30 is reached before 2 feet of penetration in this test, the test is stopped. In addition, the length of the rods, the efficiency of the driving hammer and the presence of fines can all affect the measured blowcounts. Therefore, it is difficult to estimate the density of sand layers accurately with this test, and geotechnical engineers will generally err conservatively in developing design parameters.

The following additional information would be useful in assessing a platform where axial

pile capacity is important and is affected by sand layers. Pile driving records can provide information to better estimate soil stratigraphy (e.g., is the pile tip in sand), side shear and end bearing resistance in sand layers, and pile length, which may be different from design due to driving problems that can occur when sand layers are present. Soil borings from within the vicinity of the platform, particularly any Cone Penetration Tests if available, can provide information on the possible variations in the depths and thicknesses of sand layers as well as their densities.

The following sensitivity analyses should be considered when sand layers are significant to axial pile capacity and pushover capacity:

- Increase the shear strength of the soils that are deeper than 50 feet from the mudline to confirm that the foundation capacity is governed by overturning. Increase the shear strength of both clay and sand layers. This increase will affect the axial capacity but not the lateral capacity of the piles and will increase the pushover capacity if it is governed by overturning but not if it is governed by shear.
- Upgrade the design categories for sand layers at all piles by increasing the assumed relative density (e.g., use the parameters for a Dense Sand-Silt instead of a Medium Dense Sand-Silt) or the gradation (e.g., use the parameters for a Medium Dense Sand instead of a Medium Dense Sand-Silt). This sensitivity check will indicate how potential conservatism in assigning design parameters for sand layers, particularly if the design was based on an older soil boring with Driven Penetration Testing, might affect the pushover capacity of the platform.
- If there is a question about in which layer the piles tip in (e.g., a sand versus a clay layer), then shorten or lengthen the piles to determine how this uncertainty might affect the pushover capacity. Assume reverse end bearing for piles that are in tension. There is ample evidence that has been compiled in developing foundations for deep water structures and since the API RP 2A code was developed for jackets to suggest that piles can develop reverse end bearing under rapid loading in both clay and sand layers (e.g., API RP 2SK 2005).
- Increase the yield strength for jacket members above the mudline to account for nominal bias (Energo 2009) in order to establish how the overturning capacity might be affected by the effectiveness of the structure in redistributing loads as piles reach their axial capacities.

Care is required in developing the input to a pushover analysis when sand layers are present in the foundation in order to ensure that all eight input parameters (Table 2.1) are

consistent with API RP 2A.

6.4.2. Pushover Capacity Governed by Foundation Overturning when Piles Embedded in Clays

In water depths greater than about 300 feet, marine clays are present and dominant in the subsurface profiles. These marine clays are typically normally consolidated to moderately overconsolidated. Piles in these settings tend to be relatively long and derive most of their axial capacity from side shear.

The standard of practice for soil borings until about 1980 was wireline percussion with driven sampling. In the last few decades, the standard of practice has changed to the pushed sampling method with larger thin-walled samplers and in situ testing, meaning that the measured undrained shear strengths more closely resemble the in situ conditions and tend to be higher. Quiros et al. (1983) investigated how the differences in sampling and testing affect the measured shear strengths by drilling older and modern borings adjacent to one another; they found that the older methods produced measured strengths that were about 30 percent lower than the modern methods. However, the differences in how the undrained shear strength is measured were and have been implicitly included in developing design profiles. In other words, the design profile of undrained shear strength versus depth from an older boring is expected to be about the same as that from a modern boring drilled at the same location. Gambino and Gilbert (1999) found that the difference in design undrained shear strength developed from older and modern soil borings was less than 10 percent on average in an analysis from boring data for one offshore field in Asia.

The major uncertainties in estimating axial capacity for piles in clays are the potential increases in capacity due to rate of loading and aging and the potential decreases in capacity due to cyclic degradation and strain softening. In the design method, the rate of loading and cyclic degradation effects are assumed to compensate for one another, aging is not considered and strain softening is considered.

The following sensitivity analyses should be considered when clay layers are significant to axial pile capacity and pushover capacity:

- Increase the undrained shear strength for clay layers deeper than 50 feet from the mudline to confirm that the foundation capacity is governed by overturning. This

increase will affect the axial capacity but not the lateral capacity of the piles and will increase the pushover capacity if it is governed by overturning but not if it is governed by shear.

- Increase the undrained shear strength of all clay layers by 30 percent to account for the possibility of rate effects dominating cyclic degradation effects in wave loading or the possibility of aging. An increase of much more than 30 percent is possible, but not supported by available information to date. In addition, an increase of 30 percent is not necessarily available and should not be assumed but only checked in a sensitivity analysis.
- Assume full strain softening (corresponding to 70 percent of the peak side shear) and no strain softening (corresponding to the peak side shear) to provide lower- and upper-bounds for the axial pile capacity.

6.4.3. Pushover Capacity Governed by Foundation Shear

In shallower water (relative to the width of the structure), the foundation capacity tends to be governed by shear and the lateral capacities of the piles and conductors. Because these platforms are generally located closer to the coastline, they tend to be older structures.

The lateral resistance is derived from soils in the upper 40 to 50 feet below the mudline, which are mostly very soft to soft clays. The clays near the mudline can be difficult to sample and test. Therefore, profiles of the design undrained shear strength near the mudline tend to be conservative. In addition, there is ample information (e.g., Jeanjean 2009) that the p-y curves for soft clays are stiffer and stronger than API RP 2A suggests by as much as 50 percent (e.g., Jeanjean 2009). In addition, the cyclic degradation of clay strength from wave loading will probably not affect the ultimate pushover capacity since the piles will push into undisturbed clay when they approach failure. There are two cases in our database where thin (less than 10 feet) sand layers are present immediately below the mudline. The depth of these layers can be important if they are in the vicinity of where the second hinge forms in the pile (about 40 to 50 feet below the mudline).

The capacities of foundations in shear will generally be much more sensitive to the bending moment capacities of the piles and conductors than to lateral resistance provided by the soil. Structural considerations include the yield strength of the steel, the effect of jacket legs penetrating below the mudline, the effect of inner casing strings within well conductors, and the framing details for how the conductors interact with the jacket.

The following sensitivity analyses should be considered when lateral pile capacity is important to the pushover capacity:

- Use static and not cyclic p-y curves.
- Increase the design undrained shear strength by 50 percent for clay layers within 50 feet from the mudline to increase the stiffness and lateral resistance provided by the soil. This increase in shear strength is actually a surrogate for increasing the ultimate lateral resistance that the soil provides the pile; in actuality, this increase in lateral resistance reflects a more realistic representation of the failure mechanism for the pile moving through the soil. Do not increase the undrained shear strength below 50 feet as this change will inadvertently increase the axial pile capacity as well.
- Increase the yield strength of the steel in piles and conductors to account for bias in the nominal design value (Energo 2009).
- Account for the penetration of jacket legs below the mudline.

7. Conclusions and Recommendations

The objectives of this project were to determine the level of conservatism in foundation design for the purposes of platform assessment, to identify and analyze the factors that may contribute to the conservatism, and to provide guidance on how to incorporate this information in assessing existing platforms. The methodology was to compile and analyze data for existing platforms that have been subjected to loads near or greater than the design capacity for the foundations. An expert panel of practitioners and researchers was convened to guide the work.

7.1. Conclusions

The major conclusion from this work is that the performance of platform foundations in recent hurricanes, based on the available but limited information that we have, is consistent with expectations based on their design and there is no direct evidence of excessive conservatism. In the cases we analyzed in detail, the following results were obtained:

- In five cases where the platforms were loaded to less than the design capacities of the foundation systems, there were no indications of foundation system failures.
- In four cases where the platforms were loaded to near or beyond the shear capacity of the foundation system, there were no indications of foundation system failures. This result is expected because there are many factors beyond the lateral capacity of individual piles, including reserve capacity in the structural components (e.g., steel being stronger than the nominal strength), which can contribute to the shear capacity of the foundation system for a jacket.
- In the one case we have of a reasonably definitive foundation failure, the platform was loaded to the design axial capacity of the foundation and an overturning failure of the foundation system apparently occurred. This result is not surprising because the foundation was loaded to its capacity and the platform is a tripod structure with little redundancy to overturning.
- There is one pair of bridge-connected platforms (Platforms 1 and 2) that did not experience foundation failures even though they were possibly loaded well beyond the overturning capacities of the foundation systems. However, a site-specific soil boring is not available for these platforms and the subsurface

conditions in this geologic setting are highly variable with significant layers of sand, making the inference of design capacities questionable in this case.

These results do not preclude the possibility of foundation capacities being greater than expected based on design. One of the limitations of this study was lack of cases from recent hurricanes where the ultimate strength of the foundation system was reached or exceeded in hurricanes. Foundations are designed with a factor of safety, such as a factor of 1.5 for axial loading under 100-year hurricane conditions. The magnitude of hurricane conditions required to reach this value is significant, requiring extreme waves and currents, and was not reached in most of the cases studied (i.e., a foundation failure was not expected and indeed was not observed). Of all the cases obtained from MMS files and industry sources, there were unfortunately only a few that met the high loading condition required to truly test the foundation. In addition, there is redundancy in foundation systems so that overload of a pile, either axially or laterally, does not necessarily lead to collapse or even observable damage. Finally, the study was limited to platforms that were not destroyed since little if any information is available about the performance of platforms that were destroyed.

The major factor contributing to potential conservatism is the effect of set-up or pre-loading; there is evidence from laboratory and field studies to suggest that both axial and lateral pile capacities may increase with time beyond the values that are assumed for design. However, we do not have any direct evidence of these effects in the performance of actual platform foundations. In the cases where the platform foundations survived hurricane loading, there are plausible explanations for these survivals that do not involve increasing the capacity of the foundation above the design value. Also, in the one case where we do have of a foundation failure (an axial pile failure in clay), there is no evidence of the capacity being greater than the design value.

Platform foundations can fail both in shear where the piles are failing laterally (plastic hinges forming due to bending) and overturning where the piles are failing axially (plunging or pulling out). Therefore, both axial and lateral capacities are significant for pile foundations in platforms. The axial capacity of piles is derived mostly from the soils in the bottom one-third of the pile length. The axial capacity of the piles and, therefore, the overturning capacity of the foundation are approximately proportional to the shear strength of the soils along the length and at the tip of the piles. The lateral capacities of the piles and conductors are derived mostly from the soils in the upper 40 to 50 feet

below the mudline depending on their diameters. The lateral capacities of the piles and conductors and the shear capacity of the foundation are much less sensitive to the shear strength of the soils than the axial capacity for typical soil conditions in the Gulf of Mexico.

Structural elements are important to the performance of a foundation system. Well conductors can contribute significantly to the shear capacity of a foundation system, and in some cases to the overturning capacity. The yield strength of steel in the piles also affects the shear capacity of the foundation. Increasing the nominal yield strength to reflect an average value can have a significant effect on the shear capacity for a foundation system, and a much greater effect than increasing the shear strength of the soil by the same amount.

The presence of sand layers contributing significantly to pile capacity was a notable factor in the platforms analyzed herein. Sand is significant because it generally corresponds to a geologic setting where there is significant spatial variability over rather short distances. Therefore, a soil boring not drilled at the location of a platform, even if it is within several hundred feet, may not provide representative information for the soil conditions at the platform location. In addition, most historical soil borings in the Gulf of Mexico used a Driven Penetration Test to characterize the shear strength of sand layers. This method is generally considered to be outdated, it may not have fully penetrated the sand layers due to sampler refusal, and it has been replaced over the past several decades with Cone Penetration Testing. Finally, pile capacity models when sand layers are present are more complex than for clay layers alone, and we identified numerous cases where sand layers were inappropriately modeled in pushover analyses due to this complexity.

A final conclusion is that general trends in foundation performance cannot be drawn easily based on qualitative assessments. Each platform case, considering the water depth, vintage, structure, geologic setting, hurricane loading and platform performance, is unique and a detailed analysis is required to understand how it performs.

7.2. Recommendations for Practice

The following guidelines are intended to provide a defensible and consistent approach for modeling pile foundations in platform assessments:

1. When the foundation controls the assessment, include a geotechnical engineer familiar with platform assessment.
2. Include well conductors realistically and explicitly in the structural analyses.
3. Consider using mean rather than nominal yield strength for steel piles and well conductors.
4. Use static versus cyclic p-y curves for lateral soil capacity.
5. Be careful in specifying the input for sand layers.

In addition to the specific guidelines for how foundations are modeled in platform assessments, the following general guidance is provided to improve the overall practice of platform assessment:

1. Be careful when relying on a soil boring that was not drilled at the location of the platform or was not drilled using modern methods of sampling and testing (pushed, thin-walled tube sampling for clay layers and Cone Penetration Test for sand layers).
2. Try to obtain pile driving records as well as soil boring logs to help estimate the axial pile capacities and as-built conditions.
3. When the pile foundation system is governing the capacity of the platform in a pushover analysis, check the sensitivity of the foundation system capacity to the lateral and axial capacity of the piles independently.
4. Do not arbitrarily increase the shear strength of the soil to account for perceived conservatism in foundation design.

The following recommendations are intended to improve the API Recommended Practice for Platform Assessment:

1. Provide specific guidance for characterizing pile foundations in platform assessments by incorporating the guidelines developed in this study into RP 2SIM.
2. Update p-y curves for clay in API RP 2A.
3. Better clarify and update design guidance for sand in API RP 2A.
4. Appropriately account for pile flexibility when determining the required pile length.

7.3. Recommendations for Future Work

A major limitation of this study was not analyzing platforms that were destroyed by hurricanes. If detailed analysis could be conducted on these platforms, they may provide valuable information about how pile systems and the jackets they support performed under extreme loading conditions and may allow us to refine our conclusions. In addition, there may be additional platforms that survived even though the pile systems experienced loads greater than their capacity. Such platforms should be considered for future study. Finally, performing a Cone Penetration Test at the location of the two case study platforms where we are uncertain about the geotechnical properties (Platforms 1 and 2) could provide important information to better understand why those structures survived.

8. References

- Aggarwal, R.K., Litton, R.W., Cornell, C.A., Tang, W.H., Chen, J.H. and Murff, J.D. (1996). "Development of pile foundation bias factors using observed behavior of platforms during Hurricane Andrew," Offshore Technology Conference, Houston, Texas, OTC 8078, pp. 445-455.
- American Petroleum Institute (2000). *Recommended Practice for Planning, Designing and Constructing Fixed Offshore Platforms – Working Stress Design*, API RP 2A-WSD, 21st edition (with Errata and Supplement #3, October 2007).
- American Petroleum Institute (2005). *Recommended Practice for Design and Analysis of Stationkeeping Systems for Flooding Structures*, API RP 2SK, 3rd edition.
- Bea, R.G., Jin, Z., Valle, C. and Ramos, R. (1999). "Evaluation of reliability of platform pile foundations," *Journal of Geotechnical and Geoenvironmental Engineering*, ASCE, Vol. 125, No. 8, pp. 695-704.
- Bogard, D., and Matlock, H. (1998). "Static and cyclic load testing of a 30-inch-diameter pile over a 2.5-year period." *Proc., Offshore Technol. Conf.*, Vol. 1, Houston, 455–468.
- Carpenter, J.F. (2009). *Effect of Well Conductors on the Lateral Capacity of Fixed Offshore Platforms*, Master Thesis, The University of Texas at Austin.
- Chow, F. C., Jardine, R. J., Brucy, F., and Nauroy, J. F. (1996). "The effects of time on the capacity of pipe piles in dense marine sand." *Proc., Offshore Technology Conf.*, Vol. 1, Houston, 147–160.
- EnergO Engineering, Inc. (2006). *Assessment of Fixed Offshore Platform Performance in Hurricanes Andrew, Lili and Ivan*, Final Report to Minerals Management Service.
- EnergO Engineering, Inc. (2007). *Assessment of Fixed Offshore Platform Performance in Hurricanes Katrina and Rita*, Final Report to Minerals Management Service.
- EnergO Engineering, Inc. (2009). *Evaluation of Yield Stress for Steel Members in Gulf of Mexico Fixed Platforms*, Final Report to American Petroleum Institute.
- Engineering Dynamics, Inc. (2005). *Collapse Release 6 User's Manual*.
- Engineering Dynamics, Inc. (2005). *PSI Release 6 User's Manual*.
- Engineering Dynamics, Inc. (2005). *SACS IV Release 6 User's Manual*.
- Fugro-McClelland Marine Geosciences, Inc. (2005). *Geotechnical Investigation, Confidential Platform Location, Gulf of Mexico*, Report to Confidential Client.

- Gambino, S. J. and Gilbert, R.B. (1999), "Modeling Spatial Variability in Pile Capacity for Reliability-Based Design," Analysis, Design, Construction and Testing of Deep Foundations, Roesset Ed., ASCE Geotechnical Special Publication No. 88, 135-149.
- Geoscience Earth & Marine Services, Inc. (2008). *Analysis of Foundation Collapse Loads for Shallow Water Platforms*, Letter Report to Confidential Client.
- Hamilton, J. M. and Murff, J. D. (1995) "Ultimate Lateral Capacity of Piles in Clay", OTC 7667.
- Jeanjean, P. (2009). "Re-Assessment of p-y Curves for Soft Clays from Centrifuge Testing and Finite Element Modeling," Offshore Technology Conference, Houston, Texas, OTC 20158.
- Lee, Y. (2007). *Performance of Pile Foundations for Fixed-type Platforms during Hurricane Katrina*, Master Thesis, The University of Texas at Austin.
- Long, M. (2008). "Design Parameters from In Situ Tests in Soft Ground – Recent Developments," *Proceedings of the Third International Conference on Site Characterization ISC'3*, Taipei, Taiwan, pp. 89-116.
- Materek, B.A. (2009). *An Investigation into Analytical Modeling Methods used to Determine Capacities of Offshore Jacket Type Foundations*, Master Thesis, The University of Texas at Austin.
- McClelland Engineers, Inc. (1979). *Geotechnical Investigation Boring 2, Confidential Platform Location, Gulf of Mexico*, Report to Confidential Client.
- Murff, J.D. (1987). "Plastic collapse of long piles under inclined loading," *International Journal for Numerical and Analytical Methods in Geomechanics*, Vol. 11, pp. 185-192.
- Murff, J. D. and Hamilton, J. M. (1993). "P-Ultimate for Undrained Analysis for Laterally Loaded Piles," *Journal of Geotechnical Engineering*, ASCE, Vol. 119, No. 1, pp. 91-107.
- Murff, J.D., Lacasse, S. and Young, A.G. (1993). "Discussion and summary on foundation elements, system and analysis," *Proceedings of an International Workshop Assessment and Requalification of Offshore Production Structures*, New Orleans, Louisiana, pp. 151-165.
- Murff, J.D. and Wesselink, B.D. (1986). "Collapse analysis of pile foundations," 3rd International Conference on Numerical Methods in Offshore Piling, Nantes, France, pp. 445-459.
- Najjar, S.S. (2005). *The Importance of Lower-Bound Capacities in Geotechnical Reliability Assessments*, Ph.D. Dissertation, The University of Texas at Austin.
- O'Neill, M.W. (2001). "Side Resistance in Piles and Drilled Shafts," *Journal of*

- Geotechnical and Geoenvironmental Engineering*, ASCE, Vol. 127, No. 1, pp. 3-16.
- Pelletier, J. H., Murff, J. D. and Young, A. C. (1993). "Historical Development and Assessment of the Current API Design Methods for Axially Loaded Piles," Offshore Technology Conference, Houston, Texas, OTC 7157.
- PMB Engineering, Inc. (1993). *Hurricane Andrew - Effects on Offshore Platforms*, Final Report for the Joint Industry Project.
- PMB Engineering, Inc. (1995). *Further Evaluation of Offshore Structures Performance in Hurricane Andrew – Development of Bias Factors for Pile Foundation Capacity*, Final Report to the American Petroleum Institute (Project PRAC 94-81).
- Quiros, G.W., Young, A.G., Pelletier, J.H., and Chan, J. H-C. (1983). "Shear Strength Interpretation for Gulf of Mexico Clays," *Proceedings of the Conference on Geotechnical Practice in Offshore Engineering*, Austin, Texas.
- Randolph, M. F., J. P. Carter, and C. P. Wroth (1979). "Driven Piles in Clay - The Effects of Installation and Subsequent Consolidation", *Geotechnique*, Vol. 29, No. 4, pp. 361-393.
- Randolph, M. F. and Houlsby, G. T. (1984). "The Limiting Pressure on a Circular Pile Loaded Laterally in Cohesive Soil," *Geotechnique*, Vol. 34, No. 4, pp. 613-623.
- Seed, H. B. and L. C. Reese (1957). "The Action of Soft Clay Along Friction Piles", *Transactions*, ASCE, vol. 122, pp. 731-764 (with Discussions and Response).
- Stevens, J. B. and Audibert, J. M. E. (1979). "Re-examination of p-y Curve Formulations," Offshore Technology Conference, Houston, Texas, OTC 3402.
- Tang, W.H. and Gilbert, R.B. (1992). *Offshore Pile System Reliability*, Final Report to American Petroleum Institute (Project PRAC 89-29).
- Vijayvergiya, V. N., A. P. Cheng, and H. J. Kolk (1977). "Effect of Soil Set Up on Pile Drivability in Chalk", *Journal, Geot. Engr. Div.*, ASCE, Vol. 103, No. GT10, pp. 1069-1082.

Appendix A – Excerpt of API RP 2A-WSD

smooth to a radius greater than or equal to half the branch thickness. Final grinding marks should be transverse to the weld axis and the entire finished profile should pass magnetic particle inspection.

5.5 STRESS CONCENTRATION FACTORS

The X and X' curves should be used with hot spot stress ranges based on suitable stress concentration factors. Stress concentration factors may be derived from finite element analyses, model tests or empirical equations based on such methods.

For joints not meeting the requirements of Section 4.3.1, e.g., connections in which load transfer is accomplished by overlap (Section 4.3.2), or by gusset plates, ring stiffeners, etc. (Section 4.3.5), a minimum stress concentration factor of 6.0 should be used in the brace member, in lieu of additional analysis. Where the chord and/or other joint reinforcement are not designed to develop the full static capacity of the members joined, these elements should also be checked separately.

6 Foundation Design

The recommended criteria of Section 6.1 through Section 6.11 are devoted to pile foundations, and more specifically to steel cylindrical (pipe) pile foundations. The recommended criteria of Section 6.12 through Section 6.17 are devoted to shallow foundations.

6.1 GENERAL

The foundation should be designed to carry static, cyclic and transient loads without excessive deformations or vibrations in the platform. Special attention should be given to the effects of cyclic and transient loading on the strength of the supporting soils as well as on the structural response of piles. Guidance provided in Sections 6.3, 6.4, and 6.5 is based upon static, monotonic loadings. Furthermore, this guidance does not necessarily apply to so called problem soils such as carbonate material or volcanic sands or highly sensitive clays. The possibility of movement of the seafloor against the foundation members should be investigated and the forces caused by such movements, if anticipated, should be considered in the design.

6.2 PILE FOUNDATIONS

Types of pile foundations used to support offshore structures are as follows:

6.2.1 Driven Piles

Open ended piles are commonly used in foundations for offshore platforms. These piles are usually driven into the sea-floor with impact hammers which use steam, diesel fuel,

or hydraulic power as the source of energy. The pile wall thickness should be adequate to resist axial and lateral loads as well as the stresses during pile driving. It is possible to predict approximately the stresses during pile driving using the principles of one-dimensional elastic stress wave transmission by carefully selecting the parameters that govern the behavior of soil, pile, cushions, capblock and hammer. For a more detailed study of these principles, refer to E.A.L. Smith's paper, "Pile Driving Analysis by the Wave Equation," Transactions ASCE, Vol. 127, 1962, Part 1, Paper No. 3306, pp, 1145–1193. The above approach may also be used to optimize the pile hammer cushion and capblock with the aid of computer analyses (commonly known as the Wave Equation Analyses). The design penetration of driven piles should be determined in accordance with the principles outlined in Sections 6.3 through 6.7 and 6.9 rather than upon any correlation of pile capacity with the number of blows required to drive the pile a certain distance into the seafloor.

When a pile refuses before it reaches design penetration, one or more of the following actions can be taken:

a. Review of hammer performance. A review of all aspects of hammer performance, possibly with the aid of hammer and pile head instrumentation, may identify problems which can be solved by improved hammer operation and maintenance, or by the use of a more powerful hammer.

b. Reevaluation of design penetration. Reconsideration of loads, deformations and required capacities, of both individual piles and other foundation elements, and the foundation as a whole, may identify reserve capacity available. An interpretation of driving records in conjunction with instrumentation mentioned above may allow design soil parameters or stratification to be revised and pile capacity to be increased.

c. Modifications to piling procedures, usually the last course of action, may include one of the following:

- **Plug Removal.** The soil plug inside the pile is removed by jetting and air lifting or by drilling to reduce pile driving resistance. If plug removal results in inadequate pile capacities, the removed soil plug should be replaced by a gravel grout or concrete plug having sufficient load-carrying capacity to replace that of the removed soil plug. Attention should be paid to plug/pile load transfer characteristics. Plug removal may not be effective in some circumstances particularly in cohesive soils.
- **Soil Removal Below Pile Tip.** Soil below the pile tip is removed either by drilling an undersized hole or jetting equipment is lowered through the pile which acts as the casing pipe for the operation. The effect on pile capacity of drilling an undersized hole is unpredictable unless there has been previous experience under similar conditions. Jetting below the pile tip should in general be avoided because of the unpredictability of the results.

- **Two-Stage Driven Piles.** A first stage or outer pile is driven to a predetermined depth, the soil plug is removed, and a second stage or inner pile is driven inside the first stage pile. The annulus between the two piles is grouted to permit load transfer and develop composite action.
- Drilled and grouted insert piles as described in 6.2.2(b) below.

6.2.2 Drilled and Grouted Piles

Drilled and grouted piles can be used in soils which will hold an open hole with or without drilling mud. Load transfer between grout and pile should be designed in accordance with Sections 7.4.2, 7.4.3, and 7.4.4. There are two types of drilled and grouted piles, as follows:

- Single-Stage.** For the single-staged, drilled and grouted pile, an oversized hole is drilled to the required penetration, a pile is lowered into the hole and the annulus between the pile and the soil is grouted. This type pile can be installed only in soils which will hold an open hole to the surface. As an alternative method, the pile with expendable cutting tools attached to the tip can be used as part of the drill stem to avoid the time required to remove the drill bit and insert a pile.
- Two-Stage.** The two-staged, drilled and grouted pile consists of two concentrically placed piles grouted to become a composite section. A pile is driven to a penetration which has been determined to be achievable with the available equipment and below which an open hole can be maintained. This outer pile becomes the casing for the next operation which is to drill through it to the required penetration for the inner or "insert" pile. The insert pile is then lowered into the drilled hole and the annuli between the insert pile and the soil and between the two piles are grouted. Under certain soil conditions, the drilled hole is stopped above required penetration, and the insert pile is driven to required penetration. The diameter of the drilled hole should be at least 6 inches (150 mm) larger than the pile diameter.

6.2.3 Belled Piles

Bells may be constructed at the tip of piles to give increased bearing and uplift capacity through direct bearing on the soil. Drilling of the bell is carried out through the pile by under-reaming with an expander tool. A pilot hole may be drilled below the bell to act as a sump for unrecoverable cuttings. The bell and pile are filled with concrete to a height sufficient to develop necessary load transfer between the bell and the pile. Bells are connected to the pile to transfer full uplift and bearing loads using steel reinforcing such as structural members with adequate shear lugs, deformed reinforcement bars or prestressed tendons. Load transfer into the concrete should be designed in accordance with ACI 318. The steel reinforcing should be enclosed for their full length below the pile with

spiral reinforcement meeting the requirements of ACI 318. Load transfer between the concrete and the pile should be designed in accordance with Sections 7.4.2, 7.4.3, and 7.4.4.

6.3 PILE DESIGN

6.3.1 Foundation Size

When sizing a pile foundation, the following items should be considered: diameter, penetration, wall thickness, type of tip, spacing, number of piles, geometry, location, mudline restraint, material strength, installation method, and other parameters as may be considered appropriate.

6.3.2 Foundation Response

A number of different analysis procedures may be utilized to determine the requirements of a foundation. At a minimum, the procedure used should properly simulate the non-linear response behavior of the soil and assure load-deflection compatibility between the structure and the pile-soil system.

6.3.3 Deflections and Rotations

Deflections and rotations of individual piles and the total foundation system should be checked at all critical locations which may include pile tops, points of contraflexure, mudline, etc. Deflections and rotations should not exceed serviceability limits which would render the structure inadequate for its intended function.

6.3.4 Pile Penetration

The design pile penetration should be sufficient to develop adequate capacity to resist the maximum computed axial bearing and pullout loads with an appropriate factor of safety. The ultimate pile capacities can be computed in accordance with Sections 6.4 and 6.5 or by other methods which are supported by reliable comprehensive data. The allowable pile capacities are determined by dividing the ultimate pile capacities by appropriate factors of safety which should not be less than the following values:

Load Condition	Factors of Safety
1. Design environmental conditions with appropriate drilling loads	1.5
2. Operating environmental conditions during drilling operations	2.0
3. Design environmental conditions with appropriate producing loads	1.5
4. Operating environmental conditions during producing operations	2.0
5. Design environmental conditions with minimum loads (for pullout)	1.5

6.3.5 Alternative Design Methods

The provisions of this recommended practice for sizing the foundation pile are based on an allowable stress (working stress) method except for pile penetration per Section 6.3.4. In this method, the foundation piles should conform to the requirements of Sections 3.2 and 6.10 in addition to the provisions of Section 6.3. Any alternative method supported by sound engineering methods and empirical evidence may also be utilized. Such alternative methods include the limit state design approach or ultimate strength design of the total foundation system.

6.3.6 Scour

Seabed scour affects both lateral and axial pile performance and capacity. Scour prediction remains an uncertain art. Sediment transport studies may assist in defining scour design criteria but local experience is the best guide. The uncertainty on design criteria should be handled by robust design, or by an operating strategy of monitoring and remediation as needed. Typical remediation experience is documented in "Erosion Protection of Production Structures," by Posey, C.J., and Sybert, J.H., Proc. 9th Conv. I.A.H.R., Dobrovnik, 1961, pp. 1157-1162, and "Scour Repair Methods in the Southern North Sea," by Angus, N.M., and Moore, R.L., OTC 4410, May 1982. Scour design criteria will usually be a combination of local and global scour.

6.4 PILE CAPACITY FOR AXIAL BEARING LOADS

6.4.1 Ultimate Bearing Capacity

The ultimate bearing capacity of piles, including belled piles, Q_d should be determined by the equation:

$$Q_d = Q_f + Q_p = fA_s + qA_p \quad (6.4.1-1)$$

where

Q_f = skin friction resistance, lb (kN),

Q_p = total end bearing, lb (kN),

f = unit skin friction capacity, lb/ft² (kPa),

A_s = side surface area of pile, ft² (m²),

q = unit end bearing capacity, lb/ft² (kPa),

A_p = gross end area of pile, ft² (m²).

Total end bearing, Q_p , should not exceed the capacity of the internal plug. In computing pile loading and capacity the weight of the pile-soil plug system and hydrostatic uplift should be considered.

In determining the load capacity of a pile, consideration should be given to the relative deformations between the soil

and the pile as well as the compressibility of the soil pile system. Eq. 6.4.1-1 assumes that the maximum skin friction along the pile and the maximum end bearing are mobilized simultaneously. However, the ultimate skin friction increments along the pile are not necessarily directly additive, nor is the ultimate end bearing necessarily additive to the ultimate skin friction. In some circumstances this effect may result in the capacity being less than that given by Eq. 6.4.1-1. In such cases a more explicit consideration of axial pile performance effects on pile capacity may be warranted. For additional discussion of these effects refer to Section 6.6 and ASCE *Journal of the Soil Mechanics and Foundations Division for Load Transfer for Axially Loaded Piles in Clay*, by H.M. Coyle and L.C. Reese, Vol. 92, No. 1052, March 1966, Murff, J.D., "Pile Capacity in a Softening Soil," *International Journal for Numerical and Analytical Methods in Geomechanics* (1980), Vol. 4, No. 2, pp. 185-189, and Randolph, H.F., "Design Considerations for Offshore Piles," *Geotechnical Practice in Offshore Engineering*, ASCE, Austin 1983, pp. 422-439.

The foundation configurations should be based on those that experience has shown can be installed consistently, practically and economically under similar conditions with the pile size and installation equipment being used. Alternatives for possible remedial action in the event design objectives cannot be obtained during installation should also be investigated and defined prior to construction.

For the pile-bell system, the factors of safety should be those given in Section 6.3.4. The allowable skin friction values on the pile section should be those given in this section and in Section 6.5. Skin friction on the upper bell surface and possibly above the bell on the pile should be discounted in computing skin friction resistance, Q_f . The end bearing area of a pilot hole, if drilled, should be discounted in computing total bearing area of the bell.

6.4.2 Skin Friction and End Bearing in Cohesive Soils

For pipe piles in cohesive soils, the shaft friction, f , in lb/ft² (kPa) at any point along the pile may be calculated by the equation.

$$f = \alpha c \quad (6.4.2-1)$$

where

α = a dimensionless factor,

c = undrained shear strength of the soil at the point in question.

The factor, α , can be computed by the equations:

$$\alpha = 0.5 \psi^{-0.5} \quad \psi \leq 1.0 \quad (6.4.2-2)$$

$$\alpha = 0.5 \psi^{-0.25} \quad \psi > 1.0$$

with the constraint that, $\alpha \leq 1.0$,

where

$$\psi = c/p'_o \text{ for the point in question,}$$

$$p'_o = \text{effective overburden pressure at the point in question lb/ft}^2 \text{ (kPa).}$$

A discussion of appropriate methods for determining the undrained shear strength, c , and effective overburden pressure, p'_o , including the effects of various sampling and testing procedures is included in the commentary. For underconsolidated clays (clays with excess pore pressures undergoing active consolidation), α , can usually be taken as 1.0. Due to the lack of pile load tests in soils having c/p'_o ratios greater than three, equation 6.4.2-2 should be applied with some engineering judgment for high c/p'_o values. Similar judgment should be applied for deep penetrating piles in soils with high undrained shear strength, c , where the computed shaft frictions, f , using equation 6.4.2-1 above, are generally higher than previously specified in RP 2A.

For very long piles some reduction in capacity may be warranted, particularly where the shaft friction may degrade to some lesser residual value on continued displacement. This effect is discussed in more detail in the commentary.

Alternative means of determining pile capacity that are based on sound engineering principles and are consistent with industry experience are permissible. A more detailed discussion of alternate prediction methods is included in the commentary.

For piles end bearing in cohesive soils, the unit end bearing q , in lb/ft^2 (kPa), may be computed by the equation

$$q = 9c \quad (6.4.2-3)$$

The shaft friction, f , acts on both the inside and outside of the pile. The total resistance is the sum of: the external shaft friction; the end bearing on the pile wall annulus; the total internal shaft friction or the end bearing of the plug, whichever is less. For piles considered to be plugged, the bearing pressure may be assumed to act over the entire cross section of the pile. For unplugged piles, the bearing pressure acts on the pile wall annulus only. Whether a pile is considered plugged or unplugged may be based on static calculations. For example, a pile could be driven in an unplugged condition but act plugged under static loading.

For piles driven in undersized drilled holes, piles jetted in place, or piles drilled and grouted in place the selection of shaft friction values should take into account the soil disturbance resulting from installation. In general f should not exceed values for driven piles; however, in some cases for drilled and grouted piles in overconsolidated clay, f may exceed these values. In determining f for drilled and grouted piles, the strength of the soil-grout interface, including poten-

tial effects of drilling mud, should be considered. A further check should be made of the allowable bond stress between the pile steel and the grout as recommended in Section 7.4.3. For further discussion refer to "State of the Art: Ultimate Axial Capacity of Grouted Piles" by Kraft and Lyons, OTC 2081, May, 1974.

In layered soils, shaft friction values, f , in the cohesive layers should be as given in Eq. (6.4.2-1). End bearing values for piles tipped in cohesive layers with adjacent weaker layers may be as given in Eq. (6.4.2-3), assuming that the pile achieves penetration of two to three diameters or more into the layer in question and the tip is approximately three diameters above the bottom of the layer to preclude punch through. Where these distances are not achieved, some modification in the end bearing resistance may be necessary. Where adjacent layers are of comparable strength to the layer of interest, the proximity of the pile tip to the interface is not a concern.

6.4.3 Shaft Friction and End Bearing in Cohesionless Soils

For pipe piles in cohesionless soils, the shaft friction, f , in lb/ft^2 (kPa) may be calculated by the equation:

$$f = Kp_o \tan \delta \quad (6.4.3-1)$$

where

K = coefficient of lateral earth pressure (ratio of horizontal to vertical normal effective stress),

p_o = effective overburden pressure lb/ft^2 (kPa) at the point in question,

δ = friction angle between the soil and pile wall.

For open-ended pipe piles driven unplugged, it is usually appropriate to assume K as 0.8 for both tension and compression loadings. Values of K for full displacement piles (plugged or closed end) may be assumed to be 1.0. Table 6.4.3-1 may be used for selection of δ if other data are not available. For long piles f may not indefinitely increase linearly with the overburden pressure as implied by Eq. 6.4.3-1. In such cases it may be appropriate to limit f to the values given in Table 6.4.3-1.

For piles end bearing in cohesionless soils the unit end bearing q in lb/ft^2 (kPa) may be computed by the equation

$$q = p_o N_q \quad (6.4.3-2)$$

where

p_o = effective overburden pressure lb/ft^2 (kPa) at the pile tip,

N_q = dimensionless bearing capacity factor.

Table 6.4.3-1—Design Parameters for Cohesionless Siliceous Soil*

Density	Soil Description	Soil-Pile Friction Angle, δ Degrees	Limiting Skin Friction Values kips/ft ² (kPa)	N_q	Limiting Unit End Bearing Values kips/ft ² (MPa)
Very Loose	Sand	15	1.0 (47.8)	8	40 (1.9)
Loose	Sand-Silt**				
Medium	Silt				
Loose	Sand	20	1.4 (67.0)	12	60 (2.9)
Medium	Sand-Silt**				
Dense	Silt				
Medium	Sand	25	1.7 (81.3)	20	100 (4.8)
Dense	Sand-Silt**				
Dense	Sand	30	2.0 (95.7)	40	200 (9.6)
Very Dense	Sand-Silt**				
Dense	Gravel	35	2.4 (114.8)	50	250 (12.0)
Very Dense	Sand				

*The parameters listed in this table are intended as guidelines only. Where detailed information such as in situ cone tests, strength tests on high quality samples, model tests, or pile driving performance is available, other values may be justified.

**Sand-Silt includes those soils with significant fractions of both sand and silt. Strength values generally increase with increasing sand fractions and decrease with increasing silt fractions.

Recommended values of N_q are presented in Table 6.4.3-1. The shaft friction, f , acts on both the inside and outside of the piles. However, the total resistance in excess of the external shaft friction plus annular end bearing is the total internal shaft friction or the end bearing of the plug, whichever is less. For piles considered to be plugged the bearing pressure may be assumed to act over the entire cross section of the pile. For unplugged piles the bearing pressure acts on the pile annulus only. Whether a pile is considered to be plugged or unplugged may be based on static calculations. For example, a pile could be driven in an unplugged condition but act plugged under static loading.

Load test data for piles in sand (see "Comparison of Measured and Axial Load Capacities of Steel Pipe Piles in Sand with Capacities Calculated Using the 1986 API RP2A Standard," Final Report to API, Dec. 1987, by R. E. Olson) indicate that variability in capacity predictions may exceed those for piles in clay. Other data (see Toolan and Ims (1988)) (1) suggest that for piles in loose sands and long piles (> 50 m) in tension the method may be less conservative than for compression piles in medium dense to dense sands. Therefore, in unfamiliar situations, the designer may want to account for

this uncertainty through a selection of conservative design parameters and/or safety factors. This may be especially important where load shedding subsequent to peak load development leading to an abrupt (brittle) failure may occur such as the case for short piles under tension loading.

For soils that do not fall within the ranges of soil density and description given in Table 6.4.3-1, or for materials with unusually weak grains or compressible structures, Table 6.4.3-1 may not be appropriate for selection of design parameters. For example, very loose silts or soils containing large amounts of mica or volcanic grains may require special laboratory or field tests for selection of design parameters. Of particular importance are sands containing calcium carbonate which are found extensively in many areas of the oceans. Available data suggest that driven piles in these soils may have substantially lower design strength parameters than given in Table 6.4.3-1. Drilled and grouted piles in carbonate sands, however, may have significantly higher capacities than driven piles and have been used successfully in many carbonate areas. The characteristics of carbonate sands are highly variable and local experience should dictate the design parameters selected. For example, available qualitative data

suggest that capacity is improved in carbonate soils of high densities and higher quartz contents. Cementation may increase end bearing capacity, but result in a loss of lateral pressure and a corresponding decrease in frictional capacity. These materials are discussed further in the Commentary.

For piles driven in undersized drilled or jetted holes in cohesionless soils the values of f and q should be determined by some reliable method that accounts for the amount of soil disturbance due to installation but they should not exceed values for driven piles. Except in unusual soil types such as described above, the values of f and q in Table 6.4.3-1 may be used for drilled and grouted piles, with consideration given to the strength of the soil grout interface.

In layered soils shaft friction values, f , in the cohesionless layers should be as outlined in Table 6.4.3-1. End bearing values for piles tipped in cohesionless layers with adjacent soft layers may also be taken from Table 6.4.3-1, assuming that the pile achieves penetration of two to three diameters or more into the cohesionless layer, and the tip is approximately three diameters above the bottom of the layer to preclude punch through. Where these distances are not achieved, some modification in the tabulated values may be necessary. Where adjacent layers are of comparable strength to the layer of interest, the proximity of the pile tip to the interface is not a concern.

6.4.4 Skin Friction and End Bearing of Grouted Piles in Rock

The unit skin friction of grouted piles in jetted or drilled holes in rock should not exceed the triaxial shear strength of the rock or grout, but in general should be much less than this value based on the amount of reduced shear strength from installation. For example the strength of dry compacted shale may be greatly reduced when exposed to water from jetting or drilling. The sidewall of the hole may develop a layer of slaked mud or clay which will never regain the strength of the rock. The limiting value for this type pile may be the allowable bond stress between the pile steel and the grout as recommended in 7.4.3.

The end bearing capacity of the rock should be determined from the triaxial shear strength of the rock and an appropriate bearing capacity factor based on sound engineering practice for the rock materials but should not exceed 100 tons per square foot (9.58 MPa).

6.5 PILE CAPACITY FOR AXIAL PULLOUT LOADS

The ultimate pile pullout capacity may be equal to or less than but should not exceed Q_f , the total skin friction resistance. The effective weight of the pile including hydrostatic uplift and the soil plug shall be considered in the analysis to determine the ultimate pullout capacity. For clay, f should be the same as stated in 6.4.2. For sand and silt, f should be computed according to 6.4.3.

For rock, f should be the same as stated in Section 6.4.4.

The allowable pullout capacity should be determined by applying the factors of safety in 6.3.4 to the ultimate pullout capacity.

6.6 AXIAL PILE PERFORMANCE

6.6.1 Static Load-deflection Behavior

Piling axial deflections should be within acceptable serviceability limits and these deflections should be compatible with the structural forces and movements. An analytical method for determining axial pile performance is provided in *Computer Predictions of Axially Loaded Piles with Non-linear Supports*, by P. T. Meyer, et al., OTC 2186, May 1975. This method makes use of axial pile shear transition vs. local pile deflection ($t-z$) curves to model the axial support provided by the soil along the size of the pile. An additional ($Q-z$) curve is used to model the tip and bearing vs. the deflection response. Methods for constructing $t-z$ and $Q-z$ curves are given in Section 6.7. Pile response is affected by load directions, load types, load rates, loading sequence installation technique, soil type, axial pile stiffness and other parameters.

Some of these effects for cohesive soils have been observed in both laboratory and field tests.

In some circumstances, i.e., for soils that exhibit strain-softening behavior and/or where the piles are axially flexible, the actual capacity of the pile may be less than that given by Eq. 6.4.1-1. In these cases an explicit consideration of these effects on ultimate axial capacity may be warranted. Note that other factors such as increased axial capacity under loading rates associated with storm waves may counteract the above effects. For more information see Section 6.2.2, its commentary, as well as "Effects of Cyclic Loading and Pile Flexibility on Axial Pile Capacities in Clay" by T. W. Dunnivant, E. C. Clukey and J. D. Murff, OTC 6374, May 1990.

6.6.2 Cyclic Response

Unusual pile loading conditions or limitations on design pile penetrations may warrant detailed consideration of cyclic loading effects.

Cyclic loadings (including inertial loadings) developed by environmental conditions such as storm waves and earthquakes can have two potentially counteractive effects on the static axial capacity. Repetitive loadings can cause a temporary or permanent decrease in load-carrying resistance, and/or an accumulation of deformation. Rapidly applied loadings can cause an increase in load-carrying resistance and/or stiffness of the pile. Very slowly applied loadings can cause a decrease in load-carrying resistance and/or stiffness of the pile. The resultant influence of cyclic loadings will be a function of the combined effects of the magnitudes, cycles, and rates of applied pile loads, the structural characteristics of the

pile, the types of soils, and the factors of safety used in design of the piles.

The design pile penetration should be sufficient to develop an effective pile capacity to resist the design static and cyclic loadings as discussed in 6.3.4.

The design pile penetration can be confirmed by performing pile response analyses of the pile-soil system subjected to static and cyclic loadings. Analytical methods to perform such analyses are described in the commentary to this Section. The pile-soil resistance-displacement t - z , Q - z characterizations are discussed in Section 6.7.

6.6.3 Overall Pile Response Analyses

When any of the above effects are explicitly considered in pile response analysis, the design static and cyclic loadings should be imposed on the pile top and the resistance-displacements of the pile determined. At the completion of the design loadings, the maximum pile resistance and displacement should be determined. Pile deformations should meet structure serviceability requirements. The total pile resistance after the design loadings should meet the requirements of 6.3.4.

6.7 SOIL REACTION FOR AXIALLY-LOADED PILES

6.7.1 General

The pile foundation should be designed to resist the static and cyclic axial loads. The axial resistance of the soil is provided by a combination of axial soil-pile adhesion or load transfer along the sides of the pile and end bearing resistance at the pile tip. The plotted relationship between mobilized soil-pile shear transfer and local pile deflection at any depth is described using a t - z curve. Similarly, the relationship between mobilized end bearing resistance and axial tip deflection is described using a Q - z curve.

6.7.2 Axial Load Transfer (t - z) Curves

Various empirical and theoretical methods are available for developing curves for axial load transfer and pile displacement, (t - z) curves. Theoretical curves described by Kraft, et al. (1981) may be constructed. Empirical t - z curves based on the results of model and full-scale pile load tests may follow the procedures in clay soils described by Cole and Reese (1966) or granular soils by Coyle, H.M. and Suliaman, I.H. *Skin Friction for Steel Piles in Sand*, Journal of the Soil Mechanics and Foundation Division, Proceedings of the American Society of Civil Engineers, Vol. 93, No. SM6, November, 1967, p. 261-278. Additional curves for clays and sands are provided by Vijayvergiya, V.N., *Load Movement Characteristics of Piles*, Proceedings of the Ports '77 Conference, American Society of Civil Engineers, Vol. II, p. 269-284.

Load deflection relationships for grouted piles are discussed in *Criteria for Design of Axially Loaded Drilled Shafts*, by L. C. Reese and M. O'Neill, Center for Highway Research Report, University of Texas, August 1971. Curves developed from pile load tests in representative soil profiles or based on laboratory soil tests that model pile installation may also be justified. Other information may be used, provided such information can be shown to result in adequate safeguards against excessive deflection and rotation.

In the absence of more definitive criteria, the following t - z curves are recommended for non-carbonate soils. The recommended curves are shown in Figure 6.7.2-1.

Clays	z/D	t/t_{max}
	0.0016	0.30
	0.0031	0.50
	0.0057	0.75
	0.0080	0.90
	0.0100	1.00
	0.0200	0.70 to 0.90
	∞	0.70 to 0.90

Sands	z (in.)	t/t_{max}
	0.000	0.00
	0.100	1.00
	∞	1.00

where

z = local pile deflection, in. (mm),

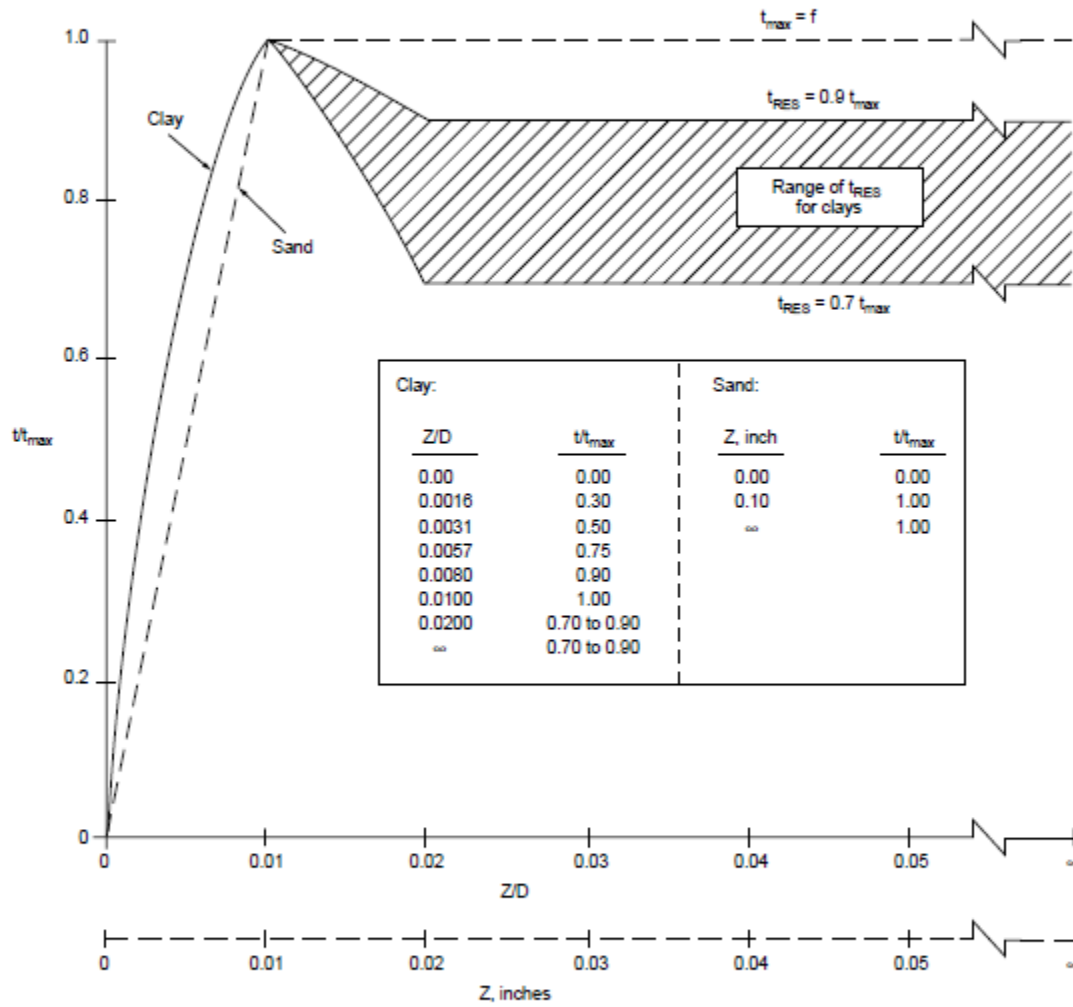
D = pile diameter, in. (mm),

t = mobilized soil pile adhesion, lb/ft² (kPa),

t_{max} = maximum soil pile adhesion or unit skin friction capacity computed according to Section 6.4, lb/ft² (kPa).

The shape of the t - z curve at displacements greater than z_{max} as shown in Figure 6.7.2-1 should be carefully considered. Values of the residual adhesion ratio t_{res}/t_{max} at the axial pile displacement at which it occurs (z_{res}) are a function of soil stress-strain behavior, stress history, pipe installation method, pile load sequence and other factors.

The value of t_{res}/t_{max} can range from 0.70 to 0.90. Laboratory, in situ or model pile tests can provide valuable information for determining values of t_{res}/t_{max} and z_{res} for various soils. For additional information see the listed references at the beginning of 6.7.2.

Figure 6.7.2-1—Typical Axial Pile Load Transfer—Displacement (t - z) Curves

6.7.3 Tip-load—Displacement Curve

The end bearing or tip-load capacity should be determined as described in 6.4.2 and 6.4.3. However, relatively large pile tip movements are required to mobilize the full end bearing resistance. A pile tip displacement up to 10 percent of the pile diameter may be required for full mobilization in both sand and clay soils. In the absence of more definitive criteria the following curve is recommended for both sands and clays.

z/D	Q/Q_p
0.002	0.25
0.013	0.50
0.042	0.75
0.073	0.90
0.100	1.00

where

- z = axial tip deflection, in. (mm),
- D = pile diameter, in. (mm),
- Q = mobilized end bearing capacity, lb (kN),
- Q_p = total end bearing, lb (kN), computed according to Section 6.4.

The recommended curve is shown in Figure 6.7.3-1.

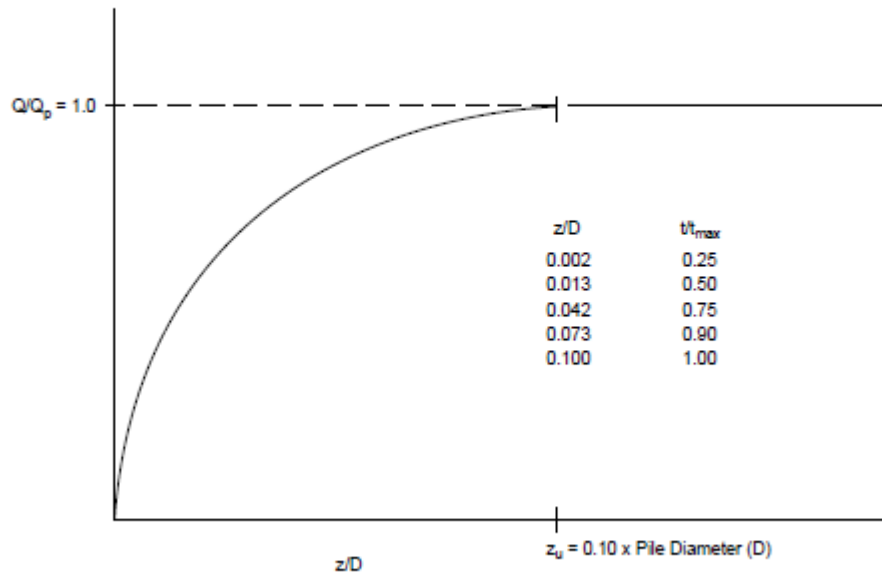


Figure 6.7.3-1—Pile Tip-load—Displacement (Q - z) curve

6.8 SOIL REACTION FOR Laterally-Loaded PILES

6.8.1 General

The pile foundation should be designed to sustain lateral loads, whether static or cyclic. Additionally, the designer should consider overload cases in which the design lateral loads on the platform foundation are increased by an appropriate safety factor. The designer should satisfy himself that the overall structural foundation system will not fail under the overloads. The lateral resistance of the soil near the surface is significant to pile design, and the effects on this resistance of scour and soil disturbance during pile installation should be considered. Generally, under lateral loading, clay soils behave as a plastic material which makes it necessary to relate pile-soil deformation to soil resistance. To facilitate this procedure, lateral soil resistance deflection (p - y) curves should be constructed using stress-strain data from laboratory soil samples. The ordinate for these curves is soil resistance, p , and the abscissa is soil deflection, y . By iterative procedures, a compatible set of load-deflection values for the pile-soil system can be developed.

For a more detailed study of the construction of p - y curves refer to the following publications.

Soft Clay: OTC 1204, Correlations for Design of Laterally Loaded Piles in Soft Clay, by H. Matlock, April 1970.

Stiff Clay: OTC 2312, Field Testing and Analysis of Laterally Loaded Piles in Stiff Clay, by L. C. Reese and W. R. Cox, April 1975.

Sand: "An Evaluation of p - y Relationships in Sands," by M. W. O'Neill and J. M. Murchinson. A report to the American Petroleum Institute, May 1983.

In the absence of more definitive criteria, procedures recommended in 6.8.2 and 6.8.3 may be used for constructing ultimate lateral bearing capacity curves and p - y curves.

6.8.2 Lateral Bearing Capacity for Soft Clay

For static lateral loads the ultimate unit lateral bearing capacity of soft clay p_u has been found to vary between $8c$ and $12c$ except at shallow depths where failure occurs in a different mode due to minimum overburden pressure. Cyclic loads cause deterioration of lateral bearing capacity below that for static loads. In the absence of more definitive criteria, the following is recommended:

p_u increases from $3c$ to $9c$ as X increases from 0 to X_R according to:

$$p_u = 3c + \gamma X + J \frac{cX}{D} \quad (6.8.2-1)$$

and

$$p_u = 9c \text{ for } X \geq X_R \quad (6.8.2-2)$$

where

- p_u = ultimate resistance, psi (kPa),
- c = undrained shear strength for undisturbed clay soil samples, psi (kPa),
- D = pile diameter, in. (mm),
- γ = effective unit weight of soil, lb/in³ (MN/m³),
- J = dimensionless empirical constant with values ranging from 0.25 to 0.5 having been determined by field testing. A value of 0.5 is appropriate for Gulf of Mexico clays,
- X = depth below soil surface, in. (mm),
- X_R = depth below soil surface to bottom of reduced resistance zone in in. (mm). For a condition of constant strength with depth, Equations 6.8.2-1 and 6.8.2-2 are solved simultaneously to give:

$$X_R = \frac{6D}{\frac{\gamma D}{c} + J}$$

Where the strength varies with depth, Equations 6.8.2-1 and 6.8.2-2 may be solved by plotting the two equations, i.e., p_u vs. depth. The point of first intersection of the two equations is taken to be X_R . These empirical relationships may not apply where strength variations are erratic. In general, minimum values of X_R should be about 2.5 pile diameters.

6.8.3 Load-deflection (p - y) Curves for Soft Clay

Lateral soil resistance-deflection relationships for piles in soft clay are generally non-linear. The p - y curves for the short-term static load case may be generated from the following table:

p/p_u	y/y_c
0.00	0.0
0.50	1.0
0.72	3.0
1.00	8.0
1.00	∞

where

- p = actual lateral resistance, psi (kPa),
- y = actual lateral deflection, in. (mm),
- $y_c = 2.5 \epsilon_c D$, in. (mm),
- ϵ_c = strain which occurs at one-half the maximum stress on laboratory undrained compression tests of undisturbed soil samples.

For the case where equilibrium has been reached under cyclic loading, the p - y curves may be generated from the following table:

$X > X_R$		$X < X_R$	
P/p_u	y/y_c	P/p_u	y/y_c
0.00	0.0	0.00	0.0
0.50	1.0	0.50	1.0
0.72	3.0	0.72	3.0
0.72	∞	0.72 X/X_R	15.0
		0.72 X/X_R	∞

6.8.4 Lateral Bearing Capacity for Stiff Clay

For static lateral loads the ultimate bearing capacity p_u of stiff clay ($c > 1 T_{5f}$ or 96 kPa) as for soft clay would vary between $8c$ and $12c$. Due to rapid deterioration under cyclic loadings the ultimate resistance will be reduced to something considerably less and should be so considered in cyclic design.

6.8.5 Load-Deflection (p - y) Curves for Stiff Clay

While stiff clays also have non-linear stress-strain relationships, they are generally more brittle than soft clays. In developing stress-strain curves and subsequent p - y curves for cyclic loads, good judgment should reflect the rapid deterioration of load capacity at large deflections for stiff clays.

6.8.6 Lateral Bearing Capacity for Sand

The ultimate lateral bearing capacity for sand has been found to vary from a value at shallow depths determined by Eq. 6.8.6-1 to a value at deep depths determined by Eq. 6.8.6-2. At a given depth the equation giving the smallest value of p_u should be used as the ultimate bearing capacity.

$$p_{us} = (C_1 \times H + C_2 \times D) \times \gamma \times H \quad (6.8.6-1)$$

$$p_{ud} = C_3 \times D \times \gamma \times H \quad (6.8.6-2)$$

where

p_u = ultimate resistance (force/unit length), lbs/in. (kN/m) (s = shallow, d = deep),

γ = effective soil weight, lb/in.³ (kN/m³),

H = depth, in. (m),

ϕ' = angle of internal friction of sand, deg.,

C_1, C_2, C_3 = Coefficients determined from Figure 6.8.6-1 as function of ϕ' ,

D = average pile diameter from surface to depth, in. (m).

6.8.7 Load-Deflection (p - y) Curves for Sand

The lateral soil resistance (p - y) relationships for sand are also non-linear and in the absence of more definitive information may be approximated at any specific depth H , by the following expression:

$$P = A \times p_u \times \tanh \left[\frac{k \times H}{A \times p_u} \times y \right] \quad (6.8.7-1)$$

where

A = factor to account for cyclic or static loading condition. Evaluated by:

$A = 0.9$ for cyclic loading.

$A = \left(3.0 - 0.8 \frac{H}{D} \right) \geq 0.9$ for static loading.

p_u = ultimate bearing capacity at depth H , lbs/in. (kN/m),

k = initial modulus of subgrade reaction, lb/in.³ (kN/m³). Determine from Figure 6.8.7-1 as function of angle of internal friction, ϕ' .

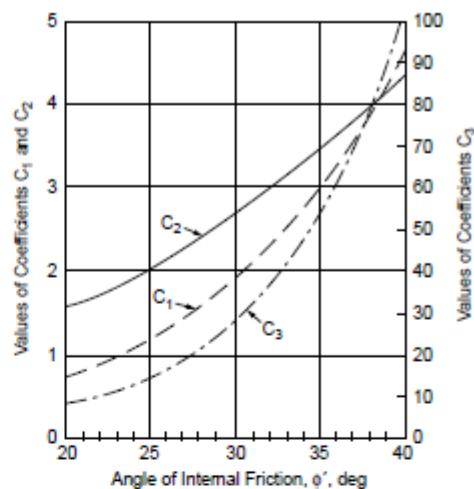


Figure 6.8.6-1—Coefficients as Function of ϕ'

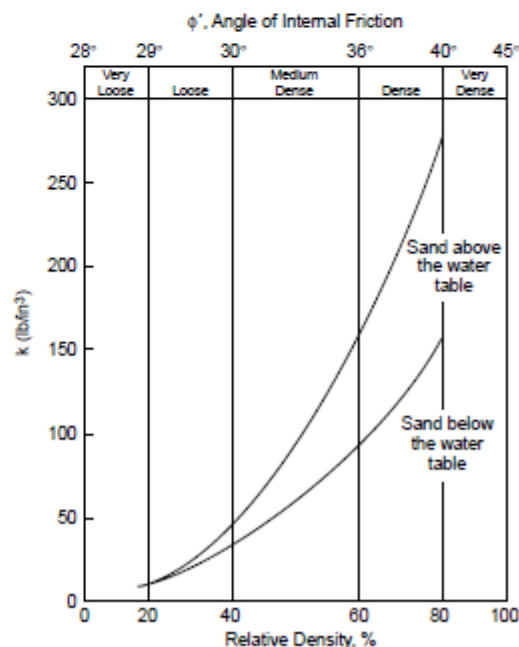


Figure 6.8.7-1—Relative Density, %

y = lateral deflection, inches (m).

H = depth, inches (m)

6.9 PILE GROUP ACTION

6.9.1 General

Consideration should be given to the effects of closely spaced adjacent piles on the load and deflection characteristics of pile groups. Generally, for pile spacing less than eight (8) diameters, group effects may have to be evaluated. For more detailed discussions refer to the following four papers: "Group Action in Offshore Piles," by O'Neill, M. W., *Proceedings, Conference on Geotechnical Practice in Offshore Engineering*, ASCE, Austin, Texas, pp. 25–64; "An Approach for the Analysis of Offshore Pile Groups," by Poulos, H. G., *Proceedings, 1st International Conference on Numerical Methods in Offshore Piling*, Institution of Civil Engineers, London, pp. 119–126; "The Analysis of Flexible Raft-Pile System" by Han, S. J., and Lee, I. K., *Geotechnique* 28, No. 1, 1978; and Offshore Technology Conference paper number OTC 2838, *Analysis of Three-Dimensional Pile Groups with Non-Linear Soil Response and Pile-Soil Interaction* by M. W. O'Neill, et al., 1977.

6.9.2 Axial Behavior

For piles embedded in clays, the group capacity may be less than a single isolated pile capacity multiplied by the number of piles in the group; conversely, for piles embedded in sands the group capacity may be higher than the sum of the capacities in the isolated piles. The group settlement in either clay or sand would normally be larger than that of a single pile subjected to the average pile load of the pile group.

In general, group effects depend considerably on pile group geometry and penetrations, and thickness of any bearing strata underneath the pile tips. Refer to "Group Action in Offshore Piles" by O'Neill, M. W., *Proceedings, Conference on Geotechnical Practice in Offshore Engineering*, ASCE, Austin, Texas, pp. 25–64; "Pile Group Analysis: A Study of Two Methods," by Poulos, H. G., and Randolph, M. F., *Journal Geotechnical Engineering Division*, ASCE, Vol. 109, No. 3, pp. 355–372.

6.9.3 Lateral Behavior

For piles with the same pile head fixity conditions and embedded in either cohesive or cohesionless soils, the pile group would normally experience greater lateral deflection than that of a single pile under the average pile load of the corresponding group. The major factors influencing the group deflections and load distribution among the piles are the pile spacing, the ratio of pile penetration to the diameter, the pile flexibility relative to the soil the dimensions of the group, and

the variations in the shear strength and stiffness modulus of the soil with depth.

O'Neill and Dunnavant (1985), in a recent API-sponsored project, [*An Evaluation of the Behavior and Analysis of Laterally Loaded Pile Groups*, API, PRAC 84-52, University of Houston, University Park, Department of Civil Engineering, Research Report No. UHCE 85-11] found of the four group analysis methods examined in this study, the following methods to be the most appropriate for use in designing group pile foundations for the given loading conditions: (a) advanced methods, such as PILGP2R, for defining initial group stiffness; (b) the Focht-Koch (1973) method ["Rational Analysis of the Lateral Performance of Offshore Pile Groups," OTC 1896] as modified by Reese et al. (1984) ["Analysis of a Pile Group Under Lateral Loading," *Laterally Loaded Deep Foundations: Analysis and Performance*, ASTM, STP 835, pp. 56–71] for defining group deflections and average maximum pile moments for design event loads—deflections are probably underpredicted at loads giving deflections of 20 percent or more of the diameter of the individual piles in the group; (c) largest value obtained from the Focht-Koch and b methods for evaluating maximum pile load at a given group deflection.

Past experience and the results of the study by O'Neill and Dunnavant (1985) confirm that the available tools for analysis of laterally loaded pile groups provide approximate answers that sometimes deviate significantly from observed behavior, particularly with regard to deflection calculations. Also, limitations in site investigation procedures and in the ability to predict single-pile soil-pile interaction behavior produce uncertainty regarding proper soil input to group analyses. Therefore multiple analyses should be performed for pile groups, using two or more appropriate methods of analysis and upper-bound and lower-bound values of soil properties in the analyses. By performing such analyses, the designer will obtain an appreciation for the uncertainty involved in his predictions of foundation performance and can make more informed decisions regarding the structural design of the foundation and superstructure elements.

6.9.4 Pile Group Stiffness and Structure Dynamics

When the dynamic behavior of a structure is determined to be sensitive to variations in foundation stiffness, parametric analyses such as those described in 6.9.3 should be performed to bound the vertical and lateral foundation stiffness values to be used in the dynamic structural analyses. For insight regarding how changes in foundation stiffness can impact the natural frequencies of tall steel jacket platforms, see K. A. Digre et al. (1989), "The Design of the Bullwinkle Platform," OTC 6060.

6.10 PILE WALL THICKNESS

6.10.1 General

The wall thickness of the pile may vary along its length and may be controlled at a particular point by any one of several loading conditions or requirements which are discussed in the paragraphs below.

6.10.2 Allowable Pile Stresses

The allowable pile stresses should be the same as those permitted by the AISC specification for a compact hot rolled section, giving due consideration to Sections 3.1 and 3.3. A rational analysis considering the restraints placed upon the pile by the structure and the soil should be used to determine the allowable stresses for the portion of the pile which is not laterally restrained by the soil. General column buckling of the portion of the pile below the mudline need not be considered unless the pile is believed to be laterally unsupported because of extremely low soil shear strengths, large computed lateral deflections, or for some other reason.

6.10.3 Design Pile Stresses

The pile wall thickness in the vicinity of the mudline, and possibly at other points, is normally controlled by the combined axial load and bending moment which results from the design loading conditions for the platform. The moment curve for the pile may be computed with soil reactions determined in accordance with Section 6.8 giving due consideration to possible soil removal by scour. It may be assumed that the axial load is removed from the pile by the soil at a rate equal to the ultimate soil-pile adhesion divided by the appropriate pile safety factor from 6.3.4. When lateral deflections associated with cyclic loads at or near the mudline are relatively large (e.g., exceeding y_c as defined in 6.8.3 for soft clay), consideration should be given to reducing or neglecting the soil-pile adhesion through this zone.

6.10.4 Stresses Due to Weight of Hammer During Hammer Placement

Each pile or conductor section on which a pile hammer (pile top drilling rig, etc.) will be placed should be checked for stresses due to placing the equipment. These loads may be the limiting factors in establishing maximum length of add-on sections. This is particularly true in cases where piling will be driven or drilled on a batter. The most frequent effects include: static bending, axial loads, and arresting lateral loads generated during initial hammer placement.

Experience indicates that reasonable protection from failure of the pile wall due to the above loads is provided if the static stresses are calculated as follows:

1. The pile projecting section should be considered as a freestanding column with a minimum effective length factor K of 2.1 and a minimum Reduction Factor C_m of 1.0.
2. Bending moments and axial loads should be calculated using the full weight of the pile hammer, cap, and leads acting through the center of gravity of their combined masses, and the weight of the pile add-on section with due consideration to pile batter eccentricities. The bending moment so determined should not be less than that corresponding to a load equal to 2 percent of the combined weight of the hammer, cap, and leads applied at the pile head and perpendicular to its centerline.
3. Allowable stresses in the pile should be calculated in accordance with Sections 3.2 and 3.3. The one third increase in stress should not be allowed.

6.10.5 Stresses During Driving

Consideration should also be given to the stresses that occur in the freestanding pile section during driving. Generally, stresses are checked based on the conservative criterion that the sum of the stresses due to the impact of the hammer (the dynamic stresses) and the stresses due to axial load and bending (the static stresses) should not exceed the minimum yield stress of the steel. Less conservative criteria are permitted, provided that these are supported by sound engineering analyses and empirical evidence. A method of analysis based on wave propagation theory should be used to determine the dynamic stresses (see 6.2.1). In general, it may be assumed that column buckling will not occur as a result of the dynamic portion of the driving stresses. The dynamic stresses should not exceed 80 to 90 percent of yield depending on specific circumstances such as the location of the maximum stresses down the length of pile, the number of blows, previous experience with the pile-hammer combination and the confidence level in the analyses. Separate considerations apply when significant driving stresses may be transmitted into the structure and damage to appurtenances must be avoided. The static stress during driving may be taken to be the stress resulting from the weight of the pile above the point of evaluation plus the pile hammer components actually supported by the pile during the hammer blows, including any bending stresses resulting there from. When using hydraulic hammers it is possible that the driving energy may exceed the rated energy and this should be considered in the analyses. Also, the static stresses induced by hydraulic hammers need to be computed with special care due to the possible variations in driving configurations, for example when driving vertical piles without lateral restraint and exposed to environmental forces (see also 12.5.7.a). Allowable static stresses in the pile should be calculated in accordance with Sections 3.2 and 3.3. The one-third increases in stress should not be allowed. The pile hammers evaluated for use during driving should be noted by the designer on the installation drawings or specifications.

6.10.6 Minimum Wall Thickness

The D/t ratio of the entire length of a pile should be small enough to preclude local buckling at stresses up to the yield strength of the pile material. Consideration should be given to the different loading situations occurring during the installation and the service life of a piling. For in-service conditions, and for those installation situations where normal pile-driving is anticipated or where piling installation will be by means other than driving, the limitations of Section 3.2 should be considered to be the minimum requirements. For piles that are to be installed by driving where sustained hard driving (250 blows per foot [820 blows per meter] with the largest size hammer to be used) is anticipated, the minimum piling wall thickness used should not be less than

$$\left. \begin{aligned} t &= 0.25 + \frac{D}{100} \\ \text{Metric Formula} & \\ t &= 6.35 + \frac{D}{100} \end{aligned} \right\} \quad (6.10.6-1)$$

where

t = wall thickness, in. (mm),

D = diameter, in. (mm).

Minimum wall thickness for normally used pile sizes should be as listed in the following table:

Minimum Pile Wall Thickness			
Pile Diameter		Nominal Wall Thickness, t	
in.	mm	in.	mm
24	610	$\frac{1}{2}$	13
30	762	$\frac{9}{16}$	14
36	914	$\frac{5}{8}$	16
42	1067	$\frac{11}{16}$	17
48	1219	$\frac{3}{4}$	19
60	1524	$\frac{7}{8}$	22
72	1829	1	25
84	2134	$1\frac{1}{8}$	28
96	2438	$1\frac{1}{4}$	31
108	2743	$1\frac{3}{8}$	34
120	3048	$1\frac{1}{2}$	37

The preceding requirement for a lesser D/t ratio when hard driving is expected may be relaxed when it can be shown by past experience or by detailed analysis that the pile will not be damaged during its installation.

6.10.7 Allowance for Underdrive and Overdrive

With piles having thickened sections at the mudline, consideration should be given to providing an extra length of

heavy wall material in the vicinity of the mudline so the pile will not be overstressed at this point if the design penetration is not reached. The amount of underdrive allowance provided in the design will depend on the degree of uncertainty regarding the penetration that can be obtained. In some instances an overdrive allowance should be provided in a similar manner in the event an expected bearing stratum is not encountered at the anticipated depth.

6.10.8 Driving Shoe

The purpose of driving shoes is to assist piles to penetrate through hard layers or to reduce driving resistances allowing greater penetrations to be achieved than would otherwise be the case. Different design considerations apply for each use. If an internal driving shoe is provided to drive through a hard layer it should be designed to ensure that unacceptably high driving stresses do not occur at and above the transition point between the normal and the thickened section at the pile tip. Also it should be checked that the shoe does not reduce the end bearing capacity of the soil plug below the value assumed in the design. External shoes are not normally used as they tend to reduce the skin friction along the length of pile above them.

6.10.9 Driving Head

Any driving head at the top of the pile should be designed in association with the installation contractor to ensure that it is fully compatible with the proposed installation procedures and equipment.

6.11 LENGTH OF PILE SECTIONS

In selecting pile section lengths consideration should be given to: 1) the capability of the lift equipment to raise, lower and stab the sections; 2) the capability of the lift equipment to place the pile driving hammer on the sections to be driven; 3) the possibility of a large amount of downward pile movement immediately following the penetration of a jacket leg closure; 4) stresses developed in the pile section while lifting; 5) the wall thickness and material properties at field welds; 6) avoiding interference with the planned concurrent driving of neighboring piles; and 7) the type of soil in which the pile tip is positioned during driving interruptions for field welding to attach additional sections. In addition, static and dynamic stresses due to the hammer weight and operation should be considered as discussed in 6.10.4 and 6.10.5.

Each pile section on which driving is required should contain a cutoff allowance to permit the removal of material damaged by the impact of the pile driving hammer. The normal allowance is 2 to 5 ft. (0.5 to 1.5 meters) per section. Where possible the cut for the removal of the cutoff allowance should be made at a conveniently accessible elevation.

6.12 SHALLOW FOUNDATIONS

Shallow foundations are those foundations for which the depth of embedment is less than the minimum lateral dimension of the foundation element. The design of shallow foundations should include, where appropriate to the intended application, consideration of the following:

1. Stability, including failure due to overturning, bearing, sliding or combinations thereof.
2. Static foundation deformations, including possible damage to components of the structure and its foundation or attached facilities.
3. Dynamic foundation characteristics, including the influence of the foundation on structural response and the performance of the foundation itself under dynamic loading.
4. Hydraulic instability such as scour or piping due to wave pressures, including the potential for damage to the structure and for foundation instability.
5. Installation and removal, including penetration and pull out of shear skirts or the foundation base itself and the effects of pressure build up or draw down of trapped water underneath the base.

Recommendations pertaining to these aspects of shallow foundation design are given in 6.13 through 6.17.

6.13 STABILITY OF SHALLOW FOUNDATIONS

The equations of this paragraph should be considered in evaluating the stability of shallow foundations. These equations are applicable to idealized conditions, and a discussion of the limitations and of alternate approaches is given in the Commentary. Where use of these equations is not justified, a more refined analysis or special considerations should be considered.

6.13.1 Undrained Bearing Capacity ($\phi = 0$)

The maximum gross vertical load which a footing can support under undrained conditions is

$$Q = (cN_cK_c + \gamma D)A' \quad (6.13.1-1)$$

where

- Q = maximum vertical load at failure,
- c = undrained shear strength of soil,
- N_c = a dimensionless constant, 5.14 for $\phi = 0$,
- ϕ = undrained friction angle = 0,
- γ = total unit weight of soil,

D = depth of embedment of foundation,

A' = effective area of the foundation depending on the load eccentricity,

K_c = correction factor which accounts for load inclination, footing shape, depth of embedment, inclination of base, and inclination of the ground surface.

A method for determining the correction factor and the effective area is given in the Commentary. Two special cases of Eq. 6.13.1-1 are frequently encountered. For a vertical concentric load applied to a foundation at ground level where both the foundation base and ground are horizontal, Eq. 6.13.1-1 is reduced below for two foundation shapes.

1. Infinitely Long Strip Footing.

$$Q_0 = 5.14cA_0 \quad (6.13.1-2)$$

where

Q_0 = maximum vertical load per unit length of footing

A_0 = actual foundation area per unit length

2. Circular or Square Footing.

$$Q = 6.17cA \quad (6.13.1-3)$$

where

A = actual foundation area

6.13.2 Drained Bearing Capacity

The maximum net vertical load which a footing can support under drained conditions is

$$Q' = (c'N_cK_c + qN_qK_q + \frac{1}{2}\gamma'BN_\gamma K_\gamma)A' \quad (6.13.2-1)$$

where

Q' = maximum net vertical load at failure,

c' = effective cohesion intercept of Mohr Envelope,

N_q = $(\text{Exp} [\pi \tan \phi']) (\tan^2(45^\circ + \phi'/2))$, a dimensionless function of ϕ' ,

N_c = $(N_q - 1) \cot \phi'$, a dimensionless function of ϕ' ,

N_γ = an empirical dimensionless function of ϕ' that can be approximated by $2(N_q + 1) \tan \phi'$,

ϕ' = effective friction angle of Mohr Envelope,

γ' = effective unit weight,

$q = \gamma D$, where D = depth of embedment of foundation,

B = minimum lateral foundation dimension,

A' = effective area of the foundation depending on the load eccentricity,

K_c, K_q, K_γ = correction factors which account for load inclination, footing shape, depth of embedment, inclination of base, and inclination of the ground surface, respectively. The subscripts $c, q,$ and γ refer to the particular term in the equation.

A complete description of the K factors, as well as curves showing the numerical values of $N_q, N_c,$ and N_γ as a function of ϕ' are given in the Commentary.

Two special cases of Eq. 6.13.2-1 for $c' = 0$ (usually sand) are frequently encountered. For a vertical, centric load applied to a foundation at ground level where both the foundation base and ground are horizontal, Eq. 6.13.2-1 is reduced below for two foundation shapes.

1. Infinitely Long Strip Footing.

$$Q_o = 0.5 v' BN_\gamma A_o \quad (6.13.2-2)$$

2. Circular or Square Footing.

$$Q = 0.3 v' BN_\gamma A \quad (6.13.2-3)$$

6.13.3 Sliding Stability

The limiting conditions of the bearing capacity equations in 6.13.1 and 6.13.2, with respect to inclined loading, represent sliding failure and result in the following equations:

1. Undrained Analysis:

$$H = cA \quad (6.13.3-1)$$

where

H = horizontal load at failure.

2. Drained Analysis:

$$H = c'A + Q \tan \phi' \quad (6.13.3-2)$$

6.13.4 Safety Factors

Foundations should have an adequate margin of safety against failure under the design loading conditions. The following factors of safety should be used for the specific failure modes indicated:

Failure Mode	Safety Factor
Bearing Failure	2.0
Sliding Failure	1.5

These values should be used after cyclic loading effects have been taken into account. Where geotechnical data are sparse or site conditions are particularly uncertain, increases in these values may be warranted. See the Commentary for further discussion of safety factors.

6.14 STATIC DEFORMATION OF SHALLOW FOUNDATIONS

The maximum foundation deformation under static or equivalent static loading affects the structural integrity of the platform, its serviceability, and its components. Equations for evaluating the static deformation of shallow foundations are given in 6.14.1 and 6.14.2 below. These equations are applicable to idealized conditions. A discussion of the limitations and of alternate approaches is given in the Commentary.

6.14.1 Short Term Deformation

For foundation materials which can be assumed to be isotropic and homogeneous and for the condition where the structure base is circular, rigid, and rests on the soil surface, the deformations of the base under various loads are as follows:

$$\text{Vertical: } u_v = \left(\frac{1-v}{4GR} \right) Q \quad (6.14.1-1)$$

$$\text{Horizontal: } u_h = \left(\frac{7-8v}{32(1-v)GR} \right) H \quad (6.14.1-2)$$

$$\text{Rocking: } \theta_r = \left(\frac{3(1-v)}{8GR^3} \right) M \quad (6.14.1-3)$$

$$\text{Torsion: } \theta_t = \left(\frac{3}{16GR^3} \right) T \quad (6.14.1-4)$$

where

u_v, u_h = vertical and horizontal displacements,

Q, H = vertical and horizontal loads,

θ_r, θ_t = overturning and torsional rotations,

M, T = overturning and torsional moments,

G = elastic shear modulus of the soil,

v = poisson's ratio of the soil,

R = radius of the base.

These solutions can also be used for approximating the response of a square base of equal area.

6.14.2 Long Term Deformation

An estimate of the vertical settlement of a soil layer under an imposed vertical load can be determined by the following equation:

$$u_v = \frac{hC}{1 + e_o} \log_{10} \frac{q_o + \Delta q}{q_o} \quad (6.14.2-1)$$

where

- u_v = vertical settlement,
- h = layer thickness,
- e_o = initial void ratio of the soil,
- C = compression index of the soil over the load range considered,
- q_o = initial effective vertical stress,
- Δq = added effective vertical stress.

Where the vertical stress varies within a thin layer, as in the case of a diminishing stress, estimates may be determined by using the stress at the midpoint of the layer. Thick homogeneous layers should be subdivided for analysis. Where more than one layer is involved, the estimate is simply the sum of the settlement of the layers. Compression characteristics of the soil are determined from one-dimensional consolidation tests.

6.15 DYNAMIC BEHAVIOR OF SHALLOW FOUNDATIONS

Dynamic loads are imposed on a structure-foundation system by current, waves, ice, wind, and earthquakes. Both the influence of the foundation on the structural response and the integrity of the foundation itself should be considered.

6.16 HYDRAULIC INSTABILITY OF SHALLOW FOUNDATIONS

6.16.1 Scour

Positive measures should be taken to prevent erosion and undercutting of the soil beneath or near the structure base due to scour. Examples of such measures are (1) scour skirts penetrating through erodible layers into scour resistant materials or to such depths as to eliminate the scour hazard, or (2) riprap emplaced around the edges of the foundation. Sediment transport studies may be of value in planning and design.

6.16.2 Piping

The foundation should be so designed to prevent the creation of excessive hydraulic gradients (piping conditions) in the soil due to environmental loadings or operations carried out during or subsequent to structure installation.

6.17 INSTALLATION AND REMOVAL OF SHALLOW FOUNDATIONS

Installation should be planned to ensure the foundation can be properly seated at the intended site without excessive disturbance to the supporting soil. Where removal is anticipated an analysis should be made of the forces generated during removal to ensure that removal can be accomplished with the means available.

Reference

1. Toolan, F. E., and Ims, B. W., "Impact of Recent Changes in the API Recommended Practice for Offshore Piles in and Sand Clays, *Underwater Technology*, V. 14, No. 1 (Spring 1988) pp. 9–13.29.

7 Other Structural Components and Systems

7.1 SUPERSTRUCTURE DESIGN

The superstructure may be modeled in a simplified form for the analysis of the platform jacket, or substructure; however, recognition should be given to the vertical and horizontal stiffnesses of the system and the likely effect on the substructure. This modeling should consider the overturning effects of wind load for environmental loading conditions, the proper location of superstructure and equipment masses for seismic loading conditions, and the alternate locations of heavy gravity loads such as the derrick.

The superstructure itself may be analyzed as one or more independent structures depending upon its configuration; however, consideration should be given to the effect of deflections of the substructure in modeling the boundary supports. Differential deflections of the support points of heavy deck modules placed on skid beams or trusses at the top of the substructure may result in a significant redistribution of the support reactions. In such a case, the analysis model should include the deck modules and the top bay or two of the substructure to facilitate accurate simulation of support conditions. This model should be analyzed to develop support reaction conditions which reflect these effects.

Depending upon the configuration of a platform designed with a modular superstructure, consideration should be given to connecting adjacent deck modules to resist lateral environmental forces. Connection may also have the advantage of providing additional redundancy to the platform in the event of damage to a member supporting the deck modules.

In areas where seismic forces may govern the design of superstructure members, a pseudo-static analysis may be used. The analysis should be based on peak deck accelerations determined from the overall platform seismic analysis. The height at which the acceleration is selected should be based upon the structural configuration and the location of the dominant superstructure masses.

Appendix B – Platform Database

Platform Database No.	Hurricane Exposure Event(s)	Number of Piles	Length of Piles (ft)	Year of Installation	Age of Piles	Soil Stratigraphy	Tip Bearing Stratum	Sampling and Testing Method	Water Depth (ft)	Number of Well Conductors	Maximum Wave Height, H _{max} (ft)	API Section 17 A-2 ULS Wave Height, H _{dgn} (ft)	(H _{max} /H _{dgn}) ²	Expected Mode of Failure for the Piles
1	Katrina	8	135	1965	40	Stratum 1: very soft to firm clay (90') Stratum 2: fine sand (12') Stratum 3: firm clay (12') Stratum 4: interbedded sandy silt and firm silty clay (19') Stratum 5: sandy silt (10') Stratum 6: silty fine sand (10')	Stratum 5: sandy silt	Sampling Method: driven Testing Method: miniature vane, torvane, unconfined compression and UU triaxial tests	140	18	59	55	1.14	Axial
2	Katrina	6	140	1966	39	Stratum 1: very soft to firm clay (90') Stratum 2: fine sand (12') Stratum 3: firm clay (12') Stratum 4: interbedded sandy silt and firm silty clay (19') Stratum 5: sandy silt (10') Stratum 6: silty fine sand (10')	Stratum 5: sandy silt	Sampling Method: driven Testing Method: miniature vane, torvane, unconfined compression and UU triaxial tests	140	12	59	55	1.14	Axial
3	Andrew	8	175	1963	29	Stratum 1: firm to very stiff clay (184') Stratum 2: dense to very dense fine sand (93') Stratum 3: very stiff to hard clay (118')	Stratum 1: very stiff clay	Sampling Method: both driven and pushed Testing Method: miniature vane, torvane, unconfined compression and UU triaxial tests	140	12	61	55	1.23	Combined Axial/ Lateral
4	Andrew	4	165	1969	23	Stratum 1: firm clay (158') Stratum 2: fine sand (14') Stratum 3: silty clay (6') Stratum 4: fine-to-medium sand (78')	Stratum 2: fine sand	Sampling Method: driven Testing Method: miniature vane, unconfined compression and UU triaxial tests	60	0	51	46	1.21	Lateral

Platform Database No.	Hurricane Exposure Event(s)	Number of Piles	Length of Piles (ft)	Year of Installation	Age of Piles	Soil Stratigraphy	Tip Bearing Stratum	Sampling and Testing Method	Water Depth (ft)	Number of Well Conductors	Maximum Wave Height, H _{max} (ft)	API Section 17 A-2 ULS Wave Height, H _{dgn} (ft)	(H _{max} /H _{dgn}) ²	Expected Mode of Failure for the Piles
5	Andrew	8	187	1965	27	Stratum 1: soft to stiff clay (141') Stratum 2: clayey silt (4') Stratum 3: silty fine sand (13') Stratum 4: laminated clay, silt & sandy silt (178') Stratum 5: stiff clay (13') Stratum 6: silty fine sand (8') Stratum 7: stiff silty clay (32') Stratum 8: stiff clay (92')	Stratum 5: stiff clay	Sampling Method: driven Testing Method: miniature vane, unconfined compression and UU triaxial tests	140	16	60	55	1.20	Axial
6		8							290	40		60		Lateral
7	Katrina	4	360						470	21		>62		
8	Katrina	4	274	1984	21	Stratum 1: very soft to soft clay (30') Stratum 2: silty fine to fine sand (56') Stratum 3: interbedded firm to stiff clay and fine to silty fine sand (37') Stratum 4: firm to very stiff clay (56') Stratum 5: silty fine sand (101') Stratum 6: very stiff clay (52')	Stratum 5: silty fine sand	Sampling Method: both driven and pushed Testing Method: miniature vane, torvane, unconfined compression and UU triaxial tests	220	12	77	59	1.70	Axial
9	Katrina	4	118	1989	16	Stratum 1: silty fine sand (5') Stratum 2: firm clay (20') Stratum 3: silty fine sand (11') Stratum 4: fine sand (71') Stratum 5: interbedded very stiff clay and silty fine sand (44') Stratum 6: fine sand (50')	Stratum 5: interbedded very stiff clay and silty fine sand	Sampling Method: driven Testing Method: miniature vane, torvane, unconfined compression and UU triaxial tests	60	1	56	45	1.55	Combined Axial/ Lateral

Platform Database No.	Hurricane Exposure Event(s)	Number of Piles	Length of Piles (ft)	Year of Installation	Age of Piles	Soil Stratigraphy	Tip Bearing Stratum	Sampling and Testing Method	Water Depth (ft)	Number of Well Conductors	Maximum Wave Height, H _{max} (ft)	API Section 17 A-2 ULS Wave Height, H _{dgn} (ft)	(H _{max} /H _{dgn}) ²	Expected Mode of Failure for the Piles
10	Ike	3	220/ 265	2001	5	Stratum 1: very soft clay (11') Stratum 2: soft to hard clay (337')	Stratum 2: very stiff clay	Sampling Method: pushed Testing Method: miniature vane, torvane, pocket penetrometer and UU triaxial tests	360	1	71	61	1.35	Axial
11	Katrina	4	239/ 309	2000	5	Stratum 1: fine sand (9') Stratum 2: soft to firm clay (27') Stratum 3: fine sand (64') Stratum 4: stiff clay (8') Stratum 5: fine sand (9') Stratum 6: stiff to very stiff clay (6.5') Stratum 7: silty fine to fine sand (13.5') Stratum 8: stiff to very stiff clay (71') Stratum 9: silty fine to fine sand (73') Stratum 10: very stiff silty clay (7') Stratum 11: fine sand (27')	Stratum 9: silty fine to fine sand/ Stratum 11: fine sand	Sampling Method: both driven and pushed Testing Method: miniature vane, torvane, unconfined compression and UU triaxial tests	120	4	67	54	1.54	Lateral
12	Rita	4	255	1972	33	Stratum 1: stiff to firm clay (37.5') Stratum 2: medium dense silty fine sand grading to clay silt below 56' (34.5) Stratum 3: stiff to very stiff clay (144') Stratum 4: very dense (silty) fine sand (100') Stratum 5: very stiff clay (25') Stratum 6: very dense sandy silt (15') Stratum 7: very stiff clay (N/A)	Stratum 4: very dense (silty) fine sand	Sampling Method: driven Testing Method: miniature vane, unconfined compression and UU triaxial tests	190	12	67	58	1.33	Lateral

Platform Database No.	Hurricane Exposure Event(s)	Number of Piles	Length of Piles (ft)	Year of Installation	Age of Piles	Soil Stratigraphy	Tip Bearing Stratum	Sampling and Testing Method	Water Depth (ft)	Number of Well Conductors	Maximum Wave Height, H _{max} (ft)	API Section 17 A-2 ULS Wave Height, H _{dgn} (ft)	(H _{max} /H _{dgn}) ²	Expected Mode of Failure for the Piles
13		12	372/ 374/ 230			Stratum 1: very soft to medium stiff clay (20') Stratum 2: stiff clay (170') Stratum 3: stiff to hard clay (>261')	Stratum 3: stiff to hard clay	Sampling Method: both driven and pushed Testing Method: miniature vane, torvane, unconfined compression and UU triaxial tests	270	18		60		Lateral
14		12	365						1030	30		>62		
15		12	350 to 357			Stratum 1: very soft to firm clay (66' to 86') Stratum 2: medium sandy silt (12' to 20') Stratum 3: firm to very stiff clay (226' to 229') Stratum 4: medium silty fine sand (55' to 60') Stratum 5: very stiff clay (72' to 74') Stratum 6: medium silty fine sand (>11')	Stratum 4: medium silty fine sand	Sampling Method: driven Testing Method: miniature vane, torvane, unconfined compression and UU triaxial tests	400	18		62		
16	Ivan	8	400	1971	33				190			57		Lateral
17	Ivan	8	400	1971	33				210			58		
18	Ivan	8	400	1973	31				190			58		
19	Ivan	8	398	1971	33				190			58		
20	Ivan	8	400	1980	24				210			58		
21	Ivan	8	400	1986	18				190			58		

Platform Database No.	Hurricane Exposure Event(s)	Number of Piles	Length of Piles (ft)	Year of Installation	Age of Piles	Soil Stratigraphy	Tip Bearing Stratum	Sampling and Testing Method	Water Depth (ft)	Number of Well Conductors	Maximum Wave Height, H _{max} (ft)	API Section 17 A-2 ULS Wave Height, H _{dgn} (ft)	(H _{max} /H _{dgn}) ²	Expected Mode of Failure for the Piles
22	Rita	4	290	1976	29	Stratum 1: very soft to firm clay (106') Stratum 2: silty fine sand (21') Stratum 3: stiff clay (13.5') Stratum 4: silty fine sand (27.5') Stratum 5: stiff clay (49.5') Stratum 6: laminated stiff clay and silty fine sand (27.5') Stratum 7: silty fine sand (26') Stratum 8: firm to stiff silty clay (69')	Stratum 8: firm to stiff silty clay	Sampling Method: driven Testing Method: miniature vane, torvane, unconfined compression and UU triaxial tests	110	0	57	53	1.16	Lateral
23	Katrina	8		1964	41	Stratum 1: very soft to soft clay (40') Stratum 2: soft to medium stiff clay (30') Stratum 3: stiff clay (110') Stratum 4: very stiff clay (225')			150	8		56		
24	Katrina	8	128 /102 /132	1956	49	Stratum 1: firm clay (5') Stratum 2: medium dense silty fine sand (12') Stratum 3: firm to very stiff clay (146') Stratum 4: dense fine sand (>43')	Stratum 3: firm to very stiff clay	Sampling Method: both driven and pushed Testing Method: miniature vane, torvane, pocket penetrometer and UU triaxial tests	100	6		52		
25	Katrina	4	169	1967	38	Stratum 1: firm clay (5') Stratum 2: medium dense silty fine sand (12') Stratum 3: firm to very stiff clay (146') Stratum 4: dense fine sand (>43')	Stratum 4: dense fine sand	Sampling Method: both driven and pushed Testing Method: miniature vane, torvane, pocket penetrometer and UU triaxial tests	90	4	44	51	0.74	Lateral
26	Rita	4	181	1994	11				100	2		52		Lateral

Platform Database No.	Hurricane Exposure Event(s)	Number of Piles	Length of Piles (ft)	Year of Installation	Age of Piles	Soil Stratigraphy	Tip Bearing Stratum	Sampling and Testing Method	Water Depth (ft)	Number of Well Conductors	Maximum Wave Height, H _{max} (ft)	API Section 17 A-2 ULS Wave Height, H _{dgn} (ft)	(H _{max} /H _{dgn}) ²	Expected Mode of Failure for the Piles
27	Rita	4	281/ 264	2000	5	Stratum 1: very soft clay (14') Stratum 2: firm to stiff clay (86') Stratum 3: medium dense sand (15') Stratum 4: very stiff clay (>185')	Stratum 4: very stiff clay		300	2	75	61	1.51	Lateral
28	Rita	8		1981	24	Stratum 1: stiff clay (10') Stratum 2: very stiff clay (15') Stratum 3: medium dense sand (170') Stratum 4: very stiff sandy clay to silt (15') Stratum 5: medium dense sand (130') Stratum 6: hard clay (10')			60	15		45		Lateral
29	Katrina	8	140	1967	38	Stratum 1: very soft to firm clay (75') Stratum 2: dense to very dense sand (80') Stratum 3: silty clay (5.5') Stratum 4: dense to very dense sand (N/A)	Stratum 2: dense to very dense sand	Sampling Method: driven Testing Method: miniature vane, unconfined compression and UU triaxial tests	150	12	63	56	1.27	Lateral
30	Katrina	6	210	1973	32	Stratum 1: very soft to firm clay (75') Stratum 2: dense to very dense sand (80') Stratum 3: silty clay (5.5') Stratum 4: dense to very dense sand (N/A)	Stratum 4: dense to very dense sand	Sampling Method: driven Testing Method: miniature vane, unconfined compression and UU triaxial tests	150	12	63	56	1.27	Lateral

Appendix C – Description of 3-D FEM Model

Structural Analysis Computer Software (SACS™) was used to conduct 3-Dimensional Finite Element Method analyses of the case study platforms. SACS™ is a suite of modular software developed by Engineering Dynamics, Inc. for use in both offshore structures and general civil engineering applications (Engineering Dynamics 2005). Use of this software was donated in-kind for this project by Engineering Dynamics, Inc. The inputs to this model are the structural properties of all members and connections including the piles, the behavior of the soil surrounding the piles (i.e., t-z and p-y curves as a function of depth along each pile and a Q-z curve at the tip), and the environmental loading including the magnitude and direction of waves, wind and current. The primary output from this model includes the total load on the structure, typically expressed as a base shear, the displacement of the deck, and the loads, moments and deformations in individual members.

The software uses large deflection, elasto-plastic, nonlinear, finite-element analysis to determine the load-displacement relationship of a jacket structure. When a full plastic collapse (pushover) analysis is performed, the software also determines the load at which the structure collapses. The solution process involves three levels of iteration. For any global load increment, a beam-column solution is performed for each plastic member using the cross section sub-element details. The global stiffness iteration is then performed including the effects of connection flexibility, plasticity and failure and the foundation stiffness iteration including the nonlinear pile/soil effects. During any global solution iteration, the deflected shape of the structure is determined and compared to the displacements of the previous solution iteration. If convergence is not achieved, the new global displacements of the joints along with the beam internal and external loads are used to recalculate the elemental stiffness matrices. The structural stiffness iteration is then repeated including the effect of the foundation until the displacements meet the convergence tolerance.

The solution of the pile/soil foundation also requires an iterative procedure. Initially, soil forces and stiffness is calculated assuming deflections and rotations are zero along the full length of the pile. For the given pilehead displacement, the pile deflections and rotations are then determined. New soil forces and stiffness are calculated based on these

new displacements and rotations. Using the segment deflections and rotations, the program computes the pile segment internal loads and then calculates the pile segment plasticity. The resulting plastic forces are then applied to the pile segment for the next iteration. This procedure is repeated until all of the deflections and rotations along the pile length have converged. At the final deflected position, the program calculates the pilehead stiffness matrix by incrementally varying the pilehead deflections and rotations and computing the pilehead restraining forces and moments. The resulting pilehead plastic forces are transformed into the global coordinates and added to the global plastic force vector for the next global increment or iteration.

Brief discussions of various modules of the software and how to perform a pushover analysis and a hindcast analysis are provided herein. More details of the software can be found in the user's manuals (Engineering Dynamics 2005).

Description of Various Software Modules

The SACS IV module is an executive module. It utilizes the COLLAPSE and PSI modules to perform a pushover analysis to determine the ultimate capacity of an offshore jacket platform. The SACS IV model input file, designated as "sacs.inp," contains pertinent information for the program to function and can be developed using the graphical user interface within the program or using a text file. The model input file consists of the analysis option, post processing option, material and section property data, element data, joint data and load data. This model input file contains the information of the entire structure and is called upon when any type of analysis is performed using the SACS™ suite of software.

The SEASTATE module is an environmental load module that operates within the SACS IV module to generate load data for the analysis. The user can input parameters for the wave, wind and current conditions, dead load, and buoyancy of the structure. SEASTATE takes the environmental load parameters and generates distributed loads that vary along the members of the platform. Together with the SACS IV module, SEASTATE can reduce all environmental loads to a resultant horizontal force and overturning moment at various locations on the structure. At the mudline elevation, these forces represent the base shear and overturning moment that the foundation system would be subjected to during a storm.

The COLLAPSE module is a large deflection, elasto-plastic, nonlinear finite-element analysis module used to perform the pushover analysis of the structure. The collapse input file, designated as “clp.inp” tells the SACSTTM suite of software the types of analysis to perform, options to consider while performing the analysis and the convergence criteria that must be satisfied to terminate the analysis. The collapse input file also specifies the load combinations and incremental load factors for the analysis. Additionally, it tells the SACSTTM suite of software whether to include the effects of a non-linear pile/soil foundation. The COLLAPSE module uses the information from the collapse input file to apply a series of incremental loads to the structure until it collapses.

The Pile Structure Interaction (PSI) module analyzes the behavior of a pile-supported structure by representing the structure above the mudline as a linear elastic model, while the pile below the mudline is represented as a beam-column on a nonlinear elastic foundation. The module reduces the loads on the linear structure above the mudline to an equivalent linear stiffness matrix involving only six degrees of freedom at each pile head joint. It then uses a finite difference method to obtain the pile axial solution and then uses the resulting internal axial forces to obtain the lateral solution of the pile. The nonlinear foundation model, including the pile and soil, is specified in the PSI input file designated as “psi.inp.”

The PSI input file contains information related to the analysis option, tolerance and convergence criteria. It contains all information about the piles and well conductors, including the diameter, wall thickness, Young’s modulus, shear modulus, nominal yield strength, unit weight of steel and segment length. It also contains the soil parameters to generate the axial, lateral and torsional responses of the pile/soil foundation. The PSI module uses these soil parameters to generate the axial load transfer (t-z) curves, tip load-displacement (Q-z) curves and lateral load-deflection (p-y) curves based on API RP 2A-WSD (2000).

To illustrate, the structural model for Platform 1 developed in SACSTTM is shown in Figure C.1 and the geotechnical design information used to estimate pile capacity and establish t-z, Q-z and p-y curves is shown in Figure C.2.

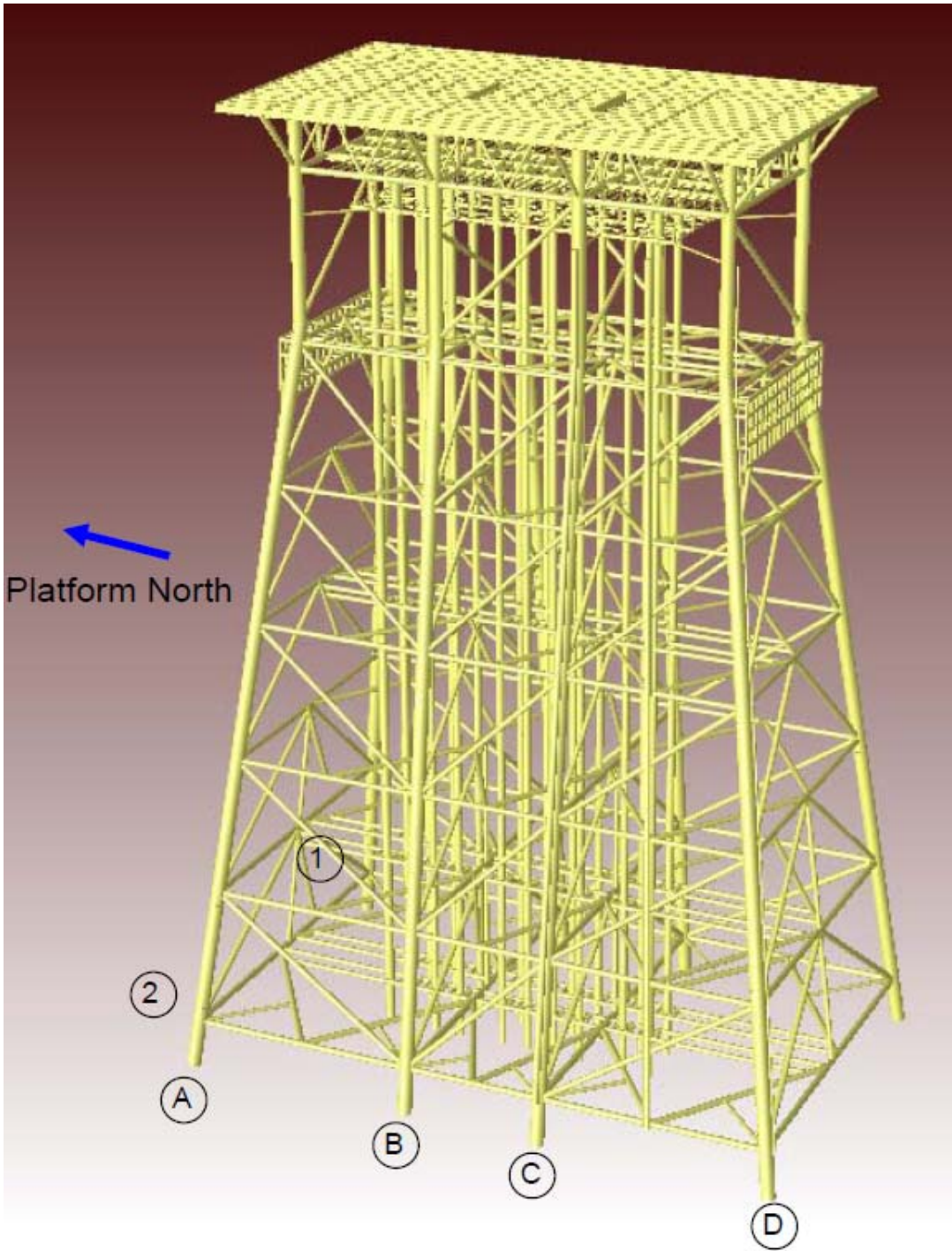


Figure C.1 An Illustration of the SACSTM model for Platform 1 (Energ0 2006)

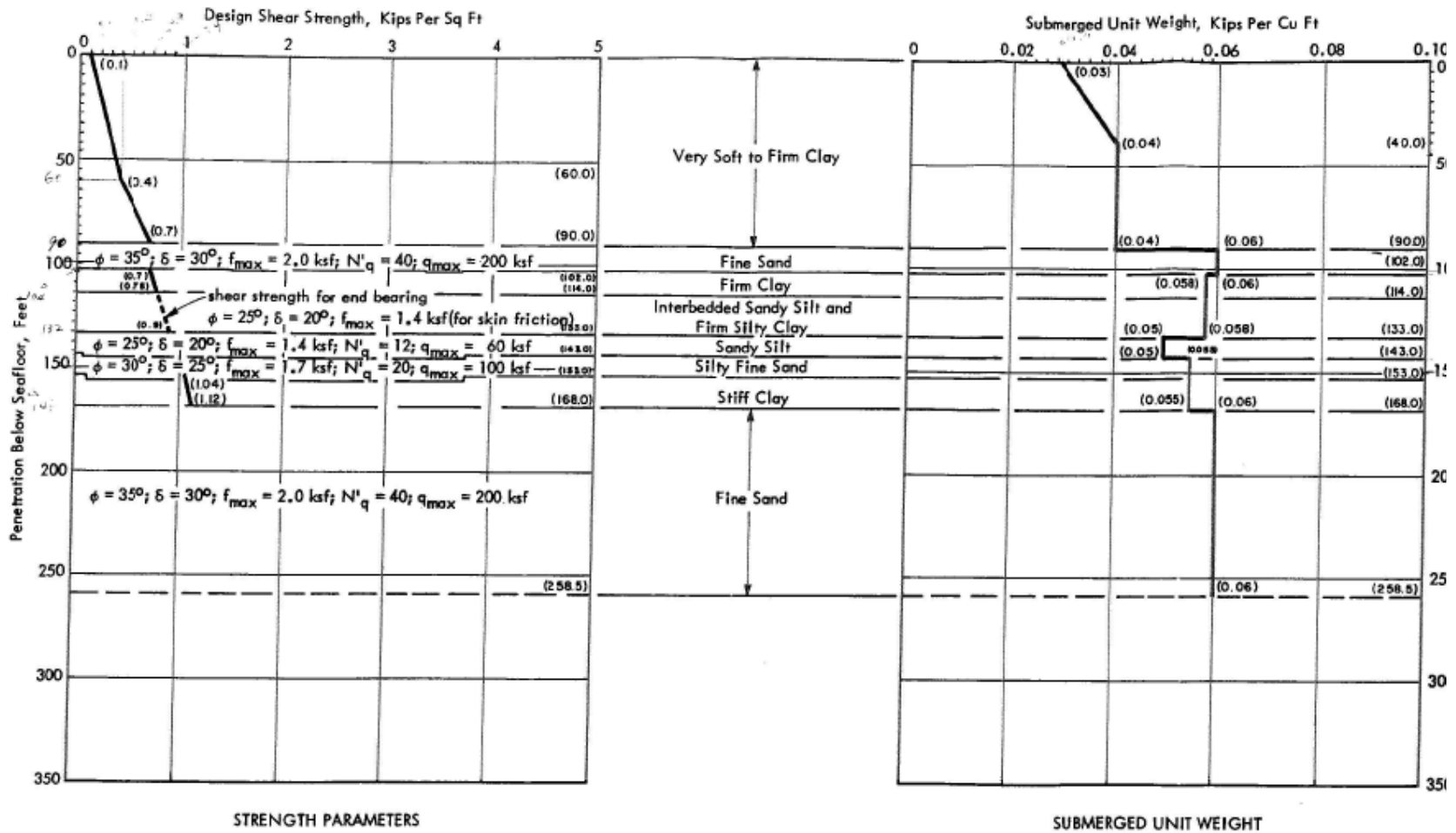


Figure C.2 Recommended Geotechnical Design Parameters for Platform 1 (McClelland 1979)

Hindcast Analysis

The hindcast analysis can be performed using the SACS IV module with the SEASTATE and PSI modules. The environmental load parameters for the hurricane are entered into the SEASTATE module. Each environmental load parameter has a set of inputs that must be specified. For the waves, the wave height, period and direction are required. The wind and current are both defined in terms of velocity and direction. In order to account for the worst-case scenario where the waves, wind and current all approach the structure from the same direction, the environmental load parameters are defined in the same direction in this study. The loading direction is typically governed by the direction of the waves because the waves generate a significant portion of the horizontal environmental load. To illustrate, the environmental load parameters used to develop the hindcast base shear and overturning moment on the foundation of Platform 1 are presented in Table C.1. Since the direction of the waves is approximately the end-on direction of this platform (toward Platform North in Figure C.1), the environmental load parameters in Table C.1 are all defined in the end-on direction.

Once the environmental load parameters are defined, a “Linear Static Analysis with Pile Soil Interaction” can be performed to determine the hindcast base shear and overturning moment. The output of the analysis is documented in the “psilst” file, under the heading “Seastate Basic Load Case Descriptions Relative to Mudline Elevations.” The output hindcast forces on the foundation are reported in 6 degrees of freedom (F_x , F_y , F_z , M_x , M_y , M_z), where the x- and y-directions are the two horizontal directions and the z-direction is the vertical direction. In order to obtain the hindcast base shear ($P_{H,Hindcast}$) and overturning moment ($M_{Hindcast}$) on the foundation, these forces are resolved using the following equations.

$$P_{H,Hindcast} = \sqrt{F_x^2 + F_y^2}$$

$$M_{Hindcast} = \sqrt{M_x^2 + M_y^2}$$

For example, the hindcast base shear and overturning moment (Table C.1) on the foundation of Platform 1 are determine to be approximately 4,000 kips and 362,000 ft-kips, respectively.

Table C.1 Environmental Load Parameters for the Hindcast Analysis of Platform 1 in the
End-on Direction

Wave Height (ft)	Wave Period (sec)	Wind Speed (knots)	Current Velocity (knots)	Vertical Load (kips)	Hindcast Base Shear (kips)	Hindcast Overturning Moment (ft-kips)
58.7	16.1	68.9	1.9	2500	4053	362323

Pushover Analysis

The pushover analysis can be performed similarly as the hindcast analysis. The environmental load parameters used in the pushover analysis may or may not correspond to those used in the hindcast analysis and will depend on the load factor at which failure occurs in the pushover analysis. If the load factor at failure is higher than 1.2 or lower than 0.8, the environmental load parameters used in the hindcast analysis are not suitable for use in the pushover analysis as explained in the next paragraph. With the environmental load parameters defined in the SEASTATE module and the SACS IV, COLLAPSE and PSI input files developed, the user can select the “Full Plastic Collapse Analysis” option in the SACS™ suite of software to perform a pushover analysis.

The SEASTATE module will propagate the waves, wind and current through the structure to determine the maximum loading condition and transform the environmental loads into distributed loads that vary along the member lengths. The COLLAPSE module will multiply the maximum load determined by the SEASTATE module by a load factor. The distributed loads are increased monotonically with an increasing load factor and applied to the structure until it collapses. For example, at a load factor of 0.0 there would be no environmental loads applied to the structure whereas at a load factor of 1.0 the full environmental loads would be applied. The COLLAPSE module starts at a load factor of 0.0 and increases at a specified interval until either the maximum load factor specified by the user is reached or until the structure collapses. Ideally, the load factor at failure should be between 0.8 and 1.2. If the load factor at failure is higher than 1.2 or lower than 0.8, the shapes of the environmental load profiles may change significantly from the hindcast conditions and scaling of the environmental load profiles linearly with a load factor may not be representative of the load causing the structure to fail. For example, the load factor at failure for Platform 1 in the initial pushover analysis using the same environmental load parameters as in the hindcast analysis is approximately 0.4. Consequently, the wave height and wave period used in the subsequent pushover analysis (Table C.2) are reduced

from the values used in the hindcast analysis (Table C.1) and the load factor at failure becomes 0.84, which is within the reasonable range.

Table C.2 Environmental Load Parameters and Results of the Pushover Analysis of Platform 1 in the End-on Direction

Wave Height (ft)	Wave Period (sec)	Pushover Failure Load Factor	Pushover Failure Base Shear (kips)	Pushover Failure Overturning Moment (ft-kips)
50	12.5	0.84	2305	214614

An example output from the pushover analysis of Platform 1 in the end-on direction is shown in Table C.3. This table shows the joint displacement report from the “clprst” output file from the pushover analysis of Platform 1, where some load steps are removed for clarity. The load step, load factor and displacements in the x-, y- and z-direction (δ_x , δ_y and δ_z) are taken directly from the output file. The base shear and overturning moment corresponding to a load factor of 1.0 [$P_{H(LF=1)}$ and $M_{(LF=1)}$] can be determined from the “psilst” output file under the heading “Seastate Basic Load Case Descriptions Relative to Mudline Elevations” similarly as the hindcast base shear and overturning moment. The horizontal deck displacement (δ_h), base shear (P_H) and overturning moment (M) corresponding to each load factor can be calculated using the following equations.

$$\delta_h = \sqrt{\delta_x^2 + \delta_y^2}$$

$$P_H = P_{H(LF=1)} \cdot LF$$

$$M = M_{(LF=1)} \cdot LF$$

where:

LF is the load factor.

The results from the above calculations are summarized in Table C.3. The base shear versus horizontal deck displacement relationship is usually presented graphically. This relationship for Platform 1 in the end-on direction is shown in Figure C.3. Tables C.2 and C.3 show that Platform 1 fails at a load factor of 0.84, a horizontal deck displacement of 32 inches, a base shear of 2,300 kips and an overturning moment of 215,000 ft-kips, approximately. The failure in the pushover analysis is contributed by a failure in the foundation, which consequently causes the entire platform to collapse. Specifically, piles A1 and A2 (Figure C.1) are overloaded in compression and start to plunge, which then causes piles D1 and D2 to be loaded to capacity in tension. According to the pushover analysis, the failure is an overturning failure of the foundation, as none of the piles reaches 50 percent of their available structural capacity.

Table C.3 Partial Output from the Pushover Analysis of Platform 1 in the End-on Direction

Load Step	Load Factor, LF	Displacements (in.)			Horizontal Deck Displacement, δ_h (in.)	Base Shear, P_H (kips)	Overturning Moment, M (ft-kips)	
		δ_x	δ_y	δ_z				
		5	0.19	2.62				-0.03
10	0.41	6.23	0.00	-0.40	6	1125	104752	
15	0.58	9.73	0.04	-0.35	10	1591	148186	
20	0.69	13.71	0.09	-0.92	14	1893	176290	
25	0.79	26.92	0.92	-3.41	27	2167	201840	
27	0.84	32.05	0.61	-4.37	32	2305	214614	
28	0.86	Platform collapsed – numerical analysis did not converge						

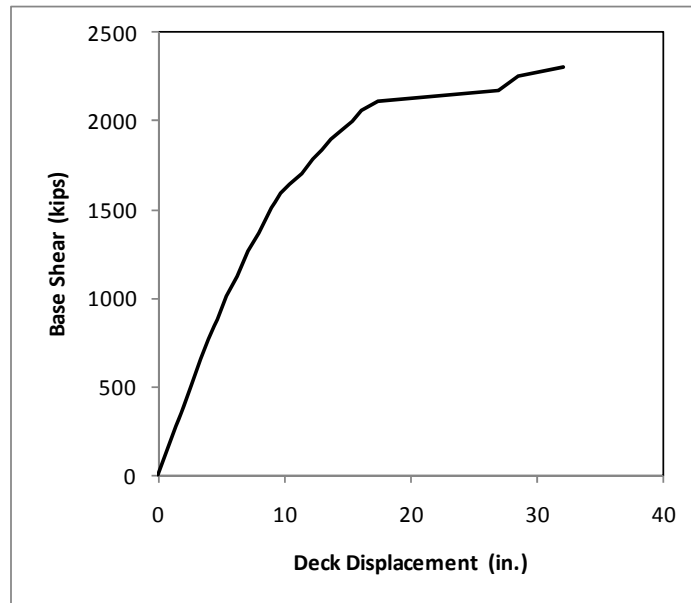


Figure C.3 Base Shear versus Deck Displacement for Platform 1 in the End-on Direction

Appendix D – Description of Simplified Plasticity Model

The simplified plastic collapse model uses an upper-bound kinematically admissible solution to define the combinations of base shear and overturning moment that cause the complete collapse of the foundation system (Murff and Wesselink 1986). The upper-bound method assumes a plastic collapse mechanism, where all elements of resistance are characterized as rigid and perfectly plastic (Murff 1987). The piles in the system collapse when one hinge forms at the pile head and a second hinge forms at some depth below the pile head. The collapse of the entire system occurs when two hinges form in each of the piles in the system as shown schematically in Figure D.1.

The performance of the foundation system is measured by comparing the ratio of the rate of internal dissipation of energy related to the resistance provided by the piles embedded in soils (\dot{W}_{int}) to the rate of external work related to the system loads applied to the foundation (\dot{W}_{ext}) as shown by the performance function, $g(x)$, presented below (Tang and Gilbert 1992).

$$g(x) = \frac{\dot{W}_{int}}{\dot{W}_{ext}} - 1.0$$

The rate of internal dissipation of energy can be separated into the following four components:

- the dissipation of energy due to the axial deformation of the soil between the two plastic hinges that form at the pile head and at depth,
- the dissipation of energy due to the lateral deformation of the soil between the two plastic hinges,
- the dissipation of energy due to the plastic yield of the pile at the first hinge that forms at the pile head, and
- the dissipation of energy due to the plastic yield of the pile at the second hinge at depth.

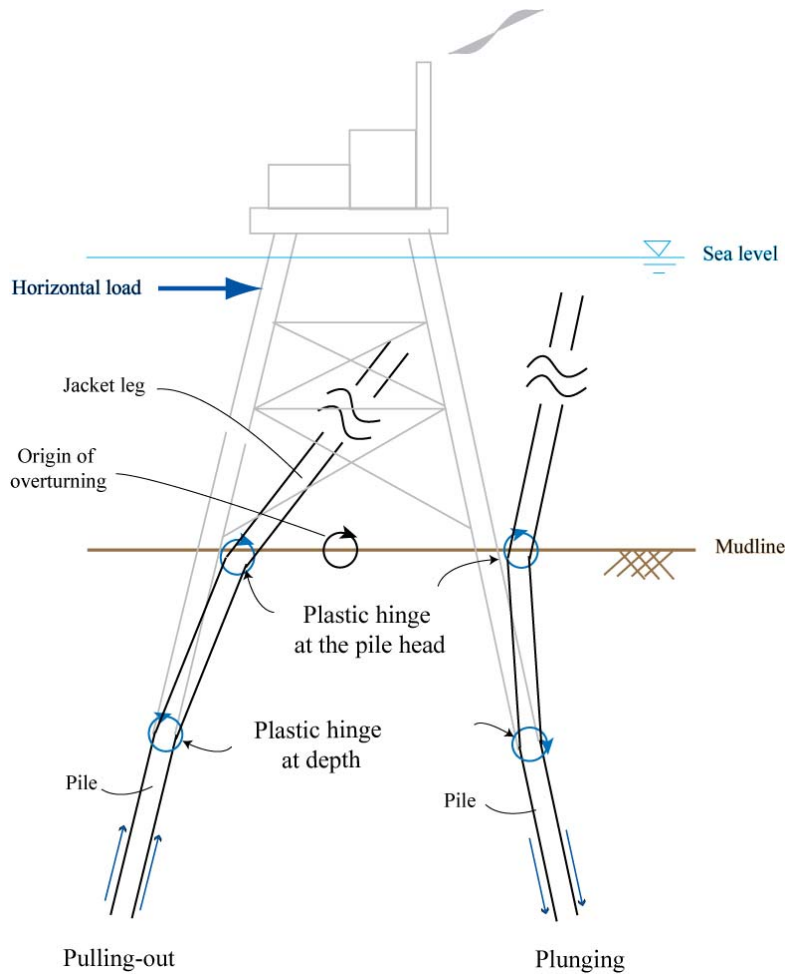


Figure D.1 Schematic of Pile System Collapse Due to the Formation of Plastic Hinges (Lee 2007)

The external work rate consists of the contributions from the vertical and horizontal loads on the foundation system due to the platform base translating laterally and rotating about a point at the mudline. The foundation system collapses when the external work rate is equal to the rate of internal dissipation of energy, i.e. $\dot{g}(x) = 0.0$. The solution is an upper-bound approximation to the system capacity because it does not explicitly satisfy force and moment equilibrium. Also, the structure supported by the piles is assumed to be perfectly rigid and can distribute loads as necessary cause a complete collapse of the foundation system. Comparisons between this upper-bound solution and more rigorous pushover analyses indicate that the upper-bound model overestimates the total horizontal force causing failure by about 10 percent (Murff and Wesselink 1986).

The original model developed by Murff and Wesselink (1986) and extended by Tang and

Gilbert (1992) was updated for this study to incorporate multiple soil layers and pile wall thicknesses below the mudline. In addition, the contribution of well conductors to the foundation system capacity was included. The conductors are modeled as piles that are connected to the structure with rollers (Figure D.2) such that the structure can move the conductors horizontally but not vertically (that is, the conductors contribute lateral resistance but not axial resistance to the foundation system).

To account for the modifications made to the simplified plastic collapse model, the input structure of the program was re-arranged to offer more flexibility and transparency to the user. The model requires four different types of input files, all of which are text files that can be developed using a text editing program such as Microsoft® Notepad. The four input file types can be considered as:

- the routing input file
- the executive input file
- the pile structural capacity input file
- the pile geotechnical capacity input file

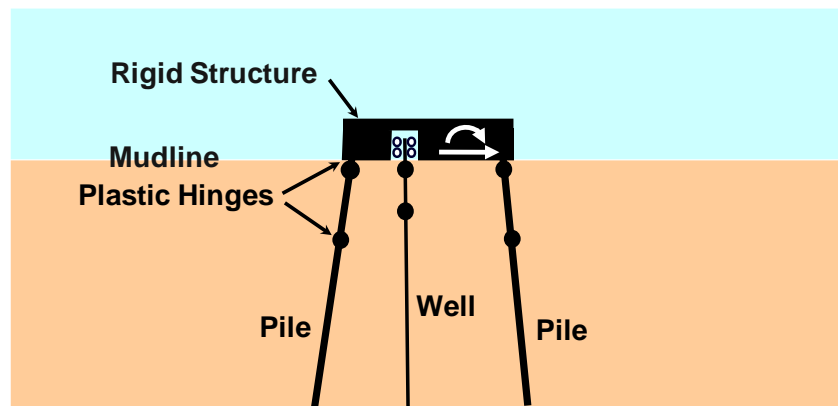


Figure D.2 Schematic of the Updated Plastic Collapse Model for Piles and Wells

The routing input file, designated as “TOPCATF.inp,” contains only the name of the executive input file. This allows for several executive input files containing differing parameters to be developed so that a parametric analysis can be performed simply by changing the name of the executive input file specified herein.

The executive input file contains the system load data, number of piles and conductors, pile and conductor geometry, pile structural capacity input file name, and pile

geotechnical capacity input file name. Under the system load data section of the executive input file, there are six lines of text which represent:

- the horizontal load (P_H),
- the moment arm of the horizontal load above the mudline (h),
- the eccentricity of the horizontal load in the y -direction (r),
- the skew angle measured counterclockwise from the positive x -axis (α),
- the vertical load applied to the platform (P_V), and
- the eccentricity of the vertical load (e)

The above system load parameters are shown schematically in Figures D.3 and D.4.

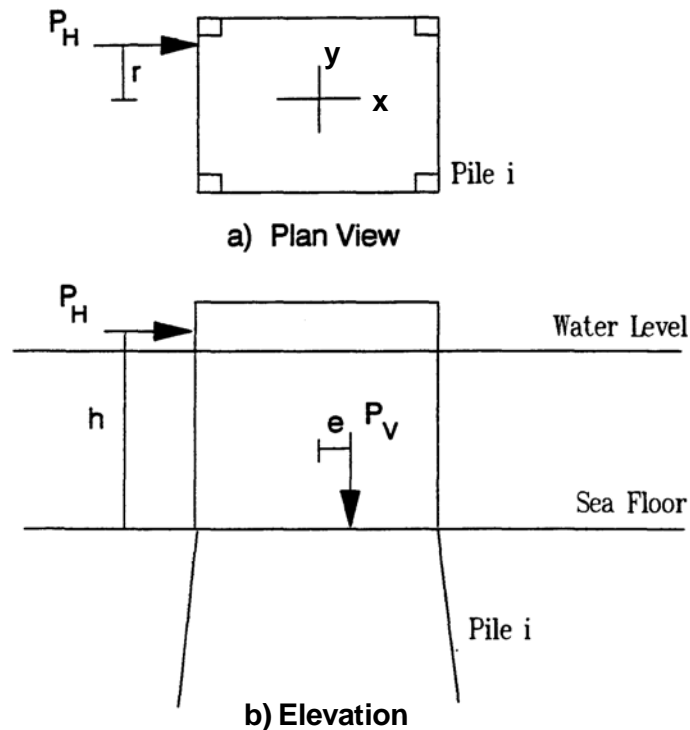


Figure D.3 System Load Parameters for the Simplified Plastic Collapse Model (Tang and Gilbert 1992)

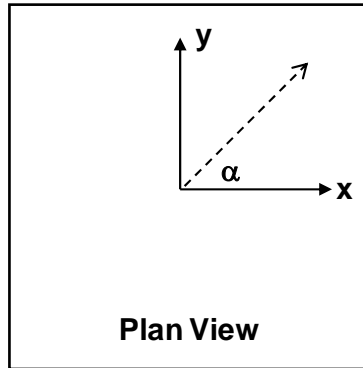


Figure D.4 Orientation of the Skew Angle in the Simplified Plastic Collapse Model (Tang and Gilbert 1992)

The next section of the executive input file contains information about the piles and conductors. The number of piles is specified in the input file, where conductors of the same size are usually accounted for as one additional pile regardless of the number of conductors that the platform is actually equipped with. For example, in an 8-pile platform with 20 identical conductors, the number of piles specified in the input file would be 9. If the same platform were to be analyzed without considering the conductors, the number of piles can simply be changed from 9 to 8. Each pile is given a number in the input file and seven pile geometric parameters are defined on a single line of the input separated by a space between each of them. The geometric parameters are:

- the x-coordinate (X),
- the y-coordinate (Y),
- the batter angle in the x-direction (THETAX),
- the batter angle in the y-direction (THETAY),
- the pile length (L),
- the axial constraint parameter (0 or 1), and
- the number of piles or conductors in the group (NGROUP).

The axial constraint parameter defines whether the pile is constrained axially. A value of 0 denotes that the pile is not constrained in the axial direction and is free to move independently of the platform in the axial direction. This assumption is used to model the conductors. A value of 1 denotes that the pile is constrained in the axial direction and is used to model the pile. NGROUP is typically set to 1 when modeling the pile since every pile has unique geometric parameters. When conductors are modeled in the analysis, NGROUP can be set to the number of conductors to account for the contribution of many

conductors of the same size. Considering the previous example of an 8-pile platform with 20 conductors, the ninth pile in the input would have an axial constrain parameter of 0 and an NGROUP value of 20. The x- and y-coordinates of the conductor group should be the center of the entire conductor group.

The final two input parameters defined for each pile in the executive input file are the names of the pile structural capacity input file and pile geotechnical capacity input file. The updated plastic collapse model no longer calculates the pile structural capacity and geotechnical capacity internally. Instead, it allows the user to perform the calculations externally (for example, using Microsoft® Excel) and import the calculated structural and geotechnical capacities into these input files. Only the names of the pile structural capacity input file and pile geotechnical capacity input file are specified in the executive input file. The pile structural capacity input file and geotechnical capacity input file are typically designated as “WPILE.inp” and “WSOIL.inp,” respectively. A letter “C” is usually added to denote that the file is for conductors, and a number “1” or “2” is usually added to denote how many directions the foundation pile is battered in.

The pile structural capacity input file contains the axial structural capacity in compression and tension (Q_{\max}) and the moment capacity in bending (M_{\max}) over a given pile length (Z). The recent update to the program allows up to three pile sections to be defined. The following equations are used to calculate the axial structural capacity and moment capacity of a steel pipe pile with a diameter of D and a pile wall thickness of t .

$$Q_{\max} = \frac{\pi}{4} [D^2 - (D - 2t)^2] \cdot f_Y$$

$$M_{\max} = \frac{1}{6} [D^3 - (D - 2t)^3] \cdot f_Y$$

where:

f_Y is the nominal yield strength of the steel.

The pile geotechnical capacity input file contains the number of rows of data in the input file (NDEPTH) and the depth increment (DZ). Following these, it contains four columns of data which from left to right correspond to:

- the length along the pile (Z),

- the axial capacity of the pile in compression at length Z (Q_C),
- the axial capacity of the pile in tension at length Z (Q_T), and
- the lateral capacity of the pile at length Z (R).

This input file defines the capacity of a pile at specified intervals along the pile. The geotechnical capacity input file is developed using a custom-built spreadsheet that calculates Z, Q_C , Q_T and R based on the recommended design parameters in the geotechnical report for the study platform. The calculations in the spreadsheet follow the recommendations in API RP 2A-WSD (2000), which is included in Appendix A.

The critical horizontal collapse load (that is, base shear, P_H) of the foundation system at a specified moment arm above the mudline (h) can be determined by varying the horizontal load such that the external work applied by the system load is equal to the internal work associated with the system capacity. When this occurs, the performance function, $g(x)$, should be sufficiently close to 0.0 (less than 1×10^{-3}). The critical collapse loads at various moment arms can be determined for a foundation system. A base shear versus overturning moment (M) interaction curve for a foundation system can be developed from the combinations of critical collapse load and its moment arm, using the following equation.

$$M = P_H \times h$$

To illustrate, the foundation system capacity interaction curve for Platform 1 in the end-on loading direction is shown in Figure D.5. This interaction curve includes the contribution from the 8 piles as well as the 18 well conductors. The interaction curve is an envelope; for hurricane loads located within the envelope, the foundation system is expected to be stable. The first zone corresponds to the shear failure mechanism, which is the initial part of the interaction curve at a small overturning moment. This part of the interaction curve slopes upward gently (increases in base shear with increasing overturning moment) because of pile batters. In this portion of the interaction curve, the capacity of the foundation system is governed by the lateral capacities of the piles and conductors. The other extreme at a large overturning moment corresponds to an overturning failure mechanism. This part of the interaction curve shows a steep downward slope (critical base shear decreasing rapidly with increasing overturning moment). In this portion of the interaction curve, the capacity of the foundation system is

governed by the axial capacities of the piles. The zone between these two extremes on the interaction curve corresponds to a combination of shear and overturning (i.e., both lateral and axial capacities are contributing to total system capacity).

The foundation system capacity can be compared to the hindcast loading. The maximum base shear and overturning moment applied by Hurricane Katrina in the end-on direction (Appendix C) are also plotted in Figure D.5. The applied loading is significantly greater than the estimated capacity from the upper-bound plasticity model for this platform.

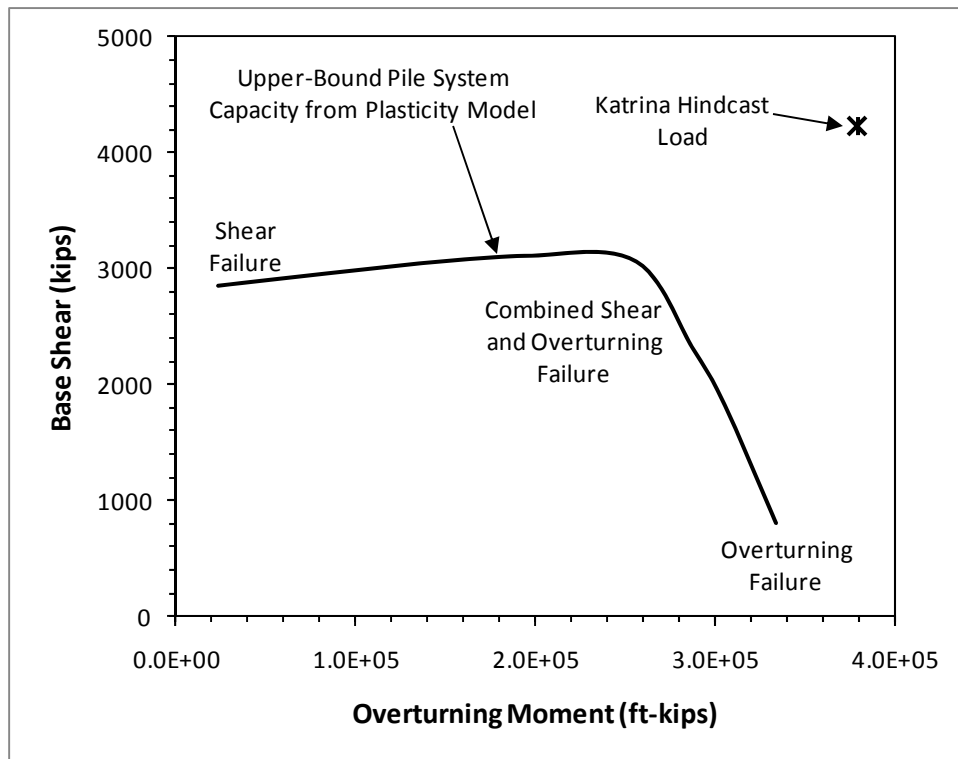


Figure D.5 Foundation System Capacity Interaction Curve from Plasticity Model of Platform 1 in the End-on Loading Direction

Appendix E – Quantitative Analyses of Case Study Platforms

The details of the quantitative analyses of the 12 case study platforms are presented in this Appendix. Simplified plastic collapse analyses of the foundations were performed for all case study platforms. Parametric analyses using the simplified plasticity models were also performed for selected platforms. The results from these analyses form the basis for evaluating the performance of the case study platforms in the hurricanes, upon which the major findings in this study were synthesized.

The inputs to the simplified plasticity model are the loads on the foundation system, the geometry of the piles and conductors including locations and batters, the axial and lateral resistance versus depth for each pile and conductor, and the structural capacity of each pile and conductor. The above inputs for each case study platform are documented in this Appendix. Specifically, the loads on the foundation system and geometry of the piles and conductors can be found in the executive input file of each platform presented herein. A description of the input parameters in the executive input file is provided in Appendix D. The axial and lateral resistance versus depth for each pile and conductor (provided in the pile geotechnical capacity input file) can be determined using the custom-built spreadsheet developed for this study, based on the recommended design soil profile and parameters for each case study platform, following the recommendations in API RP 2A-WSD (2000). The input parameters for this custom-built spreadsheet as well as the axial and lateral capacities versus depth for the piles and conductors of each case study platform are presented herein. The structural capacity of each pile and conductor can be found in the pile structural capacity input file, which is summarized in a tabular format in this Appendix.

Typically, foundation system capacity interaction curves in the 3 principal loading directions, namely the end-on, broadside and diagonal directions, are presented. The hurricane hindcast loads on the foundations were estimated from the hindcast analyses (Appendix C) in the approximate loading direction of the waves. These hindcast loads on the foundations are compared only with the foundation system capacity interaction curves in the directions of the waves. Parametric analyses, if performed, are also in terms of those directions. For each loading direction, the foundation system capacity interaction curves with and without the contribution of the well conductors are both presented. Due

to confidentiality considerations, details of the platforms, such as platform designations, locations, structural drawings and geotechnical information, are not presented herein. However, Table 3.1 and Appendix B provide the critical information of each case study platform and can be referenced if some levels of details about each platform are desired.

E.1 Platform 1

Platform 1 is an 8-leg structure supported by 8 piles and equipped with 20 conductors. The direction of the waves in Hurricane Katrina is approximately the end-on direction of this platform. The executive input file of this platform in the end-on direction is presented hereafter.

Executive Input File for Platform 1

PLATFORM 1 (ALL UNITS IN LB., IN., AND DEGREES)

SYSTEM LOAD DATA (PH,H,R,SKEW,PV,ECCENT)

2.0E6

1.0E2

1.00E-10

90.0

2.557E6

1.00E-10

NUMBER OF PILES (NPILE)

9

PILE 1

GEOMETRY (X,Y,THETAX,THETAY,L,AXIAL CONSTRAINT,NGROUP)

-4.66625E+02 -7.66625E+02 -7.13 -7.13 1.668E+03 1 1

PILE STRUCTURAL CAPACITY (INPUT FILE)

WPILE.INP

SOIL CAPACITY (INPUT FILE)

WSOIL2.INP

PILE 2

GEOMETRY (X,Y,THETAX,THETAY,L,AXIAL CONSTRAINT,NGROUP)

4.66625E+02 -7.66625E+02 7.13 -7.13 1.668E+03 1 1

PILE STRUCTURAL CAPACITY (INPUT FILE)

WPILE.INP

SOIL CAPACITY (INPUT FILE)

WSOIL2.INP

PILE 3

GEOMETRY (X,Y,THETAX,THETAY,L,AXIAL CONSTRAINT,NGROUP)

-4.66625E+02 7.66625E+02 -7.13 7.13 1.668E+03 1 1

PILE STRUCTURAL CAPACITY (INPUT FILE)

WPILE.INP

SOIL CAPACITY (INPUT FILE)

WSOIL2.INP

PILE 4

GEOMETRY (X,Y,THETAX,THETAY,L,AXIAL CONSTRAINT,NGROUP)

4.66625E+02 7.66625E+02 7.13 7.13 1.668E+03 1 1

PILE STRUCTURAL CAPACITY (INPUT FILE)

WPILE.INP

SOIL CAPACITY (INPUT FILE)

WSOIL2.INP

PILE 5

GEOMETRY (X,Y,THETAX,THETAY,L,AXIAL CONSTRAINT,NGROUP)

-4.66625E+02 -1.80E+02 -7.13 0 1.668E+03 1 1

PILE STRUCTURAL CAPACITY (INPUT FILE)

WPILE.INP

SOIL CAPACITY (INPUT FILE)

WSOIL1.INP

PILE 6

GEOMETRY (X,Y,THETAX,THETAY,L,AXIAL CONSTRAINT,NGROUP)

4.66625E+02 -1.80E+02 7.13 0 1.668E+03 1 1

PILE STRUCTURAL CAPACITY (INPUT FILE)

WPILE.INP

SOIL CAPACITY (INPUT FILE)

WSOIL1.INP

PILE 7

GEOMETRY (X,Y,THETAX,THETAY,L,AXIAL CONSTRAINT,NGROUP)

-4.66625E+02 1.80E+02 -7.13 0 1.668E+03 1 1

PILE STRUCTURAL CAPACITY (INPUT FILE)

WPILE.INP

SOIL CAPACITY (INPUT FILE)

WSOIL1.INP

PILE 8

GEOMETRY (X,Y,THETAX,THETAY,L,AXIAL CONSTRAINT,NGROUP)

4.66625E+02 1.80E+02 7.13 0 1.668E+03 1 1

PILE STRUCTURAL CAPACITY (INPUT FILE)

WPILE.INP

SOIL CAPACITY (INPUT FILE)

WSOIL1.INP

CONDUCTORS

GEOMETRY (X,Y,THETAX,THETAY,L,AXIAL CONSTRAINT,NGROUP)

0.00E+00 0.00E+00 0.00 0.00 1.62E+03 0 20

PILE STRUCTURAL CAPACITY (INPUT FILE)

WPILEC.INP

SOIL CAPACITY (INPUT FILE)

WSOILC.INP

The input parameters for the custom-built spreadsheet to calculate the axial and lateral resistance of the 4 corner piles battered in 2 directions, the 4 side piles battered in 1 direction, and the 20 conductors are presented in Tables E.1, E.2 and E.3, respectively. The design soil profile and parameters common for all piles and conductors are presented in Table E.4. The axial capacities of the 4 corner piles in compression and in tension are presented in Figure E.1. The lateral resistance of these piles is presented in Figure E.2. The same figures for the 4 side piles are not presented since they are similar to those for the corner piles. The lateral resistance of the conductors is presented in Figure E.3.

Table E.1 Input Parameters for the Piles of Platform 1 Battered in 2 Directions

Seafloor Elevation (ft, MSL)	-140
Seasurface Elevation (ft, MSL)	0
Top of Pile Elevation (ft,MSL)	-140
Pile Length (ft)	139
Pile Diameter (ft)	2.75
Pile Tip Wall Thickness (in.)	0.5
Unit Weight of Water (pcf)	62.4
Depth Increment (ft)	1
Open- or Close-ended	Open
Open-ended Pile Tip Condition	Plugged
Loading Condition	Cyclic
K Compression	0.8
K Tension	0.8
Pile Batter in x-direction (deg.)	7.125
Pile Batter in y-direction (deg.)	7.125
X_R (ft)	16.2

Table E.2 Input Parameters for the Piles of Platform 1 Battered in 1 Direction

Seafloor Elevation (ft, MSL)	-140
Seasurface Elevation (ft, MSL)	0
Top of Pile Elevation (ft,MSL)	-140
Pile Length (ft)	139
Pile Diameter (ft)	2.75
Pile Tip Wall Thickness (in.)	0.5
Unit Weight of Water (pcf)	62.4
Depth Increment (ft)	1
Open- or Close-ended	Open
Open-ended Pile Tip Condition	Plugged
Loading Condition	Cyclic
K Compression	0.8
K Tension	0.8
Pile Batter in x-direction (deg.)	0
Pile Batter in y-direction (deg.)	0
X_R (ft)	16.5

Table E.3 Input Parameters for the Conductors of Platform 1

Seafloor Elevation (ft, MSL)	-140
Seasurface Elevation (ft, MSL)	0
Top of Pile Elevation (ft,MSL)	-140
Pile Length (ft)	135
Pile Diameter (ft)	1.67
Pile Tip Wall Thickness (in.)	0.5
Unit Weight of Water (pcf)	62.4
Depth Increment (ft)	1
Open- or Close-ended	Open
Open-ended Pile Tip Condition	Plugged
Loading Condition	Cyclic
K Compression	0.8
K Tension	0.8
Pile Batter in x-direction (deg.)	0
Pile Batter in y-direction (deg.)	0
X_R (ft)	11.5

Table E.4 Design Soil Profile and Parameters for All Piles and Conductors of Platform 1

Layer	Soil Type	Top Elevation (ft, MSL)	Bottom Elevation (ft, MSL)	Thickness (ft)	Total Unit Weight (pcf)	Submerged Unit Weight (pcf)	c_u at the Top of Layer (psf)	dc_u/dz (psf/ft)	Friction Angle, ϕ' (deg.)	Soil Pile Friction Angle, δ (deg.)	f_{max} (ksf)	N_q	q_{max} (ksf)	C_1	C_2	C_3
1	Cohesive	-140	-177	37	97.4	35	100	5								
2	Cohesive	-177	-197	20	102.4	40	300	5								
3	Cohesive	-197	-227	30	102.4	40	400	10								
4	Cohesionless	-227	-239	12	122.4	60			35	30	2.0	40	200	3.0	3.4	54
5	Cohesive	-239	-251	12	120.4	58	700	6.67								
6	Cohesionless	-251	-270	19	120.4	58			25	20	1.4	12	60	1.2	2.0	15
7	Cohesionless	-270	-280	10	112.4	50			25	20	1.4	12	60	1.2	2.0	15

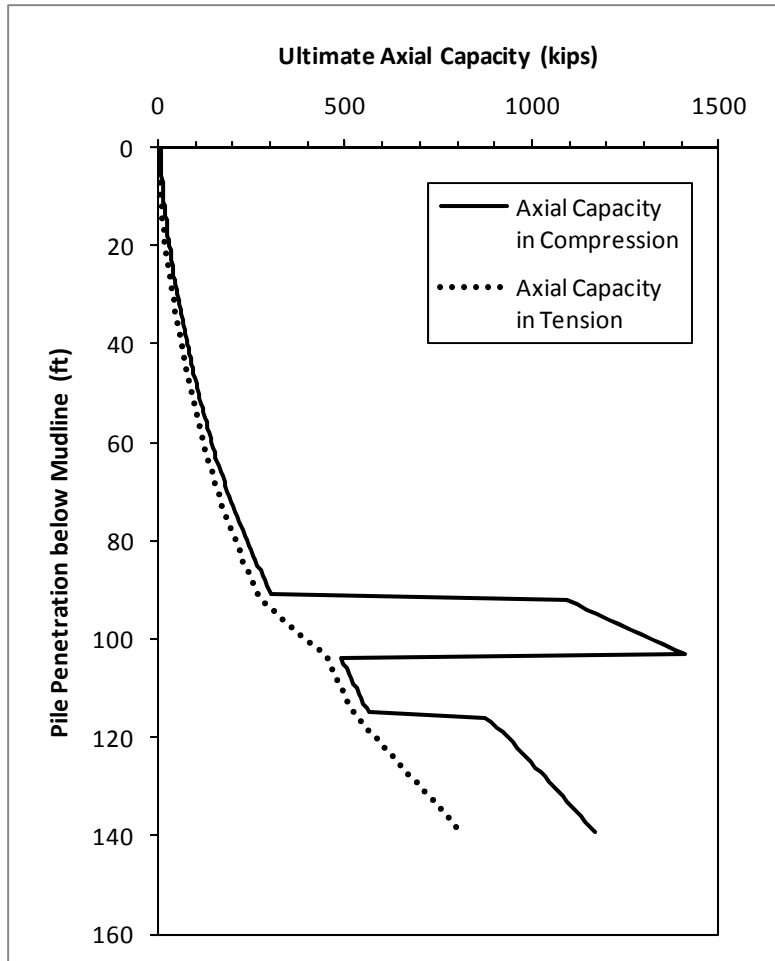


Figure E.1 Ultimate Axial Capacities of the Corner Piles of Platform 1

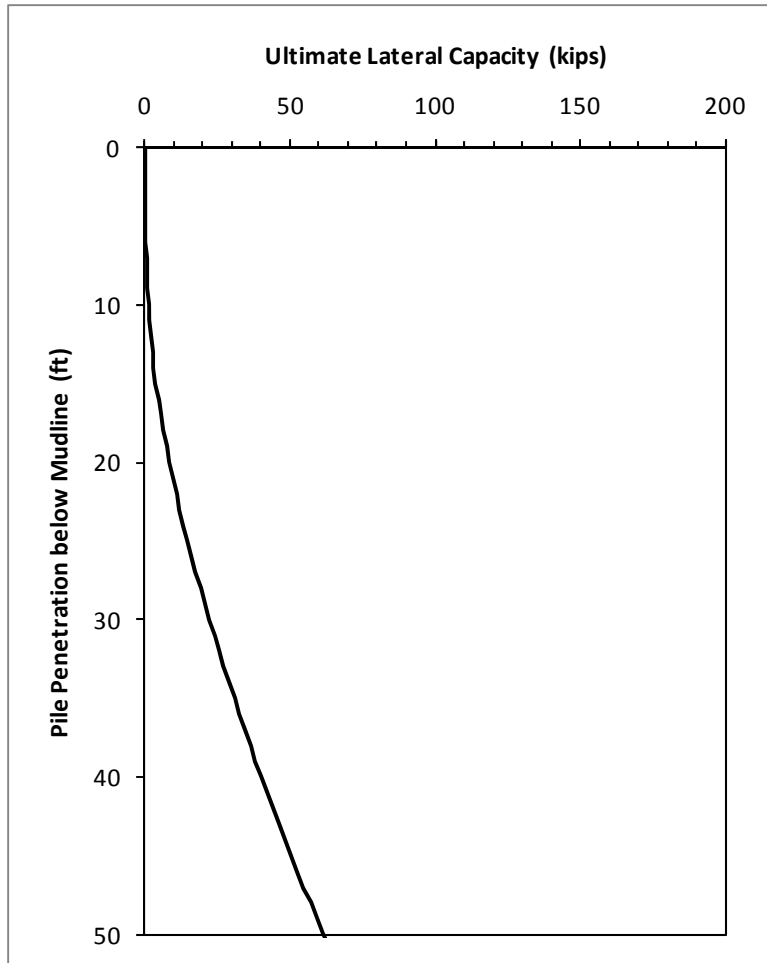


Figure E.2 Ultimate Lateral Capacity of the Corner Piles of Platform 1

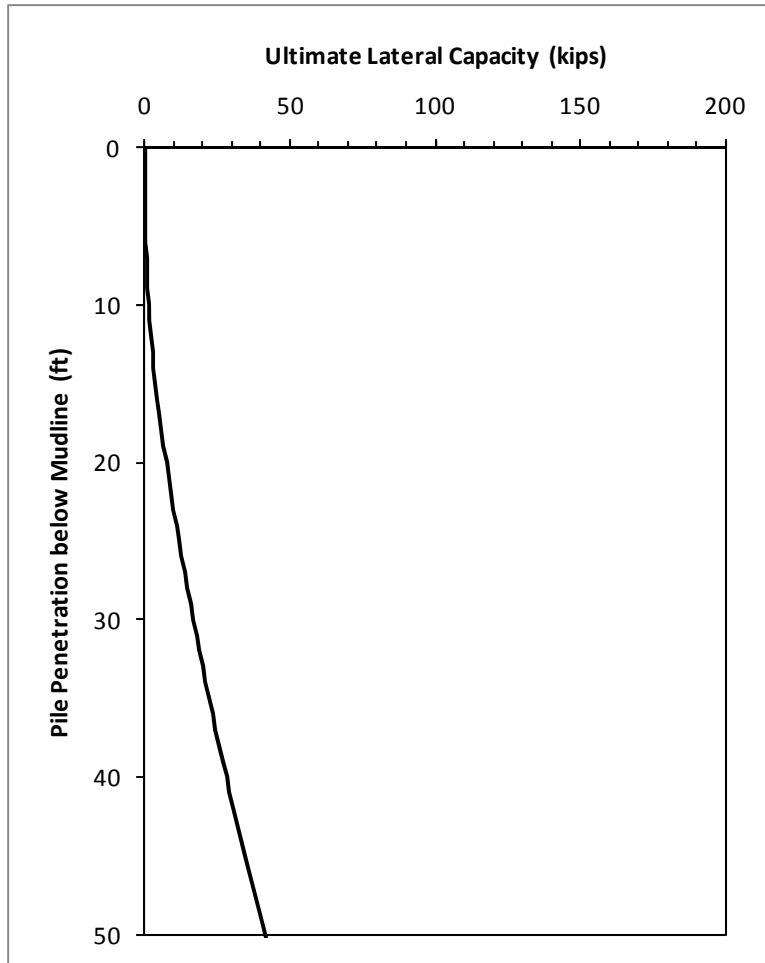


Figure E.3 Ultimate Lateral Capacity of the Conductors of Platform 1

The structural capacity input files of the piles and conductors are summarized in Tables E.5 and E.6, respectively.

Table E.5 Structural Capacity of the Piles of Platform 1

Wall Thickness, t (in.)	Starting Length along Pile, z (in.)	Axial Structural Capacity, Q (lbs)	Moment Capacity, M (in.-lbs)
1.5	0	5.344E+06	5.362E+07
0.75	480	2.736E+06	2.809E+07
0.5	972	1.838E+06	1.901E+07

Table E.6 Structural Capacity of the Conductors of Platform 1

Wall Thickness, t (in.)	Starting Length along Pile, z (in.)	Axial Structural Capacity, Q (lbs)	Moment Capacity, M (in.-lbs)
0.5	0	1.103E+06	6.846E+06
0.5	600	1.103E+06	6.846E+06
0.5	1200	1.103E+06	6.846E+06

Based on the above input parameters, the base case foundation system capacity interaction curves in the end-on, broadside and diagonal directions are presented in Figures E.4, E.5 and E.6, respectively. The direction of the waves is approximately the end-on direction of this platform. Therefore, the hurricane hindcast load on the foundation is also presented in the interaction diagram for the end-on direction.

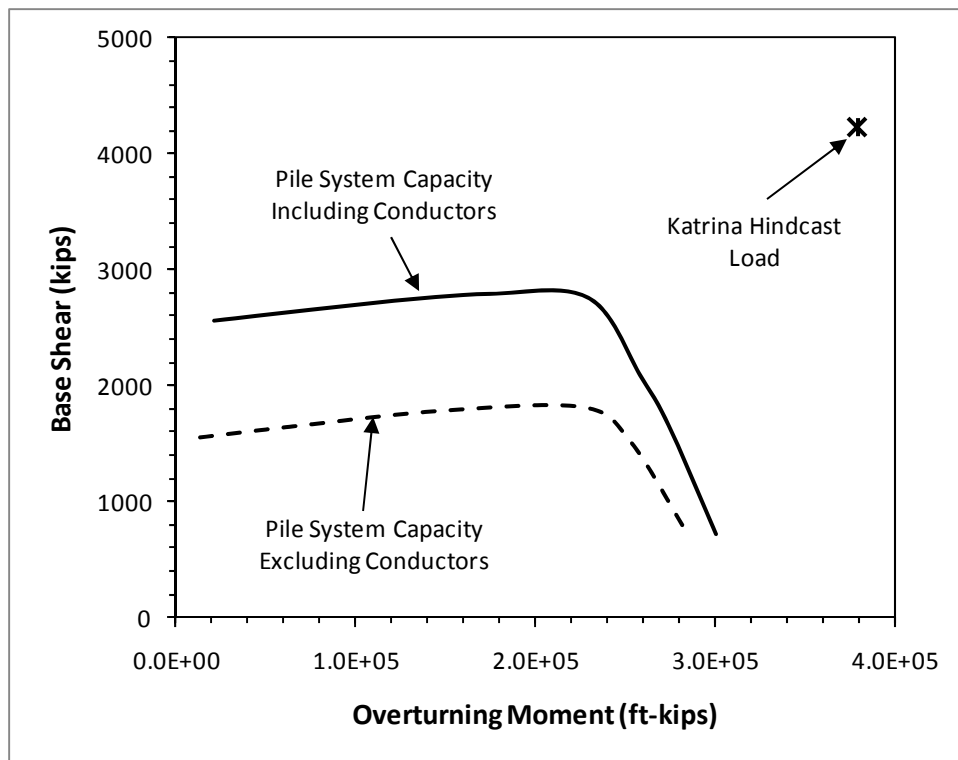


Figure E.4 Base Case Foundation System Capacity Interaction Diagram of Platform 1 in the End-on Direction

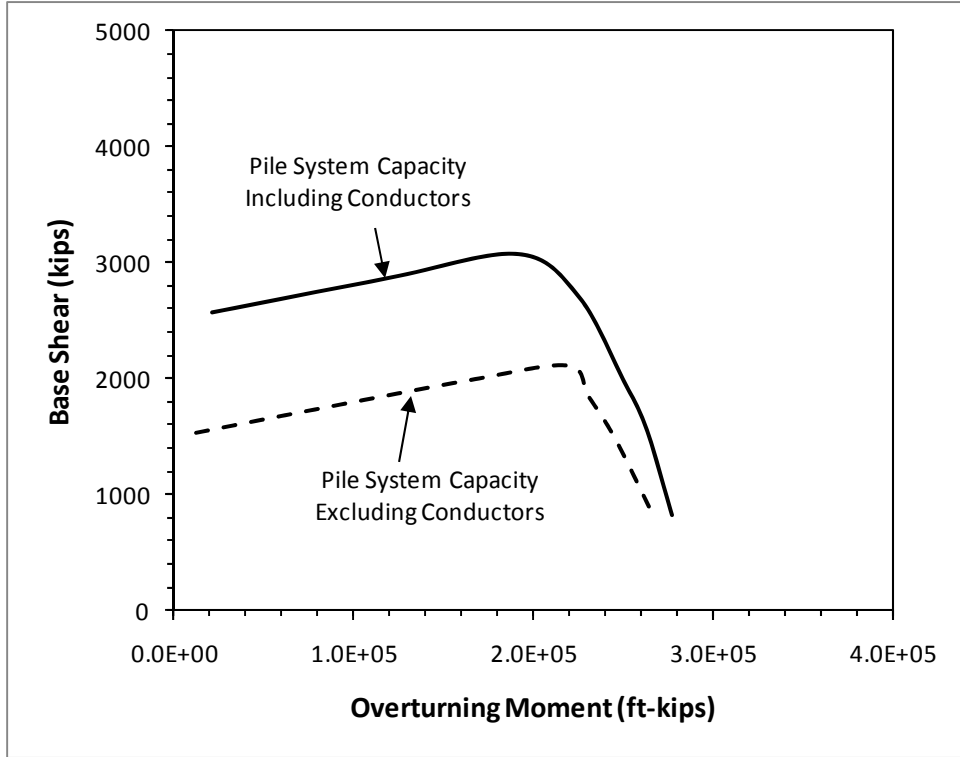


Figure E.5 Base Case Foundation System Capacity Interaction Diagram of Platform 1 in the Broadside Direction

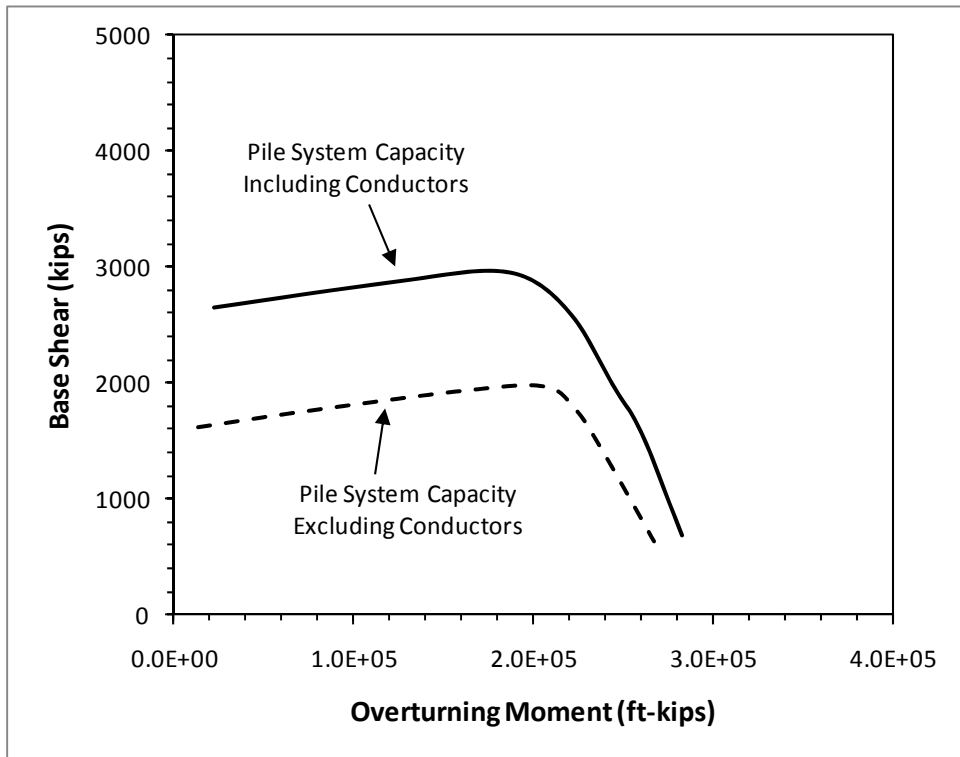


Figure E.6 Base Case Foundation System Capacity Interaction Diagram of Platform 1 in the Diagonal Direction

In addition to the base case, parametric analyses were also performed for Platform 1 in the end-on direction. The unit side shear and end bearing, which are roughly proportional to the shear strength of the soil in the lower third of the pile, can be increased by a multiplier, NQ_{ax} , for all piles. The unit lateral resistance, which is roughly proportional to the shear strength of the soil over the upper 50 feet of the pile or conductor, can also be increased by a multiplier, NQ_{lat} , for all piles and conductors. Parametric analyses performed using these two multipliers are insightful in understanding the effects of axial and lateral capacities on the overturning and shear capacities of the foundation because the axial capacity can be increased independently of the lateral capacity and vice versa. Results from the parametric analyses performed using a combination of these two multipliers are presented in Figure E.7. Discussions on the sensitivity of shear versus overturning capacity of the foundation to the shear strength of the soil are provided in Section 5.2.1.

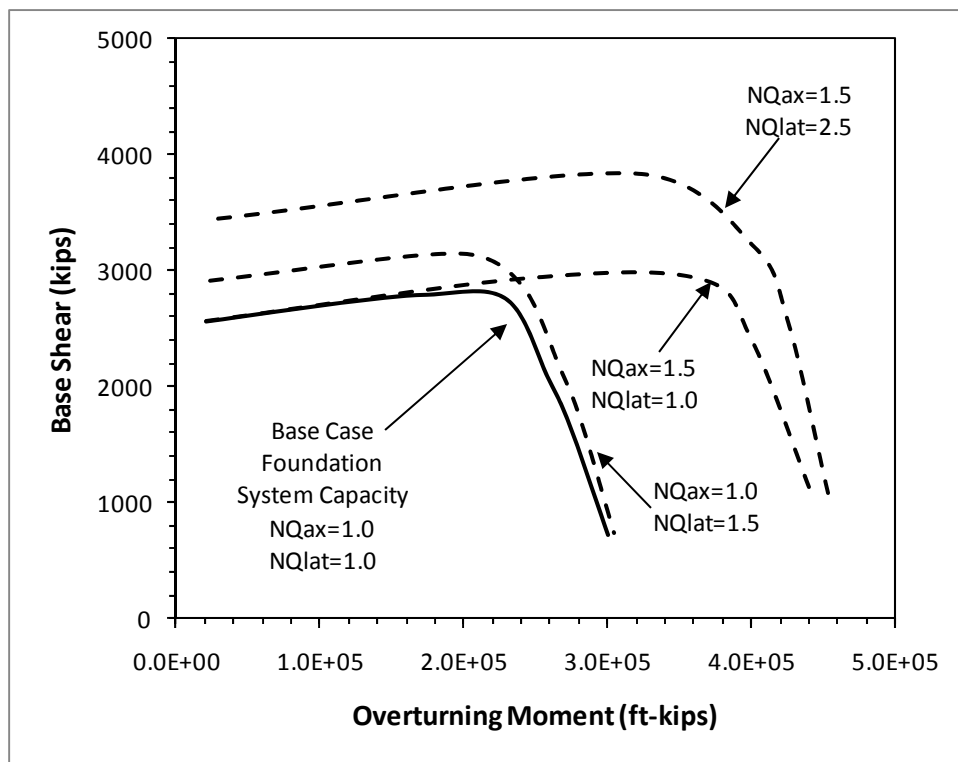


Figure E.7 Parametric Analyses for Platform 1 in the End-on Direction Using Capacity Multipliers

Other types of parametric analyses (ones without using the capacity multipliers) can also be performed. For example, a parametric analysis was performed using the lateral resistance corresponding to the static (versus cyclic) loading condition in the end-on

direction. The result of this analysis is shown and compared to the result from the base case assuming the cyclic loading condition. As shown in Figure E.8, the lateral capacities of the piles and conductors and, therefore, the shear capacity of the foundation are higher assuming the static loading condition than the cyclic loading condition.

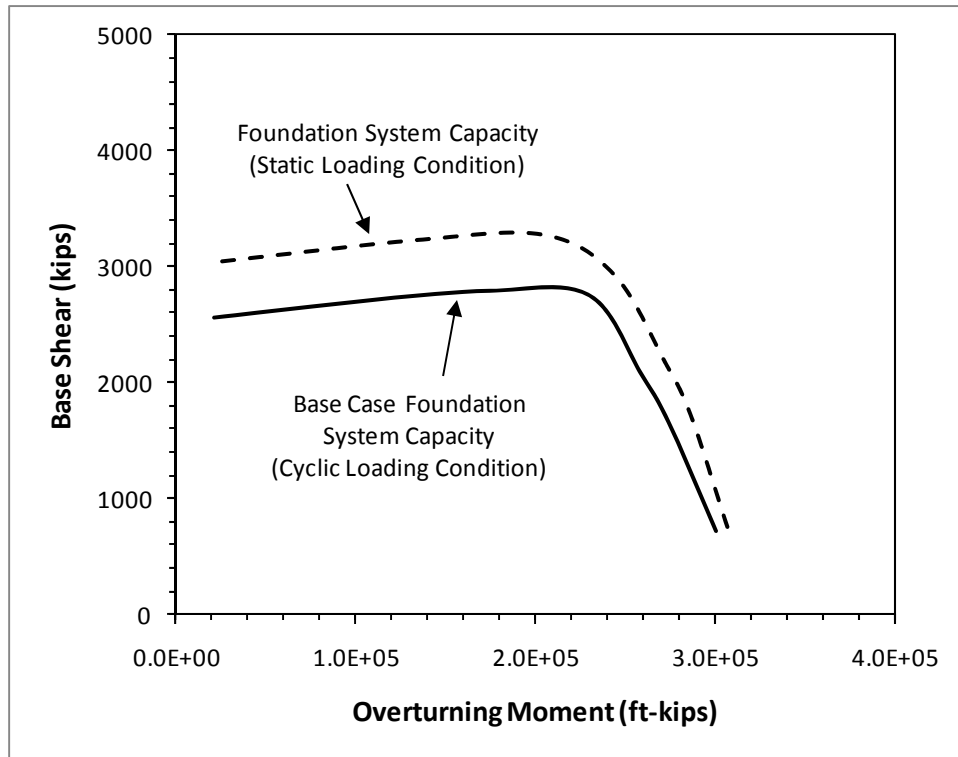


Figure E.8 Parametric Analysis for Platform 1 in the End-on Direction Assuming Static (versus Cyclic) Loading Condition

The density of the pile tipping layer can be increased independently of other input parameters. Figure E.9 shows the result of the analysis of increasing the density of the pile tipping layer from “Medium Sand-Silt” to “Very Dense Sand.” As shown, such an increase has a significant effect on the overturning capacity of the foundation.

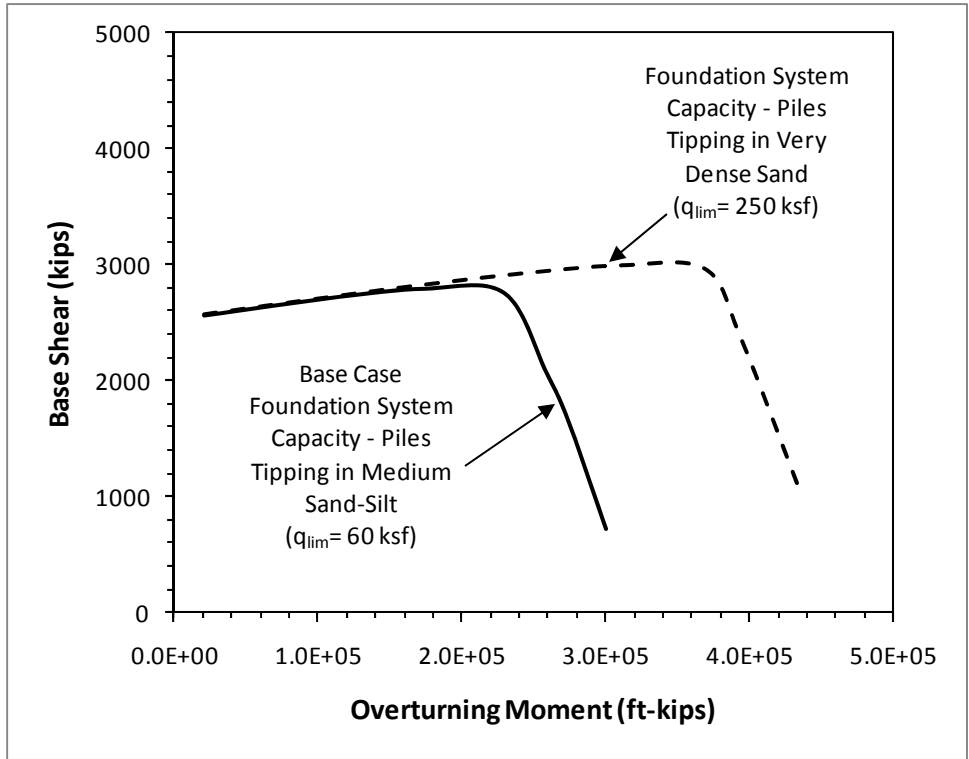


Figure E.9 Parametric Analysis for Platform 1 in the End-on Direction Increasing the Density of the Pile Tipping Layer

The yield strength of the steel piles and conductors can also be increased independently of other input parameters. Figure E.10 shows the result of the analysis of increasing the yield strength from the nominal value of 36 ksi using in the base case to 41.2 ksi, which is more representative of the average value. As shown, such an increase changes the shear capacity of the foundation proportionally.

A variety of parametric analyses with combinations of changes (as illustrated above) can also be performed as necessary with the flexibility of the custom-built spreadsheet to calculate the axial and lateral resistance of the foundation elements. However, only those that provide insight into the behavior of the foundation system and those that are reasonable to explain the survival of the platform are presented herein.

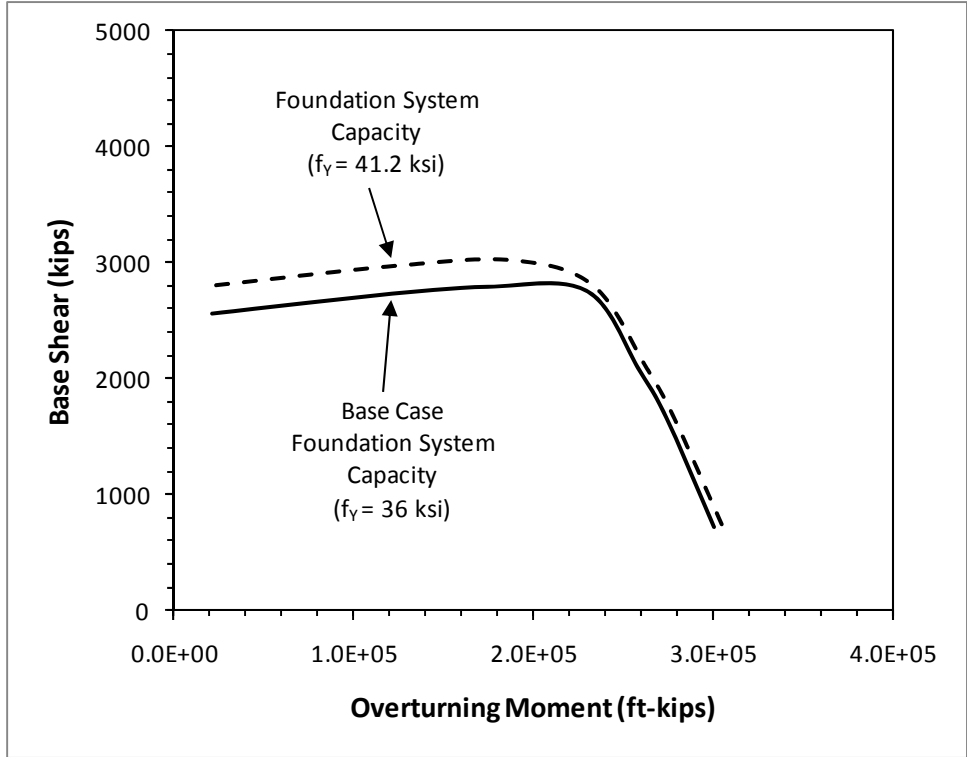


Figure E.10 Parametric Analysis for Platform 1 in the End-on Direction Increasing the Yield Strength of the Steel Piles and Conductors

E.2 Platform 2

Platform 2 is a 6-leg structure supported by 6 piles and equipped with 12 conductors. The direction of the waves in Hurricane Katrina is approximately the end-on direction of this platform. The executive input file of this platform in the end-on direction is presented hereafter.

Executive Input File for Platform 2

PLATFORM 2 (ALL UNITS IN LB., IN., AND DEGREES)

SYSTEM LOAD DATA (PH,H,R,SKEW,PV,ECCENT)

2.5E6

1.0E3

1.0E-10

00.0

2.20E6

1.0E-10

NUMBER OF PILES (NPILE)

7

PILE 1

GEOMETRY (X,Y,THETAX,THETAY,L,AXIAL CONSTRAINT,NGROUP)

-4.665E+02 -5.865E+02 -7.13 -7.13 1.680E+03 1 1

PILE STRUCTURAL CAPACITY (INPUT FILE)

WPILE.INP

SOIL CAPACITY (INPUT FILE)

WSOIL2.INP

PILE 2

GEOMETRY (X,Y,THETAX,THETAY,L,AXIAL CONSTRAINT,NGROUP)

4.665E+02 -5.865E+02 7.13 -7.13 1.680E+03 1 1

PILE STRUCTURAL CAPACITY (INPUT FILE)

WPILE.INP

SOIL CAPACITY (INPUT FILE)

WSOIL2.INP

PILE 3

GEOMETRY (X,Y,THETAX,THETAY,L,AXIAL CONSTRAINT,NGROUP)

-4.665E+02 5.865E+02 -7.13 7.13 1.680E+03 1 1

PILE STRUCTURAL CAPACITY (INPUT FILE)

WPILE.INP

SOIL CAPACITY (INPUT FILE)

WSOIL2.INP

PILE 4

GEOMETRY (X,Y,THETAX,THETAY,L,AXIAL CONSTRAINT,NGROUP)

4.665E+02 5.865E+02 7.13 7.13 1.680E+03 1 1

PILE STRUCTURAL CAPACITY (INPUT FILE)

WPILE.INP

SOIL CAPACITY (INPUT FILE)

WSOIL2.INP

PILE 5

GEOMETRY (X,Y,THETAX,THETAY,L,AXIAL CONSTRAINT,NGROUP)

-4.665E+02 1.0E-10 -7.13 0.00 1.680E+03 1 1

PILE STRUCTURAL CAPACITY (INPUT FILE)

WPILE.INP

SOIL CAPACITY (INPUT FILE)

WSOIL1.INP

PILE 6

GEOMETRY (X,Y,THETAX,THETAY,L,AXIAL CONSTRAINT,NGROUP)

4.665E+02 1.0E-10 7.13 0.00 1.680E+03 1 1

PILE STRUCTURAL CAPACITY (INPUT FILE)

WPILE.INP

SOIL CAPACITY (INPUT FILE)

WSOIL1.INP

CONDUCTORS

GEOMETRY (X,Y,THETAX,THETAY,L,AXIAL CONSTRAINT,NGROUP)

0.00E1 0.00E1 0.00 0.00 1.680E+03 0 12

PILE STRUCTURAL CAPACITY (INPUT FILE)

WPILEC.INP

SOIL CAPACITY (INPUT FILE)

WSOILC.INP

The input parameters for the custom-built spreadsheet to calculate the axial and lateral resistance of the 4 corner piles battered in 2 directions, the 2 side piles battered in 1 direction, and the 12 conductors are presented in Tables E.7, E.8 and E.9, respectively. The design soil profile and parameters common for all piles and conductors are presented in Table E.10. The axial capacities of the 4 corner piles in compression and in tension are presented in Figure E.11. The lateral resistance of these piles is presented in Figure E.12. The same figures for the 2 side piles are not presented since they are similar to those for the corner piles. The lateral resistance of the conductors is presented in Figure E.13.

Table E.7 Input Parameters for the Piles of Platform 2 Battered in 2 Directions

Seafloor Elevation (ft, MSL)	-140
Seasurface Elevation (ft, MSL)	0
Top of Pile Elevation (ft,MSL)	-140
Pile Length (ft)	140
Pile Diameter (ft)	3
Pile Tip Wall Thickness (in.)	0.625
Unit Weight of Water (pcf)	62.4
Depth Increment (ft)	1
Open- or Close-ended	Open
Open-ended Pile Tip Condition	Plugged
Loading Condition	Cyclic
K Compression	0.8
K Tension	0.8
Pile Batter in x-direction (deg.)	7.125
Pile Batter in y-direction (deg.)	7.125
X_R (ft)	17.2

Table E.8 Input Parameters for the Piles of Platform 2 Battered in 1 Direction

Seafloor Elevation (ft, MSL)	-140
Seasurface Elevation (ft, MSL)	0
Top of Pile Elevation (ft,MSL)	-140
Pile Length (ft)	140
Pile Diameter (ft)	3
Pile Tip Wall Thickness (in.)	0.625
Unit Weight of Water (pcf)	62.4
Depth Increment (ft)	1
Open- or Close-ended	Open
Open-ended Pile Tip Condition	Plugged
Loading Condition	Cyclic
K Compression	0.8
K Tension	0.8
Pile Batter in x-direction (deg.)	7.125
Pile Batter in y-direction (deg.)	0
X_R (ft)	16.4

Table E.9 Input Parameters for the Conductors of Platform 2

Seafloor Elevation (ft, MSL)	-140
Seasurface Elevation (ft, MSL)	0
Top of Pile Elevation (ft,MSL)	-140
Pile Length (ft)	140
Pile Diameter (ft)	2
Pile Tip Wall Thickness (in.)	0.5
Unit Weight of Water (pcf)	62.4
Depth Increment (ft)	1
Open- or Close-ended	Open
Open-ended Pile Tip Condition	Plugged
Loading Condition	Cyclic
K Compression	0.8
K Tension	0.8
Pile Batter in x-direction (deg.)	0
Pile Batter in y-direction (deg.)	0
X_R (ft)	12.5

Table E.10 Design Soil Profile and Parameters for All Piles and Conductors of Platform 2

Layer	Soil Type	Top Elevation (ft, MSL)	Bottom Elevation (ft, MSL)	Thickness (ft)	Total Unit Weight (pcf)	Submerged Unit Weight (pcf)	c_u at the Top of Layer (psf)	dc_u/dz (psf/ft)	Friction Angle, ϕ' (deg.)	Soil Pile Friction Angle, δ (deg.)	f_{max} (ksf)	N_q	q_{max} (ksf)	C_1	C_2	C_3
1	Cohesive	-140	-177	37	97.4	35	100	5								
2	Cohesive	-177	-197	20	102.4	40	300	5								
3	Cohesive	-197	-227	30	102.4	40	400	10								
4	Cohesionless	-227	-239	12	122.4	60			35	30	2.0	40	200	3.0	3.4	54
5	Cohesive	-239	-251	12	120.4	58	700	6.67								
6	Cohesionless	-251	-270	19	120.4	58			25	20	1.4	12	60	1.2	2.0	15
7	Cohesionless	-270	-280	10	112.4	50			25	20	1.4	12	60	1.2	2.0	15

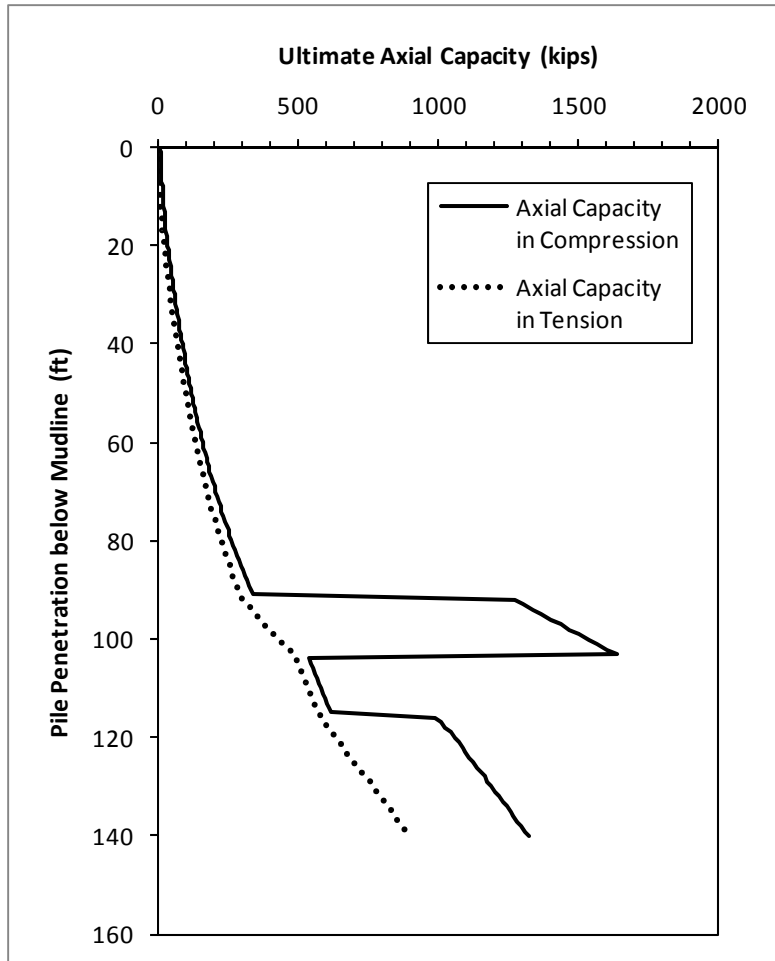


Figure E.11 Ultimate Axial Capacities of the Corner Piles of Platform 2

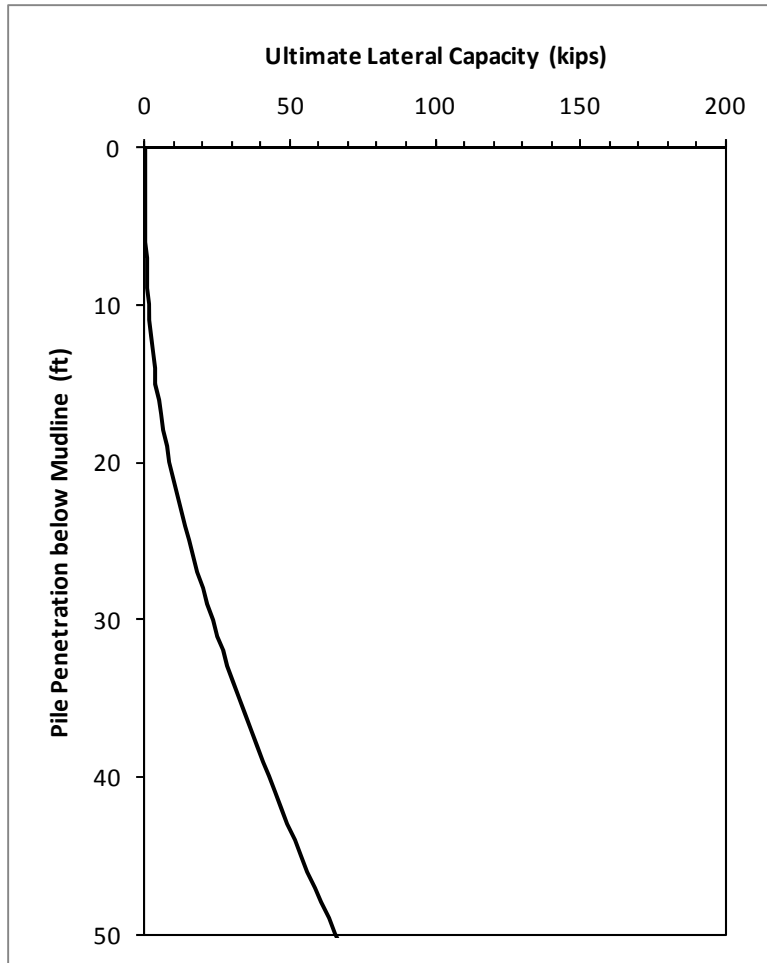


Figure E.12 Ultimate Lateral Capacity of the Corner Piles of Platform 2

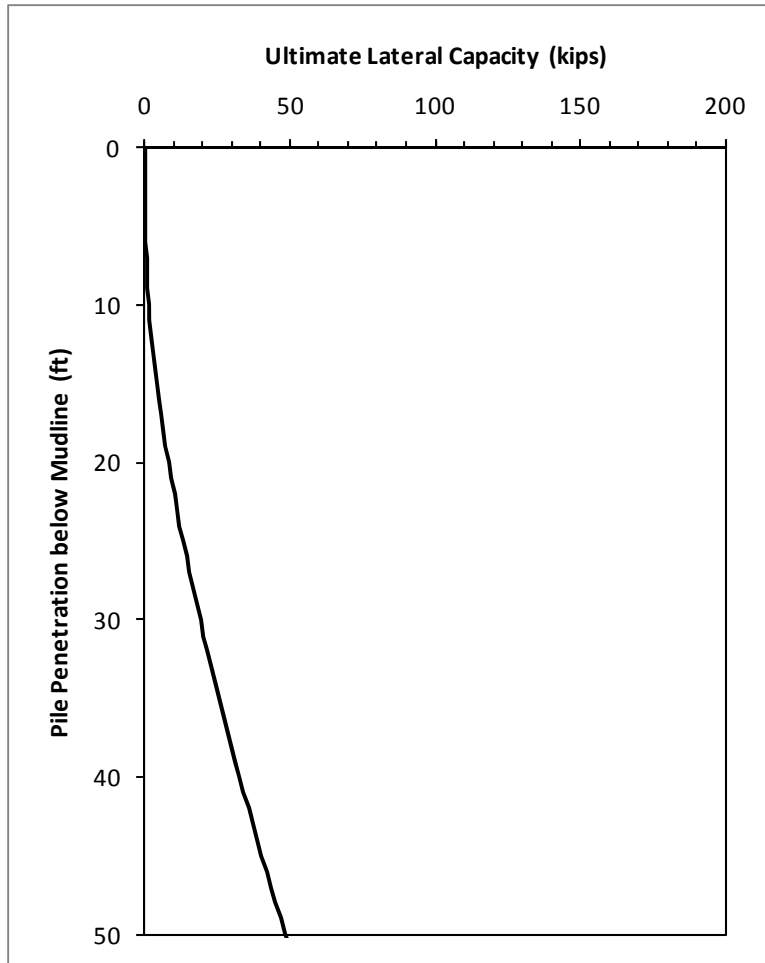


Figure E.13 Ultimate Lateral Capacity of the Conductors of Platform 2

The structural capacity input files of the piles and conductors are summarized in Tables E.11 and E.12, respectively.

Table E.11 Structural Capacity of the Piles of Platform 2

Wall Thickness, t (in.)	Starting Length along Pile, z (in.)	Axial Structural Capacity, Q (lbs)	Moment Capacity, M (in.-lbs)
1.75	0	6.779E+06	7.397E+07
1.5	780	5.853E+06	6.431E+07
1	1020	3.958E+06	4.411E+07

Table E.12 Structural Capacity of the Conductors of Platform 2

Wall Thickness, t (in.)	Starting Length along Pile, z (in.)	Axial Structural Capacity, Q (lbs)	Moment Capacity, M (in.-lbs)
0.75	0	1.972E+06	1.460E+07
0.75	600	1.972E+06	1.460E+07
0.75	1200	1.972E+06	1.460E+07

Based on the above input parameters, the base case foundation system capacity interaction curves in the end-on, broadside and diagonal directions are presented in Figures E.14, E.15 and E.16, respectively. The direction of the waves is approximately the end-on direction of this platform. Therefore, the hurricane hindcast load on the foundation is also presented in the interaction diagram for the end-on direction.

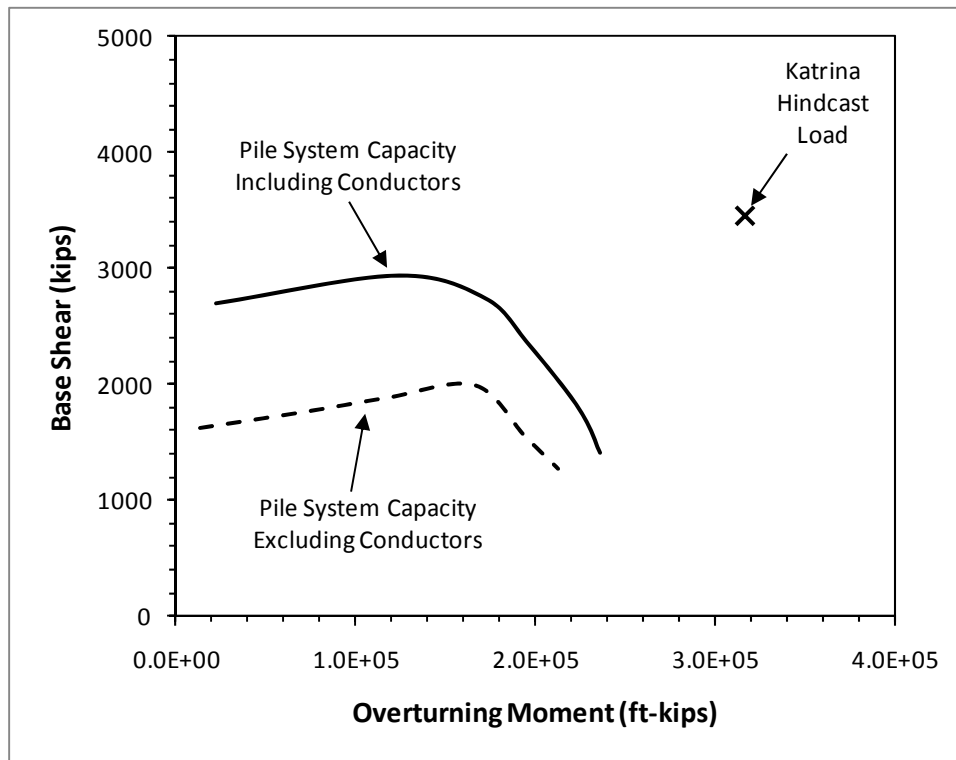


Figure E.14 Base Case Foundation System Capacity Interaction Diagram of Platform 2 in the End-on Direction

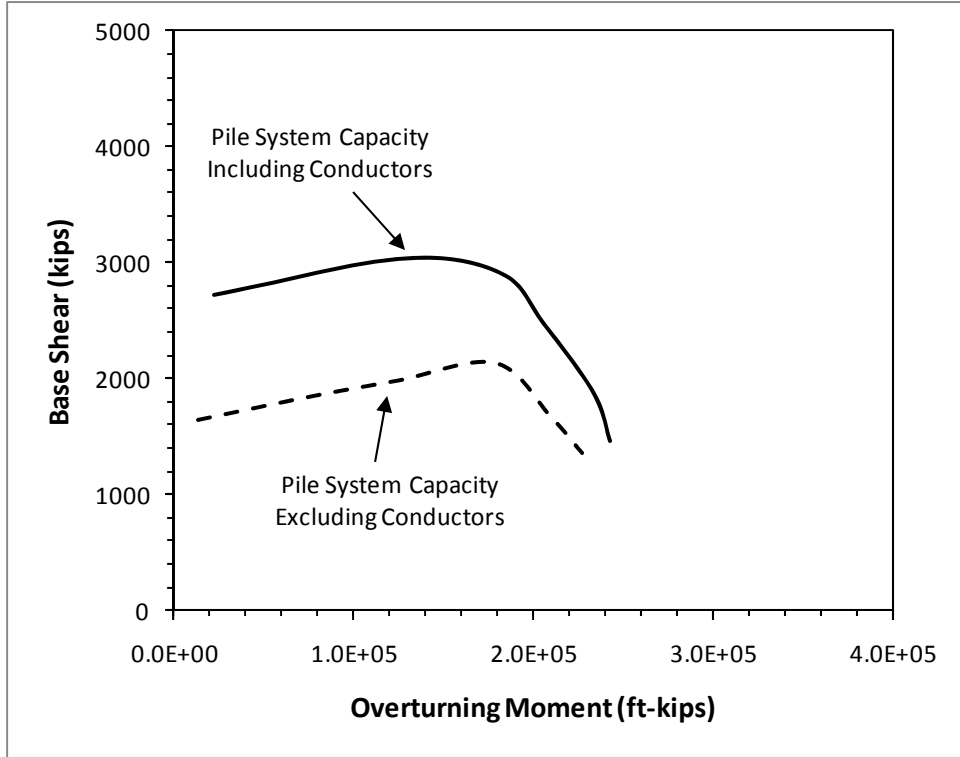


Figure E.15 Base Case Foundation System Capacity Interaction Diagram of Platform 2 in the Broadside Direction

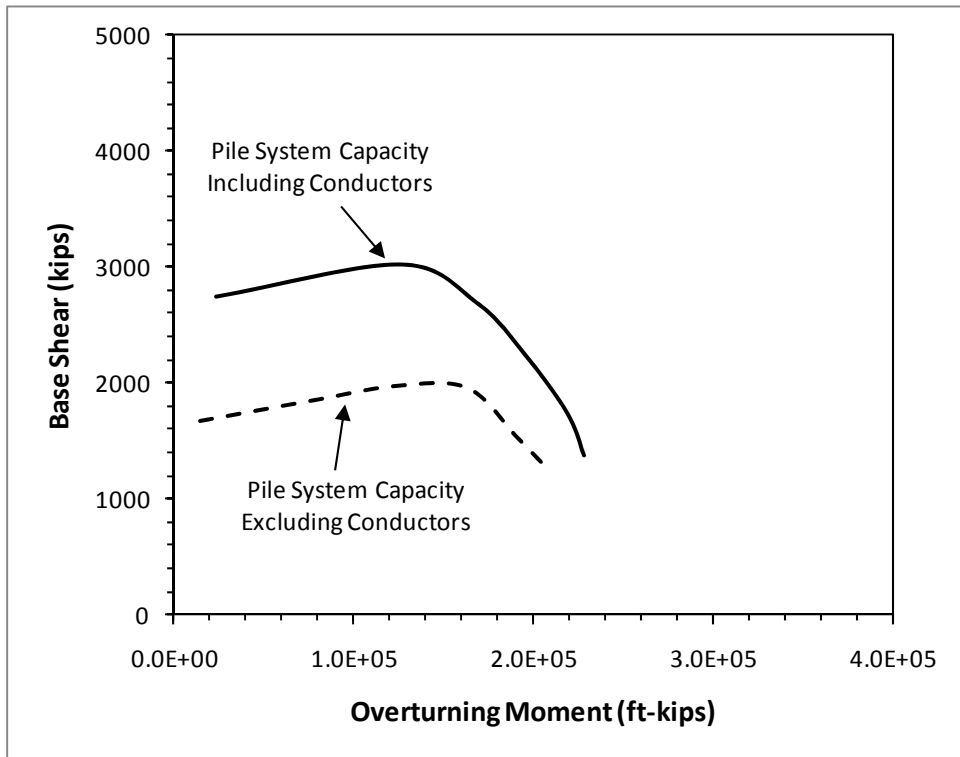


Figure E.16 Base Case Foundation System Capacity Interaction Diagram of Platform 2 in the Diagonal Direction

A parametric analysis was performed to investigate why the foundation of Platform 2 survived the loading in Hurricane Katrina while the analysis (Figure E.14) indicated otherwise. In this analysis, the density of the pile tipping layer was increased from “Medium Sand-Silt” to “Very Dense Sand.” As shown in Figure E.17, such an increase has a significant effect on the overturning capacity of the foundation and is enough to make the predicted capacity nearly the same as the hurricane loading.

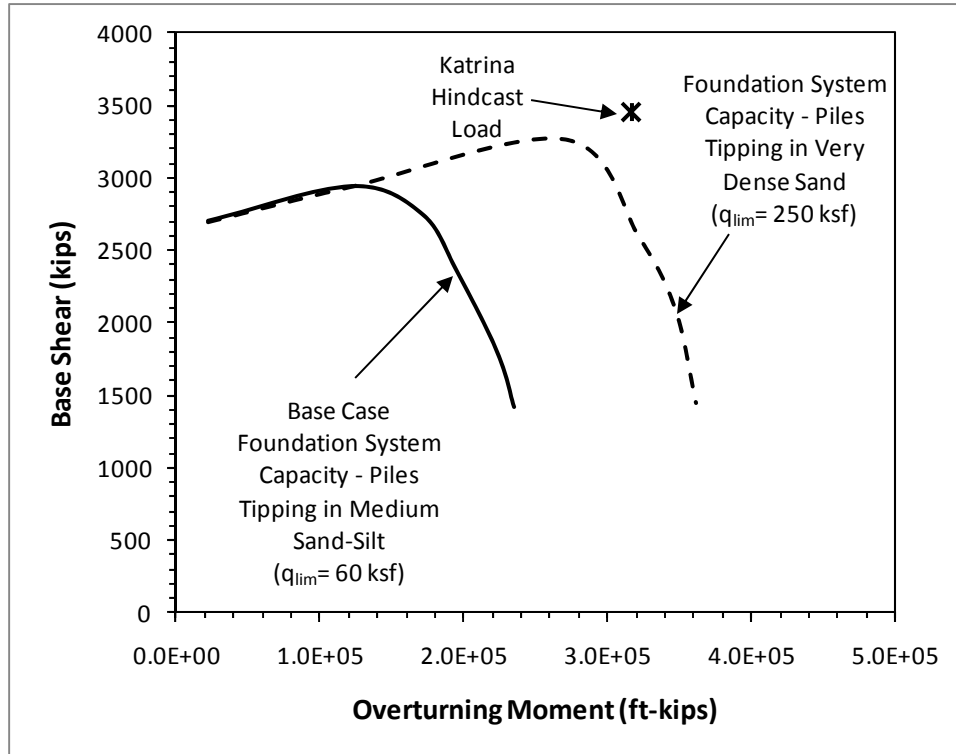


Figure E.17 Parametric Analysis for Platform 2 in the End-on Direction Increasing the Density of the Pile Tipping Layer

E.3 Platform 8

Platform 8 is a 4-leg structure supported by 4 piles that are symmetrical and equipped with 12 conductors. Seven of the conductors are 26 inches in diameter and five of the conductors are 24 inches in diameter. In the foundation model, an equivalent of ten 26-inch diameter conductors was assumed for the foundation. The executive input file of this platform in the diagonal direction is presented hereafter.

Executive Input File for Platform 8

PLATFORM 8 (ALL UNITS IN LB., IN., AND DEGREES)

SYSTEM LOAD DATA (PH,H,R,SKEW,PV,ECCENT)

1.859E6

4E3

1.00E-11

45.0

2.955E6

1.00E-10

NUMBER OF PILES (NPILE)

5

PILE 1

GEOMETRY (X,Y,THETAX,THETAY,L,AXIAL CONSTRAINT,NGROUP)

-4.536E+02 -4.536E+02 -5.6 -5.6 3.288E+03 1 1

PILE STRUCTURAL CAPACITY (INPUT FILE)

WPILE.INP

SOIL CAPACITY (INPUT FILE)

WSOIL2.INP

PILE 2

GEOMETRY (X,Y,THETAX,THETAY,L,AXIAL CONSTRAINT,NGROUP)

4.536E+02 -4.536E+02 5.6 -5.6 3.288E+03 1 1

PILE STRUCTURAL CAPACITY (INPUT FILE)

WPILE.INP

SOIL CAPACITY (INPUT FILE)

WSOIL2.INP

PILE 3

GEOMETRY (X,Y,THETAX,THETAY,L,AXIAL CONSTRAINT,NGROUP)

-4.536E+02 4.536E+02 -5.6 5.6 3.288E+03 1 1

PILE STRUCTURAL CAPACITY (INPUT FILE)

WPILE.INP

SOIL CAPACITY (INPUT FILE)

WSOIL2.INP

PILE 4

GEOMETRY (X,Y,THETAX,THETAY,L,AXIAL CONSTRAINT,NGROUP)

4.536E+02 4.536E+02 5.6 5.6 3.288E+03 1 1

PILE STRUCTURAL CAPACITY (INPUT FILE)

WPILE.INP

SOIL CAPACITY (INPUT FILE)

WSOIL2.INP

CONDUCTORS

GEOMETRY (X,Y,THETAX,THETAY,L,AXIAL CONSTRAINT,NGROUP)

-6.00E+01 0.00E+02 0.00 0.00 3.288E+03 0 10

PILE STRUCTURAL CAPACITY (INPUT FILE)

WPILEC.INP

SOIL CAPACITY (INPUT FILE)

WSOILC.INP

The input parameters for the custom-built spreadsheet to calculate the axial and lateral resistance of the 4 piles battered in 2 directions and the ten 26-inch diameter conductors are presented in Tables E.13 and E.14, respectively. The design soil profile and parameters common for all piles and conductors are presented in Table E.15. The axial capacities of the 4 piles in compression and in tension are presented in Figure E.18. The lateral resistance of these piles is presented in Figure E.19. The lateral resistance of the conductors is presented in Figure E.20.

Table E.13 Input Parameters for the Piles of Platform 8

Seafloor Elevation (ft, MSL)	-220
Seasurface Elevation (ft, MSL)	0
Top of Pile Elevation (ft,MSL)	-225
Pile Length (ft)	274
Pile Diameter (ft)	4
Pile Tip Wall Thickness (in.)	1.5
Unit Weight of Water (pcf)	62.4
Depth Increment (ft)	1
Open- or Close-ended	Open
Open-ended Pile Tip Condition	Plugged
Loading Condition	Cyclic
K Compression	0.8
K Tension	0.8
Pile Batter in x-direction (deg.)	5.6
Pile Batter in y-direction (deg.)	5.6
X_R (ft)	9.5

Table E.14 Input Parameters for the Conductors of Platform 8

Seafloor Elevation (ft, MSL)	-220
Seasurface Elevation (ft, MSL)	0
Top of Pile Elevation (ft,MSL)	-225
Pile Length (ft)	274
Pile Diameter (ft)	2.17
Pile Tip Wall Thickness (in.)	0.75
Unit Weight of Water (pcf)	62.4
Depth Increment (ft)	1
Open- or Close-ended	Open
Open-ended Pile Tip Condition	Unplugged
Loading Condition	Cyclic
K Compression	0.8
K Tension	0.8
Pile Batter in x-direction (deg.)	0
Pile Batter in y-direction (deg.)	0
X_R (ft)	8.5

Table E.15 Design Soil Profile and Parameters for All Piles and Conductors of Platform 8

Layer	Soil Type	Top Elevation (ft, MSL)	Bottom Elevation (ft, MSL)	Thickness (ft)	Total Unit Weight (pcf)	Submerged Unit Weight (pcf)	c_u at the Top of Layer (psf)	dc_u/dz (psf/ft)	Friction Angle, ϕ' (deg.)	Soil Pile Friction Angle, δ (deg.)	f_{max} (ksf)	N_q	q_{max} (ksf)	C_1	C_2	C_3
1	Cohesive	-220	-232	12	87.4	25	50	0								
2	Cohesive	-232	-247	15	107.4	45	50	10								
3	Cohesionless	-247	-303	56	122.4	60			30	25	1.7	20	100	1.9	2.7	29
4	Cohesionless	-303	-340	37	112.4	50			30	25	1.7	20	100	1.9	2.7	29
5	Cohesive	-340	-387	47	109.4	47	800	14.89								
6	Cohesive	-387	-396	9	106.4	44	1500	103.33								
7	Cohesionless	-396	-497	101	122.4	60			30	25	1.7	20	100	1.9	2.7	29

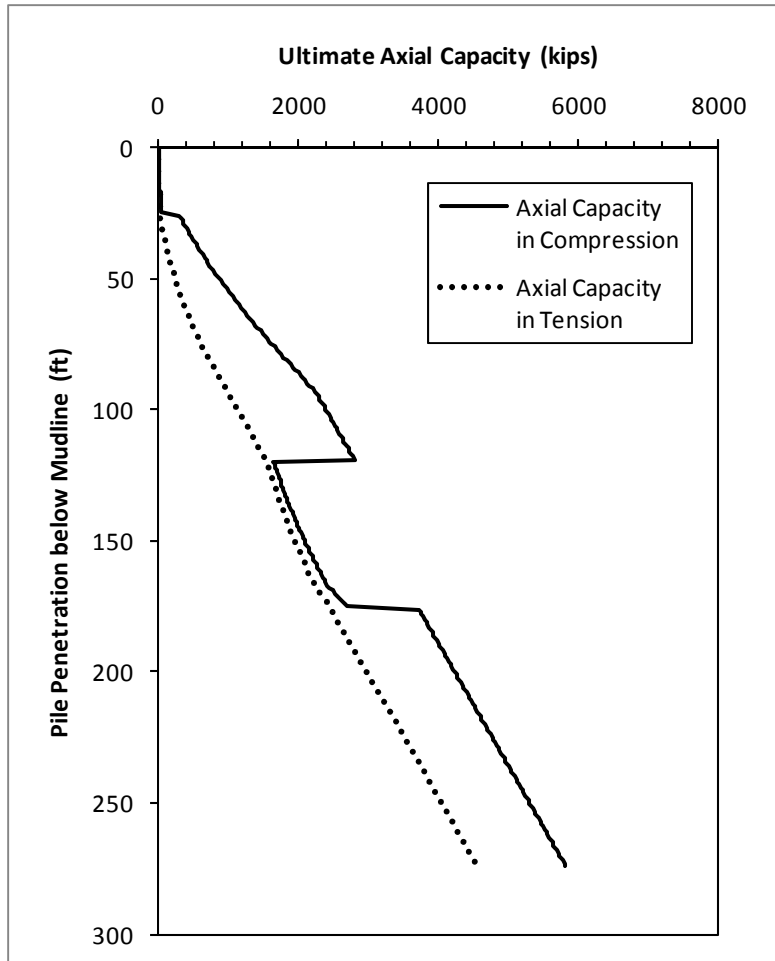


Figure E.18 Ultimate Axial Capacities of the Piles of Platform 8

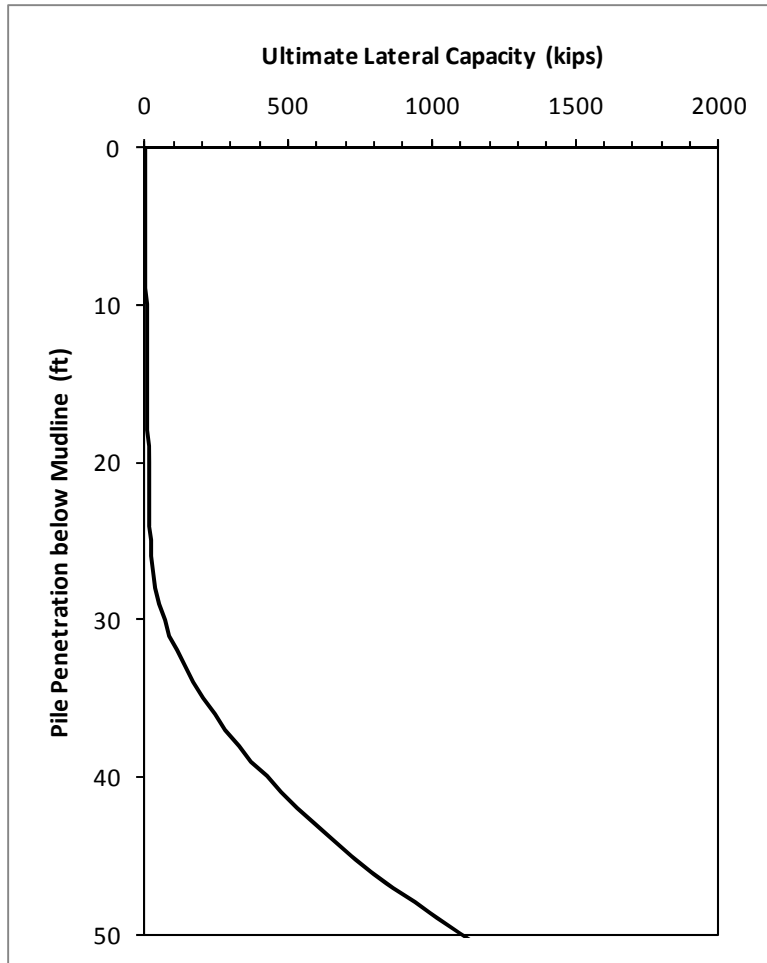


Figure E.19 Ultimate Lateral Capacity of the Piles of Platform 8

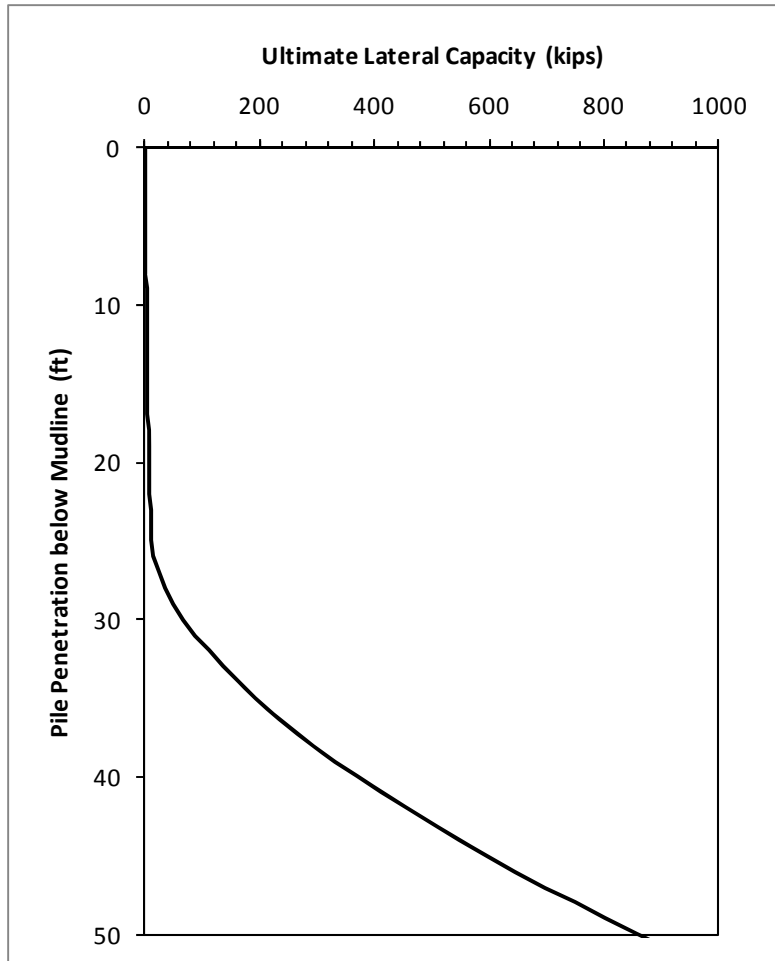


Figure E.20 Ultimate Lateral Capacity of the Conductors of Platform 8

The structural capacity input files of the piles and conductors are summarized in Tables E.16 and E.17, respectively.

Table E.16 Structural Capacity of the Piles of Platform 8

Wall Thickness, t (in.)	Starting Length along Pile, z (in.)	Axial Structural Capacity, Q (lbs)	Moment Capacity, M (in.-lbs)
2	0	1.040E+07	1.524E+08
1.75	528	9.154E+06	1.348E+08
1.5	648	7.889E+06	1.168E+08

Table E.17 Structural Capacity of the Conductors of Platform 8

Wall Thickness, t (in.)	Starting Length along Pile, z (in.)	Axial Structural Capacity, Q (lbs)	Moment Capacity, M (in.-lbs)
0.75	0	2.142E+06	1.722E+07
0.75	600	2.142E+06	1.722E+07
0.75	1200	2.142E+06	1.722E+07

Based on the above input parameters, the base case foundation system capacity interaction curves in the end-on and diagonal directions are presented in Figures E.21 and E.22, respectively. Due to the symmetry of the piles, the foundation capacity in the broadside direction is the same as that in the end-on direction. The direction of the waves is approximately the diagonal direction of this platform. Therefore, the hurricane hindcast load on the foundation is also presented in the interaction diagram for the diagonal direction. The magnitudes of the base shear and overturning moment on the foundation in Katrina were estimated to be 2,600 kips and 419,700 ft-kips. Note that these estimates were not obtained from the detailed hindcast analysis using a 3-D model. Rather, they were inferred from the results of ultimate strength analysis using metocean criteria that are similar to the Katrina hindcast conditions. The overturning capacity of the foundation in end-on direction is apparently greater than that in the diagonal direction while the shear capacity is similar in these two directions (Figures E.21 and E.22). From Figure E.22, the failure mechanism of the foundation is dominated by overturning. The Katrina hindcast load on the foundation is apparently lower than the base case foundation system capacity.

Due to the uncertainty in the magnitudes of hindcast base shear and overturning moment and the fact that the base case foundation system capacity is already higher than the Katrina hindcast load, parametric analyses were not performed.

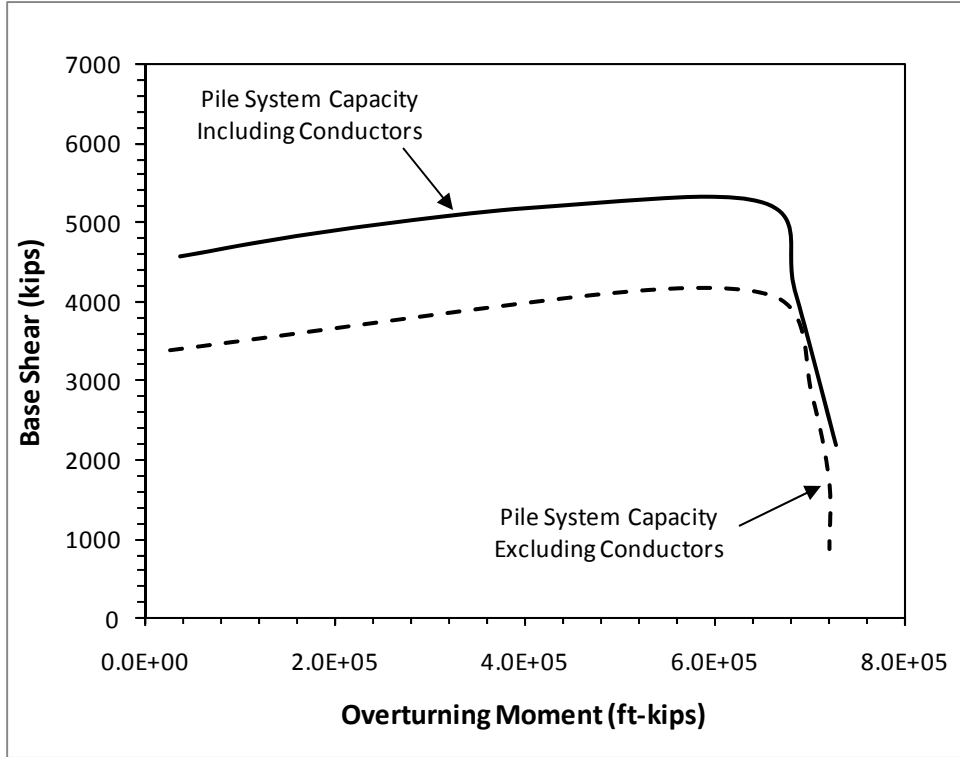


Figure E.21 Base Case Foundation System Capacity Interaction Diagram of Platform 8 in the End-on Direction

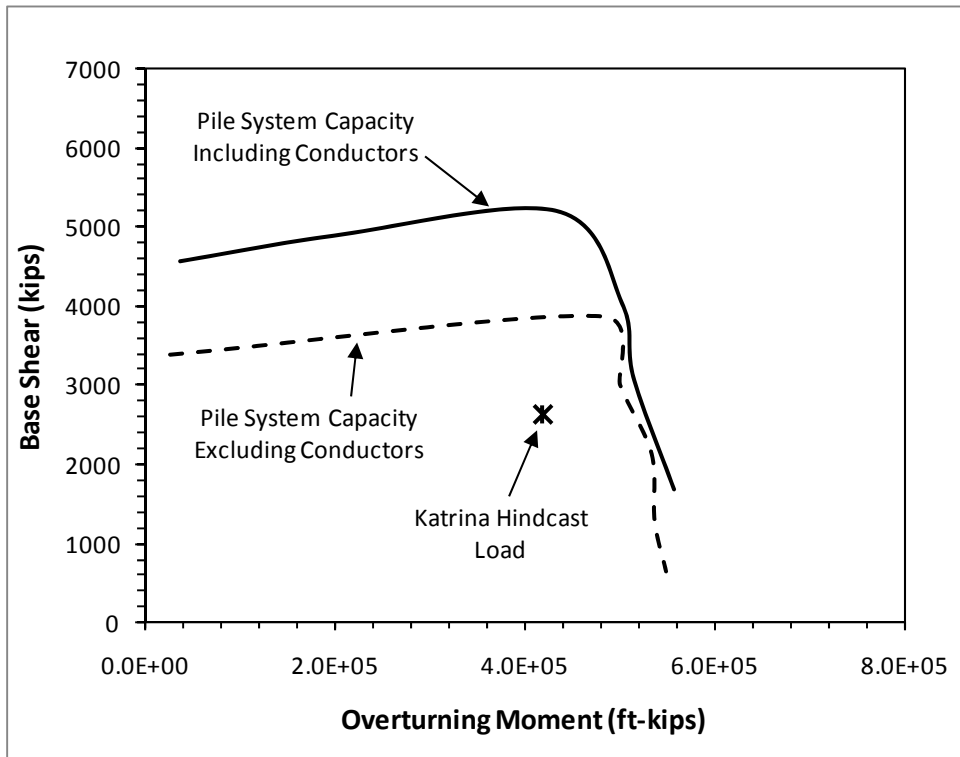


Figure E.22 Base Case Foundation System Capacity Interaction Diagram of Platform 8 in the Diagonal Direction

E.4 Platform 9

Platform 9 is a 4-leg structure supported by 4 piles that are symmetrical and equipped with one 72-inch diameter conductor. The direction of the waves in Hurricane Katrina is approximately the end-on direction of this platform. The executive input file of this platform in the end-on direction is presented hereafter.

Executive Input File for Platform 9

PLATFORM 9 (ALL UNITS IN LB., IN., AND DEGREES)

SYSTEM LOAD DATA (PH,H,R,SKEW,PV,ECCENT)

0.901E6

1.5E3

1.00E-11

90.0

0.640E6

1.00E-10

NUMBER OF PILES (NPILE)

5

PILE 1

GEOMETRY (X,Y,THETAX,THETAY,L,AXIAL CONSTRAINT,NGROUP)

-2.58E+02 -2.58E+02 -7.13 -7.13 1.44E+03 1 1

PILE STRUCTURAL CAPACITY (INPUT FILE)

WPILE1.INP

SOIL CAPACITY (INPUT FILE)

WSOIL1.INP

PILE 2

GEOMETRY (X,Y,THETAX,THETAY,L,AXIAL CONSTRAINT,NGROUP)

2.58E+02 -2.58E+02 7.13 -7.13 1.44E+03 1 1

PILE STRUCTURAL CAPACITY (INPUT FILE)

WPILE1.INP

SOIL CAPACITY (INPUT FILE)

WSOIL1.INP

PILE 3

GEOMETRY (X,Y,THETAX,THETAY,L,AXIAL CONSTRAINT,NGROUP)

-2.58E+02 2.58E+02 -7.13 7.13 1.44E+03 1 1

PILE STRUCTURAL CAPACITY (INPUT FILE)

WPILE1.INP

SOIL CAPACITY (INPUT FILE)

WSOIL1.INP

PILE 4

GEOMETRY (X,Y,THETAX,THETAY,L,AXIAL CONSTRAINT,NGROUP)

2.58E+02 2.58E+02 7.13 7.13 1.44E+03 1 1

PILE STRUCTURAL CAPACITY (INPUT FILE)

WPILE1.INP

SOIL CAPACITY (INPUT FILE)

WSOIL1.INP

CONDUCTOR

GEOMETRY (X,Y,THETAX,THETAY,L,AXIAL CONSTRAINT,NGROUP)

0.78E+00 0.00E+02 0.00 0.00 1.236E+03 0 1

PILE STRUCTURAL CAPACITY (INPUT FILE)

WPILEC72.INP

SOIL CAPACITY (INPUT FILE)

WSOILC72.INP

The input parameters for the custom-built spreadsheet to calculate the axial and lateral resistance of the 4 piles battered in 2 directions and the 72-inch diameter conductor are presented in Tables E.18 and E.19, respectively. The design soil profile and parameters common for all piles and conductor are presented in Table E.20. The axial capacities of the 4 piles in compression and in tension are presented in Figure E.23. The lateral resistance of these piles is presented in Figure E.24. The lateral resistance of the 72-inch diameter conductor is presented in Figure E.25.

Table E.18 Input Parameters for the Piles of Platform 9

Seafloor Elevation (ft, MSL)	-60
Seasurface Elevation (ft, MSL)	0
Top of Pile Elevation (ft, MSL)	-60
Pile Length (ft)	120
Pile Diameter (ft)	2.5
Pile Tip Wall Thickness (in.)	0.75
Unit Weight of Water (pcf)	62.4
Depth Increment (ft)	1
Open- or Close-ended	Open
Open-ended Pile Tip Condition	Plugged
Loading Condition	Cyclic
K Compression	0.8
K Tension	0.8
Pile Batter in x-direction (deg.)	7.125
Pile Batter in y-direction (deg.)	7.125
X_R (ft)	24.1

Table E.19 Input Parameters for the Conductor of Platform 9

Seafloor Elevation (ft, MSL)	-60
Seasurface Elevation (ft, MSL)	0
Top of Pile Elevation (ft, MSL)	-60
Pile Length (ft)	103
Pile Diameter (ft)	6
Pile Tip Wall Thickness (in.)	1
Unit Weight of Water (pcf)	62.4
Depth Increment (ft)	1
Open- or Close-ended	Open
Open-ended Pile Tip Condition	Plugged
Loading Condition	Cyclic
K Compression	0.8
K Tension	0.8
Pile Batter in x-direction (deg.)	0
Pile Batter in y-direction (deg.)	0
X_R (ft)	23.5

Table E.20 Design Soil Profile and Parameters for All Piles and Conductor of Platform 9

Layer	Soil Type	Top Elevation (ft, MSL)	Bottom Elevation (ft, MSL)	Thickness (ft)	Total Unit Weight (pcf)	Submerged Unit Weight (pcf)	c_u at the Top of Layer (psf)	dc_u/dz (psf/ft)	Friction Angle, ϕ' (deg.)	Soil Pile Friction Angle, δ (deg.)	Limiting Skin Friction Value (ksf)	N_q	Limiting End Bearing Value (ksf)	C_1	C_2	C_3
1	Cohesionless	-60	-66	6	112.4	50			30	25	1.7	20	100	1.9	2.7	29
2	Cohesive	-66	-86	20	102.4	40	500	15								
3	Cohesionless	-86	-97	11	122.4	60			30	25	1.7	20	100	1.9	2.7	29
4	Cohesionless	-97	-142	45	122.4	60			35	30	2.0	40	200	3.0	3.5	55
5	Cohesionless	-142	-168	26	122.4	60			40	35	2.4	50	250	4.7	4.3	100
6	Cohesive	-168	-190	22	112.4	50	2000	22.73								
7	Cohesive	-190	-212	22	112.4	50	2500	22.73								

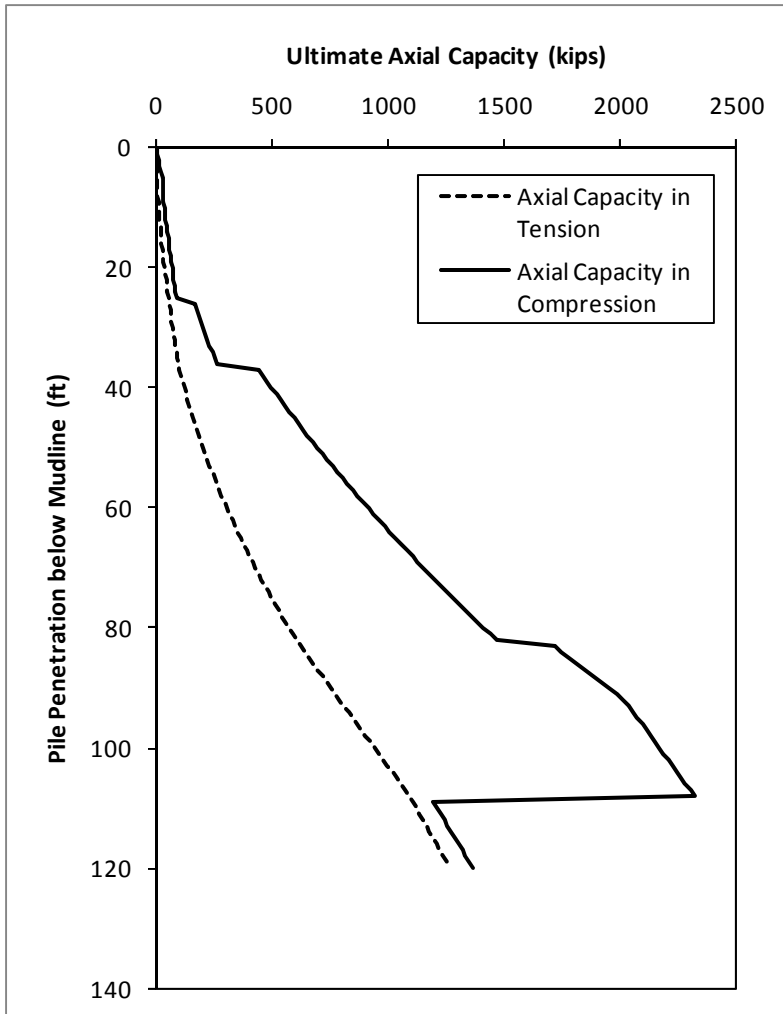


Figure E.23 Ultimate Axial Capacities of the Piles of Platform 9

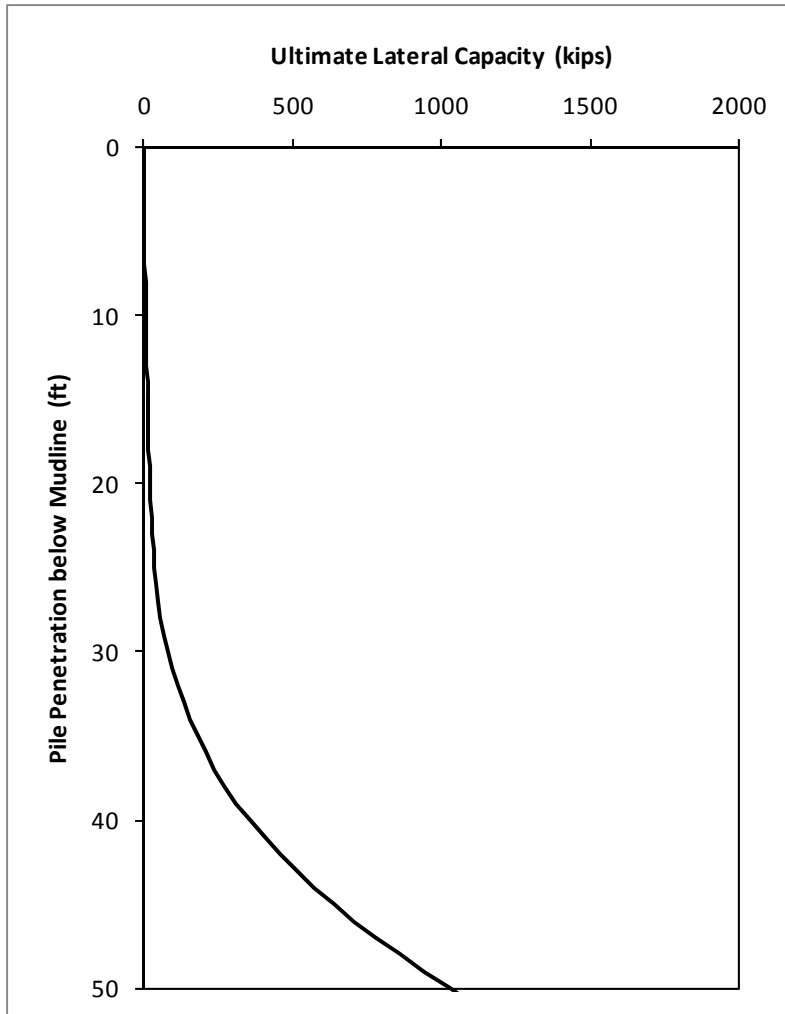


Figure E.24 Ultimate Lateral Resistance of the Piles of Platform 9

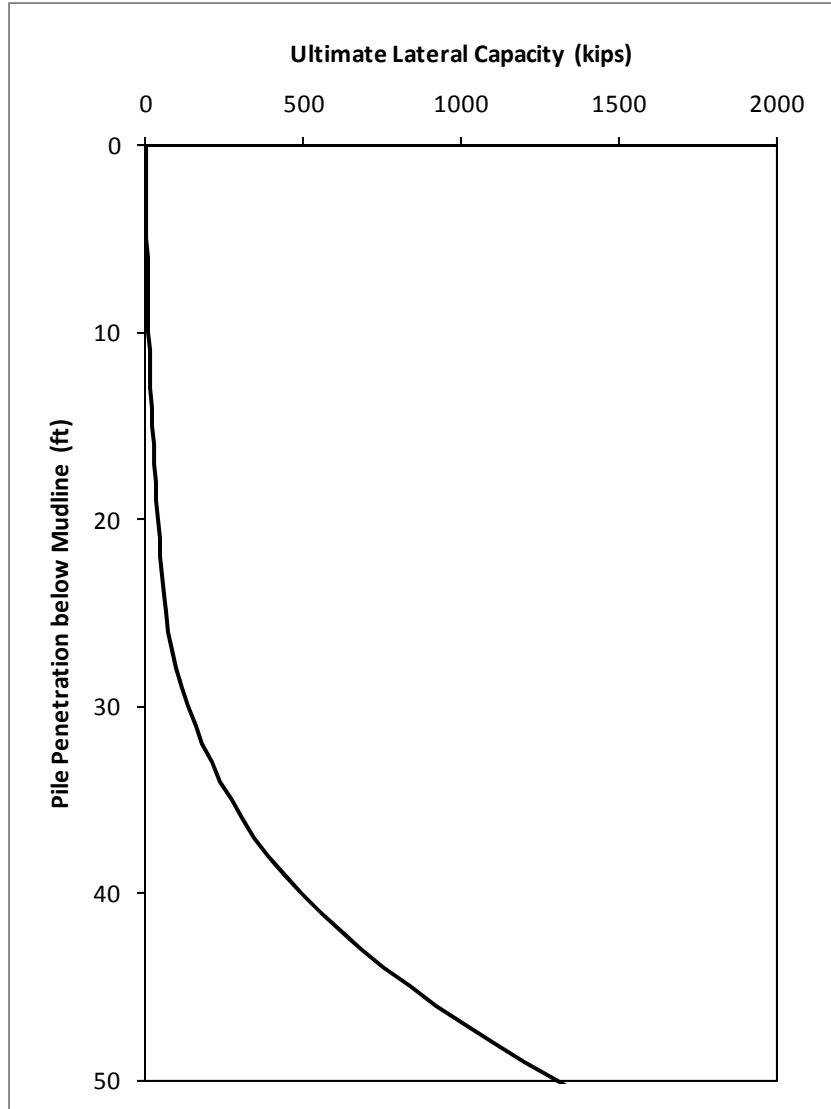


Figure E.25 Ultimate Lateral Resistance of the Conductor of Platform 9

The structural capacity input files of the piles and conductor are summarized in Tables E.21 and E.22, respectively.

Table E.21 Structural Capacity of the Piles of Platform 9

Wall Thickness, t (in.)	Starting Length along Pile, z (in.)	Axial Structural Capacity, Q (lbs)	Moment Capacity, M (in.-lbs)
1	0	3.280E+06	3.029E+07
0.75	1200	2.481E+06	2.311E+07
1	1380	3.280E+06	3.029E+07

Table E.22 Structural Capacity of the Conductor of Platform 9

Wall Thickness, t (in.)	Starting Length along Pile, z (in.)	Axial Structural Capacity, Q (lbs)	Moment Capacity, M (in.-lbs)
1.5	0	1.196E+07	2.684E+08
1.75	120	1.390E+07	3.110E+08
1.5	564	1.196E+07	2.684E+08

Based on the above input parameters, the base case foundation system capacity interaction curves in the end-on and diagonal directions are presented in Figures E.26 and E.27, respectively. Due to the symmetry of the piles, the foundation capacity in the broadside direction is the same as that in the end-on direction. The direction of the waves is approximately the end-on direction of this platform. Therefore, the hurricane hindcast load on the foundation is also presented in the interaction diagram for the end-on direction.

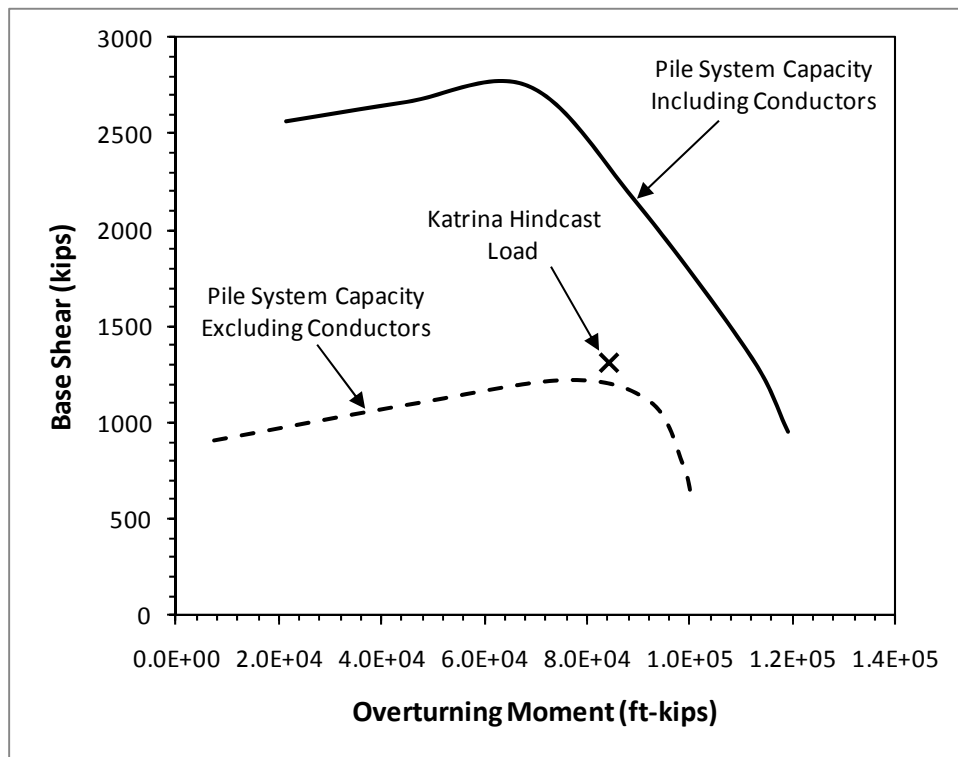


Figure E.26 Base Case Foundation System Capacity Interaction Diagram of Platform 9 in the End-on Direction

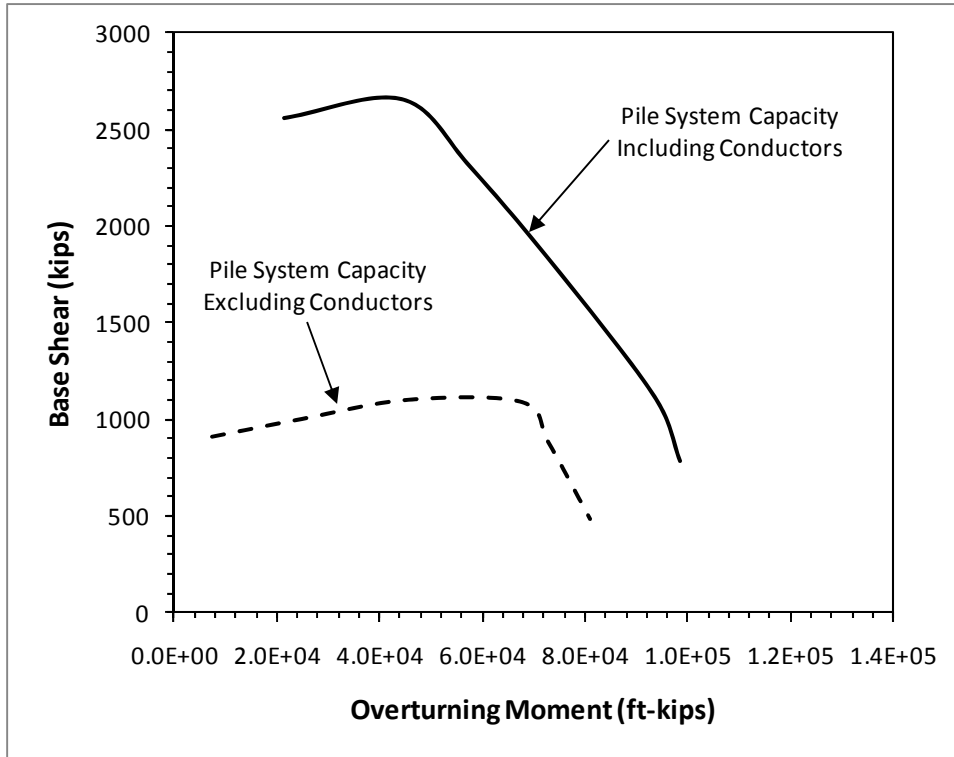


Figure E.27 Base Case Foundation System Capacity Interaction Diagram of Platform 9 in the Diagonal Direction

As shown in Figures E.26 and E.27, the presence of the 72-inch diameter conductor contributes significantly to the shear and overturning capacities of the foundation. Also, the overturning capacities of the foundation in the end-on and diagonal directions are notably different. This is due to the non-redundant nature of this 4-pile structure. Parametric analyses were performed in the end-on direction to investigate the effects of the lateral resistance of the soil and the yield strength of the steel for the conductor on the foundation system capacity. In the first analysis, the ultimate lateral resistance, which is roughly proportional to the shear strength of the soil over the upper 50 feet of the conductor, was increased by 50 percent with a multiplier, N_{Qlat} , of 1.5. Unlike the parametric analysis for Platform 1, the multiplier was only applied for the conductor in this analysis. In the second analysis, the yield strength of the steel conductor was increased by 15 percent beyond its nominal value ($f_Y = 41.4$ ksi). The results of these two parametric analyses are presented in Figure E.28 where the base case foundation system capacity interaction curve is also presented. As shown, the increase in the shear capacity of the foundation due to increasing the ultimate lateral resistance of the conductor by 50 percent is very similar to that due to increasing the yield strength of the conductor by 15 percent. Increasing the yield strength of the conductor also increases the overturning

capacity of the foundation marginally because the plastic moment capacity of the conductor contributes to the overturning capacity of the foundation. However, increasing the ultimate lateral resistance of the conductor does not increase the overturning capacity.

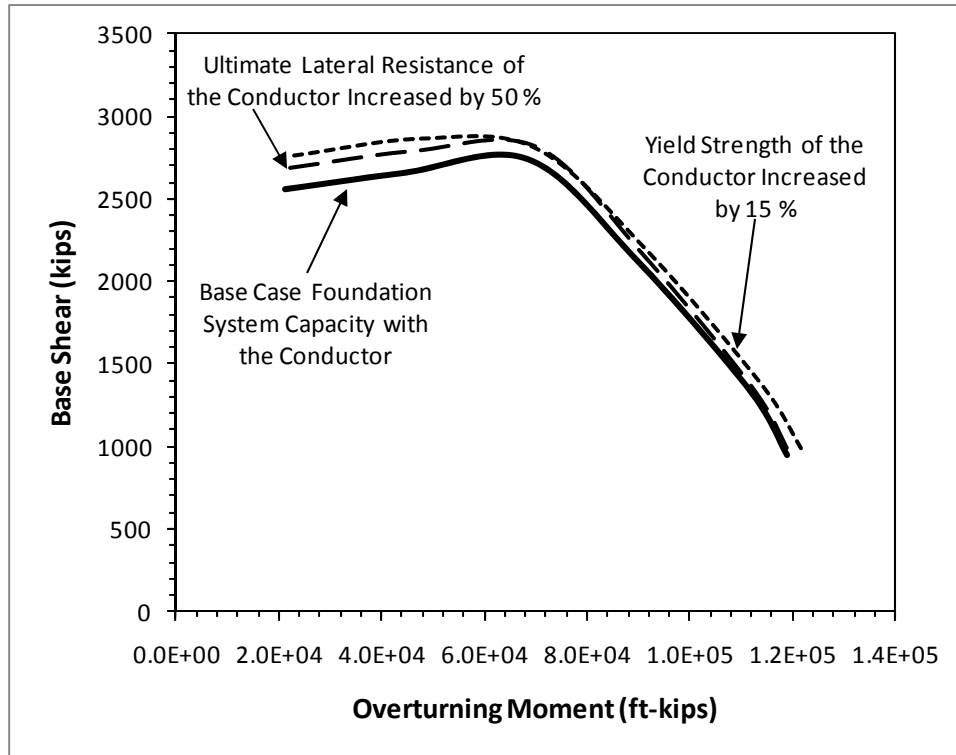


Figure E.28 Parametric Analyses for Platform 9 in the End-on Direction Increasing the Ultimate Lateral Resistance and Yield Strength of the 72-inch Diameter Conductor

E.5 Platform 10

Platform 10 is a 3-leg structure supported by 3 piles and equipped with one 20-inch diameter conductor (Figure E.29). The foundation system is highly asymmetrical. Pile A is a vertical pile with a diameter of 48 inches and a length of 265 feet. This pile also houses a well inside with a series of casing strings. Piles B and C are battered in 2 directions. The diameter and length of these two piles are 48 inches and 220 feet, respectively. The direction of the waves in Hurricane Ike is approximately from the southeast to the northwest (290 degrees clockwise from the true north). The executive input file of this platform in the direction of the waves is presented hereafter.

Executive Input File for Platform 10

PLATFORM 10 (ALL UNITS IN LB., IN., AND DEGREES)

SYSTEM LOAD DATA (PH,H,R,SKEW,PV,ECCENT)

1.4E6

4E3

1.00E-11

160.0

3.116E6

1.00E-10

NUMBER OF PILES (NPILE)

4

PILE 1

GEOMETRY (X,Y,THETAX,THETAY,L,AXIAL CONSTRAINT,NGROUP)

0.0E+02 5.435E+02 0.0 0.0 3.18E+03 1 1

PILE STRUCTURAL CAPACITY (INPUT FILE)

WPILE0.INP

SOIL CAPACITY (INPUT FILE)

WSOIL0.INP

PILE 2

GEOMETRY (X,Y,THETAX,THETAY,L,AXIAL CONSTRAINT,NGROUP)

-6.276E+02 -5.435E+02 -5.71 -9.83 2.64E+03 1 1

PILE STRUCTURAL CAPACITY (INPUT FILE)

WPILE2.INP

SOIL CAPACITY (INPUT FILE)

WSOIL2.INP

PILE 3

GEOMETRY (X,Y,THETAX,THETAY,L,AXIAL CONSTRAINT,NGROUP)

6.276E+02 -5.435E+02 5.71 -9.83 2.64E+03 1 1

PILE STRUCTURAL CAPACITY (INPUT FILE)

WPILE2.INP

SOIL CAPACITY (INPUT FILE)

WSOIL2.INP

CONDUCTOR

GEOMETRY (X,Y,THETAX,THETAY,L,AXIAL CONSTRAINT,NGROUP)

0.0E+02 6.335E+02 0.0 0.0 3.18E+03 0 1

PILE STRUCTURAL CAPACITY (INPUT FILE)

WPILEC.INP

SOIL CAPACITY (INPUT FILE)

WSOILC.INP

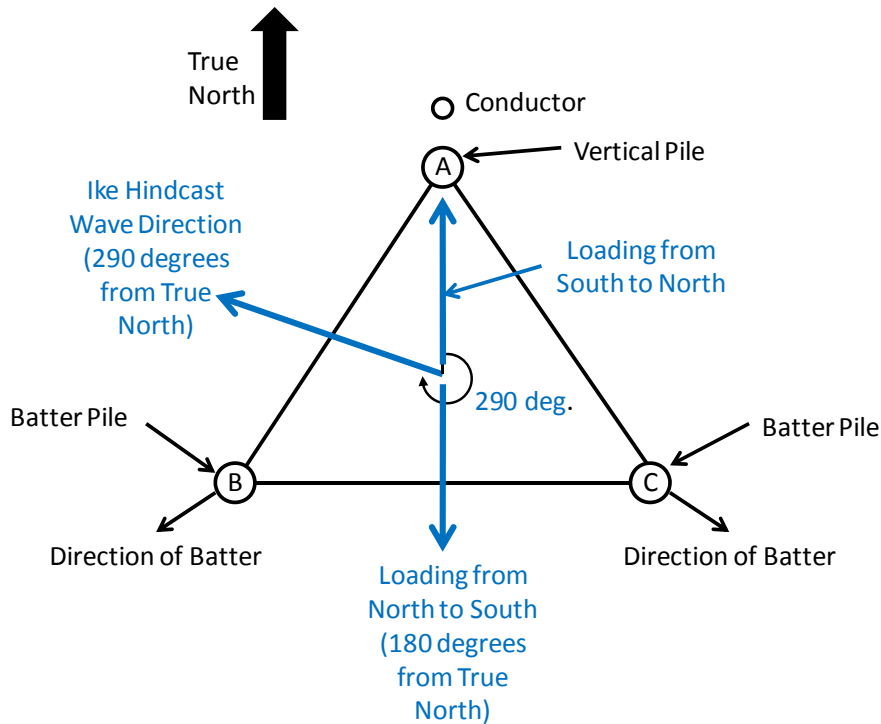


Figure E.29 Plan View of Foundation System for Platform 10

The input parameters for the custom-built spreadsheet to calculate the axial and lateral resistance of Pile A, Piles B and C, and the 20-inch diameter conductor are presented in Tables E.23, E24 and E.25, respectively. The design soil profile and parameters common for all piles and conductor are presented in Table E.26. The axial capacities of Pile A in compression and in tension are presented in Figure E.30. The lateral resistance of Pile A is presented in Figure E.31. The axial capacities of Piles B and C in compression and in tension are presented in Figure E.32. The lateral resistance of Piles B and C is presented

in Figure E.33. The lateral resistance of the 20-inch diameter conductor is presented in Figure E.34.

Note that the axial capacity profiles presented herein represent the residual (versus peak) side shear with a residual adhesion ratio, t_{res}/t_{max} , of 0.8, because the piles are embedded entirely in clays where strain softening will affect the axial pile capacity adversely.

Table E.23 Input Parameters for Pile A of Platform 10

Seafloor Elevation (ft, MSL)	-360
Seasurface Elevation (ft, MSL)	0
Top of Pile Elevation (ft,MSL)	-360
Pile Length (ft)	265
Pile Diameter (ft)	4
Pile Tip Wall Thickness (in.)	1.25
Unit Weight of Water (pcf)	62.4
Depth Increment (ft)	1
Open- or Close-ended	Open
Open-ended Pile Tip Condition	Plugged
Loading Condition	Cyclic
K Compression	0.8
K Tension	0.8
Pile Batter in x-direction (deg.)	0
Pile Batter in y-direction (deg.)	0
X_R (ft)	35.5

Table E.24 Input Parameters for Piles B and C of Platform 10

Seafloor Elevation (ft, MSL)	-360
Seasurface Elevation (ft, MSL)	0
Top of Pile Elevation (ft,MSL)	-360
Pile Length (ft)	220
Pile Diameter (ft)	4
Pile Tip Wall Thickness (in.)	1.25
Unit Weight of Water (pcf)	62.4
Depth Increment (ft)	1
Open- or Close-ended	Open
Open-ended Pile Tip Condition	Plugged
Loading Condition	Cyclic
K Compression	0.8
K Tension	0.8
Pile Batter in x-direction (deg.)	5.71
Pile Batter in y-direction (deg.)	9.83
X_R (ft)	35.8

Table E.25 Input Parameters for the Conductor of Platform 10

Seafloor Elevation (ft, MSL)	-360
Seasurface Elevation (ft, MSL)	0
Top of Pile Elevation (ft,MSL)	-360
Pile Length (ft)	265
Pile Diameter (ft)	1.67
Pile Tip Wall Thickness (in.)	0.5
Unit Weight of Water (pcf)	62.4
Depth Increment (ft)	1
Open- or Close-ended	Open
Open-ended Pile Tip Condition	Unplugged
Loading Condition	Cyclic
K Compression	0.8
K Tension	0.8
Pile Batter in x-direction (deg.)	0
Pile Batter in y-direction (deg.)	0
X_R (ft)	15.5

Table E.26 Design Soil Profile and Parameters for All Piles and Conductor of Platform 10

Layer	Soil Type	Top Elevation (ft, MSL)	Bottom Elevation (ft, MSL)	Thickness (ft)	Total Unit Weight (pcf)	Submerged Unit Weight (pcf)	c_u at the Top of Layer (psf)	dc_u/dz (psf/ft)	Friction Angle, ϕ' (deg.)	Soil Pile Friction Angle, δ (deg.)	f_{max} (ksf)	N_q	q_{max} (ksf)	C_1	C_2	C_3
1	Cohesive	-360	-369	9	92.4	30	30	9.09								
2	Cohesive	-369	-381	12	105.4	43	320	40.42								
3	Cohesive	-381	-408	27	106.4	44	805	16.85								
4	Cohesive	-408	-447	39	108.4	46	1260	10.5								
5	Cohesive	-447	-508	61	109.4	47	1669.5	10.5								
6	Cohesive	-508	-574	66	109.4	47	2310	10.5								
7	Cohesive	-574	-706	132	113.4	51	3003	10.5								

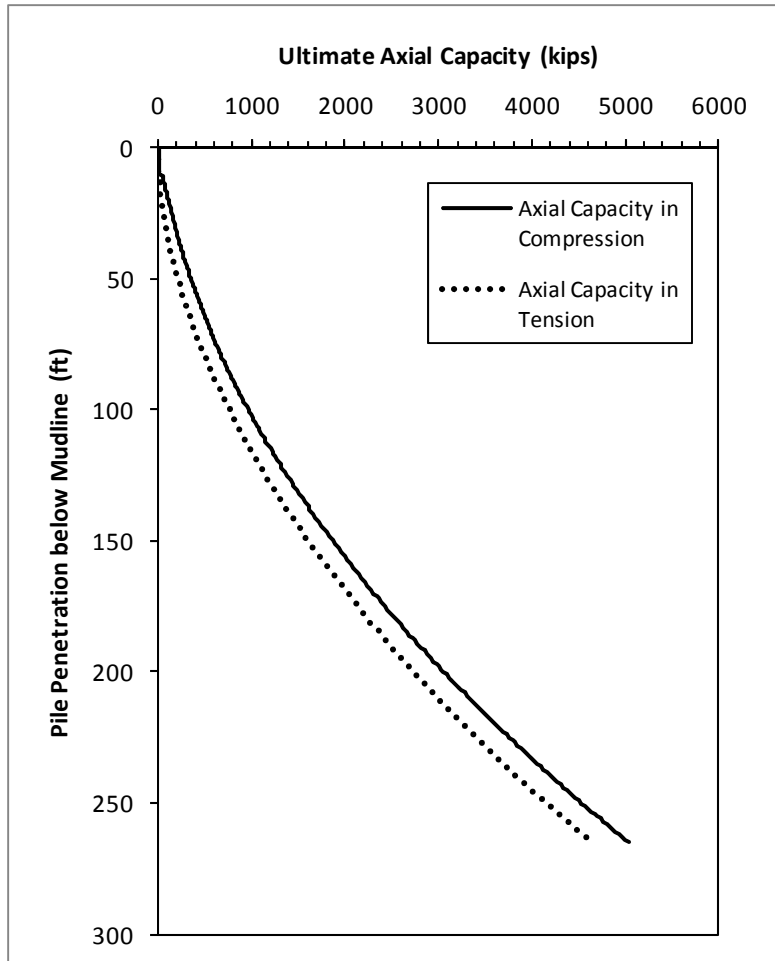


Figure E.30 Ultimate Axial Capacities of Pile A of Platform 10

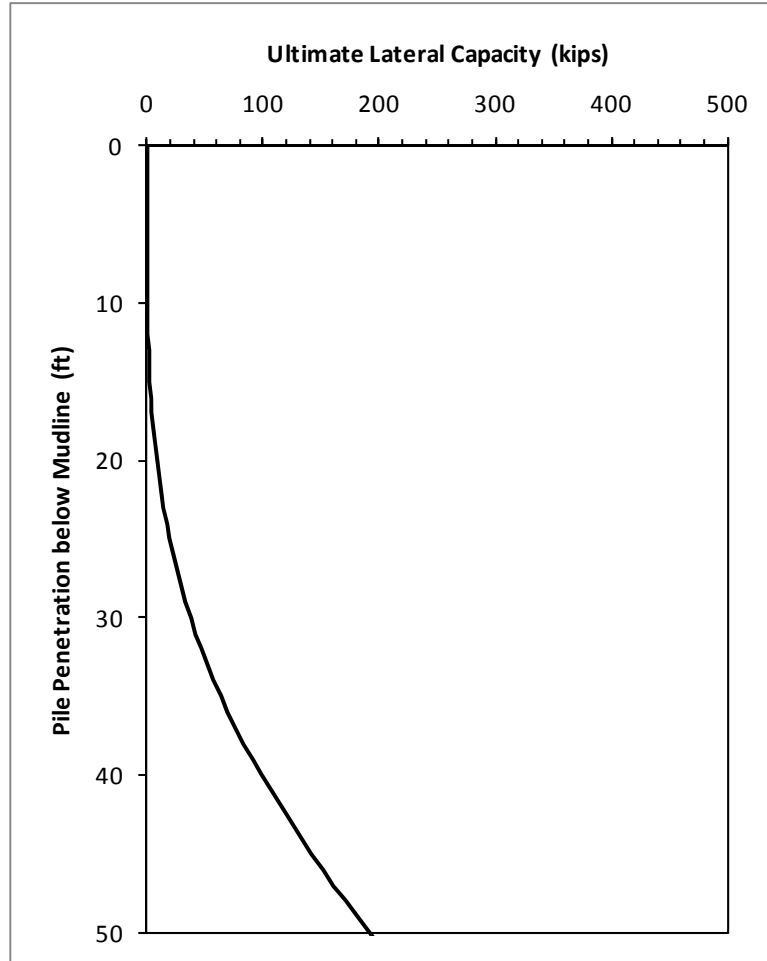


Figure E.31 Ultimate Lateral Resistance of Pile A of Platform 10

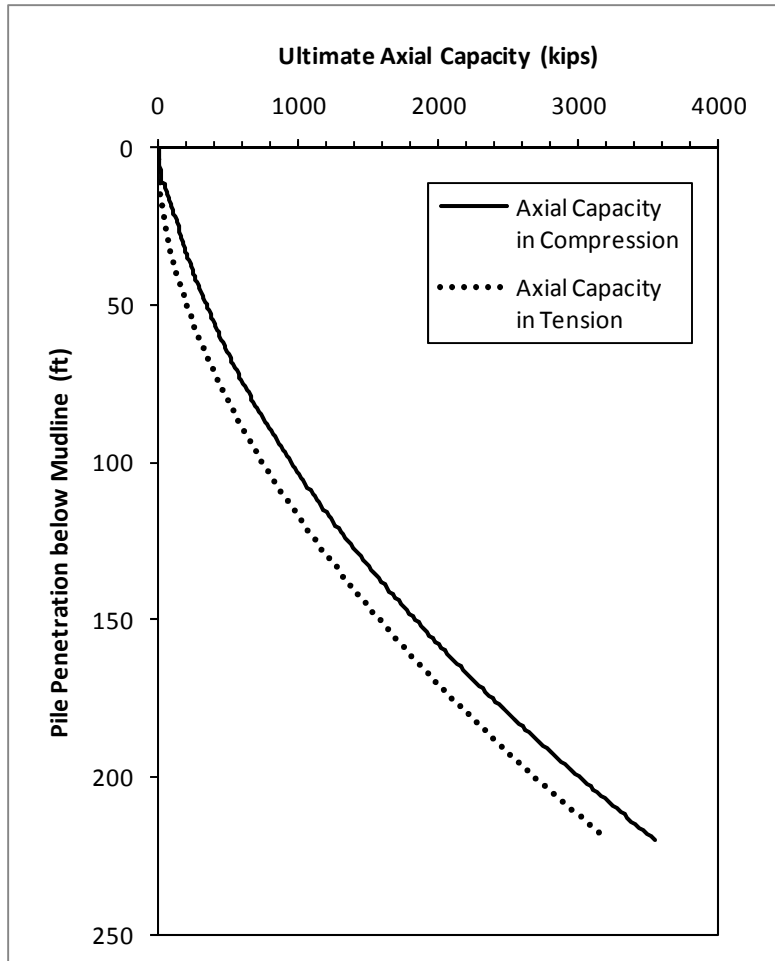


Figure E.32 Ultimate Axial Capacities of Piles B and C of Platform 10

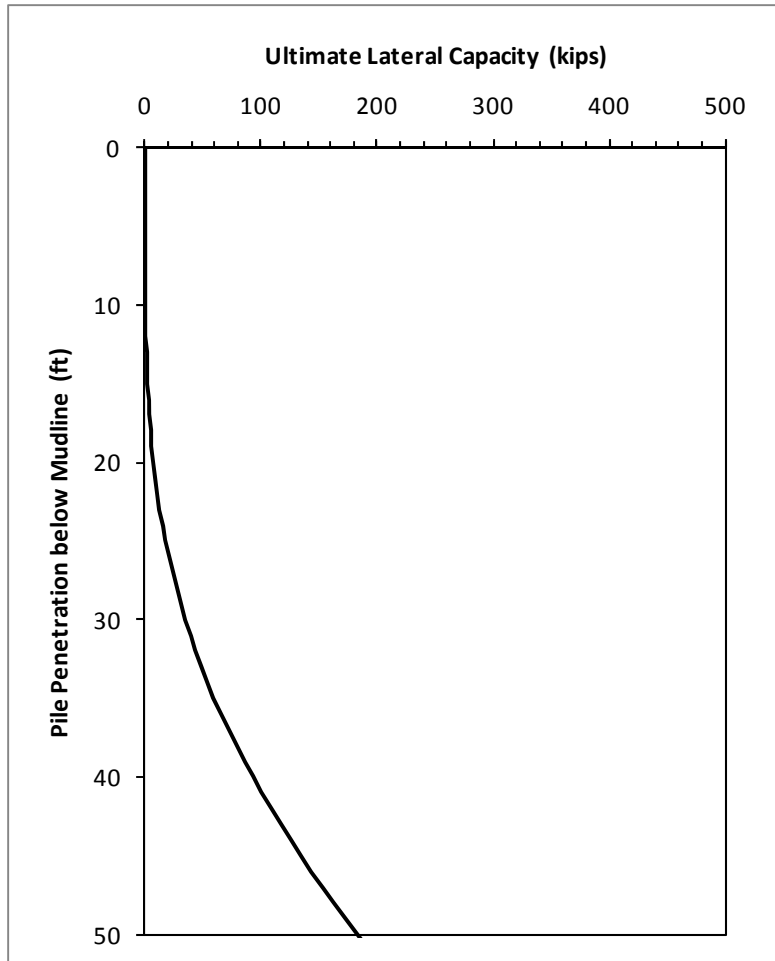


Figure E.33 Ultimate Lateral Resistance of Piles B and C of Platform 10

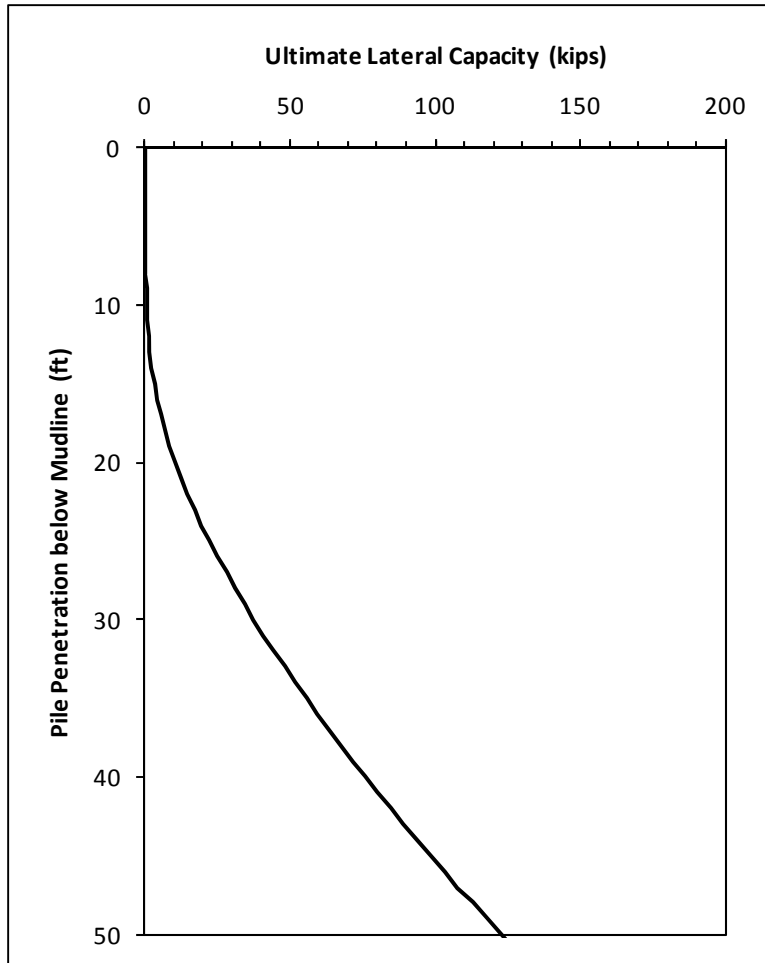


Figure E.34 Ultimate Lateral Resistance of the Conductor of Platform 10

The structural capacity input files of Pile A, Piles B and C, and the conductor are summarized in Tables E.27, E.28 and E.29, respectively.

Table E.27 Structural Capacity of Pile A of Platform 10

Wall Thickness, t (in.)	Starting Length along Pile, z (in.)	Axial Structural Capacity, Q (lbs)	Moment Capacity, M (in.-lbs)
1.75	0	9.154E+06	1.348E+08
1.5	600	7.889E+06	1.168E+08
1.25	1080	6.609E+06	9.837E+07

Table E.28 Structural Capacity of Piles B and C of Platform 10

Wall Thickness, t (in.)	Starting Length along Pile, z (in.)	Axial Structural Capacity, Q (lbs)	Moment Capacity, M (in.-lbs)
1.5	0	7.889E+06	1.168E+08
1.25	660	6.609E+06	9.837E+07
1	900	5.316E+06	7.954E+07

Table E.29 Structural Capacity of the Conductor of Platform 10

Wall Thickness, t (in.)	Starting Length along Pile, z (in.)	Axial Structural Capacity, Q (lbs)	Moment Capacity, M (in.-lbs)
0.5	0	1.103E+06	6.846E+06
0.5	600	1.103E+06	6.846E+06
0.5	1080	1.103E+06	6.846E+06

Based on the above input parameters, the base case foundation system capacity interaction curves corresponding to the direction of the waves in Hurricane Ike (Figure E.29), loading from south to north, loading from north to south, and loading from east to west are presented in Figures E.35, E.36, E.37 and E.38, respectively. Note that these interaction diagrams were developed using the residual side shear, which corresponds to 80 percent of the peak side shear along the entire length of the piles. As shown in these figures, the 20-inch diameter conductor contributes insignificantly to the foundation system capacity.

The foundation system capacities (without the contribution of the conductor) in different loading directions are compared in Figure E.39. As shown, both the shear and overturning capacities of the foundation are very different in different loading directions. This is due to the asymmetrical and non-redundant nature of the foundation.

A parametric analysis was performed in the hindcast wave direction using the peak side shear. The result of this analysis is shown in Figure E.40. As shown, the overturning capacities of the foundation using the peak and residual side shear values are very different. It underscores the importance of considering the effect of strain softening on pile capacity for long, flexible piles embedded in clays.

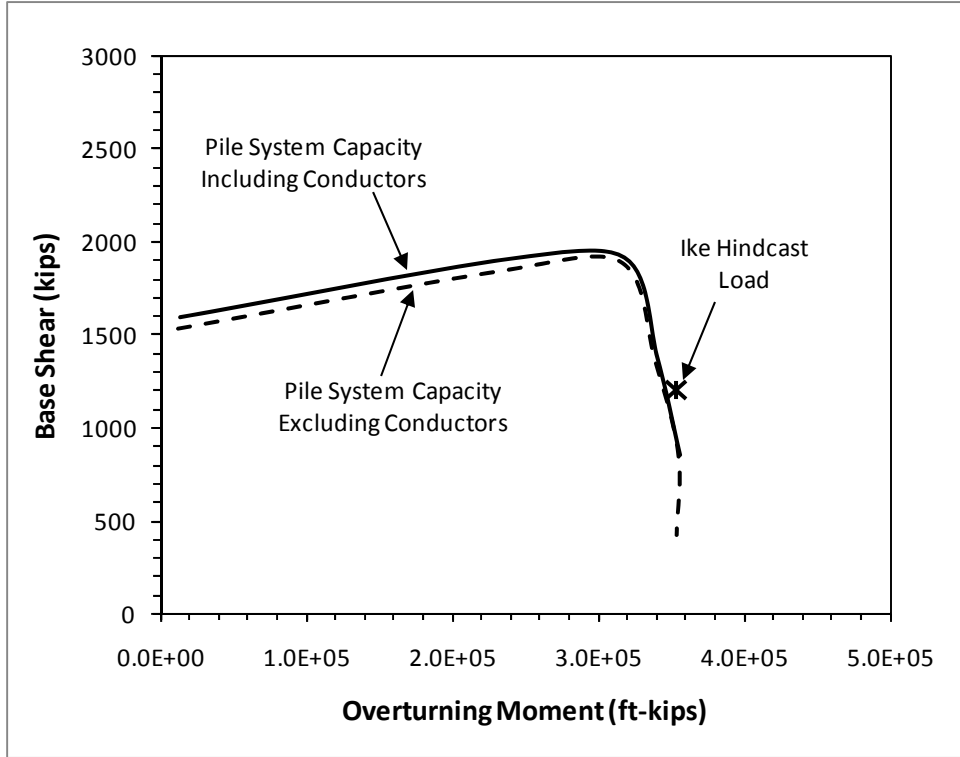


Figure E.35 Base Case Foundation System Capacity Interaction Diagram of Platform 10 in the Direction of the Waves in Hurricane Ike

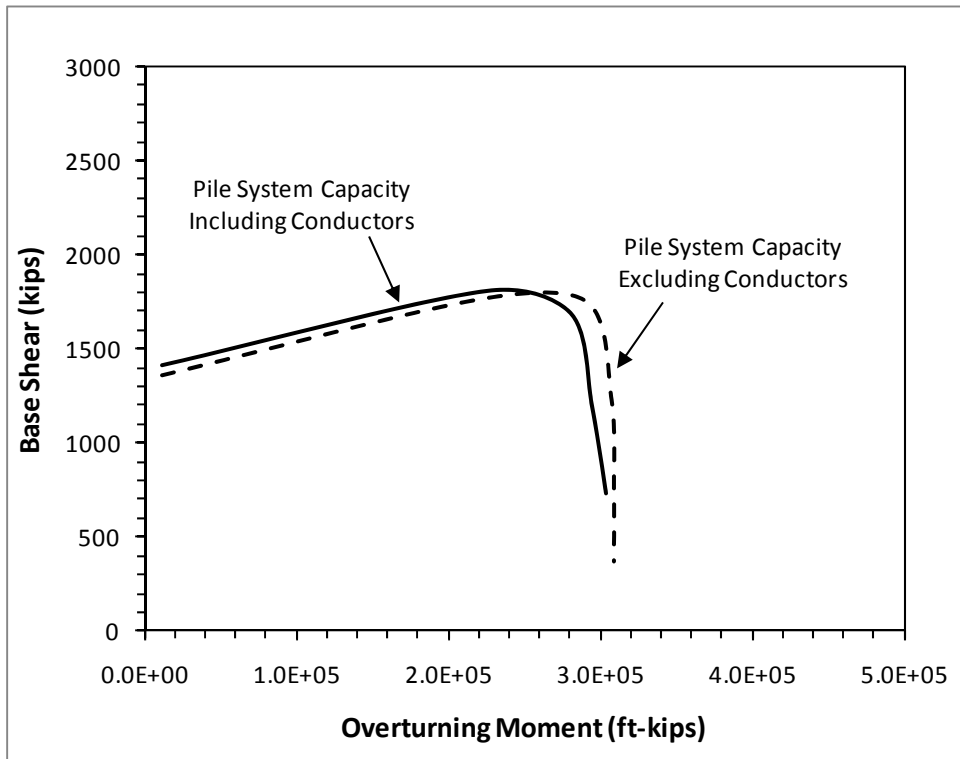


Figure E.36 Base Case Foundation System Capacity Interaction Diagram of Platform 10 Corresponding to Loading from South to North

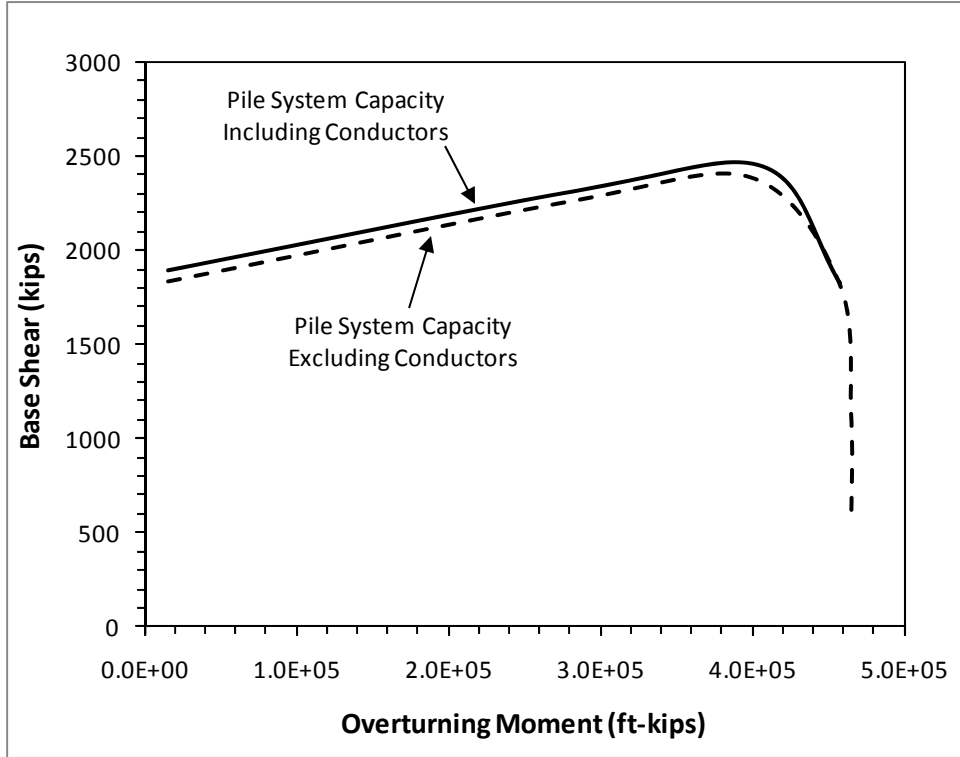


Figure E.37 Base Case Foundation System Capacity Interaction Diagram of Platform 10 Corresponding to Loading from North to South

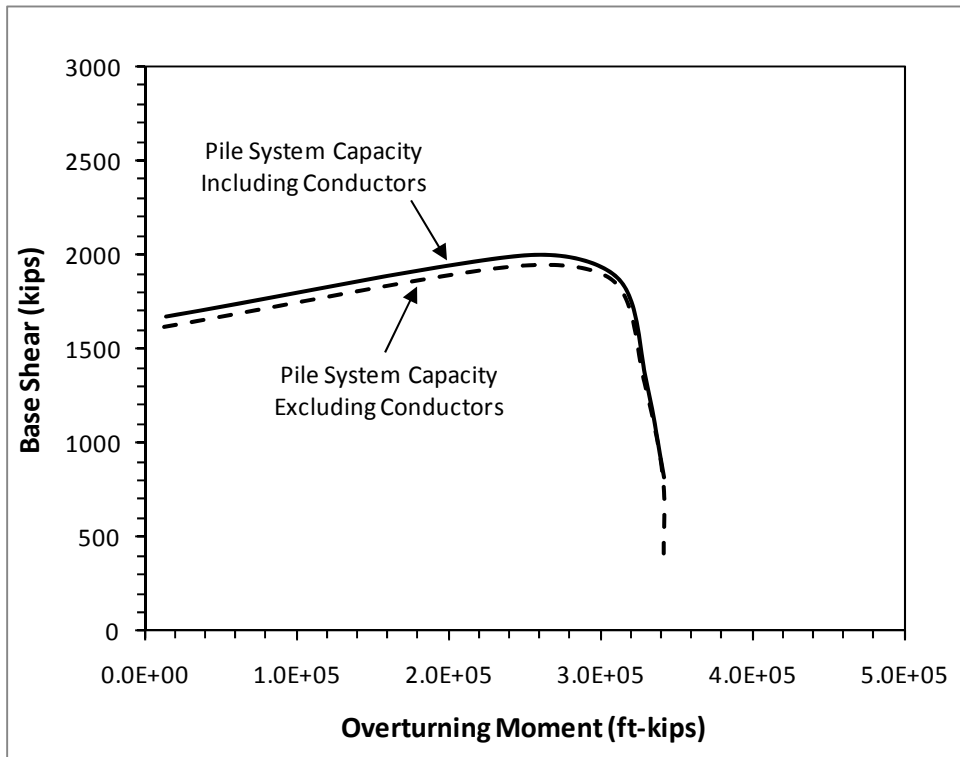


Figure E.38 Base Case Foundation System Capacity Interaction Diagram of Platform 10 Corresponding to Loading from East to West

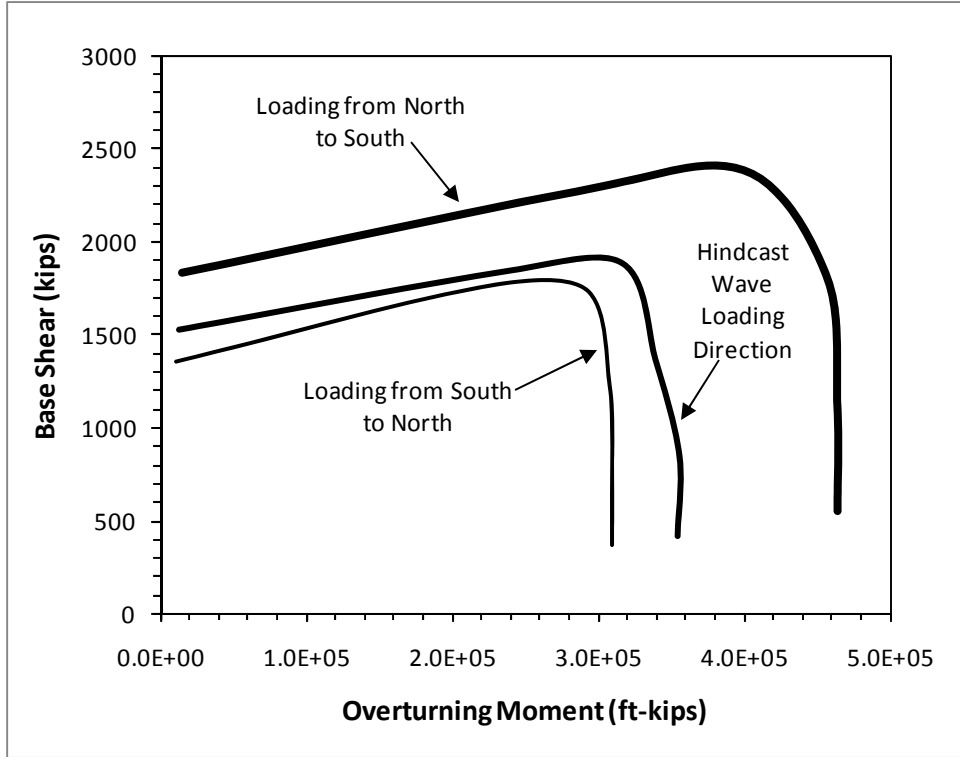


Figure E.39 Comparison of Foundation Capacities in Different Loading Directions for Platform 10

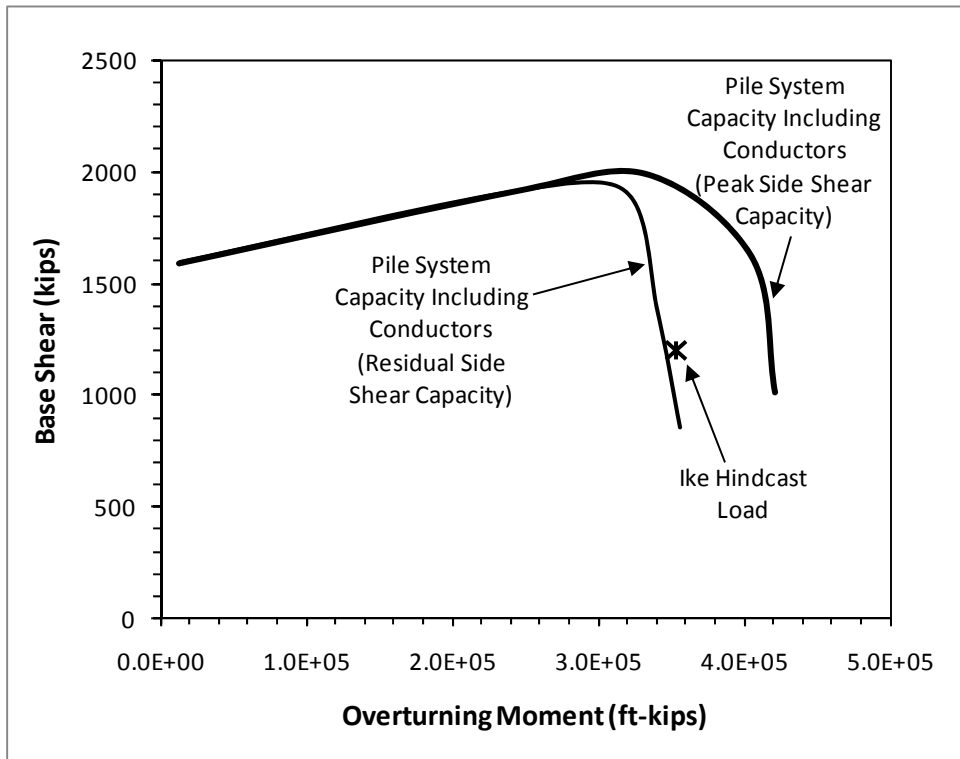


Figure E.40 Parametric Analysis for Platform 10 in the Hindcast Wave Direction Using the Peak Side Shear Capacity

E.6 Platform 11

Platform 11 is a 4-leg structure supported by 4 piles and equipped with 4 conductors. One of the conductors is 72 inches in diameter and the others are 26 inches in diameter. The 72-inch diameter conductor was included in the foundation model. The foundation system is highly asymmetrical. Two of the piles are battered in 2 directions (double batter piles) and they are 239 feet long. The other two piles battered in 1 direction (single batter piles) are 309 feet long. All of the piles are 42 inches in diameter. The direction of the waves in Hurricane Katrina is approximately the end-on direction of this platform (loading from the side of the double batter piles to the side of the single batter piles). The executive input file of this platform in the end-on direction is presented hereafter.

Executive Input File for Platform 11

PLATFORM 11 (ALL UNITS IN LB., IN., AND DEGREES)

SYSTEM LOAD DATA (PH,H,R,SKEW,PV,ECCENT)

2.0E6

1.0E2

1.00E-10

270.0

6.0E6

1.00E-10

NUMBER OF PILES (NPILE)

5

PILE 1

GEOMETRY (X,Y,THETAX,THETAY,L,AXIAL CONSTRAINT,NGROUP)

-4.2E+02 3.747E+02 -7.13 7.13 2.868E+03 1 1

PILE STRUCTURAL CAPACITY (INPUT FILE)

WPILE2.INP

SOIL CAPACITY (INPUT FILE)

WSOIL2.INP

PILE 2

GEOMETRY (X,Y,THETAX,THETAY,L,AXIAL CONSTRAINT,NGROUP)

4.2E+02 3.747E+02 7.13 7.13 2.868E+03 1 1

PILE STRUCTURAL CAPACITY (INPUT FILE)

WPILE2.INP

SOIL CAPACITY (INPUT FILE)

WSOIL2.INP

PILE 3

GEOMETRY (X,Y,THETAX,THETAY,L,AXIAL CONSTRAINT,NGROUP)

-4.2E+02 -3.747E+02 -7.13 0 3.708E+03 1 1

PILE STRUCTURAL CAPACITY (INPUT FILE)

WPILE1.INP

SOIL CAPACITY (INPUT FILE)

WSOIL1.INP

PILE 4

GEOMETRY (X,Y,THETAX,THETAY,L,AXIAL CONSTRAINT,NGROUP)

4.2E+02 -3.747E+02 7.13 0 3.708E+03 1 1

PILE STRUCTURAL CAPACITY (INPUT FILE)

WPILE1.INP

SOIL CAPACITY (INPUT FILE)

WSOIL1.INP

CONDUCTOR

GEOMETRY (X,Y,THETAX,THETAY,L,AXIAL CONSTRAINT,NGROUP)

0.00E+00 -4.947E+02 0.00 0.00 1.560E+03 0 1

PILE STRUCTURAL CAPACITY (INPUT FILE)

WPILEC.INP

SOIL CAPACITY (INPUT FILE)

WSOILC.INP

The input parameters for the custom-built spreadsheet to calculate the axial and lateral resistance of the double batter piles, the single batter piles and the 72-inch diameter conductor are presented in Tables E.30, E.31 and E.32, respectively. The design soil profile and parameters common for all piles and conductor are presented in Table E.33. The axial capacities of the double batter piles in compression and in tension are presented

in Figure E.41. The lateral resistance of the double batter piles is presented in Figure E.42. The axial capacities of the single batter piles in compression and in tension are presented in Figure E.43. The lateral resistance of the single batter piles is presented in Figure E.44. The lateral resistance of the 72-inch diameter conductor is presented in Figure E.45.

Table E.30 Input Parameters for the Double Batter Piles of Platform 11

Seafloor Elevation (ft, MSL)	-120
Seasurface Elevation (ft, MSL)	0
Top of Pile Elevation (ft,MSL)	-120
Pile Length (ft)	239
Pile Diameter (ft)	3.5
Pile Tip Wall Thickness (in.)	0.75
Unit Weight of Water (pcf)	62.4
Depth Increment (ft)	1
Open- or Close-ended	Open
Open-ended Pile Tip Condition	Plugged
Loading Condition	Cyclic
K Compression	0.8
K Tension	0.8
Pile Batter in x-direction (deg.)	7.125
Pile Batter in y-direction (deg.)	7.125
X_R (ft)	32.0

Table E.31 Input Parameters for the Single Batter Piles of Platform 11

Seafloor Elevation (ft, MSL)	-120
Seasurface Elevation (ft, MSL)	0
Top of Pile Elevation (ft,MSL)	-120
Pile Length (ft)	309
Pile Diameter (ft)	3.5
Pile Tip Wall Thickness (in.)	0.75
Unit Weight of Water (pcf)	62.4
Depth Increment (ft)	1
Open- or Close-ended	Open
Open-ended Pile Tip Condition	Plugged
Loading Condition	Cyclic
K Compression	0.8
K Tension	0.8
Pile Batter in x-direction (deg.)	7.125
Pile Batter in y-direction (deg.)	0
X_R (ft)	32.2

Table E.32 Input Parameters for the 72-inch Diameter Conductor of Platform 11

Seafloor Elevation (ft, MSL)	-120
Seasurface Elevation (ft, MSL)	0
Top of Pile Elevation (ft,MSL)	-120
Pile Length (ft)	130
Pile Diameter (ft)	6
Pile Tip Wall Thickness (in.)	1
Unit Weight of Water (pcf)	62.4
Depth Increment (ft)	1
Open- or Close-ended	Open
Open-ended Pile Tip Condition	Plugged
Loading Condition	Cyclic
K Compression	0.8
K Tension	0.8
Pile Batter in x-direction (deg.)	0
Pile Batter in y-direction (deg.)	0
X_R (ft)	35.5

Table E.33 Design Soil Profile and Parameters for All Piles and Conductor of Platform 11

Layer	Soil Type	Top Elevation (ft, MSL)	Bottom Elevation (ft, MSL)	Thickness (ft)	Total Unit Weight (pcf)	Submerged Unit Weight (pcf)	c_u at the Top of Layer (psf)	dc_u/dz (psf/ft)	Friction Angle, ϕ' (deg.)	Soil Pile Friction Angle, δ (deg.)	f_{max} (ksf)	N_q	q_{max} (ksf)	C_1	C_2	C_3
1	Cohesionless	-120	-128	8	119.9	57.5			30	25	1.7	20	100	1.9	2.7	28
2	Cohesive	-128	-139	11	89.9	27.5	250	36.36								
3	Cohesive	-139	-155	16	94.9	32.5	650	6.25								
4	Cohesionless	-155	-219	64	124.4	62			35	30	2.0	40	200	3.0	3.4	54
5	Cohesive	-219	-227	8	113.4	51	1000	0								
6	Cohesionless	-227	-236	9	122.4	60			35	30	2.0	40	200	3.0	3.4	54
7	Cohesive	-236	-242.5	6.5	120.4	58	1800	0								
8	Cohesionless	-242.5	-256	13.5	122.4	60			30	25	1.7	20	100	1.9	2.7	28
9	Cohesive	-256	-327	71	117.9	55.5	1800	21.13								
10	Cohesionless	-327	-364	37	122.4	60			30	25	1.7	20	100	1.9	2.7	28
11	Cohesionless	-364	-400	36	122.4	60			35	30	2.0	40	200	3.0	3.4	54
12	Cohesive	-400	-407	7	120.4	58	2300	0								
13	Cohesionless	-407	-434	27	122.4	60			35	30	2.0	40	200	3.0	3.4	54

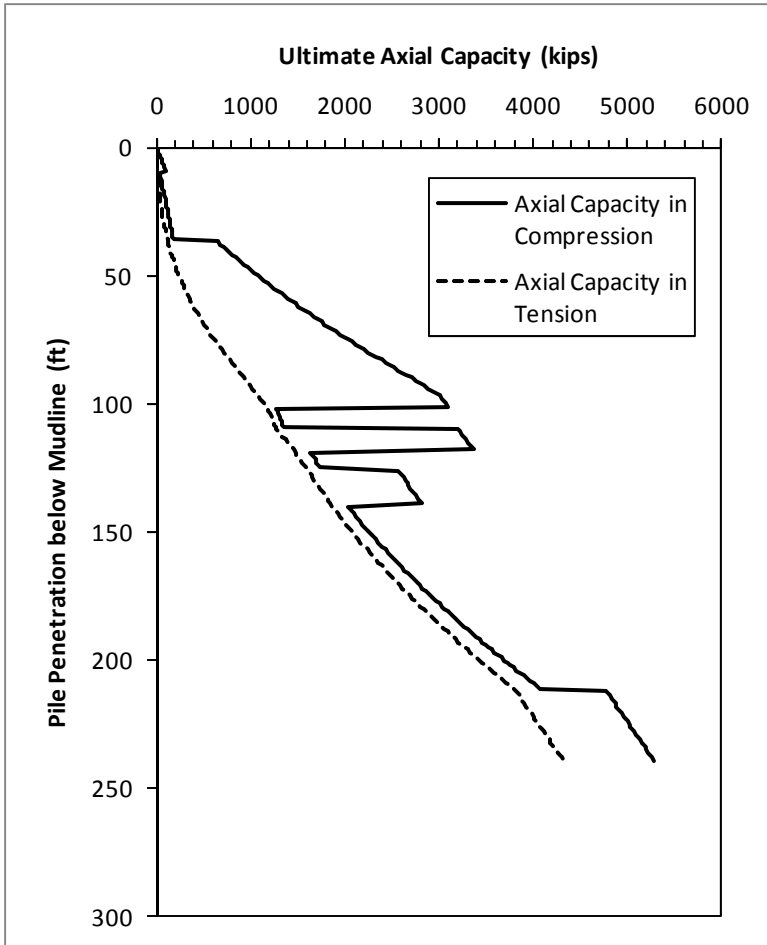


Figure E.41 Ultimate Axial Capacities of the Double Batter Piles of Platform 11

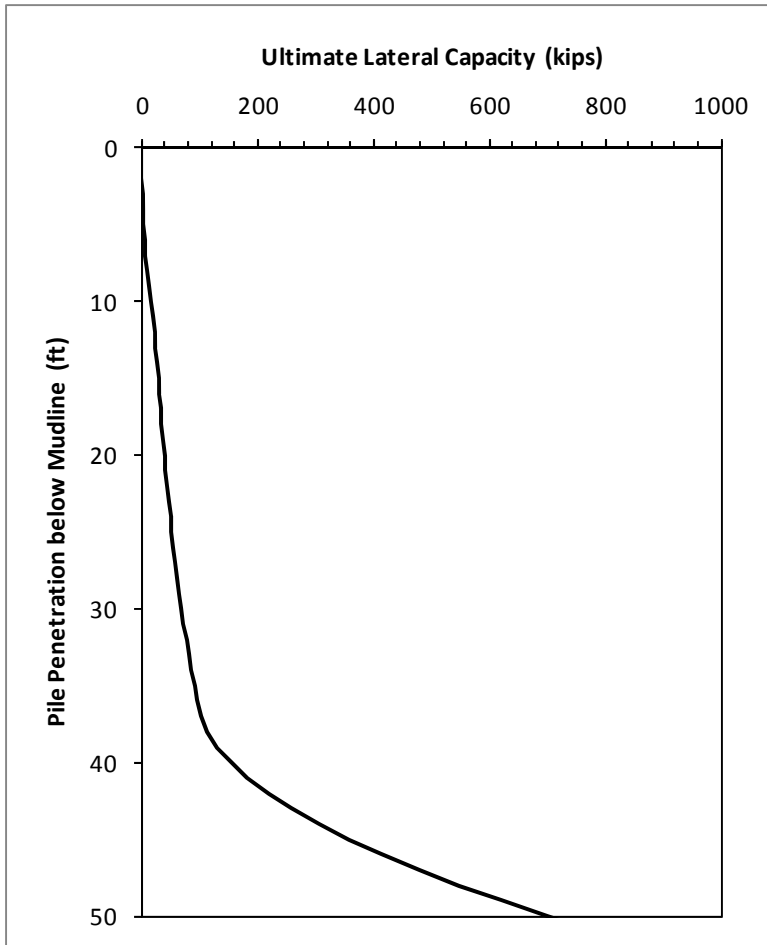


Figure E.42 Ultimate Lateral Resistance of the Double Batter Piles of Platform 11

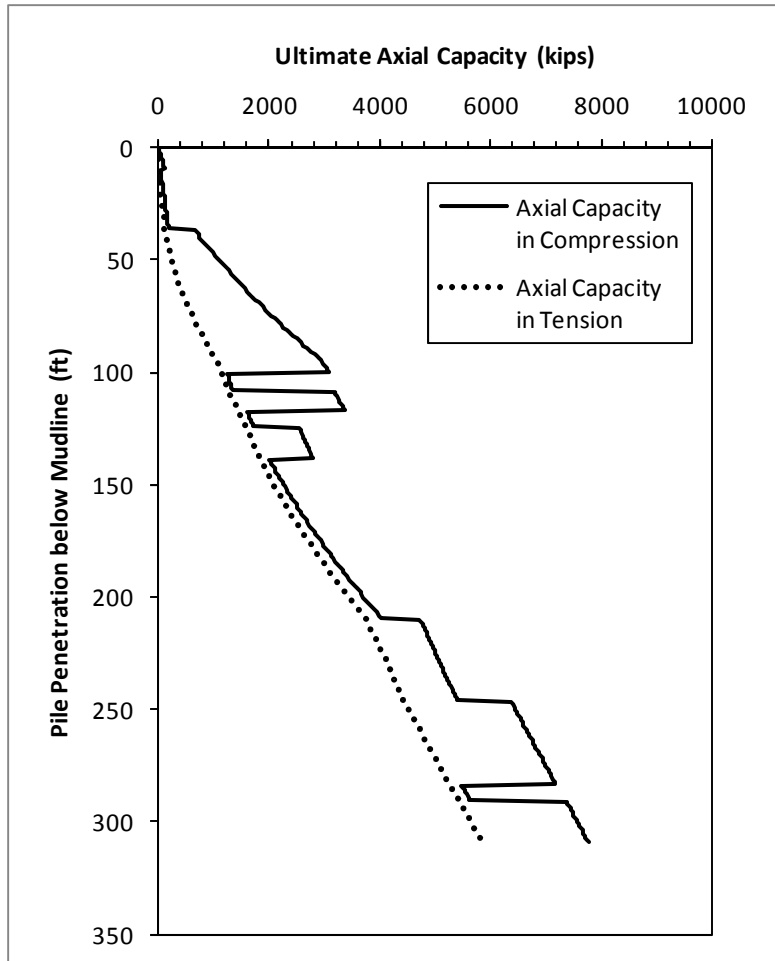


Figure E.43 Ultimate Axial Capacities of the Single Batter Piles of Platform 11

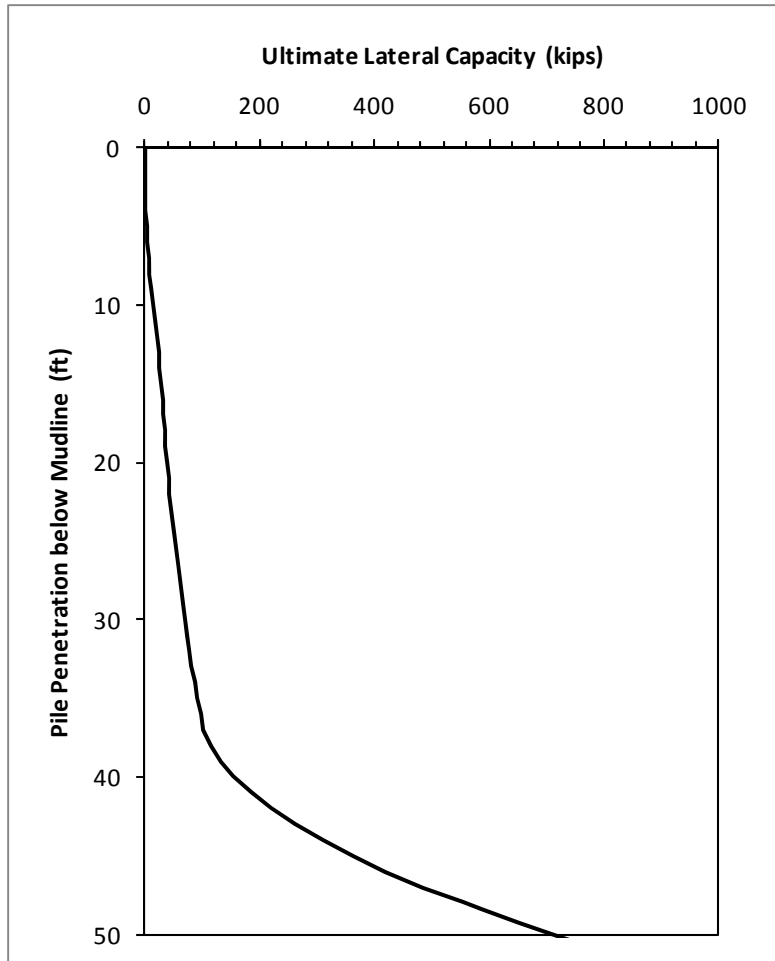


Figure E.44 Ultimate Lateral Resistance of the Single Batter Piles of Platform 11

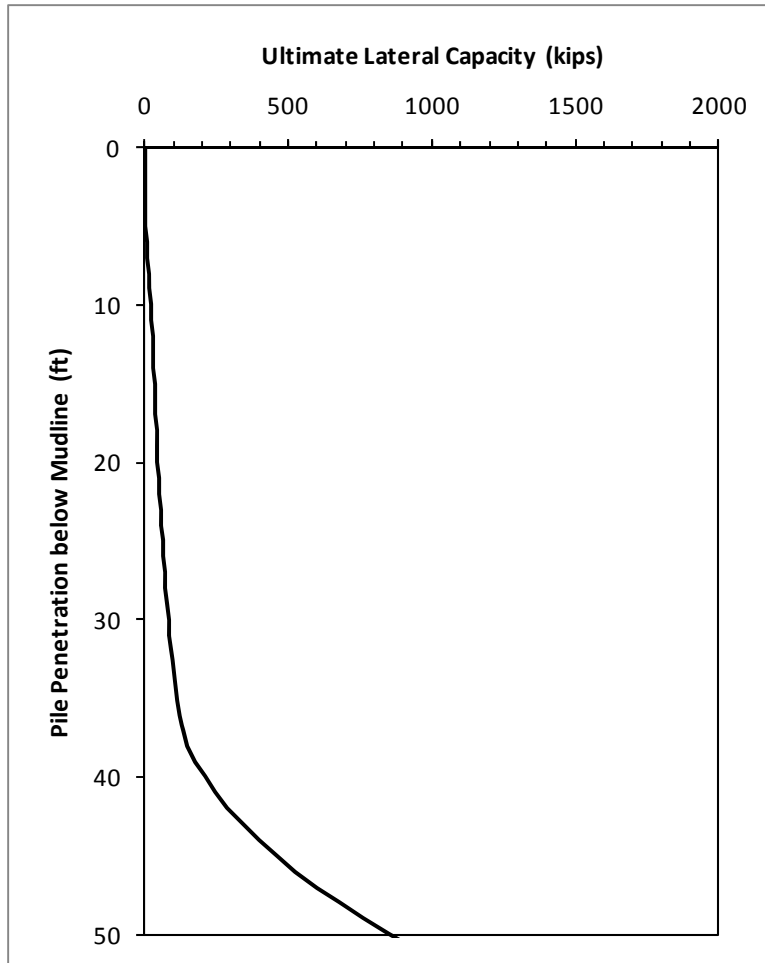


Figure E.45 Ultimate Lateral Resistance of the Conductor of Platform 11

The structural capacity input files of the double batter piles, single batter piles and conductor are summarized in Tables E.34, E.35 and E.36, respectively.

Table E.34 Structural Capacity of the Double Batter Piles of Platform 11

Wall Thickness, t (in.)	Starting Length along Pile, z (in.)	Axial Structural Capacity, Q (lbs)	Moment Capacity, M (in.-lbs)
1.75	0	7.966E+06	1.021E+08
1.5	720	6.871E+06	8.861E+07
1.25	960	5.761E+06	7.475E+07

Table E.35 Structural Capacity of the Single Batter Piles of Platform 11

Wall Thickness, t (in.)	Starting Length along Pile, z (in.)	Axial Structural Capacity, Q (lbs)	Moment Capacity, M (in.-lbs)
2	0	9.048E+06	1.153E+08
1.75	720	7.966E+06	1.021E+08
1.25	1080	5.761E+06	7.475E+07

Table E.36 Structural Capacity of the Conductor of Platform 11

Wall Thickness, t (in.)	Starting Length along Pile, z (in.)	Axial Structural Capacity, Q (lbs)	Moment Capacity, M (in.-lbs)
1.75	0	1.390E+07	3.110E+08
1.5	360	1.196E+07	2.684E+08
1	840	8.030E+06	1.815E+08

Based on the above input parameters, the base case foundation system capacity interaction curves in the end-on direction are presented in Figure E.46. The direction of the waves in Hurricane Katrina is approximately the end-on direction of this platform. The magnitude of the base shear and overturning moment on the foundation in Katrina was roughly estimated to be 3,500 kips and 213,500 ft-kips. Note that this estimate was not obtained from the detailed hindcast analysis using a 3-D model. This hindcast load is compared with the foundation system capacity interaction curves in the end-on direction.

As shown in Figure E.46, the 72-inch diameter conductor contributes significant shear capacity to the foundation. The hurricane load is nearly equivalent to the foundation capacity including the four piles and this large conductor. The foundation of this platform did survive the hurricane. Its survival is explainable if the contribution of all four conductors is included.

A parametric analysis was performed in the end-on direction to increase the yield strength of the steel for the piles and the 72-inch diameter conductor by 15 percent to represent the average value. The result is presented in Figure E.47. As shown, increasing the yield strength of steel further increases the shear capacity of the foundation. Consequently, the survival of the foundation for this platform is not a surprise.

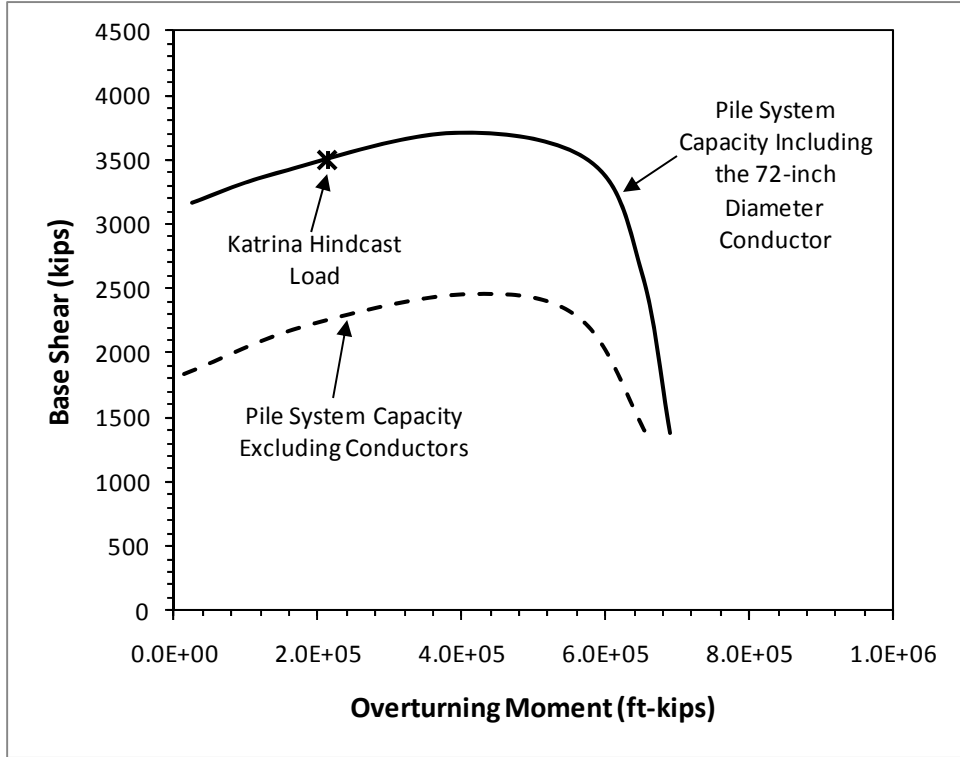


Figure E.46 Base Case Foundation System Capacity Interaction Diagram of Platform 11 in the End-on Direction

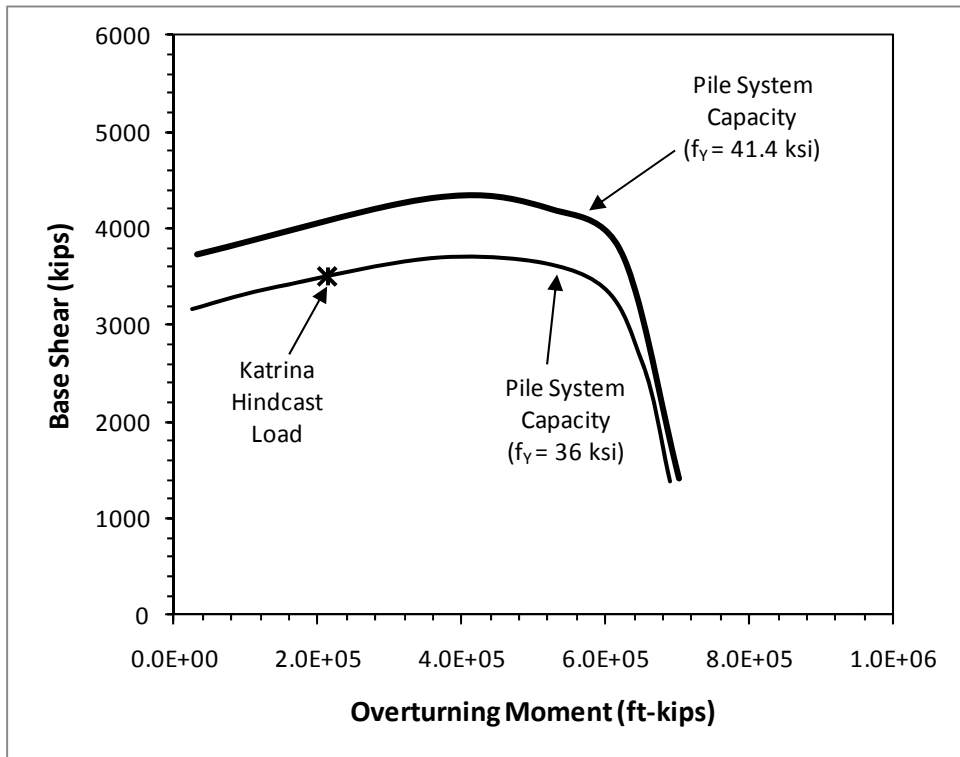


Figure E.47 Parametric Analysis for Platform 11 in the End-on Direction Increasing the Yield Strength of the Steel

E.7 Platform 12

Platform 12 is a 4-leg structure supported by 4 piles and equipped with 12 conductors. One of the conductors is 36 inches in diameter and the others are 26 inches in diameter. All conductors were included explicitly in the foundation model. The foundation system is symmetrical. All four piles are 48 inches in diameter and battered in 2 directions. The direction of the waves in Hurricane Rita is approximately the end-on direction of this platform. The executive input file of this platform in the end-on direction is presented hereafter.

Executive Input File for Platform 12

PLATFORM 12 (ALL UNITS IN LB., IN., AND DEGREES)

SYSTEM LOAD DATA (PH,H,R,SKEW,PV,ECCENT)

2.899E6

3E3

1.00E-11

90.0

3.936E6

1.00E-10

NUMBER OF PILES (NPILE)

6

PILE 1

GEOMETRY (X,Y,THETAX,THETAY,L,AXIAL CONSTRAINT,NGROUP)

-4.995E+02 -4.995E+02 -7.13 -7.13 3.06E+03 1 1

PILE STRUCTURAL CAPACITY (INPUT FILE)

WPILE1.INP

SOIL CAPACITY (INPUT FILE)

WSOIL1.INP

PILE 2

GEOMETRY (X,Y,THETAX,THETAY,L,AXIAL CONSTRAINT,NGROUP)

4.995E+02 -4.995E+02 7.13 -7.13 3.06E+03 1 1

PILE STRUCTURAL CAPACITY (INPUT FILE)

WPILE1.INP

SOIL CAPACITY (INPUT FILE)

WSOIL1.INP

PILE 3

GEOMETRY (X,Y,THETAX,THETAY,L,AXIAL CONSTRAINT,NGROUP)

-4.995E+02 4.995E+02 -7.13 7.13 3.06E+03 1 1

PILE STRUCTURAL CAPACITY (INPUT FILE)

WPILE1.INP

SOIL CAPACITY (INPUT FILE)

WSOIL1.INP

PILE 4

GEOMETRY (X,Y,THETAX,THETAY,L,AXIAL CONSTRAINT,NGROUP)

4.995E+02 4.995E+02 7.13 7.13 3.06E+03 1 1

PILE STRUCTURAL CAPACITY (INPUT FILE)

WPILE1.INP

SOIL CAPACITY (INPUT FILE)

WSOIL1.INP

CONDUCTORS

GEOMETRY (X,Y,THETAX,THETAY,L,AXIAL CONSTRAINT,NGROUP)

0.00E+00 0.68E+02 0.00 0.00 1.80E+03 0 11

PILE STRUCTURAL CAPACITY (INPUT FILE)

WPILEC26.INP

SOIL CAPACITY (INPUT FILE)

WSOILC26.INP

CONDUCTORS

GEOMETRY (X,Y,THETAX,THETAY,L,AXIAL CONSTRAINT,NGROUP)

0.00E+00 0.68E+02 0.00 0.00 1.80E+03 0 1

PILE STRUCTURAL CAPACITY (INPUT FILE)

WPILEC36.INP

SOIL CAPACITY (INPUT FILE)

WSOILC36.INP

The input parameters for the custom-built spreadsheet to calculate the axial and lateral resistance of the piles, 36-inch diameter conductor and 26-inch diameter conductors are presented in Tables E.37, E38 and E.39, respectively. The design soil profile and parameters common for all piles and conductor are presented in Table E.40. The axial capacities of the piles in compression and in tension are presented in Figure E.48. The lateral resistance of the piles is presented in Figure E.49. The lateral resistance of the 36-inch and 26-inch diameter conductors is presented in Figures E.50 and E.51, respectively.

Table E.37 Input Parameters for the Piles of Platform 12

Seafloor Elevation (ft, MSL)	-190
Seasurface Elevation (ft, MSL)	0
Top of Pile Elevation (ft, MSL)	-190
Pile Length (ft)	255
Pile Diameter (ft)	4
Pile Tip Wall Thickness (in.)	1.25
Unit Weight of Water (pcf)	62.4
Depth Increment (ft)	1
Open- or Close-ended	Open
Open-ended Pile Tip Condition	Plugged
Loading Condition	Cyclic
K Compression	0.8
K Tension	0.8
Pile Batter in x-direction (deg.)	7.125
Pile Batter in y-direction (deg.)	7.125
X_R (ft)	32.0

Table E.38 Input Parameters for the 36-inch Diameter Conductor of Platform 12

Seafloor Elevation (ft, MSL)	-190
Seasurface Elevation (ft, MSL)	0
Top of Pile Elevation (ft, MSL)	-190
Pile Length (ft)	150
Pile Diameter (ft)	3
Pile Tip Wall Thickness (in.)	0.5
Unit Weight of Water (pcf)	62.4
Depth Increment (ft)	1
Open- or Close-ended	Open
Open-ended Pile Tip Condition	Plugged
Loading Condition	Cyclic
K Compression	0.8
K Tension	0.8
Pile Batter in x-direction (deg.)	0
Pile Batter in y-direction (deg.)	0
X_R (ft)	25.5

Table E.39 Input Parameters for the 26-inch Diameter Conductors of Platform 12

Seafloor Elevation (ft, MSL)	-190
Seasurface Elevation (ft, MSL)	0
Top of Pile Elevation (ft, MSL)	-190
Pile Length (ft)	150
Pile Diameter (ft)	2.167
Pile Tip Wall Thickness (in.)	0.5
Unit Weight of Water (pcf)	62.4
Depth Increment (ft)	1
Open- or Close-ended	Open
Open-ended Pile Tip Condition	Plugged
Loading Condition	Cyclic
K Compression	0.8
K Tension	0.8
Pile Batter in x-direction (deg.)	0
Pile Batter in y-direction (deg.)	0
X_R (ft)	19.5

Table E.40 Design Soil Profile and Parameters for All Piles and Conductors of Platform 12

Layer	Soil Type	Top Elevation (ft, MSL)	Bottom Elevation (ft, MSL)	Thickness (ft)	Total Unit Weight (pcf)	Submerged Unit Weight (pcf)	c_u at the Top of Layer (psf)	dc_u/dz (psf/ft)	Friction Angle, ϕ' (deg.)	Soil Pile Friction Angle, δ (deg.)	Limiting Skin Friction Value (ksf)	N_q	Limiting End Bearing Value (ksf)	C_1	C_2	C_3
1	Cohesive	-190	-226	36	108.4	46	400	10.53								
2	Cohesionless	-226	-260	34	112.4	50			25	20	1.4	12	60	1.2	2.0	15
3	Cohesive	-260	-288	28	116.4	54	1200	8.33								
4	Cohesive	-288	-316	28	116.4	54	1433	8.33								
5	Cohesive	-316	-344	28	116.4	54	1667	8.33								
6	Cohesive	-344	-372	28	116.4	54	1900	8.33								
7	Cohesive	-372	-400	28	116.4	54	2133	8.33								

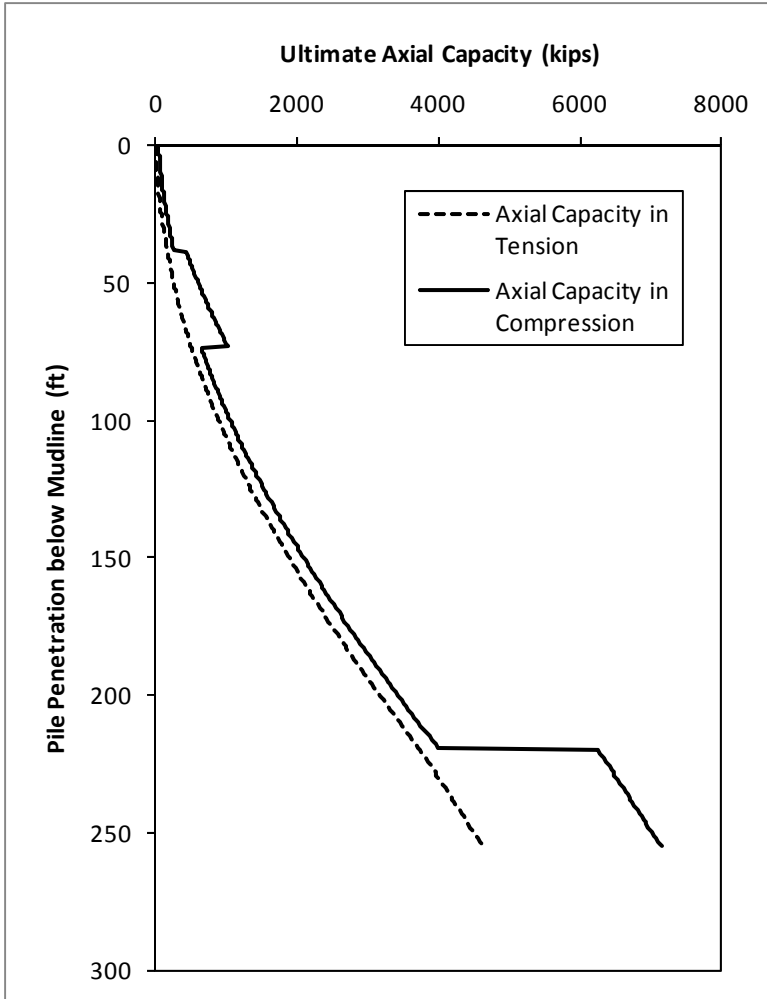


Figure E.48 Ultimate Axial Capacities of the Piles of Platform 12

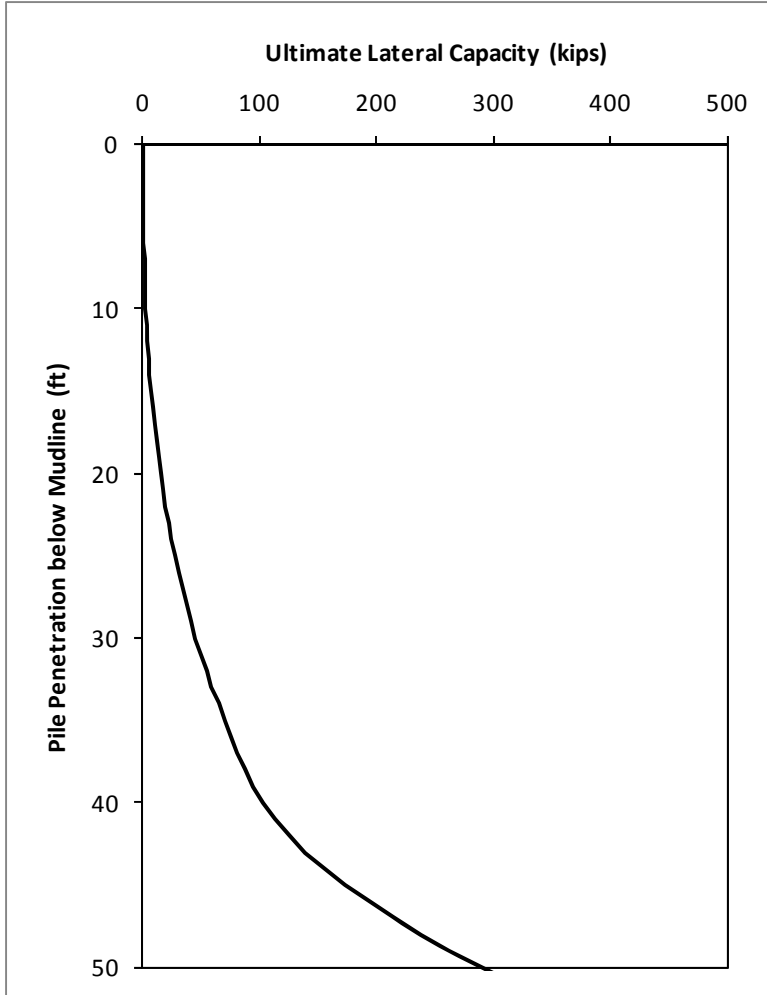


Figure E.49 Ultimate Lateral Resistance of the Piles of Platform 12

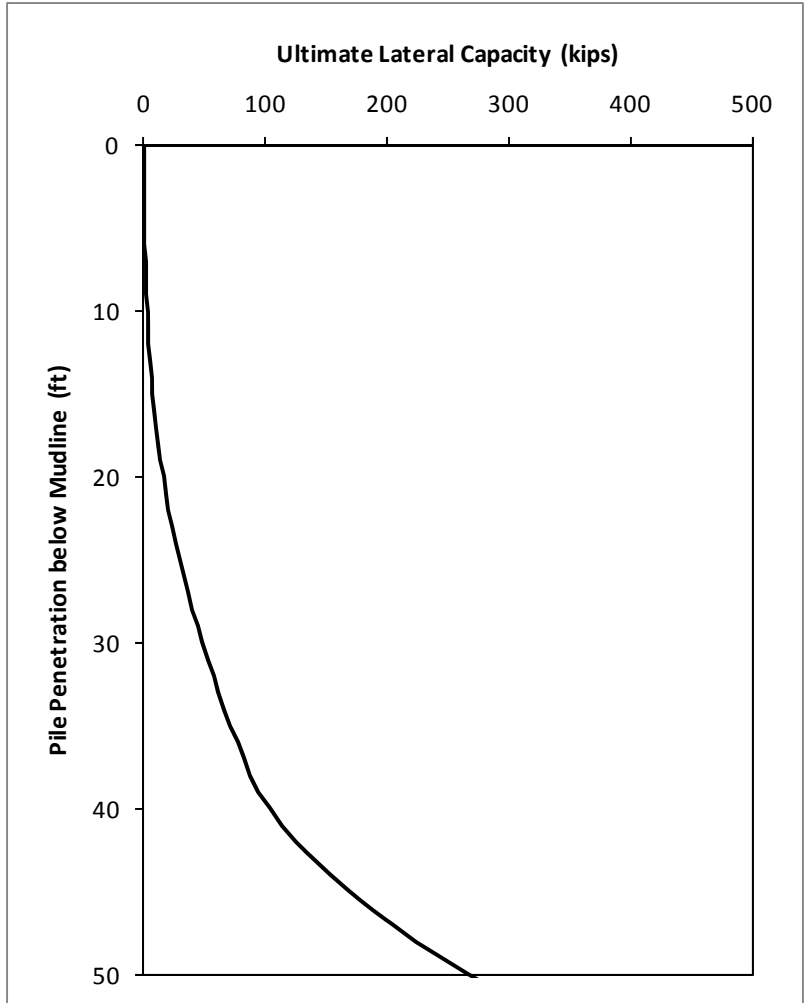


Figure E.50 Ultimate Lateral Resistance of the 36-inch Diameter Conductor of Platform 12

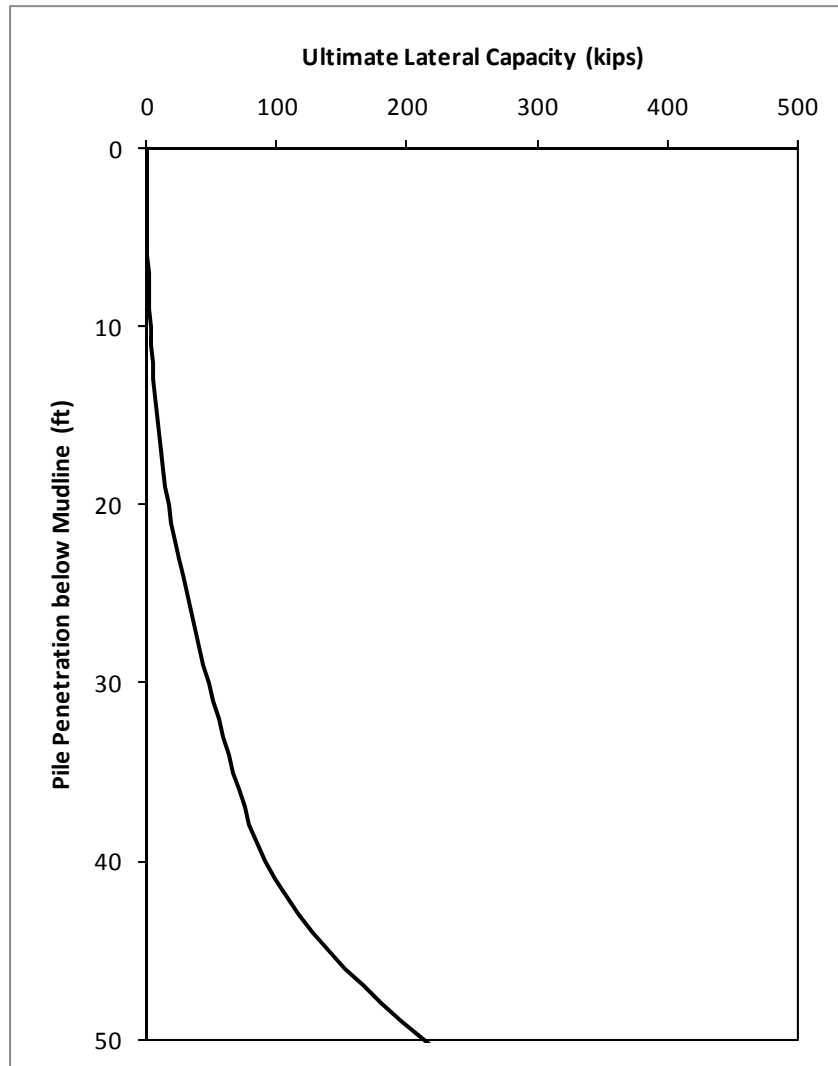


Figure E.51 Ultimate Lateral Resistance of the 26-inch Diameter Conductors of Platform 12

The structural capacity input files of the piles, 36-inch diameter conductor and 26-inch diameter conductors are summarized in Tables E.41, E.42 and E.43, respectively.

Based on the above input parameters, the base case foundation system capacity interaction curves in the end-on and diagonal directions are presented in Figures E.52 and E.53, respectively. Due to the symmetry of the piles, the foundation capacity in the broadside direction is the same as that in the end-on direction. The direction of the waves is approximately the end-on direction of this platform. Therefore, the hurricane hindcast load on the foundation is also presented in the interaction diagram for the end-on direction.

Table E.41 Structural Capacity of the Piles of Platform 12

Wall Thickness, t (in.)	Starting Length along Pile, z (in.)	Axial Structural Capacity, Q (lbs)	Moment Capacity, M (in.-lbs)
1.5	0	7.889E+06	1.168E+08
1.375	840	7.251E+06	1.076E+08
1.25	960	6.609E+06	9.837E+07

Table E.42 Structural Capacity of the 36-inch Diameter Conductor of Platform 12

Wall Thickness, t (in.)	Starting Length along Pile, z (in.)	Axial Structural Capacity, Q (lbs)	Moment Capacity, M (in.-lbs)
0.5	0	2.007E+06	2.269E+07
0.5	480	2.007E+06	2.269E+07
0.5	600	2.007E+06	2.269E+07

Table E.43 Structural Capacity of the 26-inch Diameter Conductors of Platform 12

Wall Thickness, t (in.)	Starting Length along Pile, z (in.)	Axial Structural Capacity, Q (lbs)	Moment Capacity, M (in.-lbs)
0.5	0	1.442E+06	1.171E+07
0.5	480	1.442E+06	1.171E+07
0.5	600	1.442E+06	1.171E+07

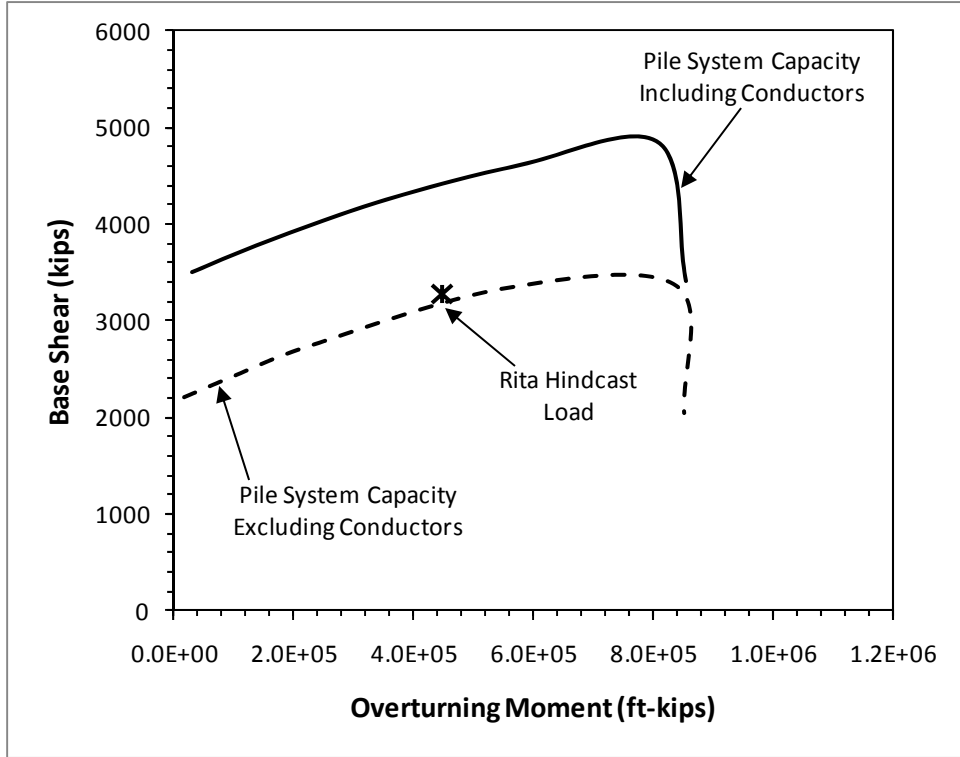


Figure E.52 Base Case Foundation System Capacity Interaction Diagram of Platform 12 in the End-on Direction

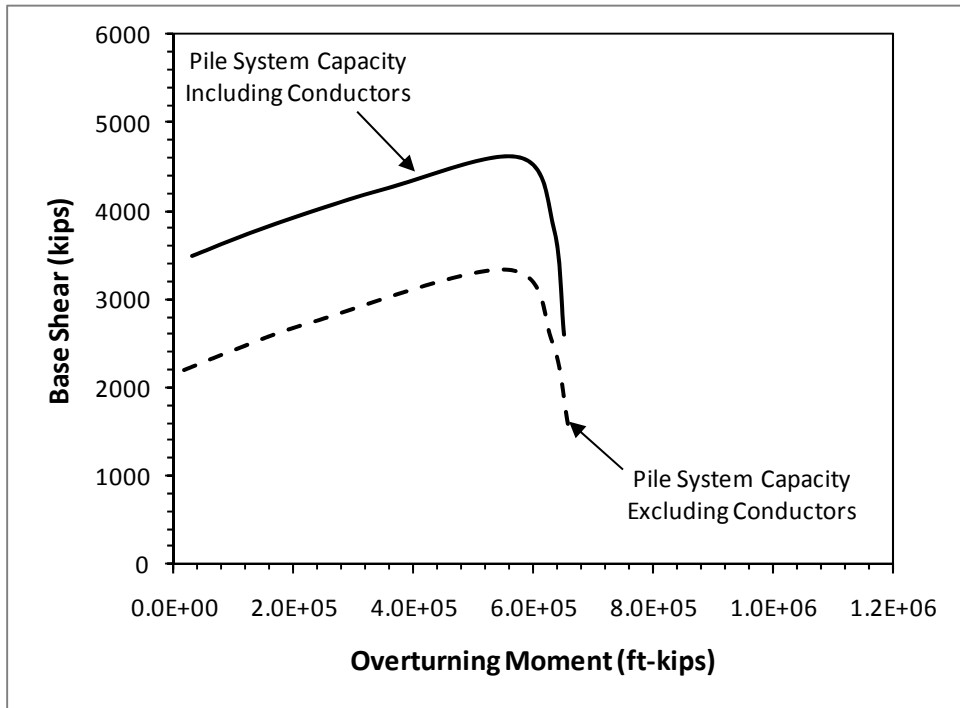


Figure E.53 Base Case Foundation System Capacity Interaction Diagram of Platform 12 in the Diagonal Direction

As shown in Figures E.52 and E.53, the presence of the 12 conductors contributes significantly to the shear capacity of the foundation. Also, the overturning capacities of the foundation in the end-on and diagonal directions are notably different. This is due to the non-redundant nature of this 4-pile structure. Parametric analyses were performed in the end-on direction to investigate the effects of the lateral resistance of the soil and the yield strength of the steel for the conductors on the foundation system capacity. In the first analysis, the ultimate lateral resistance, which is roughly proportional to the shear strength of the soil over the upper 50 feet of the conductors, was increased by 50 percent with a multiplier, NQ_{lat} , of 1.5. Unlike the parametric analysis for Platform 1, the multiplier was only applied for the conductors in this analysis. In the second analysis, the yield strength of the steel conductors was increased by 15 percent beyond its nominal value ($f_Y = 41.4$ ksi). The results of these two parametric analyses are presented in Figure E.54 where the base case foundation system capacity interaction curve is also presented. As shown, the foundation capacities as a result of increasing the ultimate lateral resistance of the conductors and increasing the yield strength of the conductors are nearly identical in this case.

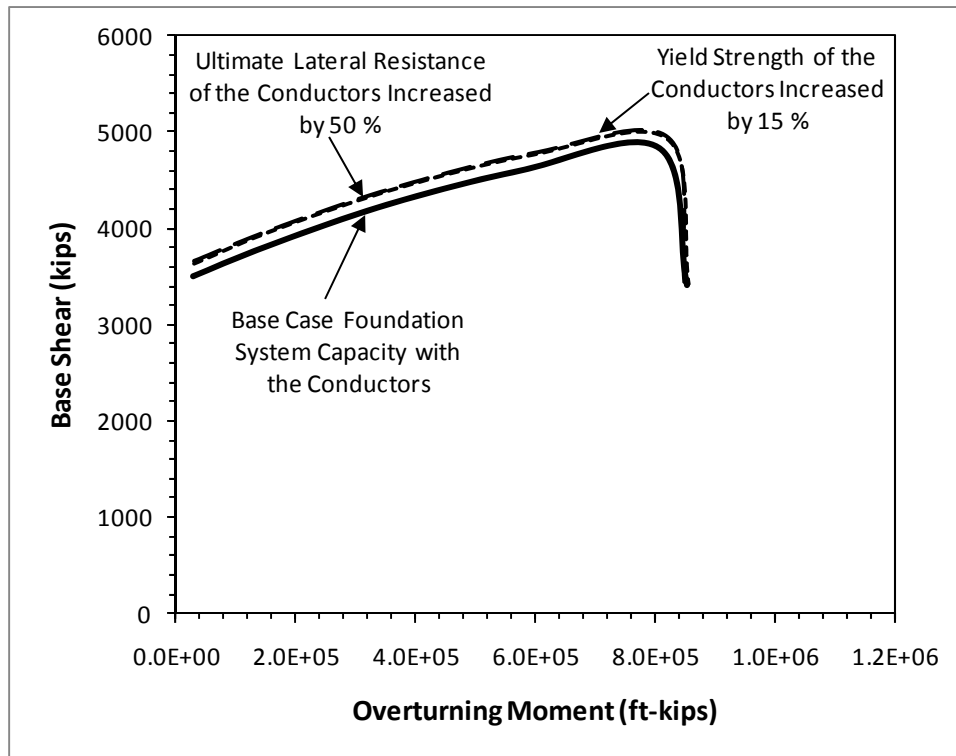


Figure E.54 Parametric Analyses for Platform 12 in the End-on Direction Increasing the Ultimate Lateral Resistance and Yield Strength of the Conductors

E.8 Platform 22

Platform 22 is a 4-leg structure supported by 4 piles. This platform is not equipped with any well conductor. The foundation system is symmetrical. All four piles are 42 inches in diameter and battered in 2 directions. The nominal yield strength of the piles is 50 ksi from the mudline to an approximate depth of 111 feet below the mudline and then it changes to 36 ksi below that depth. The direction of the waves in Hurricane Rita is approximately the end-on direction of this platform. The executive input file of this platform in the end-on direction is presented hereafter.

Executive Input File for Platform 22

PLATFORM 22 (ALL UNITS IN LB., IN., AND DEGREES)

SYSTEM LOAD DATA (PH,H,R,SKEW,PV,ECCENT)

3.5E6

1.0E2

1.00E-10

90.0

2.973E6

1.00E-10

NUMBER OF PILES (NPILE)

4

PILE 1

GEOMETRY (X,Y,THETAX,THETAY,L,AXIAL CONSTRAINT,NGROUP)

-4.125E+02 -4.125E+02 -7.13 -7.13 3.480E+03 1 1

PILE STRUCTURAL CAPACITY (INPUT FILE)

WPILE.INP

SOIL CAPACITY (INPUT FILE)

WSOIL2.INP

PILE 2

GEOMETRY (X,Y,THETAX,THETAY,L,AXIAL CONSTRAINT,NGROUP)

4.125E+02 -4.125E+02 7.13 -7.13 3.480E+03 1 1

PILE STRUCTURAL CAPACITY (INPUT FILE)

WPILE.INP

SOIL CAPACITY (INPUT FILE)

WSOIL2.INP

PILE 3

GEOMETRY (X,Y,THETAX,THETAY,L,AXIAL CONSTRAINT,NGROUP)

-4.125E+02 4.125E+02 -7.13 7.13 3.480E+03 1 1

PILE STRUCTURAL CAPACITY (INPUT FILE)

WPILE.INP

SOIL CAPACITY (INPUT FILE)

WSOIL2.INP

PILE 4

GEOMETRY (X,Y,THETAX,THETAY,L,AXIAL CONSTRAINT,NGROUP)

4.125E+02 4.125E+02 7.13 7.13 3.480E+03 1 1

PILE STRUCTURAL CAPACITY (INPUT FILE)

WPILE.INP

SOIL CAPACITY (INPUT FILE)

WSOIL2.INP

The input parameters for the custom-built spreadsheet to calculate the axial and lateral resistance of the piles are presented in Tables E.44. The design soil profile and parameters are presented in Table E.45. The axial capacities of the piles in compression and in tension are presented in Figure E.55. The lateral resistance of the piles is presented in Figure E.56. The structural capacity input file of the piles is summarized in Table E.46.

Based on the above input parameters, the base case foundation system capacity interaction curves in the end-on direction are presented in Figure E.57. Due to the symmetry of the piles, the foundation capacity in the broadside direction is the same as that in the end-on direction. The direction of the waves is approximately the end-on direction of this platform. Therefore, the hurricane hindcast load on the foundation is also presented in Figure E.57. Parametric analyses for this platform were not performed.

Table E.44 Input Parameters for the Piles of Platform 22

Seafloor Elevation (ft, MSL)	-100
Seasurface Elevation (ft, MSL)	0
Top of Pile Elevation (ft,MSL)	-100
Pile Length (ft)	290
Pile Diameter (ft)	3.5
Pile Tip Wall Thickness (in.)	1.25
Unit Weight of Water (pcf)	62.4
Depth Increment (ft)	1
Open- or Close-ended	Open
Open-ended Pile Tip Condition	Plugged
Loading Condition	Cyclic
K Compression	0.8
K Tension	0.8
Pile Batter in x-direction (deg.)	0
Pile Batter in y-direction (deg.)	0
X_R (ft)	24.5

Table E.45 Design Soil Profile and Parameters for the Piles of Platform 22

Layer	Soil Type	Top Elevation (ft, MSL)	Bottom Elevation (ft, MSL)	Thickness (ft)	Total Unit Weight (pcf)	Submerged Unit Weight (pcf)	c_u at the Top of Layer (psf)	dc_u/dz (psf/ft)	Friction Angle, ϕ' (deg.)	Soil Pile Friction Angle, δ (deg.)	f_{max} (ksf)	N_q	q_{max} (ksf)	C_1	C_2	C_3
1	Cohesive	-100	-140	40	97.4	36	100	9.43								
2	Cohesive	-140	-165	25	102.4	39	477.5	9.43								
3	Cohesive	-165	-206	41	102.4	37.5	713	9.43								
4	Cohesionless	-206	-227	21	122.4	60			30	25	1.7	20	100	1.9	2.7	28
5	Cohesive	-227	-241	13.5	120.4	40	1000	0								
6	Cohesionless	-240.5	-268	27.5	120.4	60			30	25	1.7	20	100	1.9	2.7	28
7	Cohesive	-268	-280	12	112.4	56	750	68.75								
8	Cohesive	-280	-318	37.5	112.4	56	1575	0								
9	Cohesive	-317.5	-345	27.5	112.4	56	1500	-3.6								
10	Cohesionless	-345	-371	26	112.4	60			30	25	1.7	20	100	1.9	2.7	28
11	Cohesive	-371	-400	29	112.4	60	600	82.75								
12	Cohesive	-400	-405	5	112.4	60	3000	12.5								

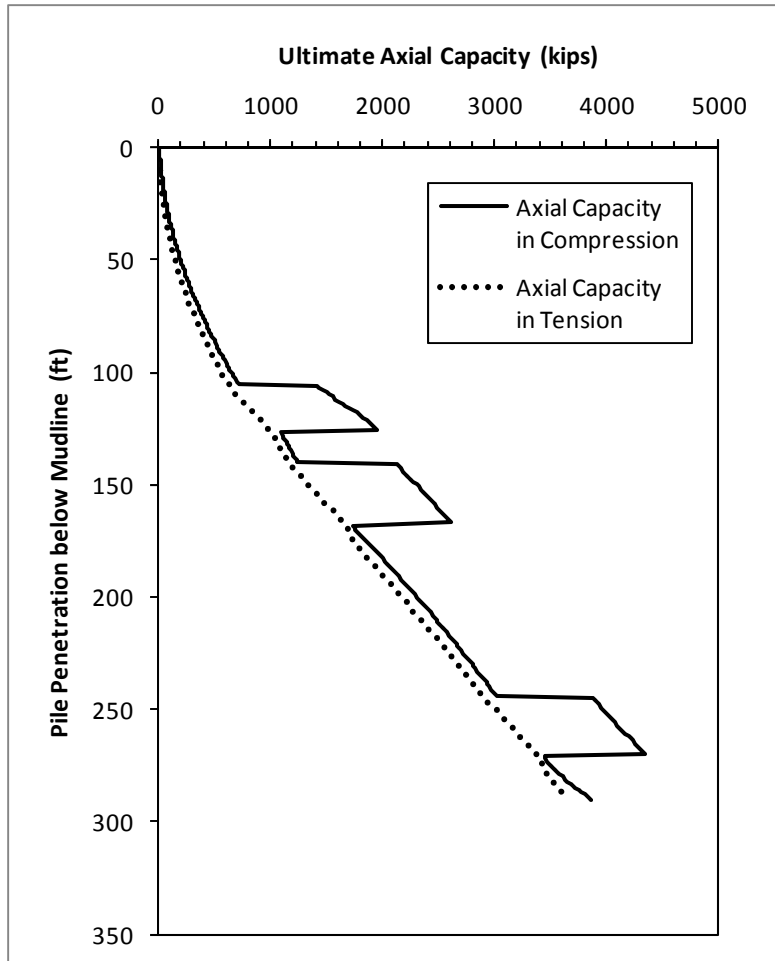


Figure E.55 Ultimate Axial Capacities of the Piles of Platform 22

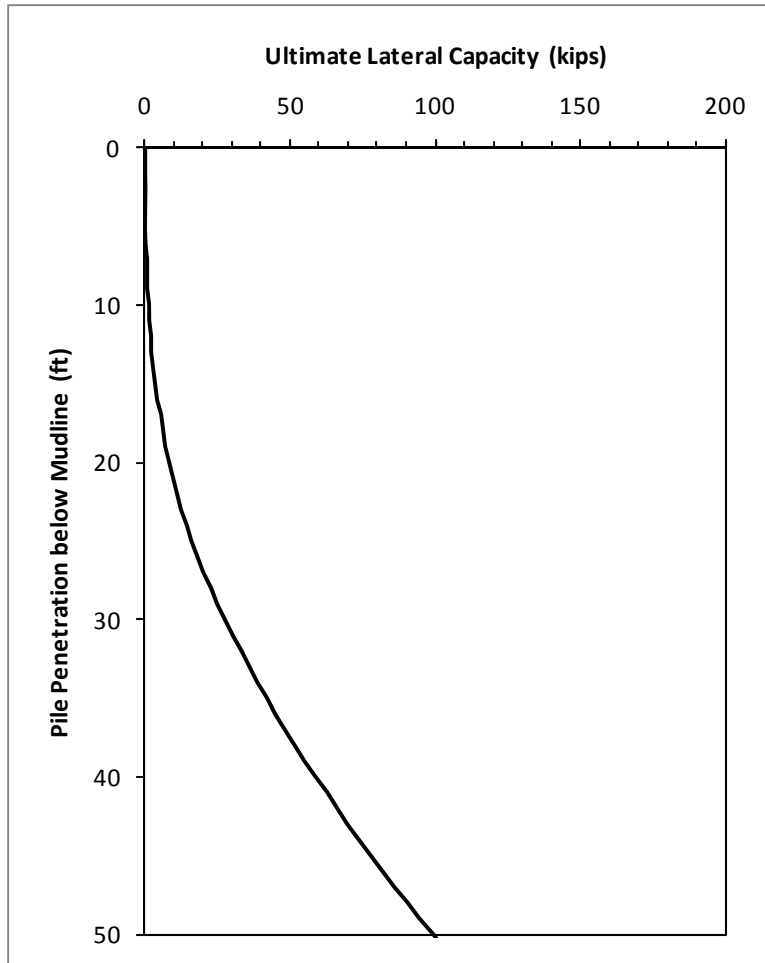


Figure E.56 Ultimate Lateral Resistance of the Piles of Platform 22

Table E.46 Structural Capacity of the Piles of Platform 22

Wall Thickness, t (in.)	Starting Length along Pile, z (in.)	Axial Structural Capacity, Q (lbs)	Moment Capacity, M (in.-lbs)
1.75	0	1.106E+07	1.418E+08
1.875	564	1.182E+07	1.510E+08
1.75	1212	1.106E+07	1.418E+08

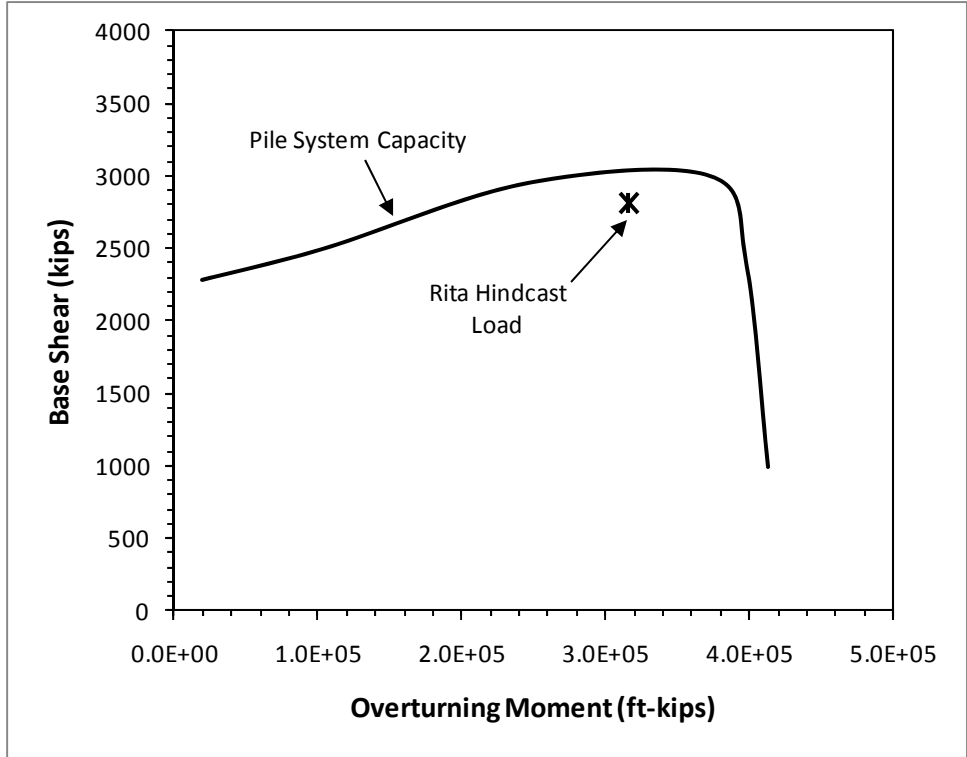


Figure E.57 Base Case Foundation System Capacity Interaction Diagram of Platform 22 in the End-on Direction

E.9 Platform 25

Platform 25 is a 4-leg structure supported by 4 piles and equipped with 4 conductors. The conductors are 30 inches in diameter and located outside the jacket. The foundation system is highly asymmetrical. Two of the piles are battered in 2 directions (double batter piles) and they are 169 feet long. The other two piles are vertical piles that are also 169 feet long. All of the piles are 36 inches in diameter. The direction of the waves in Hurricane Katrina is approximately the end-on direction of this platform (loading from the side of the double batter piles to the side of the vertical piles). The executive input file of this platform in the end-on direction is presented hereafter.

Executive Input File for Platform 25

PLATFORM 25 (ALL UNITS IN LB., IN., AND DEGREES)

SYSTEM LOAD DATA (PH,H,R,SKEW,PV,ECCENT)

3.671E6

3E2
1.00E-11
90.0
1.142E6
1.00E-10

NUMBER OF PILES (NPILE)

5

PILE 1

GEOMETRY (X,Y,THETAX,THETAY,L,AXIAL CONSTRAINT,NGROUP)

-3.56E+02 -3.73E+02 -3.576 -8.746 2.028E+03 1 1

PILE STRUCTURAL CAPACITY (INPUT FILE)

WPILE1.INP

SOIL CAPACITY (INPUT FILE)

WSOIL1.INP

PILE 2

GEOMETRY (X,Y,THETAX,THETAY,L,AXIAL CONSTRAINT,NGROUP)

3.56E+02 -3.73E+02 3.576 -8.746 2.028E+03 1 1

PILE STRUCTURAL CAPACITY (INPUT FILE)

WPILE1.INP

SOIL CAPACITY (INPUT FILE)

WSOIL1.INP

PILE 3

GEOMETRY (X,Y,THETAX,THETAY,L,AXIAL CONSTRAINT,NGROUP)

-0.54E+02 3.73E+02 0.00 0.00 2.028E+03 1 1

PILE STRUCTURAL CAPACITY (INPUT FILE)

WPILE2.INP

SOIL CAPACITY (INPUT FILE)

WSOIL2.INP

PILE 4

GEOMETRY (X,Y,THETAX,THETAY,L,AXIAL CONSTRAINT,NGROUP)

0.54E+02 3.73E+02 0.00 0.00 2.028E+03 1 1

PILE STRUCTURAL CAPACITY (INPUT FILE)

WPILE2.INP

SOIL CAPACITY (INPUT FILE)

WSOIL2.INP

CONDUCTORS

GEOMETRY (X,Y,THETAX,THETAY,L,AXIAL CONSTRAINT,NGROUP)

0.00E+00 4.72E+02 0.00 0.00 2.004E+03 0 4

PILE STRUCTURAL CAPACITY (INPUT FILE)

WPILEC30.INP

SOIL CAPACITY (INPUT FILE)

WSOILC30.INP

The input parameters for the custom-built spreadsheet to calculate the axial and lateral resistance of the vertical piles, double batter piles and conductors are presented in Tables E.47, E.48 and E.49, respectively. The design soil profile and parameters common for all piles and conductor are presented in Table E.50. The axial capacities of the double batter piles in compression and in tension are presented in Figure E.58. The lateral resistance of these piles is presented in Figure E.59. The same figures for the vertical piles are not presented since they are similar to those for the double batter piles. The lateral resistance of the conductors is presented in Figures E.60.

The structural capacity input files of the double batter piles, vertical piles and conductors are summarized in Tables E.51, E.52 and E.53, respectively.

Based on the above input parameters, the base case foundation system capacity interaction curves in the end-on, broadside and diagonal directions are presented in Figures E.61, E.62 and E.63, respectively. The direction of the waves is approximately the end-on direction of this platform. Therefore, the hurricane hindcast load on the foundation is also presented in the interaction diagram for the end-on direction.

As shown in Figures E.61, E.62 and E.63, the overturning capacity of the foundation is notably different in different loading directions (highest in the end-on and lowest in the broadside direction). This is due to the asymmetrical and non-redundant nature of the foundation. Note that even if this platform is a 4-leg structure, the two vertical legs are located close to each other. Therefore, it behaves like a 3-leg structure effectively.

Table E.47 Input Parameters for the Vertical Piles of Platform 25

Seafloor Elevation (ft, MSL)	-90
Seasurface Elevation (ft, MSL)	0
Top of Pile Elevation (ft, MSL)	-90
Pile Length (ft)	169
Pile Diameter (ft)	3
Pile Tip Wall Thickness (in.)	0.75
Unit Weight of Water (pcf)	62.4
Depth Increment (ft)	1
Open- or Close-ended	Open
Open-ended Pile Tip Condition	Plugged
Loading Condition	Cyclic
K Compression	0.8
K Tension	0.8
Pile Batter in x-direction (deg.)	0
Pile Batter in y-direction (deg.)	0
X_R (ft)	28.5

Table E.48 Input Parameters for the Double Batter Piles of Platform 25

Seafloor Elevation (ft, MSL)	-90
Seasurface Elevation (ft, MSL)	0
Top of Pile Elevation (ft, MSL)	-90
Pile Length (ft)	169
Pile Diameter (ft)	3
Pile Tip Wall Thickness (in.)	0.75
Unit Weight of Water (pcf)	62.4
Depth Increment (ft)	1
Open- or Close-ended	Open
Open-ended Pile Tip Condition	Plugged
Loading Condition	Cyclic
K Compression	0.8
K Tension	0.8
Pile Batter in x-direction (deg.)	3.576
Pile Batter in y-direction (deg.)	8.746
X_R (ft)	28.1

Table E.49 Input Parameters for the Conductors of Platform 25

Seafloor Elevation (ft, MSL)	-90
Seasurface Elevation (ft, MSL)	0
Top of Pile Elevation (ft, MSL)	-90
Pile Length (ft)	167
Pile Diameter (ft)	2.5
Pile Tip Wall Thickness (in.)	0.75
Unit Weight of Water (pcf)	62.4
Depth Increment (ft)	1
Open- or Close-ended	Open
Open-ended Pile Tip Condition	Plugged
Loading Condition	Cyclic
K Compression	0.8
K Tension	0.8
Pile Batter in x-direction (deg.)	0
Pile Batter in y-direction (deg.)	0
X_R (ft)	23.5

Table E.50 Design Soil Profile and Parameters for All Piles and Conductors of Platform 25

Layer	Soil Type	Top Elevation (ft, MSL)	Bottom Elevation (ft, MSL)	Thickness (ft)	Total Unit Weight (pcf)	Submerged Unit Weight (pcf)	c_u at the Top of Layer (psf)	dc_u/dz (psf/ft)	Friction Angle, ϕ' (deg.)	Soil Pile Friction Angle, δ (deg.)	Limiting Skin Friction Value (ksf)	N_q	Limiting End Bearing Value (ksf)	C_1	C_2	C_3
1	Cohesive	-90	-96	6	110.4	48	350	36								
2	Cohesionless	-96	-108	12	120.4	58			30	25	1.7	20	100	1.9	2.7	29
3	Cohesive	-108	-181	73	110.4	48	850	14.7								
4	Cohesive	-181	-254	73	115.4	53	1925	14.7								
5	Cohesionless	-254	-284	30	122.4	60			35	30	2.0	40	200	3.0	3.5	50
6	Cohesionless	-284	-314	30	122.4	60			35	30	2.0	40	200	3.0	3.5	50
7	Cohesionless	-314	-350	36	122.4	60			35	30	2.0	40	200	3.0	3.5	50

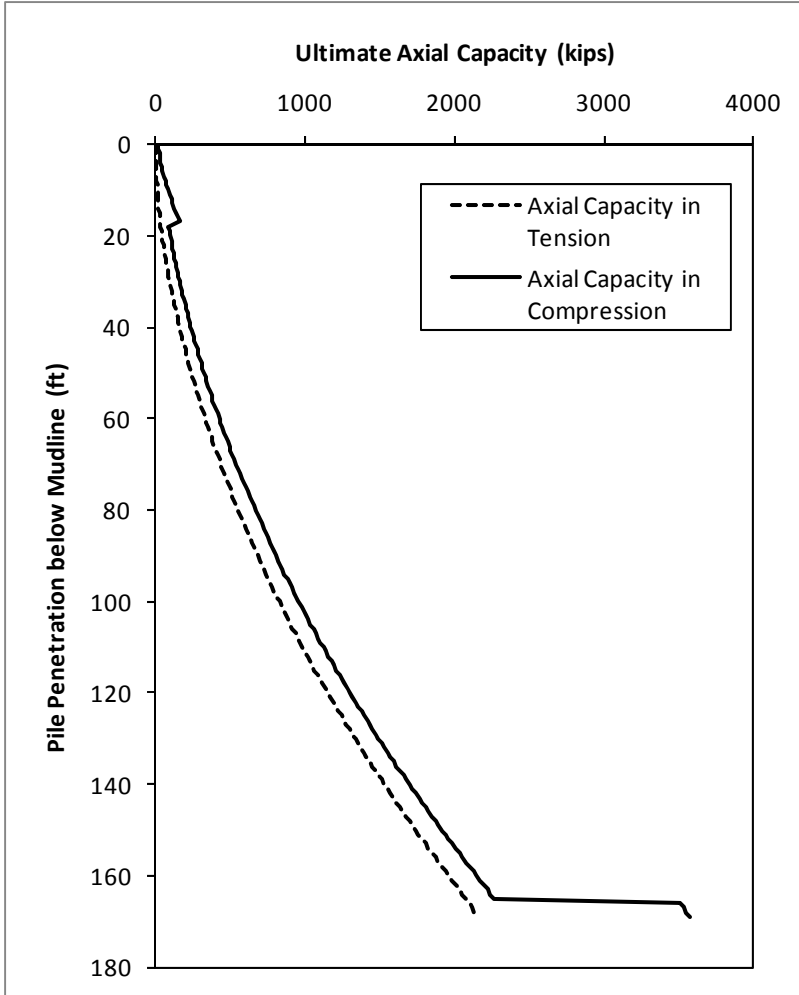


Figure E.58 Ultimate Axial Capacities of the Double Batter Piles of Platform 25

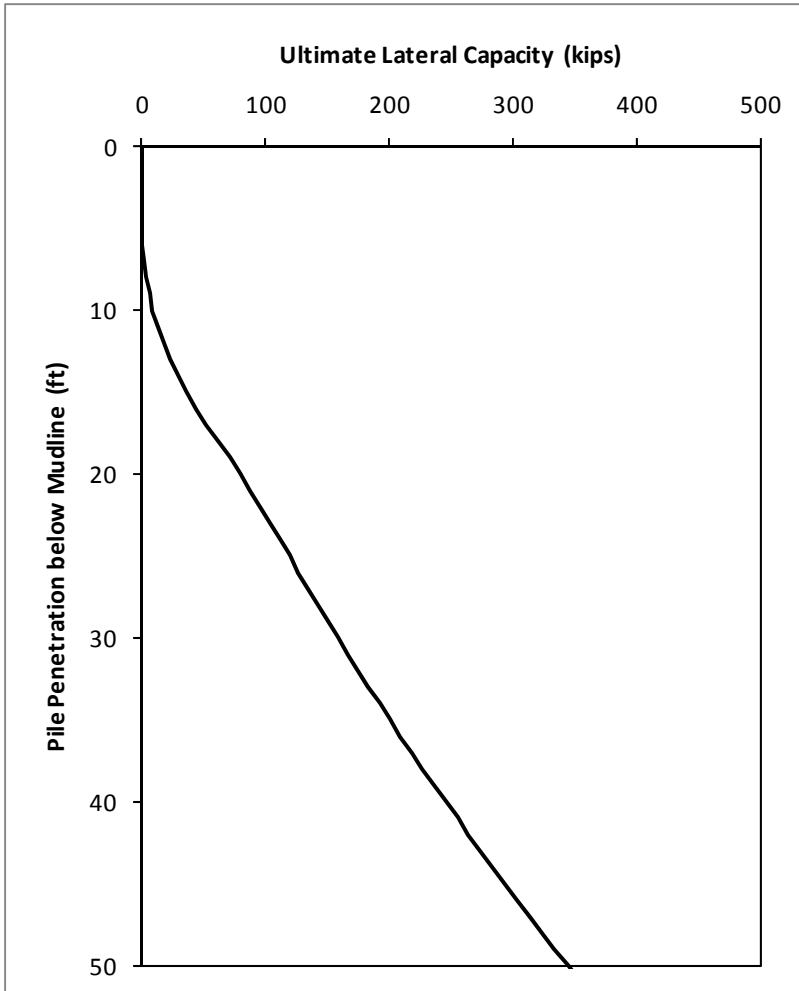


Figure E.59 Ultimate Lateral Resistance of the Double Batter Piles of Platform 25

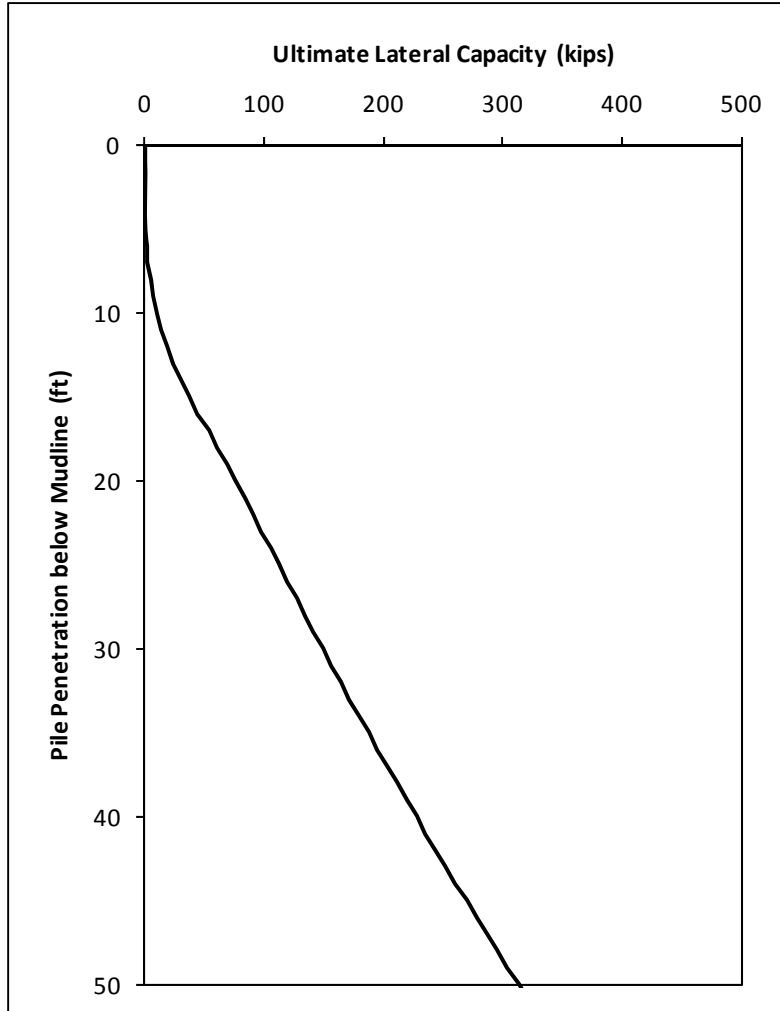


Figure E.60 Ultimate Lateral Resistance of the Conductors of Platform 25

Table E.51 Structural Capacity of the Double Batter Piles of Platform 25

Wall Thickness, t (in.)	Starting Length along Pile, z (in.)	Axial Structural Capacity, Q (lbs)	Moment Capacity, M (in.-lbs)
1.625	0	6.318E+06	6.918E+07
1.25	312	4.913E+06	5.436E+07
0.875	552	3.476E+06	3.887E+07

Table E.52 Structural Capacity of the Vertical Piles of Platform 25

Wall Thickness, t (in.)	Starting Length along Pile, z (in.)	Axial Structural Capacity, Q (lbs)	Moment Capacity, M (in.-lbs)
1.625	0	6.318E+06	6.918E+07
1.25	312	4.913E+06	5.436E+07
0.875	552	3.476E+06	3.887E+07

Table E.53 Structural Capacity of the Conductors of Platform 25

Wall Thickness, t (in.)	Starting Length along Pile, z (in.)	Axial Structural Capacity, Q (lbs)	Moment Capacity, M (in.-lbs)
1.625	0	5.215E+06	4.715E+07
1.25	312	4.064E+06	3.722E+07
0.875	552	2.882E+06	2.673E+07

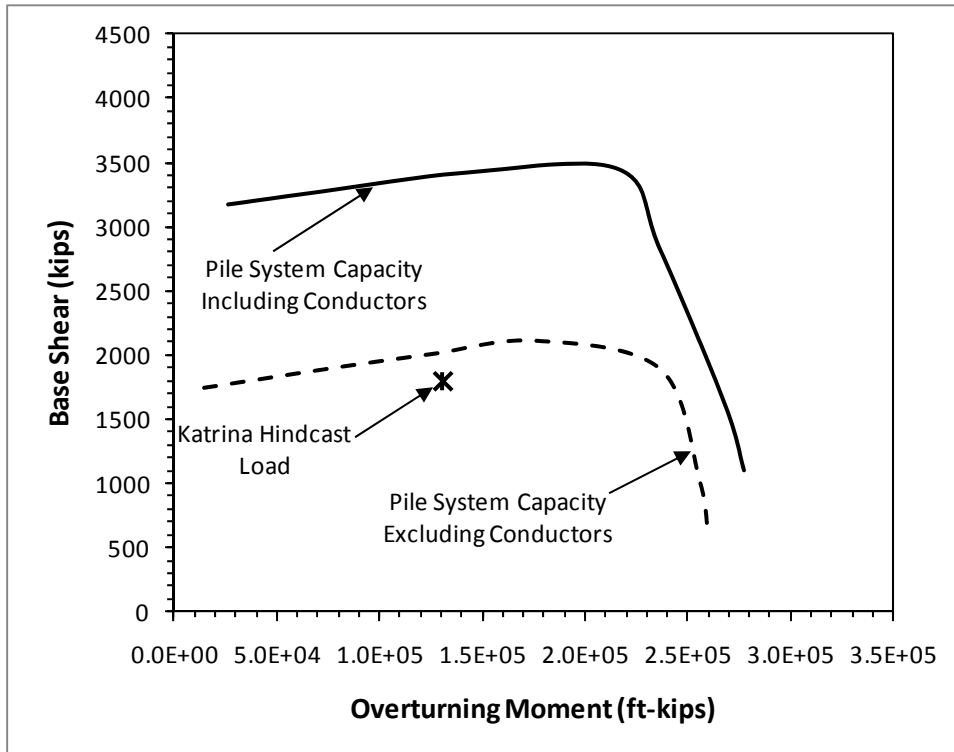


Figure E.61 Base Case Foundation System Capacity Interaction Diagram of Platform 25 in the End-on Direction

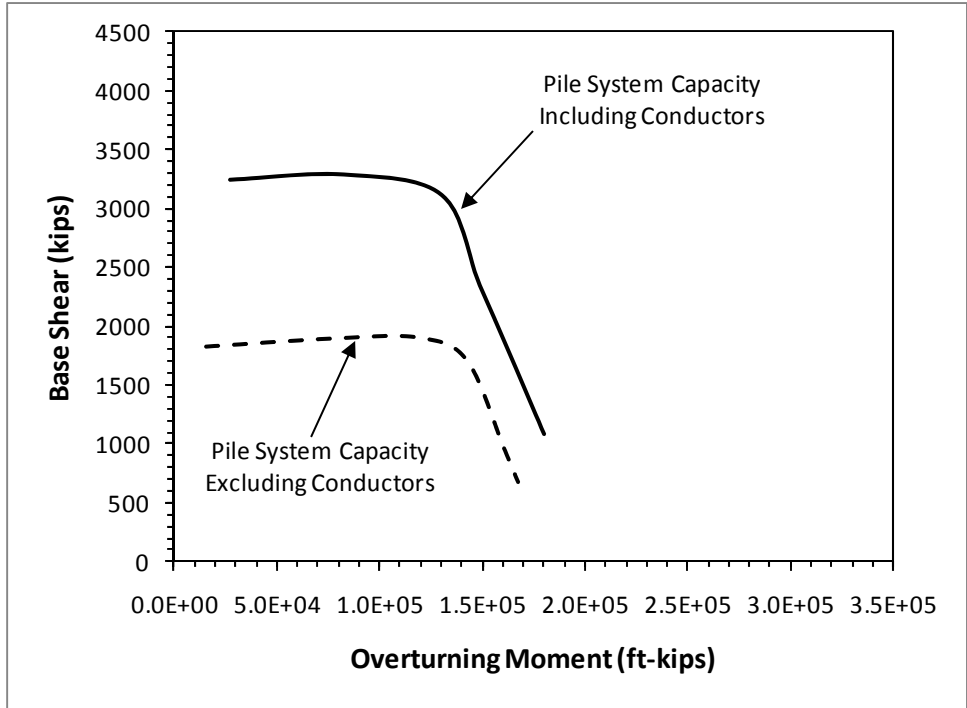


Figure E.62 Base Case Foundation System Capacity Interaction Diagram of Platform 25 in the Broadside Direction

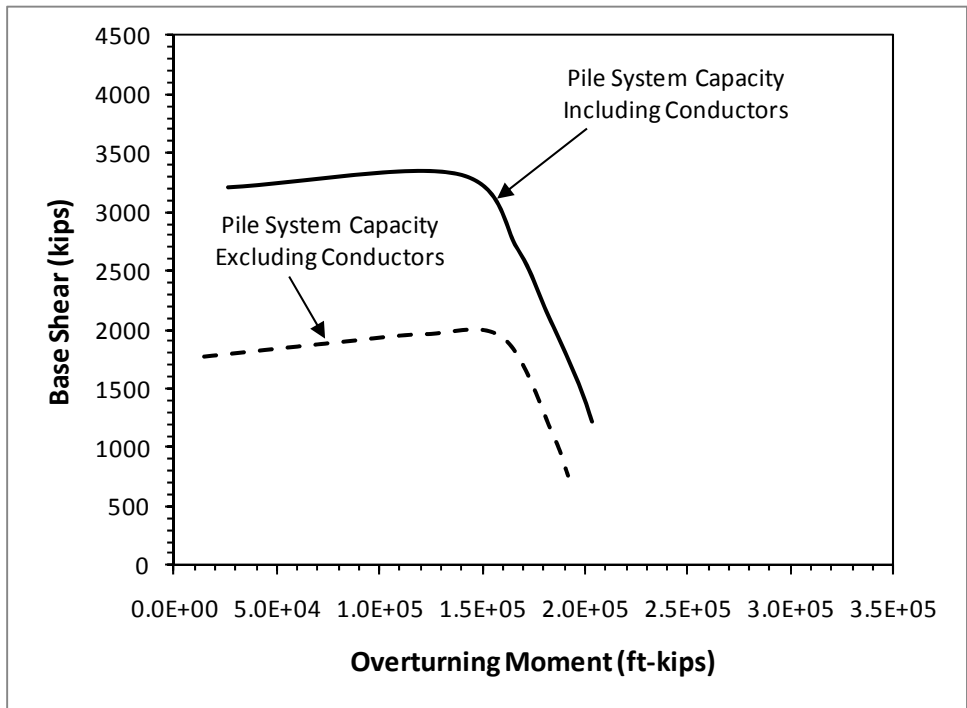


Figure E.63 Base Case Foundation System Capacity Interaction Diagram of Platform 25 in the Diagonal Direction

Parametric analyses were performed in the end-on direction to investigate the effects of the lateral resistance of the soil and the yield strength of the steel for the conductors on the foundation system capacity. In the first analysis, the ultimate lateral resistance, which is roughly proportional to the shear strength of the soil over the upper 50 feet of the conductors, was increased by 50 percent with a multiplier, N_{Qlat} , of 1.5. Unlike the parametric analysis for Platform 1, the multiplier was only applied for the conductors in this analysis. In the second analysis, the yield strength of the steel conductors was increased by 15 percent beyond its nominal value ($f_Y = 41.4$ ksi). The results of these two parametric analyses are presented in Figure E.64 where the base case foundation system capacity interaction curve is also presented. As shown, the increase in the shear capacity of the foundation due to increasing the ultimate lateral resistance of the conductors by 50 percent is very similar to that due to increasing the yield strength of the conductors by 15 percent. Increasing the ultimate lateral resistance or yield strength of the conductors does not increase the overturning capacity of the foundation since the conductors are relatively small.

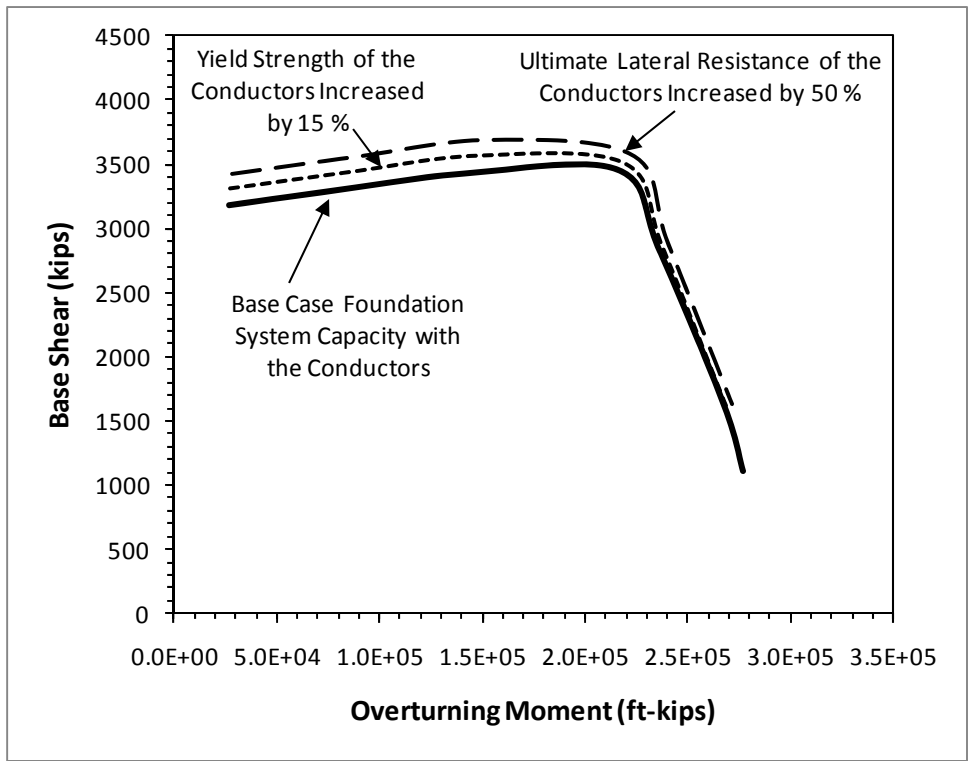


Figure E.64 Parametric Analyses for Platform 25 in the End-on Direction Increasing the Ultimate Lateral Resistance and Yield Strength of the Conductors

E.10 Platform 27

Platform 27 is a 4-leg structure supported by 4 piles and equipped with 2 conductors. The conductors are 30 inches in diameter and located outside the jacket. The foundation system is symmetrical in one direction but asymmetrical in the other direction. Two of the piles are battered in 2 directions (double batter piles). They are 264 feet long and 48 inches in diameter. The other two piles are battered in 1 direction (single batter piles). They are 281 feet long and 60 inches in diameter. The direction of the waves in Hurricane Rita is approximately the end-on direction of this platform (loading perpendicular to the plane of symmetry). The executive input file of this platform in the end-on direction is presented hereafter.

Executive Input File for Platform 27

PLATFORM 27 (ALL UNITS IN LB., IN., AND DEGREES)

SYSTEM LOAD DATA (PH,H,R,SKEW,PV,ECCENT)

2.867E6

5E3

1.00E-11

180.0

4.602E6

1.00E-10

NUMBER OF PILES (NPILE)

5

PILE 1

GEOMETRY (X,Y,THETAX,THETAY,L,AXIAL CONSTRAINT,NGROUP)

-5.62E+02 -5.491E+02 -4.76 -9.09 3.168E+03 1 1

PILE STRUCTURAL CAPACITY (INPUT FILE)

WPILE48.INP

SOIL CAPACITY (INPUT FILE)

WSOIL2.INP

PILE 2

GEOMETRY (X,Y,THETAX,THETAY,L,AXIAL CONSTRAINT,NGROUP)

5.62E+02 -5.491E+02 4.76 -9.09 3.168E+03 1 1

PILE STRUCTURAL CAPACITY (INPUT FILE)

WPILE48.INP

SOIL CAPACITY (INPUT FILE)

WSOIL2.INP

PILE 3

GEOMETRY (X,Y,THETAX,THETAY,L,AXIAL CONSTRAINT,NGROUP)

-5.62E+02 5.491E+02 -4.76 0.0 3.372E+03 1 1

PILE STRUCTURAL CAPACITY (INPUT FILE)

WPILE60.INP

SOIL CAPACITY (INPUT FILE)

WSOIL1.INP

PILE 4

GEOMETRY (X,Y,THETAX,THETAY,L,AXIAL CONSTRAINT,NGROUP)

5.62E+02 5.491E+02 4.76 0.0 3.372E+03 1 1

PILE STRUCTURAL CAPACITY (INPUT FILE)

WPILE60.INP

SOIL CAPACITY (INPUT FILE)

WSOIL1.INP

CONDUCTORS

GEOMETRY (X,Y,THETAX,THETAY,L,AXIAL CONSTRAINT,NGROUP)

0.00E+02 5.97E+02 0.00 0.00 3.372E+03 0 2

PILE STRUCTURAL CAPACITY (INPUT FILE)

WPILEC.INP

SOIL CAPACITY (INPUT FILE)

WSOILC.INP

The input parameters for the custom-built spreadsheet to calculate the axial and lateral resistance of the double batter piles, single batter piles and conductors are presented in Tables E.54, E55 and E.56, respectively. The design soil profile and parameters common for all piles and conductor are presented in Table E.57. The axial capacities of the double batter piles in compression and in tension are presented in Figure E.65. The lateral

resistance of these piles is presented in Figure E.66. The axial capacities of the single batter piles in compression and in tension are presented in Figure E.67. The lateral resistance of these piles is presented in Figure E.68. The lateral resistance of the conductors is presented in Figures E.69.

The structural capacity input files of the double batter piles, single batter piles and conductors are summarized in Tables E.58, E.59 and E.60, respectively.

Table E.54 Input Parameters for the Double Batter Piles of Platform 27

Seafloor Elevation (ft, MSL)	-300
Seasurface Elevation (ft, MSL)	0
Top of Pile Elevation (ft,MSL)	-300
Pile Length (ft)	264
Pile Diameter (ft)	4
Pile Tip Wall Thickness (in.)	1.25
Unit Weight of Water (pcf)	62.4
Depth Increment (ft)	1
Open- or Close-ended	Open
Open-ended Pile Tip Condition	Plugged
Loading Condition	Cyclic
K Compression	0.8
K Tension	0.8
Pile Batter in x-direction (deg.)	4.76
Pile Batter in y-direction (deg.)	9.09
X_R (ft)	34.0

Table E.55 Input Parameters for the Single Batter Piles of Platform 27

Seafloor Elevation (ft, MSL)	-300
Seasurface Elevation (ft, MSL)	0
Top of Pile Elevation (ft,MSL)	-300
Pile Length (ft)	281
Pile Diameter (ft)	5
Pile Tip Wall Thickness (in.)	1.5
Unit Weight of Water (pcf)	62.4
Depth Increment (ft)	1
Open- or Close-ended	Open
Open-ended Pile Tip Condition	Plugged
Loading Condition	Cyclic
K Compression	0.8
K Tension	0.8
Pile Batter in x-direction (deg.)	4.76
Pile Batter in y-direction (deg.)	0
X_R (ft)	41.4

Table E.56 Input Parameters for the Conductors of Platform 27

Seafloor Elevation (ft, MSL)	-300
Seasurface Elevation (ft, MSL)	0
Top of Pile Elevation (ft,MSL)	-300
Pile Length (ft)	281
Pile Diameter (ft)	2.5
Pile Tip Wall Thickness (in.)	0.75
Unit Weight of Water (pcf)	62.4
Depth Increment (ft)	1
Open- or Close-ended	Open
Open-ended Pile Tip Condition	Unplugged
Loading Condition	Cyclic
K Compression	0.8
K Tension	0.8
Pile Batter in x-direction (deg.)	0
Pile Batter in y-direction (deg.)	0
X_R (ft)	23.5

Table E.57 Design Soil Profile and Parameters for All Piles and Conductors of Platform 27

Layer	Soil Type	Top Elevation (ft, MSL)	Bottom Elevation (ft, MSL)	Thickness (ft)	Total Unit Weight (pcf)	Submerged Unit Weight (pcf)	c_u at the Top of Layer (psf)	dc_u/dz (psf/ft)	Friction Angle, ϕ' (deg.)	Soil Pile Friction Angle, δ (deg.)	f_{max} (ksf)	N_q	q_{max} (ksf)	C_1	C_2	C_3
1	Cohesive	-300	-317	17	92.4	30	100	4.67								
2	Cohesive	-317	-402	85	109.4	47	700	12.94								
3	Cohesionless	-402	-416	14	122.4	60			30	25	1.7	20	100	1.9	2.7	29
4	Cohesive	-416	-452	36	117.4	55	2000	10.75								
5	Cohesive	-452	-502	50	117.4	55	2387	10.75								
6	Cohesive	-502	-552	50	117.4	55	2924.5	10.75								
7	Cohesive	-552	-602	50	117.4	55	3462	10.75								

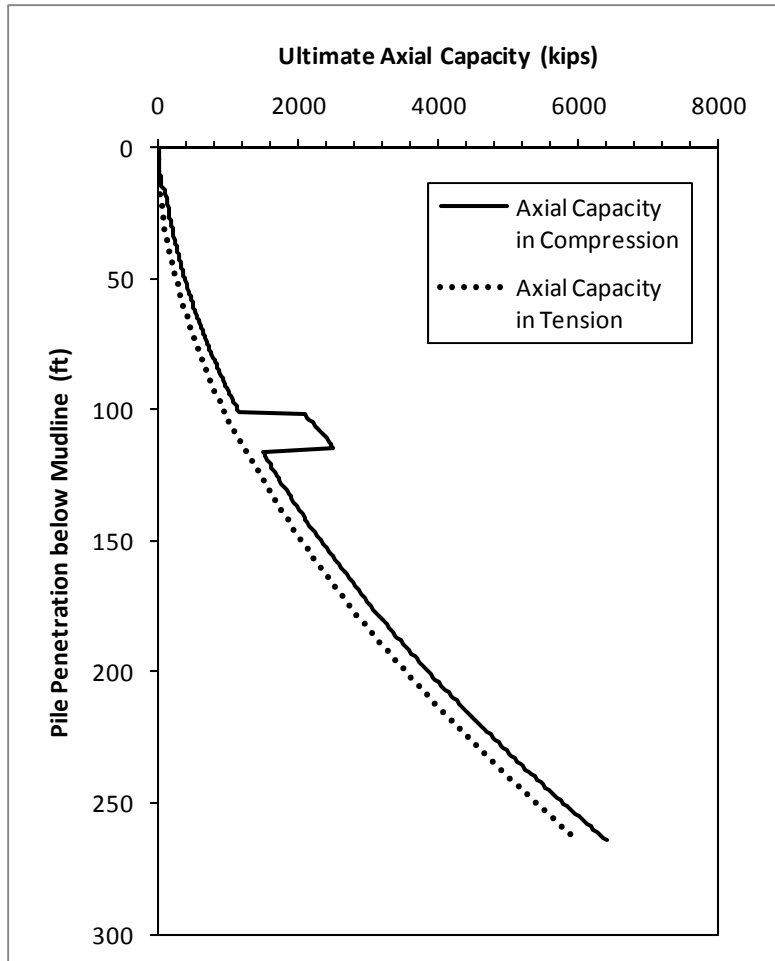


Figure E.65 Ultimate Axial Capacities of the Double Batter Piles of Platform 27

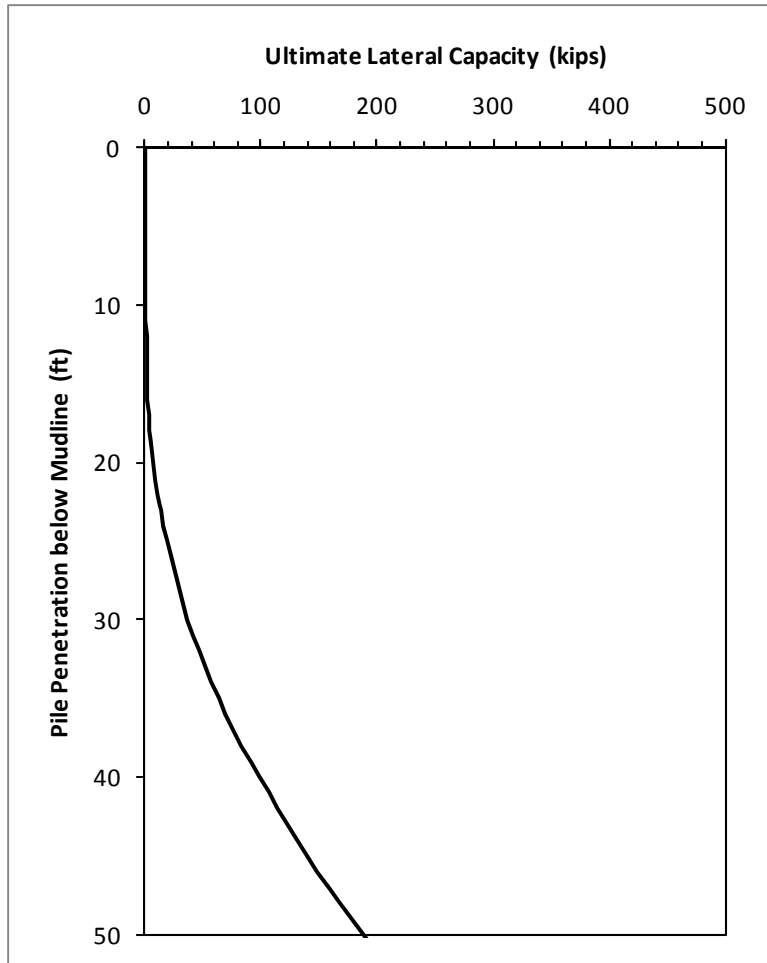


Figure E.66 Ultimate Lateral Resistance of the Double Batter Piles of Platform 27

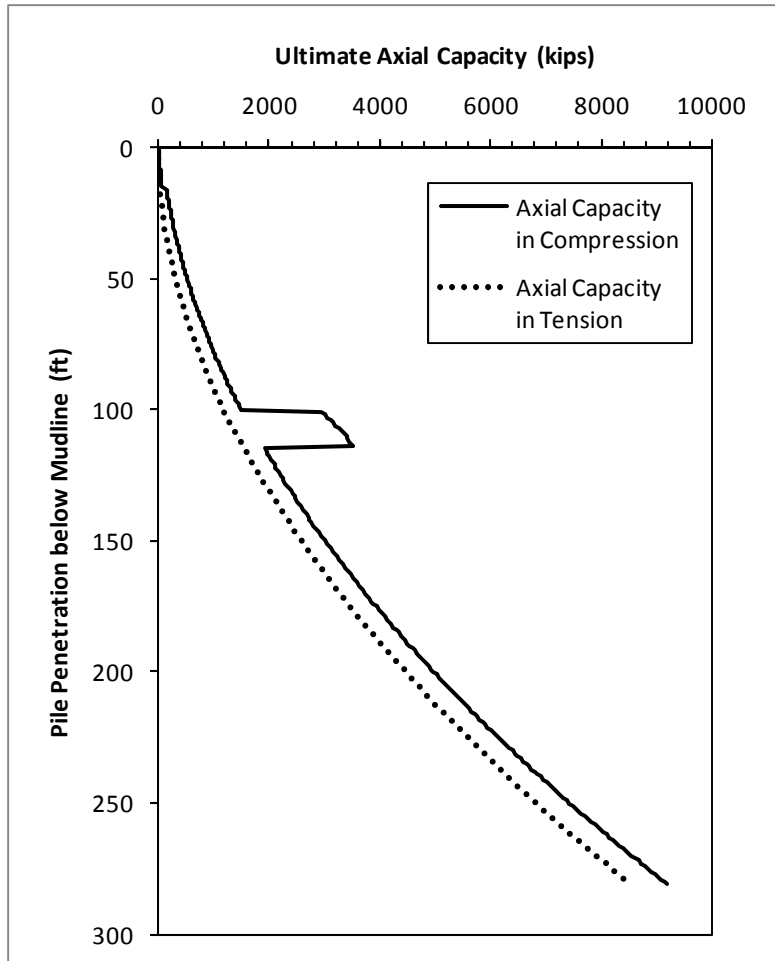


Figure E.67 Ultimate Axial Capacities of the Single Batter Piles of Platform 27

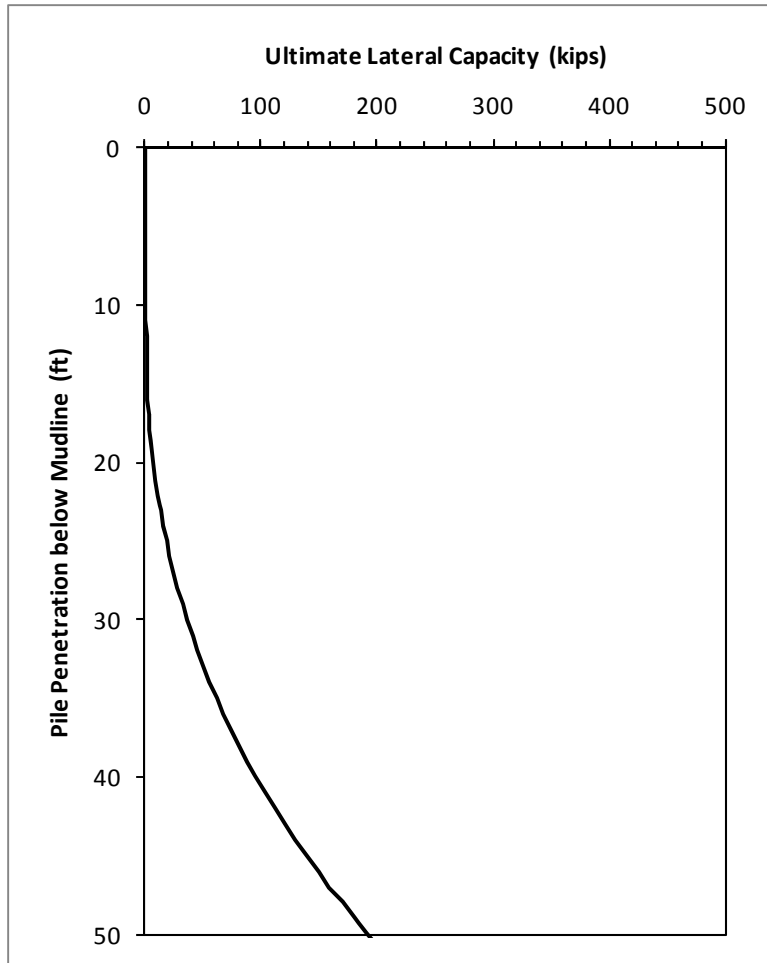


Figure E.68 Ultimate Lateral Resistance of the Single Batter Piles of Platform 27

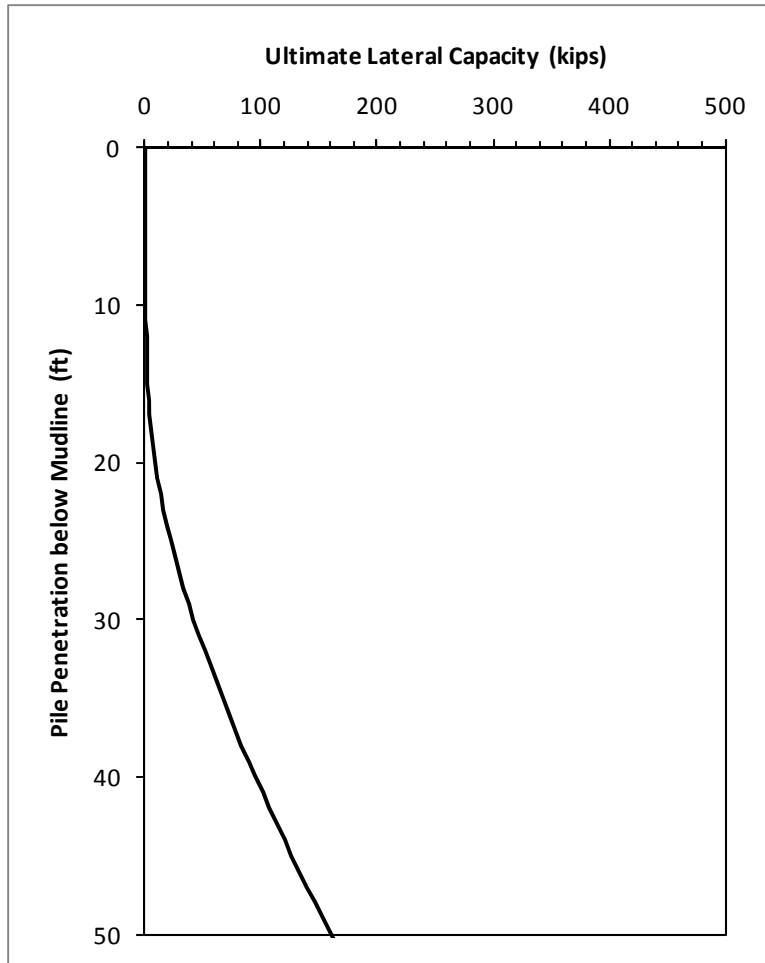


Figure E.69 Ultimate Lateral Resistance of the Conductors of Platform 27

Table E.58 Structural Capacity of the Double Batter Piles of Platform 27

Wall Thickness, t (in.)	Starting Length along Pile, z (in.)	Axial Structural Capacity, Q (lbs)	Moment Capacity, M (in.-lbs)
1.25	0	6.609E+06	9.837E+07
1	588	5.316E+06	7.954E+07
0.75	1308	4.008E+06	6.028E+07

Table E.59 Structural Capacity of the Single Batter Piles of Platform 27

Wall Thickness, t (in.)	Starting Length along Pile, z (in.)	Axial Structural Capacity, Q (lbs)	Moment Capacity, M (in.-lbs)
1.5	0	9.924E+06	1.848E+08
1.25	552	8.306E+06	1.553E+08
1	1152	6.673E+06	1.253E+08

Table E.60 Structural Capacity of the Conductors of Platform 27

Wall Thickness, t (in.)	Starting Length along Pile, z (in.)	Axial Structural Capacity, Q (lbs)	Moment Capacity, M (in.-lbs)
0.75	0	2.481E+06	2.311E+07
0.75	600	2.481E+06	2.311E+07
0.75	1200	2.481E+06	2.311E+07

Based on the above input parameters, the base case foundation system capacity interaction curves in the end-on direction are presented in Figures E.70. The direction of the waves is approximately the end-on direction of this platform. Therefore, the hurricane hindcast load on the foundation is also presented in Figure E.70.

A parametric analysis was performed to investigate the effect of loading direction on the foundation system capacity. Only the four piles were considered in this analysis. Furthermore, the yield strength of the piles was assumed to be 50 ksi (instead of 36 ksi as in the base case). The foundation system capacity interaction curves in the end-on, broadside and diagonal directions (corresponding to a skew angle, $\alpha = 180, 90$ and 135 degrees, respectively) are shown in Figure E.71. Note that the definition of the skew angle is provided in Appendix D.

As shown in Figure E.71, the overturning capacity of the foundation is notably different in different loading directions (highest in the broadside and lowest in the diagonal direction). Additionally, the shear capacity of the foundation is slightly different in different loading directions. This is due to the asymmetrical and non-redundant nature of the foundation.

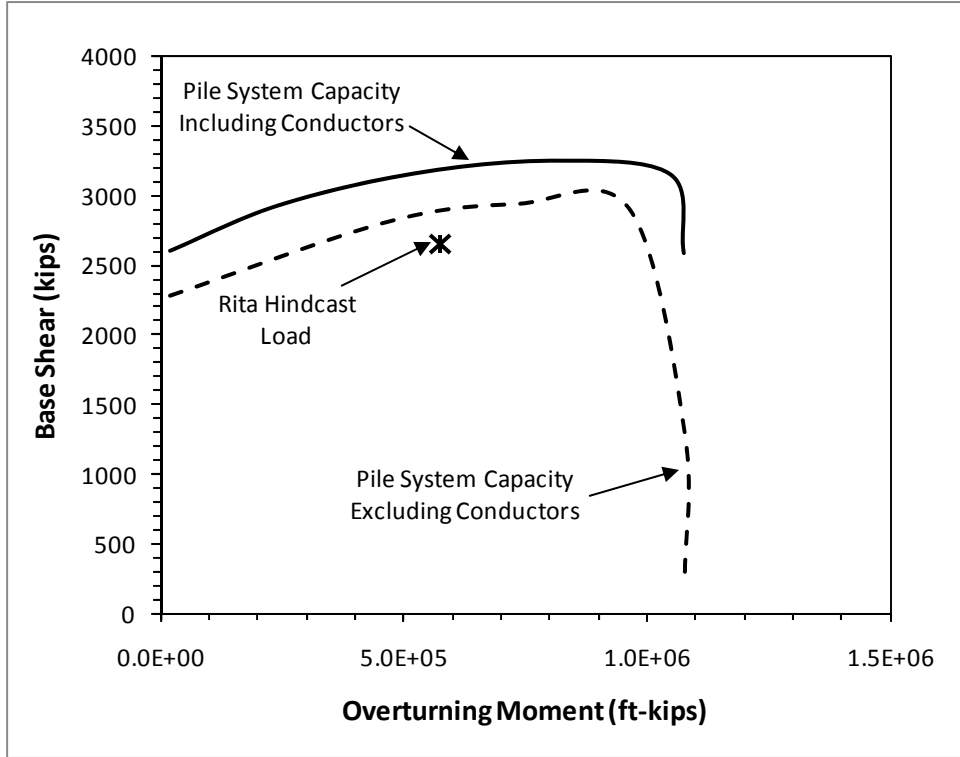


Figure E.70 Base Case Foundation System Capacity Interaction Diagram of Platform 27 in the End-on Direction

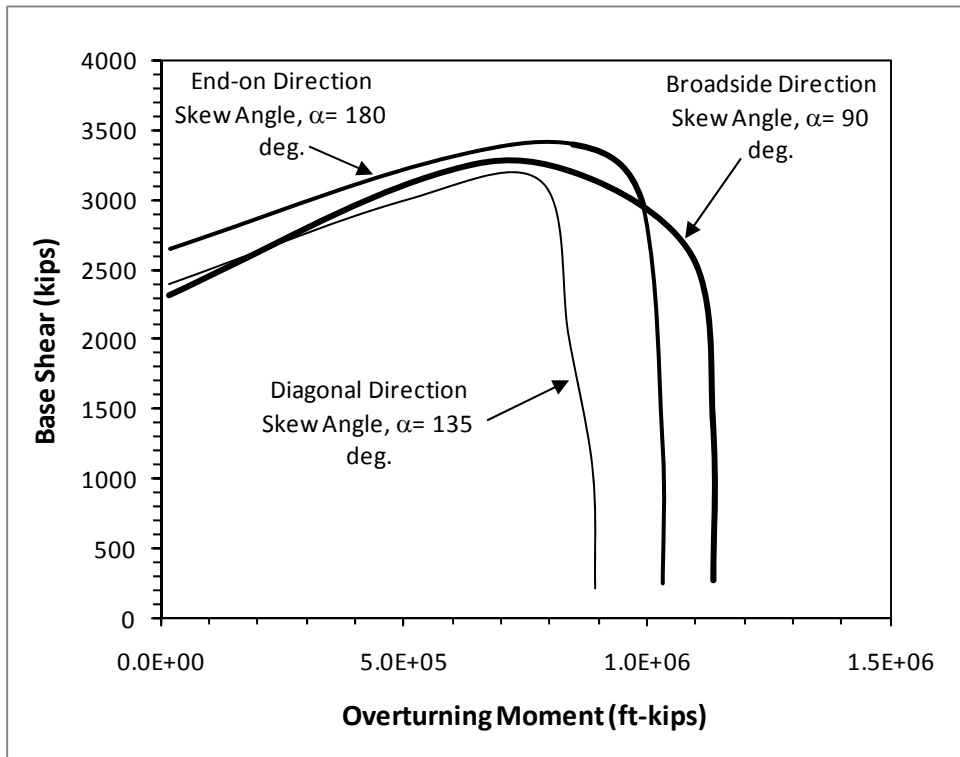


Figure E.71 Comparison of Foundation Capacities in Different Loading Directions for Platform 27

E.11 Platform 29

Platform 29 is an 8-leg structure supported by 8 piles and equipped with 12 conductors. The direction of the waves in Hurricane Katrina is approximately the broadside direction of this platform. The executive input file of this platform in the broadside direction is presented hereafter.

Executive Input File for Platform 29

PLATFORM 29 (ALL UNITS IN LB., IN., AND DEGREES)

SYSTEM LOAD DATA (PH,H,R,SKEW,PV,ECCENT)

3.0E6

1.0E2

1.00E-11

180.0

4.00E6

1.00E-10

NUMBER OF PILES (NPILE)

9

PILE 1

GEOMETRY (X,Y,THETAX,THETAY,L,AXIAL CONSTRAINT,NGROUP)

-4.935E+02 -8.415E+02 -7.13 -7.13 1.68E+03 1 1

PILE STRUCTURAL CAPACITY (INPUT FILE)

WPILE.INP

SOIL CAPACITY (INPUT FILE)

WSOIL2.INP

PILE 2

GEOMETRY (X,Y,THETAX,THETAY,L,AXIAL CONSTRAINT,NGROUP)

4.935E+02 -8.415E+02 7.13 -7.13 1.68E+03 1 1

PILE STRUCTURAL CAPACITY (INPUT FILE)

WPILE.INP

SOIL CAPACITY (INPUT FILE)

WSOIL2.INP

PILE 3

GEOMETRY (X,Y,THETAX,THETAY,L,AXIAL CONSTRAINT,NGROUP)

-4.935E+02 8.415E+02 -7.13 7.13 1.68E+03 1 1

PILE STRUCTURAL CAPACITY (INPUT FILE)

WPILE.INP

SOIL CAPACITY (INPUT FILE)

WSOIL2.INP

PILE 4

GEOMETRY (X,Y,THETAX,THETAY,L,AXIAL CONSTRAINT,NGROUP)

4.935E+02 8.415E+02 7.13 7.13 1.68E+03 1 1

PILE STRUCTURAL CAPACITY (INPUT FILE)

WPILE.INP

SOIL CAPACITY (INPUT FILE)

WSOIL2.INP

PILE 5

GEOMETRY (X,Y,THETAX,THETAY,L,AXIAL CONSTRAINT,NGROUP)

-4.935E+02 -1.80E+02 -7.13 0.00 1.68E+03 1 1

PILE STRUCTURAL CAPACITY (INPUT FILE)

WPILE.INP

SOIL CAPACITY (INPUT FILE)

WSOIL1.INP

PILE 6

GEOMETRY (X,Y,THETAX,THETAY,L,AXIAL CONSTRAINT,NGROUP)

4.935E+02 -1.80E+02 7.13 0.00 1.68E+03 1 1

PILE STRUCTURAL CAPACITY (INPUT FILE)

WPILE.INP

SOIL CAPACITY (INPUT FILE)

WSOIL1.INP

PILE 7

GEOMETRY (X,Y,THETAX,THETAY,L,AXIAL CONSTRAINT,NGROUP)

-4.935E+02 1.80E+02 -7.13 0.00 1.68E+03 1 1
PILE STRUCTURAL CAPACITY (INPUT FILE)
WPILE.INP
SOIL CAPACITY (INPUT FILE)
WSOIL1.INP

PILE 8
GEOMETRY (X,Y,THETAX,THETAY,L,AXIAL CONSTRAINT,NGROUP)
4.935E+02 1.80E+02 7.13 0.00 1.68E+03 1 1
PILE STRUCTURAL CAPACITY (INPUT FILE)
WPILE.INP
SOIL CAPACITY (INPUT FILE)
WSOIL1.INP

CONDUCTORS
GEOMETRY (X,Y,THETAX,THETAY,L,AXIAL CONSTRAINT,NGROUP)
0.00E+00 3.84E+02 0.00 0.00 1.68E+03 0 12
PILE STRUCTURAL CAPACITY (INPUT FILE)
WPILEC.INP
SOIL CAPACITY (INPUT FILE)
WSOILC.INP

The input parameters for the custom-built spreadsheet to calculate the axial and lateral resistance of the 4 corner piles battered in 2 directions, the 4 side piles battered in 1 direction, and the 12 conductors are presented in Tables E.61, E.62 and E.63, respectively. The design soil profile and parameters common for all piles and conductors are presented in Table E.64. The axial capacities of the 4 corner piles in compression and in tension are presented in Figure E.72. The lateral resistance of these piles is presented in Figure E.73. The same figures for the 4 side piles are not presented since they are similar to those for the corner piles. The lateral resistance of the conductors is presented in Figure E.74.

Table E.61 Input Parameters for the Piles of Platform 29 Battered in 2 Directions

Seafloor Elevation (ft, MSL)	-150
Seasurface Elevation (ft, MSL)	0
Top of Pile Elevation (ft,MSL)	-150
Pile Length (ft)	140
Pile Diameter (ft)	3.5
Pile Tip Wall Thickness (in.)	0.875
Unit Weight of Water (pcf)	62.4
Depth Increment (ft)	1
Open- or Close-ended	Open
Open-ended Pile Tip Condition	Plugged
Loading Condition	Cyclic
K Compression	0.8
K Tension	0.8
Pile Batter in x-direction (deg.)	7.125
Pile Batter in y-direction (deg.)	7.125
X_R (ft)	22.2

Table E.62 Input Parameters for the Piles of Platform 29 Battered in 1 Direction

Seafloor Elevation (ft, MSL)	-150
Seasurface Elevation (ft, MSL)	0
Top of Pile Elevation (ft,MSL)	-150
Pile Length (ft)	140
Pile Diameter (ft)	3.5
Pile Tip Wall Thickness (in.)	0.875
Unit Weight of Water (pcf)	62.4
Depth Increment (ft)	1
Open- or Close-ended	Open
Open-ended Pile Tip Condition	Plugged
Loading Condition	Cyclic
K Compression	0.8
K Tension	0.8
Pile Batter in x-direction (deg.)	0
Pile Batter in y-direction (deg.)	0
X_R (ft)	21.5

Table E.63 Input Parameters for the Conductors of Platform 29

Seafloor Elevation (ft, MSL)	-150
Seasurface Elevation (ft, MSL)	0
Top of Pile Elevation (ft,MSL)	-150
Pile Length (ft)	140
Pile Diameter (ft)	2
Pile Tip Wall Thickness (in.)	1
Unit Weight of Water (pcf)	62.4
Depth Increment (ft)	0.75
Open- or Close-ended	Open
Open-ended Pile Tip Condition	Plugged
Loading Condition	Cyclic
K Compression	0.8
K Tension	0.8
Pile Batter in x-direction (deg.)	0
Pile Batter in y-direction (deg.)	0
X_R (ft)	7.1

Table E.64 Design Soil Profile and Parameters for All Piles and Conductors of Platform 29

Layer	Soil Type	Top Elevation (ft, MSL)	Bottom Elevation (ft, MSL)	Thickness (ft)	Total Unit Weight (pcf)	Submerged Unit Weight (pcf)	c_u at the Top of Layer (psf)	dc_u/dz (psf/ft)	Friction Angle, ϕ' (deg.)	Soil Pile Friction Angle, δ (deg.)	f_{max} (ksf)	N_q	q_{max} (ksf)	C_1	C_2	C_3
1	Cohesive	-150	-163	13	90.9	28.5	80	0								
2	Cohesive	-163	-183	20	96.9	34.5	80	15								
3	Cohesive	-183	-228	45	101.4	39	380	7.1								
4	Cohesionless	-228	-306	78	122.4	60			35	30	2.0	40	200	3.0	3.4	54
5	Cohesionless	-306	-307	1	122.4	60			35	30	2.0	40	200	3.0	3.4	54
6	Cohesionless	-307	-308	1	122.4	60			35	30	2.0	40	200	3.0	3.4	54
7	Cohesionless	-308	-309	1	122.4	60			35	30	2.0	40	200	3.0	3.4	54

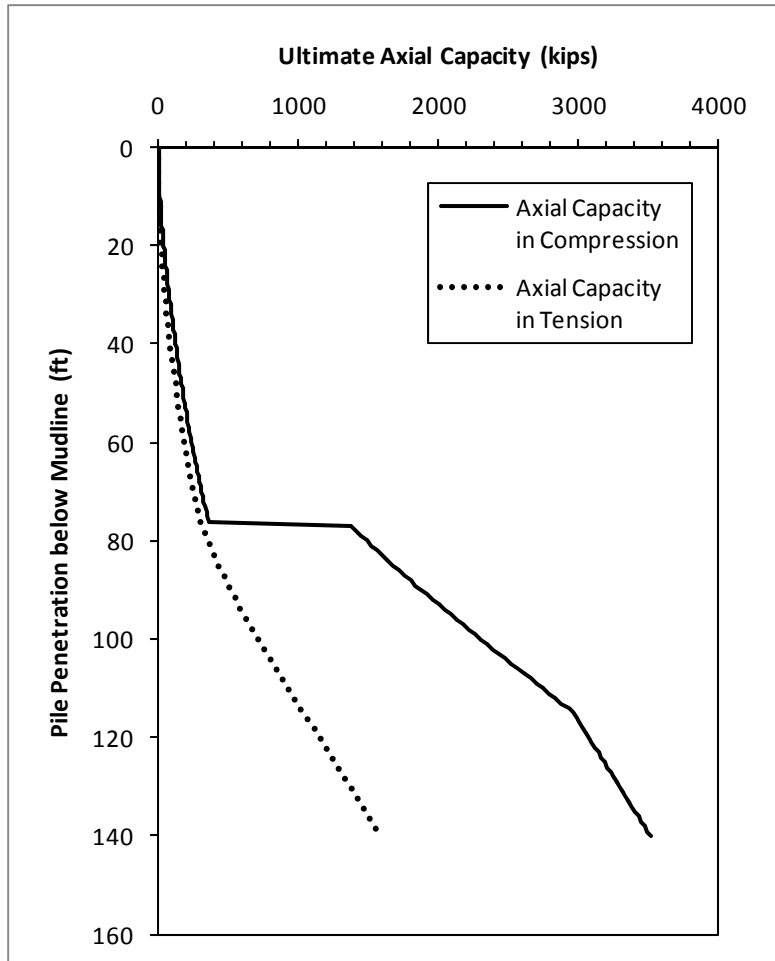


Figure E.72 Ultimate Axial Capacities of the Corner Piles of Platform 29

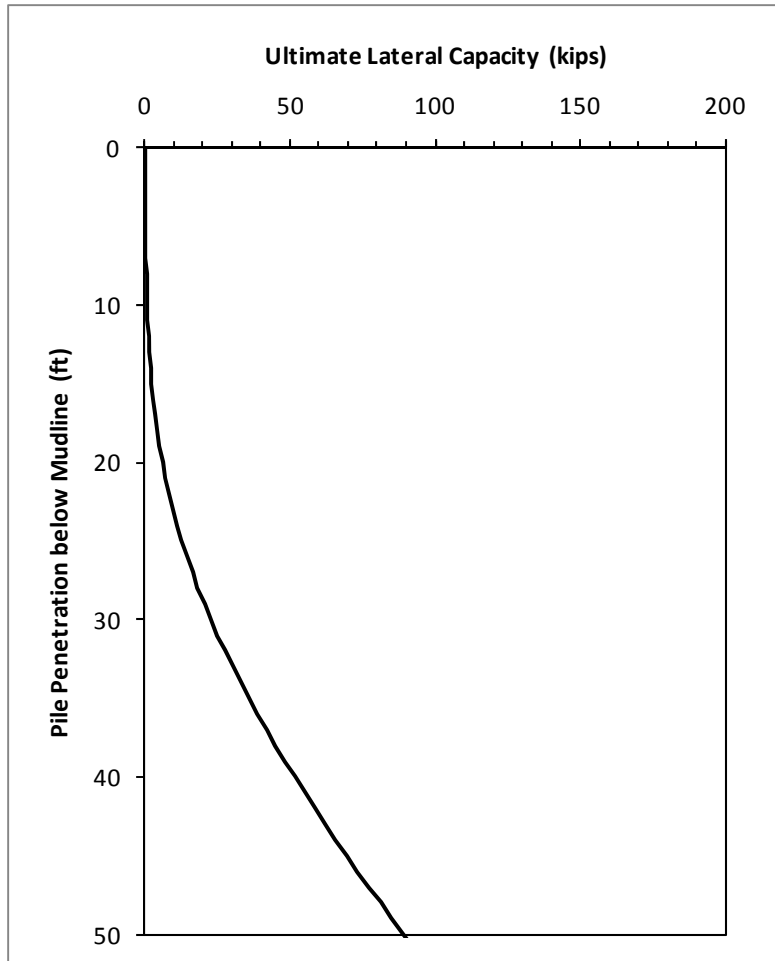


Figure E.73 Ultimate Lateral Capacity of the Corner Piles of Platform 29

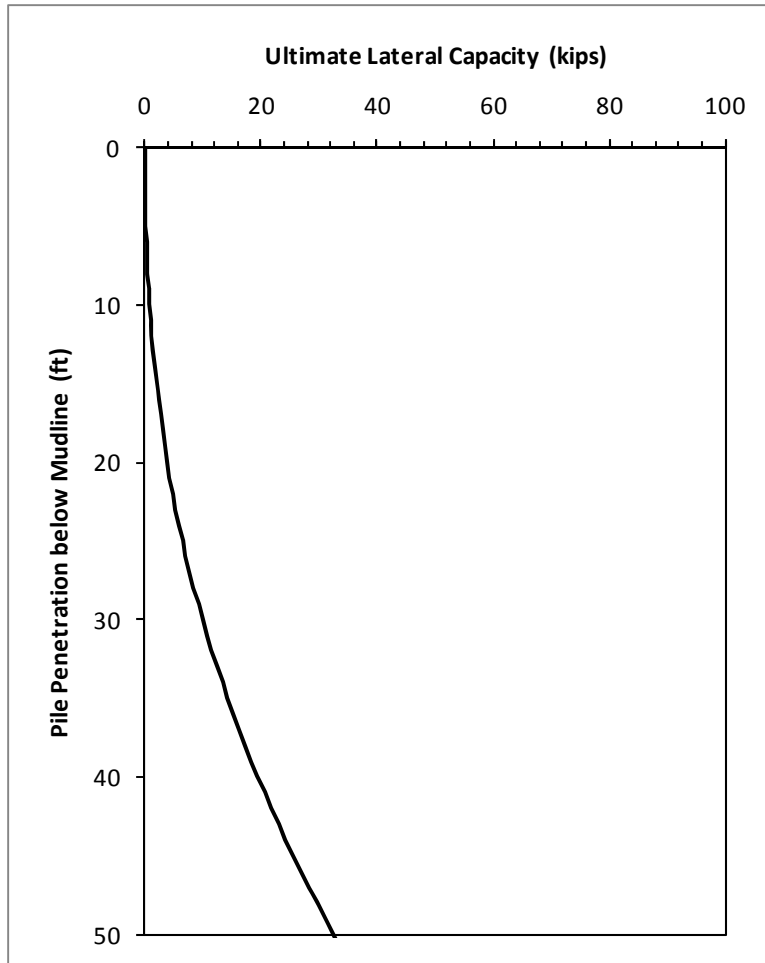


Figure E.74 Ultimate Lateral Capacity of the Conductors of Platform 29

The structural capacity input files of the piles and conductors are summarized in Tables E.65 and E.66, respectively.

Table E.65 Structural Capacity of the Piles of Platform 29

Wall Thickness, t (in.)	Starting Length along Pile, z (in.)	Axial Structural Capacity, Q (lbs)	Moment Capacity, M (in.-lbs)
1.25	0	5.761E+06	7.475E+07
1.375	216	6.318E+06	8.173E+07
1.25	816	5.761E+06	7.475E+07

Table E.66 Structural Capacity of the Conductors of Platform 29

Wall Thickness, t (in.)	Starting Length along Pile, z (in.)	Axial Structural Capacity, Q (lbs)	Moment Capacity, M (in.-lbs)
0.75	0	1.972E+06	1.460E+07
0.75	600	1.972E+06	1.460E+07
0.75	1200	1.972E+06	1.460E+07

Based on the above input parameters, the base case foundation system capacity interaction curves in the end-on, broadside and diagonal directions are presented in Figures E.75, E.76 and E.77, respectively. The direction of the waves is approximately the broadside direction of this platform. Therefore, the hurricane hindcast load on the foundation is also presented in the interaction diagram for the broadside direction. Parametric analyses were not performed for this platform.

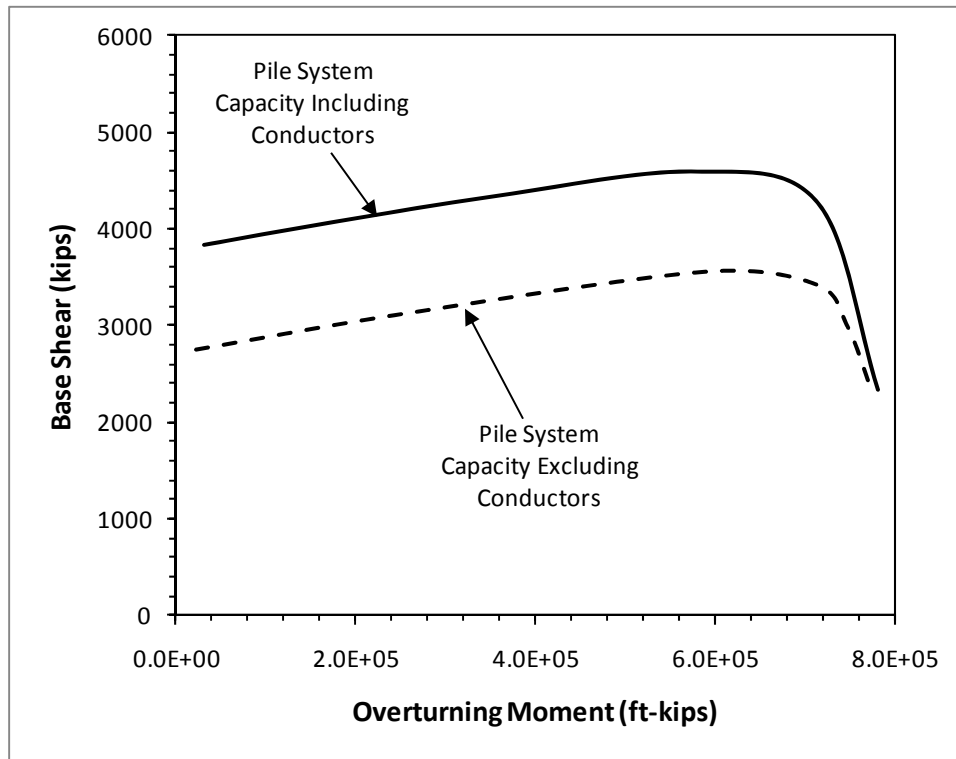


Figure E.75 Base Case Foundation System Capacity Interaction Diagram of Platform 29 in the End-on Direction

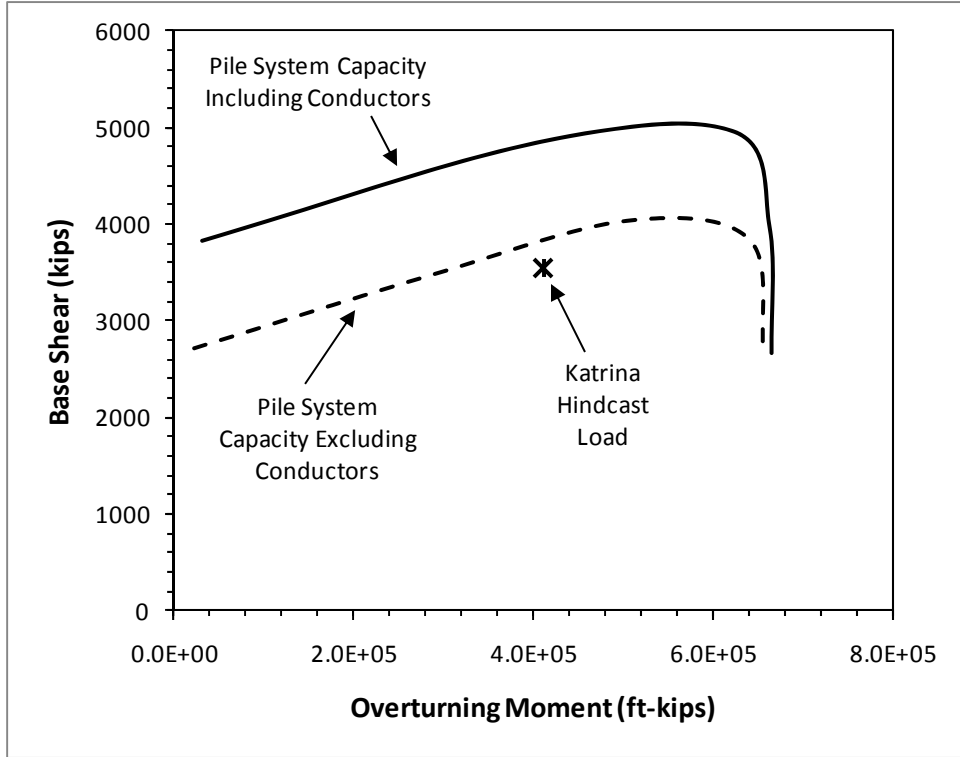


Figure E.76 Base Case Foundation System Capacity Interaction Diagram of Platform 29 in the Broadside Direction

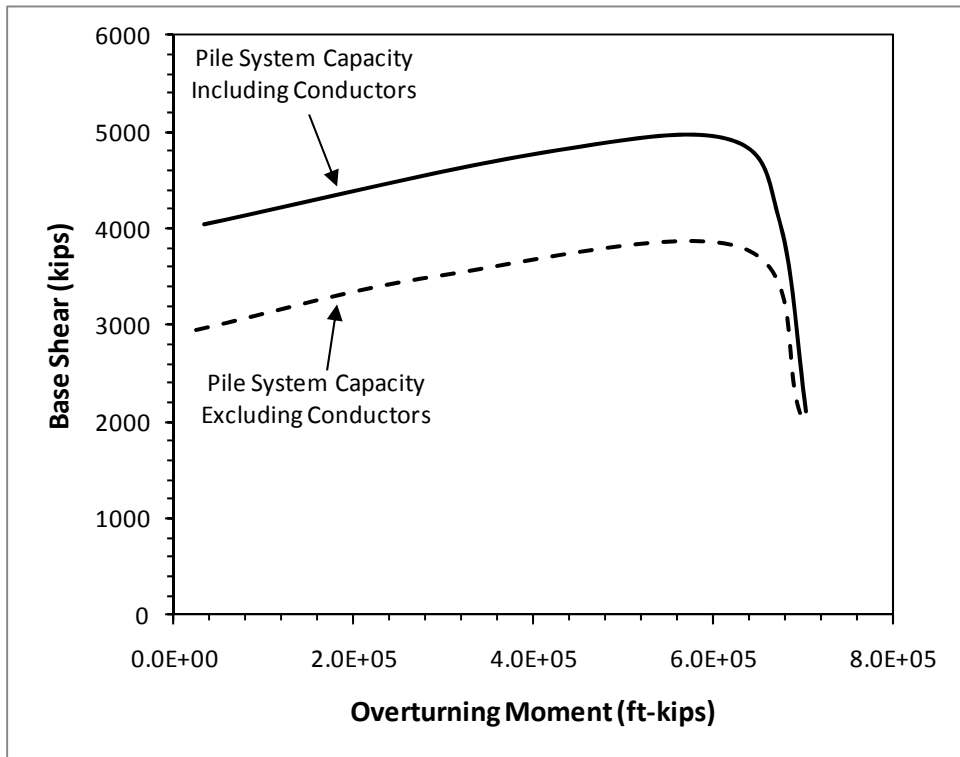


Figure E.77 Base Case Foundation System Capacity Interaction Diagram of Platform 29 in the Diagonal Direction

E.12 Platform 30

Platform 30 is a 6-leg structure supported by 6 piles and equipped with 12 conductors. The direction of the waves in Hurricane Katrina is approximately the diagonal direction of this platform. The executive input file of this platform in the diagonal direction is presented hereafter.

Executive Input File for Platform 30

PLATFORM 30 (ALL UNITS IN LB., IN., AND DEGREES)

SYSTEM LOAD DATA (PH,H,R,SKEW,PV,ECCENT)

1.181E6

1E4

1.00E-11

45.0

4.038E6

1.00E-10

NUMBER OF PILES (NPILE)

7

PILE 1

GEOMETRY (X,Y,THETAX,THETAY,L,AXIAL CONSTRAINT,NGROUP)

-4.9575E+02 -6.1575E+02 -7.13 -7.13 2.472E+03 1 1

PILE STRUCTURAL CAPACITY (INPUT FILE)

WPILE.INP

SOIL CAPACITY (INPUT FILE)

WSOIL2.INP

PILE 2

GEOMETRY (X,Y,THETAX,THETAY,L,AXIAL CONSTRAINT,NGROUP)

4.9575E+02 -6.1575E+02 7.13 -7.13 2.472E+03 1 1

PILE STRUCTURAL CAPACITY (INPUT FILE)

WPILE.INP

SOIL CAPACITY (INPUT FILE)

WSOIL2.INP

PILE 3

GEOMETRY (X,Y,THETAX,THETAY,L,AXIAL CONSTRAINT,NGROUP)

-4.9575E+02 6.1575E+02 -7.13 7.13 2.472E+03 1 1

PILE STRUCTURAL CAPACITY (INPUT FILE)

WPILE.INP

SOIL CAPACITY (INPUT FILE)

WSOIL2.INP

PILE 4

GEOMETRY (X,Y,THETAX,THETAY,L,AXIAL CONSTRAINT,NGROUP)

4.9575E+02 6.1575E+02 7.13 7.13 2.472E+03 1 1

PILE STRUCTURAL CAPACITY (INPUT FILE)

WPILE.INP

SOIL CAPACITY (INPUT FILE)

WSOIL2.INP

PILE 5

GEOMETRY (X,Y,THETAX,THETAY,L,AXIAL CONSTRAINT,NGROUP)

-4.9575E+02 0.00E+02 -7.13 0.00 2.472E+03 1 1

PILE STRUCTURAL CAPACITY (INPUT FILE)

WPILE.INP

SOIL CAPACITY (INPUT FILE)

WSOIL1.INP

PILE 6

GEOMETRY (X,Y,THETAX,THETAY,L,AXIAL CONSTRAINT,NGROUP)

4.9575E+02 0.00E+02 7.13 0.00 2.472E+03 1 1

PILE STRUCTURAL CAPACITY (INPUT FILE)

WPILE.INP

SOIL CAPACITY (INPUT FILE)

WSOIL1.INP

CONDUCTORS

GEOMETRY (X,Y,THETAX,THETAY,L,AXIAL CONSTRAINT,NGROUP)

0.00E+00 0.00E+02 0.00 0.00 1.224E+03 0 12

PILE STRUCTURAL CAPACITY (INPUT FILE)

WPILEC.INP

SOIL CAPACITY (INPUT FILE)

WSOILC.INP

The input parameters for the custom-built spreadsheet to calculate the axial and lateral resistance of the 4 corner piles battered in 2 directions, the 2 side piles battered in 1 direction, and the 12 conductors are presented in Tables E.67, E.68 and E.69, respectively. The design soil profile and parameters common for all piles and conductors are presented in Table E.70. The axial capacities of the 4 corner piles in compression and in tension are presented in Figure E.78. The lateral resistance of these piles is presented in Figure E.79. The same figures for the 2 side piles are not presented since they are similar to those for the corner piles. The lateral resistance of the conductors is presented in Figure E.80.

Table E.67 Input Parameters for the Piles of Platform 30 Battered in 2 Directions

Seafloor Elevation (ft, MSL)	-150
Seasurface Elevation (ft, MSL)	0
Top of Pile Elevation (ft,MSL)	-150
Pile Length (ft)	206
Pile Diameter (ft)	4
Pile Tip Wall Thickness (in.)	1
Unit Weight of Water (pcf)	62.4
Depth Increment (ft)	1
Open- or Close-ended	Open
Open-ended Pile Tip Condition	Plugged
Loading Condition	Cyclic
K Compression	0.8
K Tension	0.8
Pile Batter in x-direction (deg.)	7.125
Pile Batter in y-direction (deg.)	7.125
X_R (ft)	9.4

Table E.68 Input Parameters for the Piles of Platform 30 Battered in 1 Direction

Seafloor Elevation (ft, MSL)	-150
Seasurface Elevation (ft, MSL)	0
Top of Pile Elevation (ft,MSL)	-150
Pile Length (ft)	206
Pile Diameter (ft)	4
Pile Tip Wall Thickness (in.)	1
Unit Weight of Water (pcf)	62.4
Depth Increment (ft)	1
Open- or Close-ended	Open
Open-ended Pile Tip Condition	Plugged
Loading Condition	Cyclic
K Compression	0.8
K Tension	0.8
Pile Batter in x-direction (deg.)	7.125
Pile Batter in y-direction (deg.)	0
X_R (ft)	9.4

Table E.69 Input Parameters for the Conductors of Platform 30

Seafloor Elevation (ft, MSL)	-150
Seasurface Elevation (ft, MSL)	0
Top of Pile Elevation (ft,MSL)	-150
Pile Length (ft)	102
Pile Diameter (ft)	2
Pile Tip Wall Thickness (in.)	0.75
Unit Weight of Water (pcf)	62.4
Depth Increment (ft)	1
Open- or Close-ended	Open
Open-ended Pile Tip Condition	Unplugged
Loading Condition	Cyclic
K Compression	0.8
K Tension	0.8
Pile Batter in x-direction (deg.)	0
Pile Batter in y-direction (deg.)	0
X_R (ft)	8.0

Table E.70 Design Soil Profile and Parameters for All Piles and Conductors of Platform 30

Layer	Soil Type	Top Elevation (ft, MSL)	Bottom Elevation (ft, MSL)	Thickness (ft)	Total Unit Weight (pcf)	Submerged Unit Weight (pcf)	c_u at the Top of Layer (psf)	dc_u/dz (psf/ft)	Friction Angle, ϕ' (deg.)	Soil Pile Friction Angle, δ (deg.)	f_{max} (ksf)	N_q	q_{max} (ksf)	C_1	C_2	C_3
1	Cohesive	-150	-163	13	92.4	30	60	0								
2	Cohesive	-163	-183	20	97.4	35	60	14.5								
3	Cohesive	-183	-228	45	101.4	39	350	8								
4	Cohesionless	-228	-300	72	122.4	60			36	30	2.0	40	200	3.3	3.7	61
5	Cohesionless	-300	-400	100	122.4	60			36	30	2.0	40	200	3.3	3.7	61
6	Cohesionless	-400	-500	100	122.4	60			36	30	2.0	40	200	3.3	3.7	61
7	Cohesionless	-500	-600	100	122.4	60			36	30	2.0	40	200	3.3	3.7	61

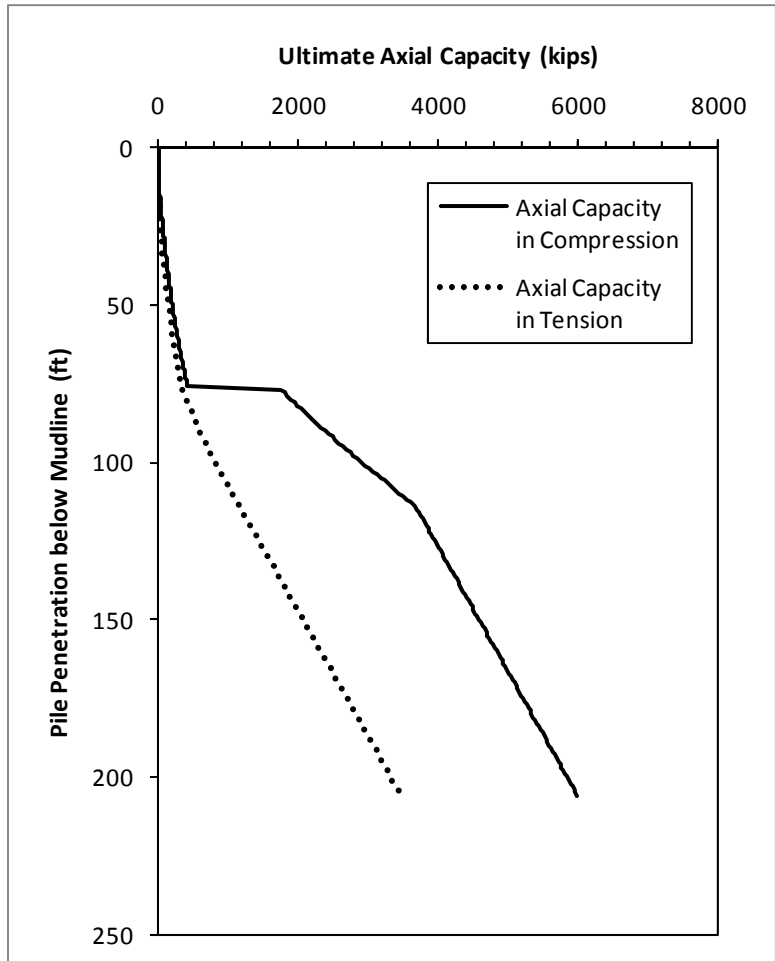


Figure E.78 Ultimate Axial Capacities of the Corner Piles of Platform 30

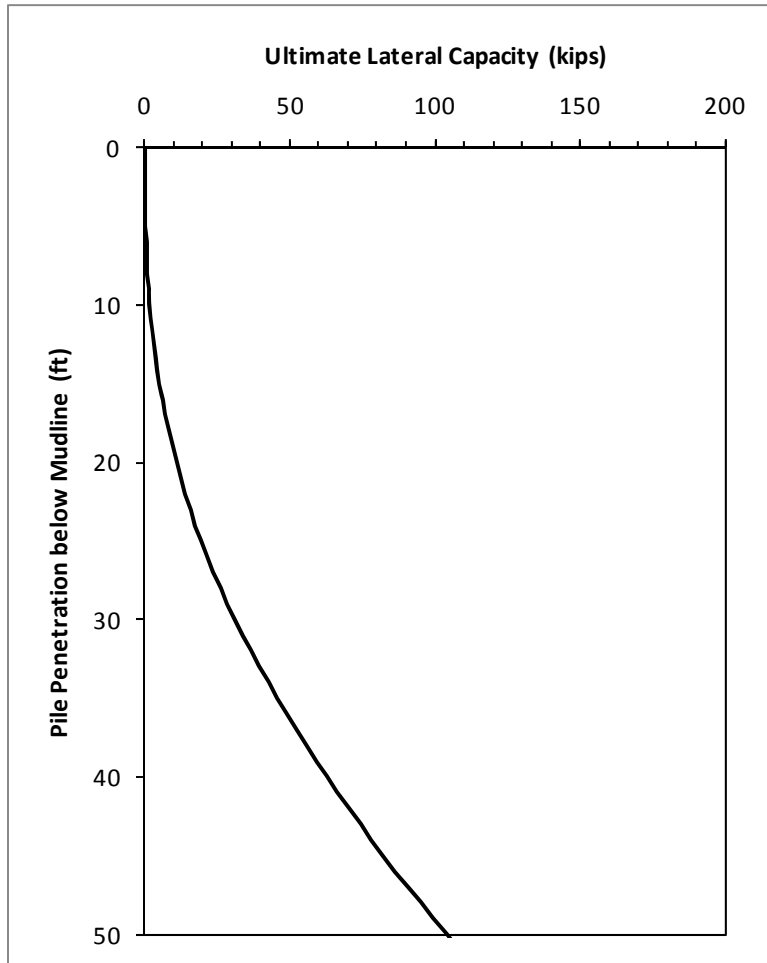


Figure E.79 Ultimate Lateral Capacity of the Corner Piles of Platform 30

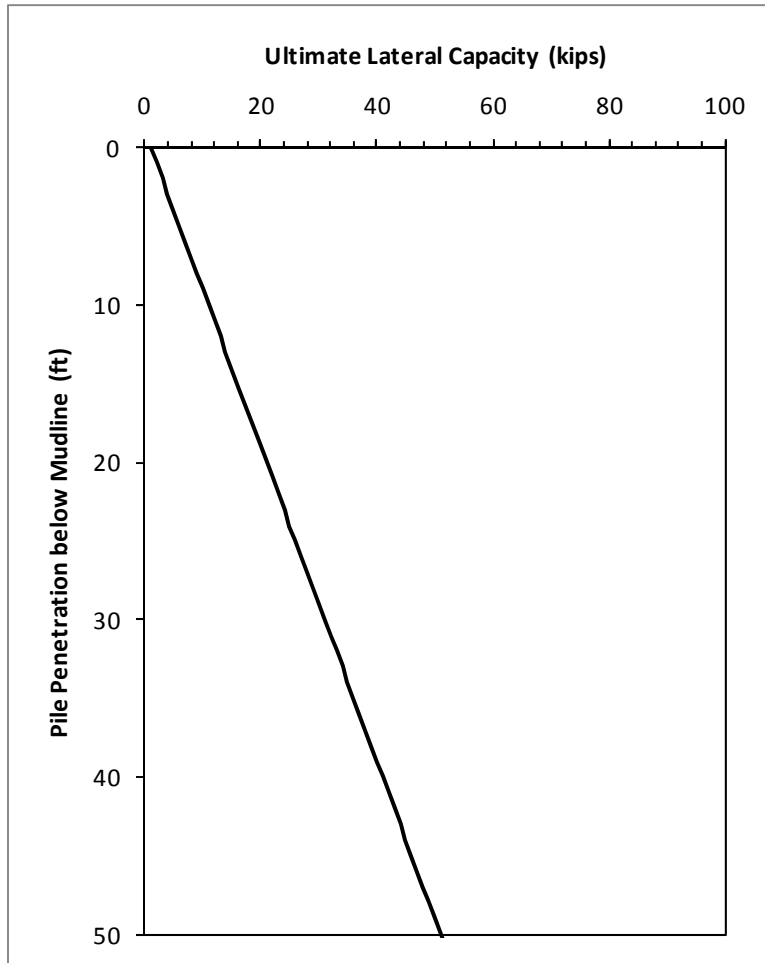


Figure E.80 Ultimate Lateral Capacity of the Conductors of Platform 30

The structural capacity input files of the piles and conductors are summarized in Tables E.71 and E.72, respectively.

Table E.71 Structural Capacity of the Piles of Platform 30

Wall Thickness, t (in.)	Starting Length along Pile, z (in.)	Axial Structural Capacity, Q (lbs)	Moment Capacity, M (in.-lbs)
1.75	0	9.154E+06	1.348E+08
1.5	1152	7.889E+06	1.168E+08
1.25	1272	6.609E+06	9.837E+07

Table E.72 Structural Capacity of the Conductors of Platform 30

Wall Thickness, t (in.)	Starting Length along Pile, z (in.)	Axial Structural Capacity, Q (lbs)	Moment Capacity, M (in.-lbs)
0.5	0	1.329E+06	9.942E+06
0.5	600	1.329E+06	9.942E+06
0.75	1164	1.972E+06	1.460E+07

Based on the above input parameters, the base case foundation system capacity interaction curves in the end-on, broadside and diagonal directions are presented in Figures E.81, E.82 and E.83, respectively. The direction of the waves is approximately the diagonal direction of this platform. Therefore, the hurricane hindcast load on the foundation is also presented in the interaction diagram for the diagonal direction.

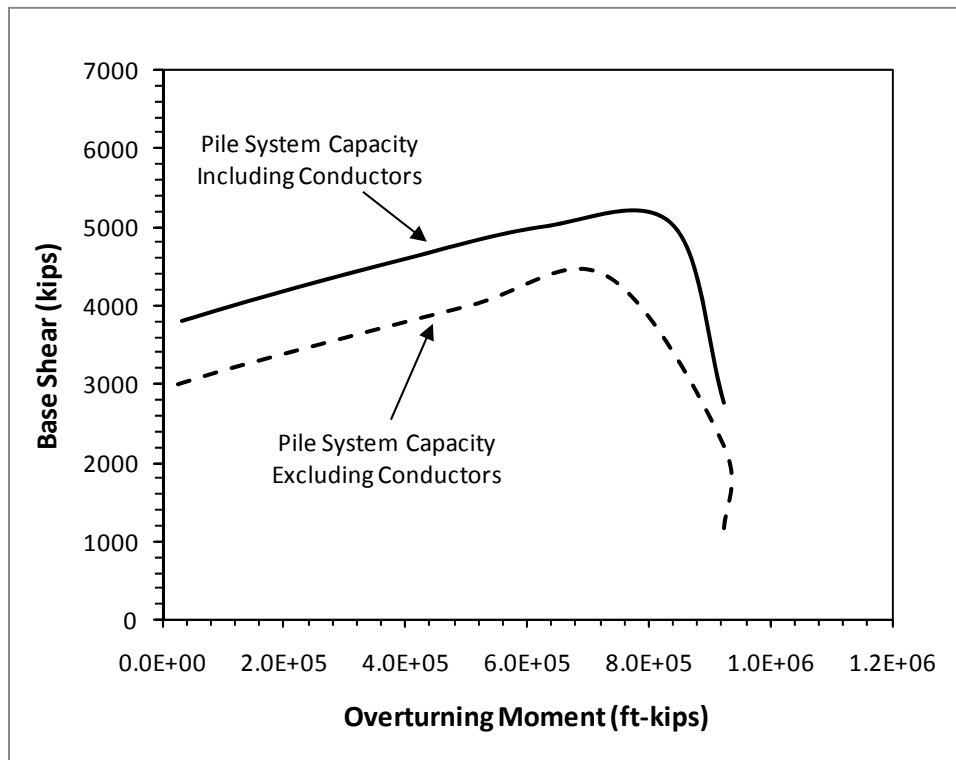


Figure E.81 Base Case Foundation System Capacity Interaction Diagram of Platform 30 in the End-on Direction

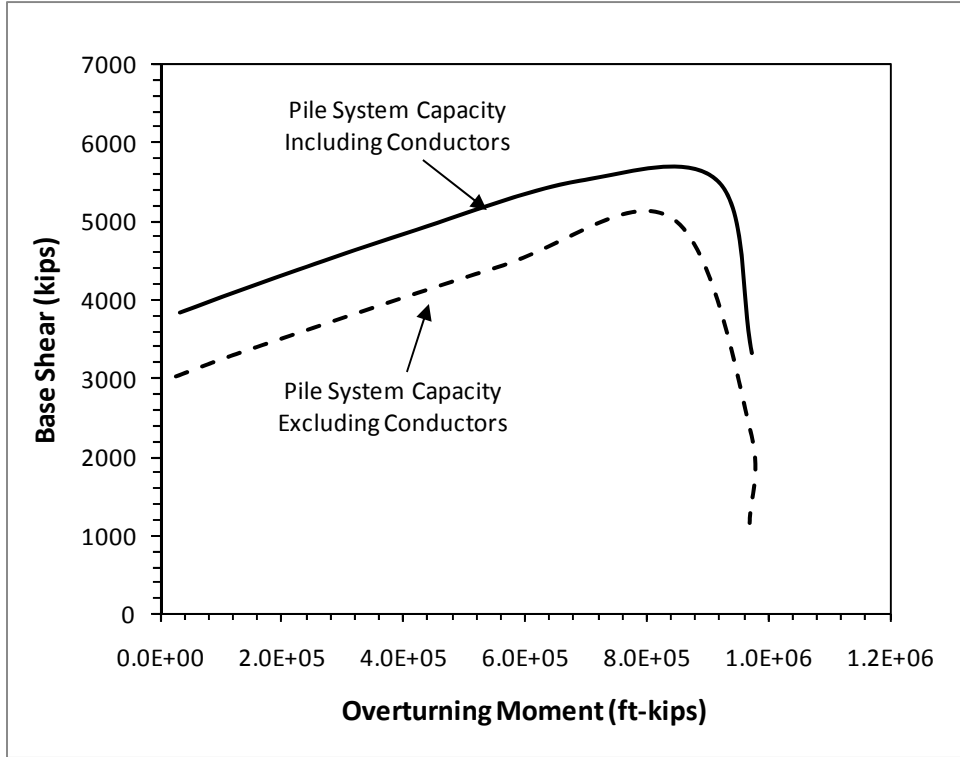


Figure E.82 Base Case Foundation System Capacity Interaction Diagram of Platform 30 in the Broadside Direction

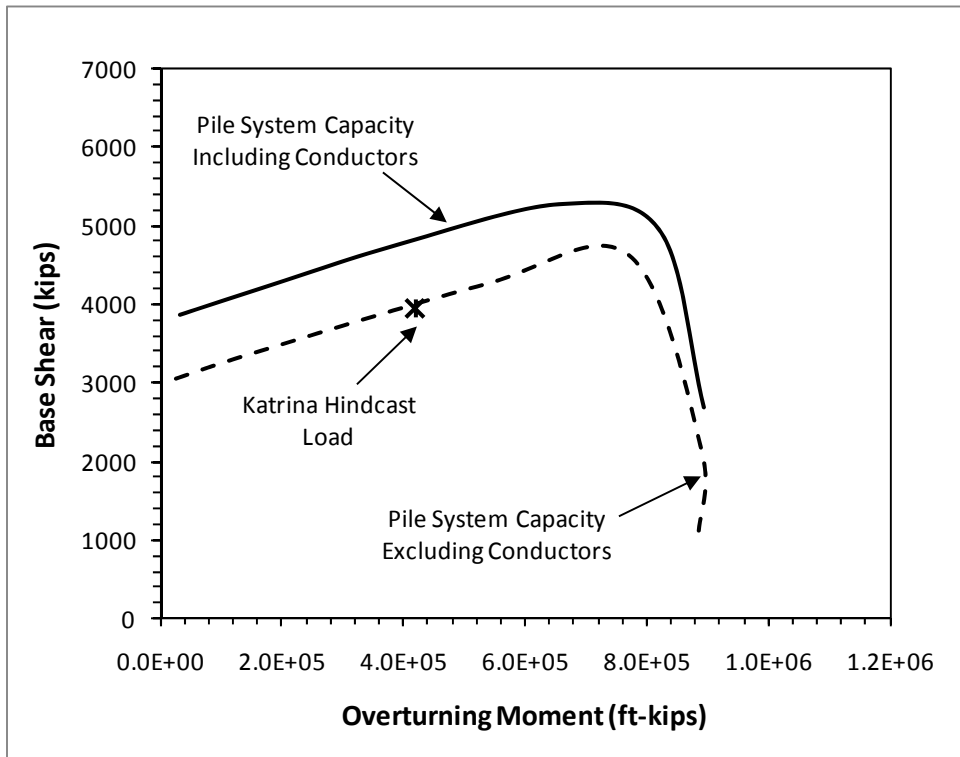


Figure E.83 Base Case Foundation System Capacity Interaction Diagram of Platform 30 in the Diagonal Direction

A parametric analysis was performed to investigate the effect of loading direction on the foundation system capacity. Only the six piles were considered in this analysis. The foundation system capacity interaction curves in the end-on, broadside and diagonal directions (corresponding to a skew angle, $\alpha = 90, 0$ and 45 degrees, respectively) are shown in Figure E.84. Note that the definition of the skew angle is provided in Appendix D.

As shown in Figure E.84, the overturning capacity of the foundation is notably different in different loading directions (highest in the broadside and lowest in the diagonal direction). This is because each individual pile contributes differently depending on the moment arm between the pile and the center of the rotation for the platform in the direction of loading. On the contrary, the shear capacity of the foundation is identical in these 3 loading directions (approximately 3,000 kips). This is because the foundation system is reasonably symmetrical and redundant. Therefore, the lateral capacity of each pile can be mobilized more uniformly than that for an asymmetrical and less redundant (i.e., 3-pile or 4-pile) foundation system.

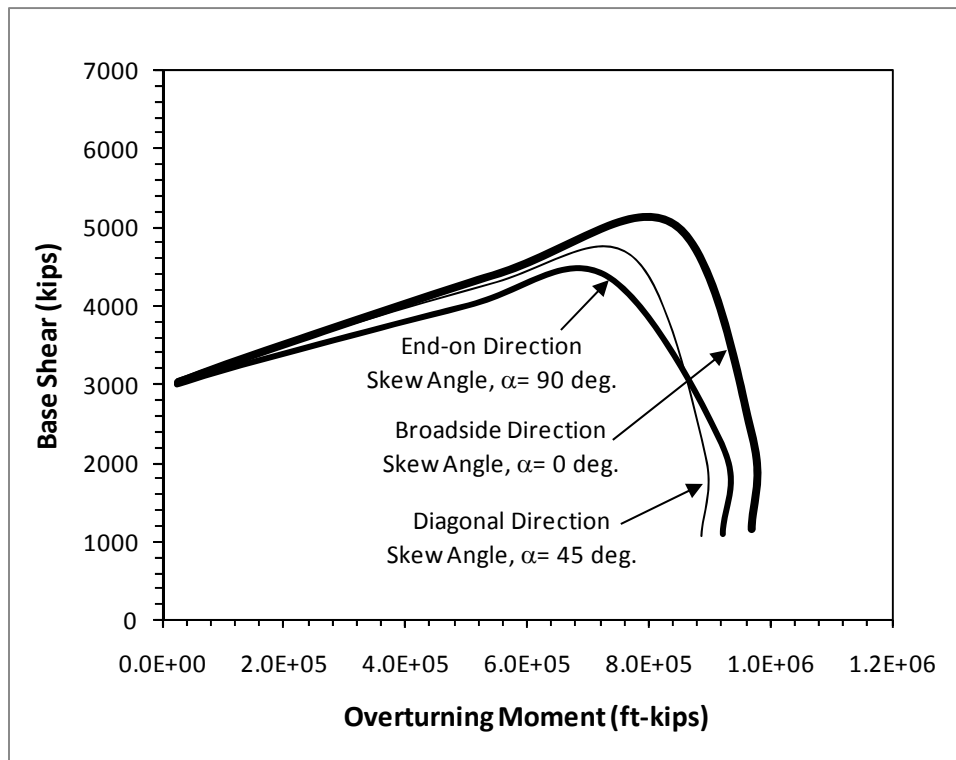


Figure E.84 Comparison of Foundation Capacities in Different Loading Directions for Platform 30

Appendix F – Expert Panel Meeting

An expert panel meeting was convened on March 23, 2009 at the University of Texas at Austin to discuss the preliminary findings in this project and solicit input from the expert panel including experienced or knowledgeable members of the industry and academia. Table F.1 shows the list of attendees in the expert panel meeting.

Table F.1 List of Attendees in the Expert Panel Meeting

Name	Affiliation
Alan Young	GEMS
Bill Quiros	Private Geotechnical Consultant
Bob Gilbert	UT-Austin
Britain Materek	UT-Austin
Christy Bohannon*	MMS
Don Murff	TAMU/Consultant
Frank Puskar	Energ Engineering
Fung Hassenboehler	MMS
Hudson Matlock	Professor Emeritus, UT-Austin
Jiun-Yih Chen	UT-Austin
John Cushing*	MMS
Justin Carpenter	UT-Austin
Lori D’Angelo*	MMS
Lymon Reese	Ensoft
Venessa Bertrand	MMS

* Participated via a teleconference call.

Important points that were discussed during the expert panel meeting are summarized below.

1. A very clear distinction should be made between assessments of existing structures, which is the focus of this project, compared to new designs.
2. Potential factors that can contribute to a difference between the design capacity and the actual capacity for platform foundations include limitations in site

characterization data (i.e., wireline percussion versus pushed sampling techniques, SPT blow counts versus CPT tip resistance), conservatism in developing design profiles of shear strength, set-up and aging increasing the pile capacity long after pile driving, periodic pre-stressing and subsequent consolidation of soils adjacent to the pile causing the shear strength to increase, actual storm loading corresponding to limited cycles of the largest storm loads in any particular direction applied at a relatively high rate, the use of cyclic p-y curves for lateral resistance that were intentionally developed to provide a lower bound on the lateral capacity, and contributions of structural elements such as mudmats and well conductors.

3. Pile driving records and as-built pile penetration are very important in understanding the actual capacity of the foundation. Consideration should be given to making these records mandatory submittal items to the MMS for new platforms so that they are available in the future for engineering studies related to platform assessments.
4. We should continue to pursue any information about potential foundation failures and attempt to obtain as much information as possible about these cases.
5. The interaction between structural and geotechnical engineers is very important in assessments. Miscommunication or no communication between the two disciplines can result in overly conservative (or un-conservative) assessments.
6. Various factors contributing to potential conservatism in pile design should be documented succinctly in the final report with key references. Presenting typical ranges of multipliers to address the discrepancy between the estimated and real capacities of foundation is not recommended as these may be used out of context and perhaps where not applicable. However, it would be useful to put a bound on what is not reasonable because it cannot be supported by any information that we have to date, such as increasing the shear strength by four times or more. Providing an illustrative example of the considerations that could go into modeling the foundation for an assessment would be valuable.
7. Both the base shear and the overturning moment are important concerning the foundation behavior. Guidance on how to obtain and make use of information about the overturning moment for a platform assessment would be helpful.

In addition to these summary points, comments provided by Dr. Lymon Reese in his letter after the expert panel meeting are presented in Figure F.1. The discussions and comments by the expert panel are incorporated in this final report. A draft of the final report was submitted to the expert panel for review and additional comments before it is finalized.



Lymon C. Reese

**105A East Walter Avenue,
Pflugerville, Texas 78660**

March 23, 2009

Dr. Robert Gilbert
Department of Civil Engineering
The University of Texas
Austin, 78712

Dear Bob:

Bob, at the outset I am amazed that no foundation failures were reported due to storm loading of offshore platforms. Is it possible that some piles moved and caused a failure which was incorrectly classified as a structural failure? By the way, how many platforms were heavily loaded by storms and how many were damaged?

After I left the meeting today, I decided to write a few comments about what you might do on the current project. The comments shown below are "rough" and not indicated to represent more than a few thoughts that arose during the meeting. Two categories of suggestion are given: the first for use in what I think to be your current study, and the second, probably much more expensive, for a follow-up study.

GEOTECHNICAL INFORMATION FOR DESIGN OF FIXED OFFSHORE PLATFORMS

The following points relate to the work of the geotechnical engineer and the manner findings are reported to the structural engineer. The Owner is also involved because appropriate funds must be authorized for the geotechnical engineer to do proper work.

1. A soil boring must be performed at the site.

The boring must be done at the location of the construction or reasonably nearby. If nearby, a geological profile must be made to show the boring is representative of the conditions at the site. Care must be exercised if a submerged river bed could have affect the boring or the construction.

2. The procedures used in making the boring must follow approved techniques. Approved techniques must be defined.

3. The properties defining the soil must be presented as a function of depth. These properties must be consistent with those employed offshore of the United States.

4. Load-transfer functions must be recommended in order to carry out structural designs. The properties should reflect the affect on the soil of pile installation, the nature of the loading, and whether for lateral loading or axial loading. The geotechnical engineer may use differing soil parameters in reflecting behavior under axial loading and behavior under lateral loading. When recommending load-transfer functions for cyclic loading, the number of cycles should be indicated. Data show that only a small number of the maximum wave loads will occur during a storm.

Phone: (512) 833-5190

Telefax 512 873 0087

e-mail: LymonReese@aol.com

Figure F.1 Comments in Dr. Lymon Reese's Letter (Part 1 of 3)

5. In developing the load-transfer functions, appropriate methods must be used to reflect the affect of close spacing of piles.
6. A uniform method must be developed to guide the geotechnical engineer in transmitting appropriate information about the soil and its behavior in designing an offshore platform.

EFFECT OF PILE INSTALLATION ON SOIL PROPERTIES

Most geotechnical engineers understand that the properties of the soil near a driven pile are very much different from the properties measured in the geotechnical investigation. Not only are the properties different but variations exist from the wall of the pile outward. Furthermore, adding to the complication is that the properties of soil around a driven pile are time-dependent. Dramatic effects are shown in some soils over a period of a few weeks but further, numerically less important changes, can continue to occur over long periods of time.

1. A document should be developed that presents general information on the subject. Some of the items to be addressed are: densification of sand and/or crushing of sand grains, general and decay of excess porewater pressure as a function of time, response of calcareous soil as an indication of the dramatic (disastrous) effect for a particular soil, and some indication of the time-dependent effect on load-transfer functions for both axial and lateral loading. The document should consider the driving of a closed-ended pile or an open ended pile.
2. With the guidance of the above document, review all of the data from pile-load tests on which the current criteria for design are based and make an estimate on soil properties of the installation of the test pile as a function of depth.
3. If possible, return to the sites where referenced tests were performed and, if the test pile still remains in place, re-load the pile to obtain information to compare with the earlier results.
4. Search the technical literature and perform Step 2 for all of the load tests where instruments were used to obtain load-transfer curves, for both axial and lateral loading.
5. Develop a laboratory testing program, perhaps employing the centrifuge, where the effect on soil properties of the passing of a metal body (the wall of a pile) through an undisturbed specimen of soil can be measured.
6. Develop detailed plans for the performance of field load tests, using piles instrumented for the measurement of load-transfer curves as a function of depth, in deposits that are principally sand and are principally clay. The instruments would include those that can measure porewater pressure as a function of time. Plan to re-load the pile with time, taking care that the loading does not cause damage to the soil surrounding the driven pile.
7. Tests as noted in Step 5 have not be performed to data and would require the development of new and unique ways to measure the properties of the along a pile, in the vicinity of the pile wall, after the time-dependent response of the soil has occurred completely. (Can devices for the

Phone: (512) 833-5190

e-mail: LymonReese@aol.com

Fax: (512) 244-8067

Figure F.1 Comments in Dr. Lymon Reese's Letter (Part 2 of 3)

sampling of soil at the wall of a driven pile be installed before driving and soil samples extracted and retrieved after the pile achieves equilibrium?)

8. Perform field load tests with heavily instrumented piles as noted in Step 7. Consider a testing program that will last a lengthy period of time, taking care that an earlier load test does not seriously affect the soil prior to a subsequent test..

CLOSING COMMENT

Bob, you can understand that the above ideas were developed "off the cuff" and not after long consideration. I hope some of the ideas above will be useful.

Your sincerely



Lyndon C. Reese

Copy: STW

Phone: (512) 833-6190

e-mail: LyndonReese@aol.com

Fax: (512) 244-6067

Figure F.1 Comments in Dr. Lyndon Reese's Letter (Part 3 of 3)